

## **Latvijas Universitātes aģentūra**



**Renovētā sārmu metālu  
laboratorija**

## **Publiskais pārskats**

**2008.gads**

## ***Misija***

Latvijas Universitātes Fizikas institūta (LU FI) misija ir iedibināta vēsturiski: zinātniskie pētījumi magnētiskajā hidrodinamikā (MHD) un ar to saistītās zinātnes nozarēs un ar to saistītu pielietojumu realizēšana un arī jauno speciālistu sagatavošanu šajās zinātnes nozarēs. LUFI darbojas kopējies Latvijas Universitātes misijas kontekstā.

## ***Latvijas Universitātes Fizikas institūta īsa vēsture.***

LU FI atrodas Salaspilī, Miera ielā 32. dibināts 1946.g. kā Latvijas PSR ZA Fizikas un matemātikas institūts, no 1950.gada Latvijas ZA Fizikas institūts, Latvijas Universitātes Fizikas institūts kopš 1997.

**Direktori:** 1946-1948 N.Brāzma ; 1948-1967 I.Kirko; 1967-1991 J.Mihailovs; 1992-1993 I.Bērsons; 1994-1997 O.Lielausis; 1998-2000 A.Gailītis.

Kopš 2001.g. direktors J.E.Freibergs. Zinātniskās padomes priekšsēdētājs A.Gailītis. Akadēmiskais personāls pašlaik ir 48 (asistenti, pētnieki un vadošie pētnieki), no tiem 6 habilitētie dokt., 35 doktori.

2006. gada 1. maijā LU Fizikas institūts atbilstoši Likumam par zinātnisko darbību tika reorganizēts par LU aģentūru.

**LU FI darbības 2008.gada pamatmērķi ir sekojoši:**

- Uzturēt LU FI kā vadošo pētniecības centru magnētiskajā hidrodinamikā un ar to saistītās zinātnēs gan Latvijā, gan Eiropā un izveidot LU FI par atzītu pētniecības iestādi Pasaules zinātniskajā telpā.
- Uzlabot sadarbību ar LU Fizikas un matemātikas fakultāti zinātnē un jauno speciālistu audzināšanā un arī ar radniecīgām fakultātēm RTU.
- Pastiprināt sadarbību ar ārzemju zinātniekiem jo sevišķi ar Franču zinātniekiem, kā arī ar Vācu, Lielbritānijas un Nīderlandes zinātniekiem.
- Turpināt strādāt pie **Ampēra iniciatīvas** projekta sagatavošanas.

**Atbilstība prioritārajiem virzieniem.**

**Materiālzinātne** (nanotehnoloģijas funkcionālo materiālu iegūšanai un jaunas paaudzes kompozītmateriāli);

**Enerģētika** – videi draudzīgi atjaunojamās enerģijas veidi, enerģijas piegādes drošība un enerģijas efektīva izmantošana.

**Lietišķo pētījumu virzieni:** šķidro metālu tehnoloģijas jaunas paaudzes kodolreaktoriem un kodolsintēzes reaktoriem (enerģijas ražošanas un piegādes drošība); MHD saules enerģijas pārveidotājs (videi draudzīgi atjaunojamās enerģijas veidi); MHD tehnoloģiju izmantošana jauna veida metālu sakausējumu iegūšanai (materiālzinātne); magnētiskie šķidrumi, magnētiskā lauka izmantošana nanoierīču vadīšanai, magnētisko parādību un kapilāro parādību mijiedarbība (nanotehnoloģijas funkcionālo materiālu un ierīču iegūšanai); starpnozaru pētījumi – magnētiski vadāmu nanoierīču izmantošana biomedicīnā.

Latvijas Universitātes dibināta Latvijas Universitātes aģentūra „Latvijas Universitātes Fizikas institūts” ; 17.03.2006.g. Latvijas Universitātes Senāta lēmums Nr.177 Reģistrēts LR VID ar kodu LV90002112199; reģistrēts Nodokļu maksātāju reģistrā ar kodu 90002112199

LR IZM Zinātniskās institūcijas reģistrācijas apliecība Nr.551021



**LU FI ir 6 zinātniskās struktūrvienības:**

Fizikālās hidromehānikas lab. (vad. E.Platacis), Siltuma un masas pārneses lab. (E.Blūms), MHD tehnoloģijas lab. (A.Bojarēvičs), MHD mašīnu teorijas lab. (A.Šiško), Elektrovirpuļplūsmu lab. (J.Freibergs), Teorētiskās fizikas lab. (A.Gailītis).

Direkcija

Grāmatvedība

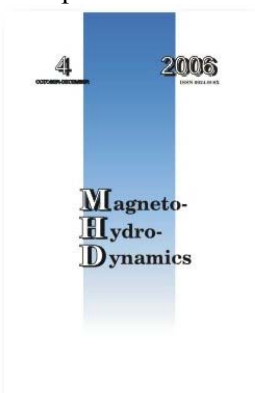
Enerģētikas un saimniecības dienests

Vidējais zinātniskā personāla skaits 44,0 2006 gadā PLE izteiksmē  
Vidējais zinātnisko darbinieku skaits 74,0 2006 gadā PLE izteiksmē

<b>Tālrunis</b>	67944700
Fakss	67901214
E-pasts	fizinst@sal.lv
Internets	<a href="http://iph.sal.lv">http://iph.sal.lv</a>
<b>Direktors</b>	<b>Dr.fiz. Jānis Freibergs</b>
Tālrunis	67944700
Fakss	67901214
E-pasts	jf@sal.lv
<b>Direktora vietnieks</b>	<b>Dr.fiz. A.Gailītis</b>
Tālrunis	67945821
e-pasts	gailitis@sal.lv
<b>Direktora palīdze</b>	<b>Maija Broka</b>
Tālrunis	67944700
Fakss	67901214
E-pasts	mbroka@sal.lv
<b>Atrodas</b>	Salaspilī, Miera ielā 32
<b>Pasta adrese</b>	Miera ielā 32, Salaspils-1, LV-2169
<b>Sadarbības fakultātes</b>	Fizikas un matemātikas fakultāte
<b>Akadēmiskā personāla skaits (asist., pētn., v.pētn., tsk.) uz 01.01.2008.</b>	<b>60</b>
	<b>doktori</b> <b>36</b>
	<b>habilitētie doktori</b> <b>6</b>

LU FI izdod starptautisku žurnālu "Magnētiskā hidrodinamika" ( kopš 1965, tagad angļu valodā, iznāk 4 reizes gadā; galvenais redaktors A.Cēbers).

LU FI organizē regulāras starptautiskas konferences.



## **Zinātniskā padome**

**Zinātniskās padomes priekšsēdētājs**

**Dr.phys. A. Gailītis**

**Sekretāre**

**R.Valdmane**

**Dr.hab.phys. E.Blūms**

**Andris Bojarēvič**

**Dr.phys. I. Bucenieks**

**Dr.phys. L. Buligins**

**Dr.hab.phys. A.Cēbers**

**Dr.phys. J.E.Freibergs**

**Dr.phys. A.Gailītis**

**Dr.hab.phys. J.Gelfgāts**

**Dr.phys. A.Mežulis**

**Dr.phys. O. Lielausis**

**Dr.phys. A. Pedčenko**

**Dr.phys. E. Platacis**

**Dr.phys. M. Zaķe**

**Jānis Zandarts.**

**LU Fizikas institūta zinātnē nodarbināto darbinieku saraksts**

N.P.K.	Vārds, uzvārds	Akadēmiskais amats	Slodze
<b>Ievēlētais zinātniskais personāls</b>			
1	Monika Abricka	pētniece	1
2	Inesa Barmina	vadošā pētniece	1
3	Elmars Blūms	vadošais pētnieks	1
4	Andris Bojarevičs	pētnieks	1
5	Valdis Bojarevičs	vadošais pētnieks	0
6	Maija Broka	zinātniskā asistente	1
7	Imants Bucenieks	vadošais pētnieks	1
8	Aleksandrs Cipiks	zinātniskais asistents	1
9	Aleksejs Flērovs	pētnieks	1
10	Jānis Freibergs	vadošais pētnieks	1
11	Vilnis Frišfelds	vadošais pētnieks	0,5
12	Agris Gailītis	vadošais pētnieks	1
13	Jurijs Geļfgats	vadošais pētnieks	1
14	Leonīds Gorbunovs	vadošais pētnieks	1
15	Ilmārs Grants	vadošais pētnieks	1
16	Maksims Igoņins	pētnieks	0
17	Sergejs Ivanovs	pētnieks	1
18	Ilga Kļaviņa	zinātniskā asistente	1
19	<u>Jānis Kļaviņš</u>	vadošais pētnieks	0,7
20	Aleksandrs Kļukins	vadošais pētnieks	1
21	Jurijs Koļesņikovs	vadošais pētnieks	0,5
22	Armands Krauze	pētnieks	1
23	Kalvis Kravalis	zinātniskais asistents	1
24	Vladislavs Kremēneckis	pētnieks	0,5
25	Stanislav Krisjko	pētnieks	1
26	Rihards Križbergs	vadošais pētnieks	1
27	Gunārs Kroņkalns	vadošais pētnieks	1
28	Agnese Līckrastiņa	vadošā pētniece	1
29	Olgerts Lielausis	vadošais pētnieks	1
30	Guntis Lipsbergs	zinātniskais asistents	1
31	Mihails Majorovs	pētnieks	1
32	Ansis Mežulis	vadošais pētnieks	1
33	Artūrs Mikelsons	vadošais pētnieks	1
34	Aleksandrs Pedčenko	vadošais pētnieks	0
35	Oksana Petričenko	zinātniskā asistente	1
36	Ernests Platacis	vadošais pētnieks	1

37	Ilgvars Platnieks	vadošais pētnieks	1
38	Alfreds Pozņaks	pētnieks	0,5
39	Jānis Priede	vadošais pētnieks	0
40	Alberts Romančuks	vadošais pētnieks	1
41	Svetlana Ščaņicina	zinātniskā asistente	1
42	Jeļena Šilova	pētnieks	0,5
43	Andrejs Šiško	vadošais pētnieks	1
44	Rita Valdmane	zinātniskā asistente	1
45	Jānis Valdmanis	vadošais pētnieks	1
46	Maija Zaķe	vadošā pētniece	1
47	Vladimirs Žuks	pētnieks	1
		<b>Kopā (PLE):</b>	<b>40,2</b>

#### Zinātniskais personāls

1	Mihails Belovs	pētnieka v.i.	0,5
2	Andrejs Cēbers	vad.pētnieka v.i.	0,5
3	Kaspars Ērglis	pētnieka v.i.	0,5
4	Jānis Gailis	zin.asistenta v.i.	0,5
5	Linards Goldšteins	zin.asistenta v.i.	0,5
6	Imants Kaldre	zin.asistenta v.i.	1
7	Līga Magone	zin.asistenta v.i.	1
8	Viesturs Šints	zin.asistenta v.i.	0,5
9	Andrejs Tatulčenkovs	zin.asistenta v.i.	1
10	Vladimirs Vorohobovs	zin.asistenta v.i.	1
11	Vladimirs Zablockis	zin.asistenta v.i.	1
		<b>Kopā (PLE):</b>	<b>8</b>

#### Zinātnes tehniskais personāls

1	Evalds Bērziņš	tehnīkis-elektroatsl.	1
2	Jānis Celmājs	tehnīkis-elektroatsl.	1
3	Jānis Ivanovs	tehnīkis-elektroatsl.	1
4	Andrejs Jurgensons	tehnīkis-frēz.	1
5	Guntis Jursons	tehnīkis-elektroatsl.	1
6	Pēteris Lūķis	tehnīkis-elektroatsl.	1
7	Dainis Mauriņš	tehnīkis-elektroatsl.	1
8	Jānis Māzers	elektriķis	1
9	Jevgēnijs Morskovs	tehnīkis-elektroatsl.	1
10	Ingus Pagasts	tehnīkis-metināt.	1
11	Roberts Parolis	tehnīkis-elektroatsl.	1
12	Jānis Peinbergs	tehnīkis-elektroatsl.	1
13	Jēkabs Šeimanis	inženieris konstr.	1
14	Juris Škapars	tehnikis	1

15	Vladimirs Soboļevs	tehnīkis-elektroatsl.	1
16	Ivars Strazdiņš	Mehāniķis	0,5
17	Juris Tobijs	tehnīkis-virp.	1
18	Nikolajs Vederņikovs	tehnīkis-elektroatsl.	1
19	Jakovs Višņakovs	tehnīkis-elektroatsl.	1
20	Jānis Zandarts	galv.inženieris	1
21	Imants Zariņš	tehnīkis-atssl.	1
22	Anatolijs Ziks	vec.inženieris	1
		<b>Kopā (PLE):</b>	<b>21,5</b>

**Zinātni apkalpojošais personāls**

1	Aida Volkova	galv.grāmatvede	1
2	Lilija Kaļčenko	grāmatvede	1
3	Ludmila Komarova	personāldaļa	1
4	Agris Strazdiņš	autobusa vadītājs	1
5	Valentīna Soboļeva	apkopēja	1
6	Valentīna sidorenko	apkopēja	1
7	Dionizija Cielava	dežurante	1
8	Jānis Cielavš	dežurants	1
9	Aleksandrs Golubevs	dežurants	1
10	Antoņina Kaminska	dežurants	1
11	Regīna Konošonoka	dežurants	1
12	Francis Ludbāržs	dežurants	1
13	Tekla Petrovska	dežurants	1
14	Peteris Rokjānis	dežurants	1
		<b>Kopā (PLE):</b>	<b>14</b>

**Latvijas Universitātes aģentūra "LU Fizikas institūts" zinātniskās darbības  
finansējums**

	Kopā, Ls
<b>Finansējums kopā</b>	1675112
tai skaitā	
<b>Valsts budžeta finansējums- kopā</b>	1409212
no tā – Eiropas Savienības struktūrfondu finansējums zinātniskajai darbībai	924766
tai skaitā VPD 2.5.1.aktivitātes projektu finansējums	924766
- Latvijas Zinātnes padomes (LZP) granti un cits LZP finansējums	92500
- zinātniskās darbības bāzes finansējums	309846
- valsts pētījumu programmu finansējums	72000
- zinātniskās darbības attīstības finansējums	0
- valsts pārvaldes institūciju pasūtītie pētījumi	0
- tirgus orientētie pētījumi	10100
- pārējais valsts budžeta finansējums (piemēram, pašvaldību finansējums)	0
<b>Augstskolas finansējums zinātnei</b>	0
<b>Finansējums no starptautiskiem avotiem - kopā</b>	265900
no tā – ienēmumi no līgumdarbiem ar ārvalstu juridiskām personām	265900
<b>Ienēmumi no līgumdarbiem ar Latvijas Republikas juridiskām personām</b>	
<b>Cits finansējums zinātniskai darbībai</b>	
no tā – ienēmumi no citām saimnieciskām darbībām	
<b>Zinātniskā institūta – komercsabiedrības vai nodibinājuma finansējums zinātniskai darbībai</b>	

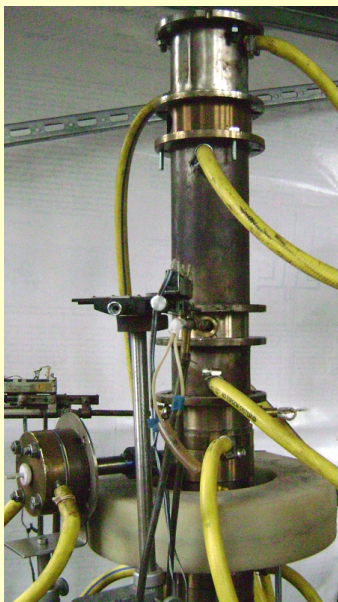
**Latvijas Universitātes aģentūra "LU Fizikas institūts" finansējuma izlietojums**

<b>Izdevumi kopā</b>	<b>1780423,0</b>
<b>Uzturēšanas izdevumi</b>	<b>940469,0</b>
<b>Kārtējie izdevumi</b>	<b>940469,0</b>
<b>Atlīdzība</b>	<b>747325,0</b>
no tā – zinātniskai darbībai	747325,0
<b>Preces un pakalpojumi</b>	<b>193144,0</b>
no tā – zinātniskai darbībai	193144,0
<b>Kapitālie izdevumi</b>	<b>839954,0</b>
<b>Pamatkapitāla veidošana</b>	<b>839954,0</b>
no tā – zinātniskai darbībai	839954,0

# The Ampere Initiative : a step into the future

## An ambitious view

The **Ampere Initiative** is a Franco-Latvian led collaborative project, aiming to create a European Centre of Excellence (“**Ampere Institute**”) in Latvia in the domain of magnetohydrodynamics and magnetic fields.

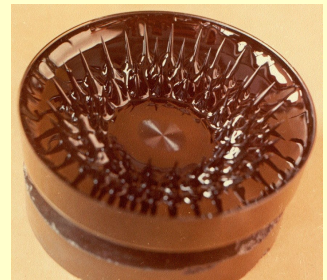
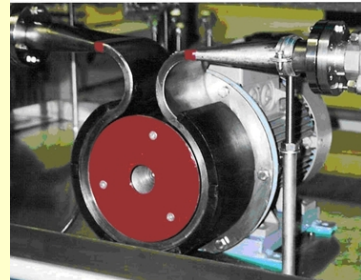


Magnetically controlled combustion apparatus in the laboratories of IPUL  
Credits : M. Zake

Since 2001, the Institute of Physics of the University of Latvia (IPUL) and the French organisms CEA and CNRS are pushing for the establishment near Riga of a large research institution making the most of Latvian excellence in these domains.

Renovation of the premises with the help of European funds will enhance IPUL world-class status and allow for the storage and study of among the world largest volumes of alkaline liquid metals (sodium and mercury).

## A push towards new technologies

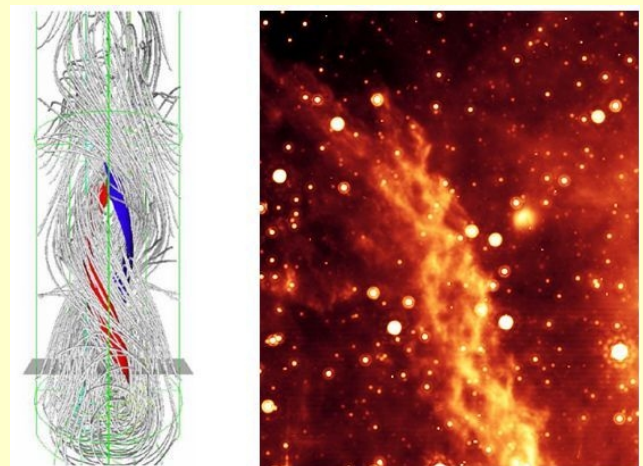


New applications of magnetic field research : a new type of electromagnetic induction pump (left) and magnetic nanocolloids (right)

Credits : I. Bucenieks, E. Blums

Applications are numerous and of prime importance : “blankets” of nuclear reactors, high-efficiency induction pumps with no moving parts, use of ferrocolloids in biomedicine, improvement of casting techniques in the metal industry, combustion or crystallization control by magnetic fields, space energy generators using magnetohydrodynamic drive, etc ... The domain of studies are among the most promising for future development.

Despite the economic crisis, the Ampere Initiative remains one of the priorities of the University of Latvia. A request of financial support to the European Regional Development Fund (ERDF) will be submitted in summer 2009 to help renew the infrastructure. The “Ampere Institute” may then come into existence as soon as 2010.



Similarities between the dynamo field at IPUL and magnetic fields of space projections events  
Credits : A. Gailitis

With the support of :

Centre National de la Recherche Scientifique (CNRS)  
Commissariat à l'Energie Atomique (CEA)



## **LUFİ zinātniskās pētniecības apakšvirzinu pašnovērtēšanas ziņojums.**

### **I apakšvirziens**

Zinātniskās pētniecības apakšvirziens, kurā LUFİ ir vadošo institūciju vidū pasaulē:

### **Šķidru metālu magnetohidrodinamika un hidrodinamika, fundamentālie un pielietojumie pētījumi.**

#### **Publikācijas:**

1. R.B.Gomes, H.Fernandes, C.Silva, A.Sarakovskis, T.Pareira, J.Figueiredo, B.Caravalho, A.Soares, C.Varandas, O.Lielais, A.Klyukin, E.Platacis, I.Tale. Interaction of a gallium jet with the tokamak ISTTOK edge plasma. *Fusion Engineering and Design*, 83 (2008)102-111
2. Gailitis, A., Gerbeth, G., Gundrum, Th., Lielausis, O., Platacis, E., Stefani, F. *History and results of the Riga dynamo experiment* Comptes Rendus Physique 9 (2008), 721-728; [arxiv.org/0807.0305](https://arxiv.org/abs/0807.0305)
3. I.Grants, C.Zhang, S.Eckert, G.Gerbeth, Experimental observation of swirl accumulation in a magnetically driven flow, *Journal of Fluid Mechanics* 616, 135 (2008)

#### **Patenti:**

1. US Patent 7,335,256, 2008. Silicon single crystal and process for producing it. Authors: W.von Ammon, H. Schmidt, J. Virbulis, Yu. Gelfgat et. al.
2. European Patent (Application No.08016830.5-2209) "Vervahren und Anordnung zur Messung des Durchflusses elektrisch leitfähiger Medien" (2008). Autori: G.Gerbeth, ... A.Bojarevics, J.Gelfgats.
3. Karcher, Ch., Kolesnikov, Y., Thess, A.: German Patent DE 10 2007 038 685 (2008).

#### **Akadēmiskais personāls:**

Dr.Phys. I.Bucenieks, J.Freibergs, A.Gailītis; I.Grants, A.Kļukins, O.Lielais; E.Platacis; I.Platnieks; A.Šiško;

### **1. Finansējuma avoti – Eiropas Savienība**

Magnetic flow tomography in technology geophysics and ocean flow research MAGFLOTOM	Commission of the EC Research DG EC 6 Framework Programm-	Contract No.028670 Specific target project
.Asociācijas EURATOM-Latvijas Universitāte Atomenerģijas kopienas (EURATOM) projektu _Fusion Physics Programme - Preparation of a gallium jet limiter for testing under reactor relevant conditions (turpmāk-projekts) ar EK kontrakta numuru Nr. FU07-CT-2007-00047	Fixed contribution contract with EURATOM EC 6 Framework Programm-	Nr. FU07-CT-2007-00047
European Isotope Separation On-Line Radiactive Ion Beam facility (EURISOL DS)	EC 6 Framework Programm	Contract 515768 (RIDS)

Virtual European Lead Laboratory (Vella)	EC 6FP: Contract type: Integrating activities implemented as integrated Infrastructure activities	Project reference 36469. NUWASTE-2005/6- 3.2.3.1-1 2006.10.01- 2009.09.30
---	---	--

### ERAFF projekts

Nr.VPD1/ERAFF/CFLA/05/APK/2.5.1./000004/004	“MHD tehnoloģija svina-litija eitektiska sakausējuma iegūšanai un pielietošanai kodolsintēzes reaktoru sistēmās”.
---	---

## 2. Latvija

### LZP sadarbības projekts

Projekts Nr. 06.0029	„Inovatīvi strukturāli integrēti kompozītmateriāli: dizains, iegūšanas un pārstrādes tehnoloģijas, ilgmūžība”.
Apakšprojekts Nr. 2.06.0029.2.09	Kompozītmateriāli un nanokompozīti. MHD metodes dispersās fāzes sadalīšanai un homogenizācijai kompozītos ar metālisku matricu

### LZP granti

## 3. Ārzemju līgumi

<i>Paul Scherer Institute</i>	<i>Switzerland</i>	<i>Modification of an electromagnetic pumps</i>
<i>Corus Research, Development and Technology</i>	<i>The Netherlands</i>	<i>Design, manufacture, test and delivery of a permanent magnet system</i>
<i>SIEMENS, Grenobles Politehniskais institūts CNRS, INPG</i>	<i>Germany France</i>	<i>Feasible study for the MHD facility with permanent magnets for the glass technology</i>
<i>Center for Automatic R&amp;D CIDAUT Foundation for R&amp;D in Automotive Sector</i>	<i>Spain</i>	<i>A research project for liquid aluminium pumps on rotating permanent magnets</i>
<i>Commissariat a l'energie atomique, Departement de technologie nucleaire</i>	<i>France</i>	<i>Assesment of possibility to design and develop pf EM pump related to m3 irradiation devices</i>
<i>Los Alamos National Laboratory (LANL)</i>	<i>ASV</i>	<i>System of electromagnetic pumps</i>
<i>Oak Ridge National Laboratory (ORNL)</i>	<i>ASV</i>	<i>Design, manufacture, test and delivery 2 electromagnetic pumps</i>

Kopējais zinātnisko darbu finansējums 2008.gadā – Ls 852900

LU Fizikas institūts – 2008

Sārmu metālu laboratorijas renovācija - Ls 697 900  
Zinātniskās iekārtas 2008.g. iegādātas par summu Ls 100400

**II apakšvirziens**  
**Latvijas kontekstā:**  
**Magnētisko nanokoloīdu fizika**

**Publikācijas:**

1. E.Blums, A.Cebers, M.M. Maiorov, *Magnetic Fluids*, Walter de Gruyter, Berlin, 1996
2. E. Blums. Mass Transfer in Non-Isothermal Ferrocolloids under the Effect of a Magnetic Field, *J. Magn. and Magn. Materials* , 1999, **201**, No. 1-3, p.242-247
3. A. Mežulis, E. Blums, The presence of microconvective instability in optically induced gratings, *Journal of Non-Equilibrium Thermodynamics* **32** (2007), 331 – 340.

**Vadošais personāls:**

E.Blūms, A. Mežulis, M. Majorovs, G.Kroņkalns.

**Finansējums:**

17 projekti, tai skaitā 1 Valsts programma, 1 LZP sadarbības projekts, 4 LZP granti, 2 Eiropas Komisijas projekti, 1 Sorosa Fonda grants, 2 Vācijas un 1 Zviedrijas sadarbības projekti, 2 Humboldta Fonda atbalsta granti, kompānijas „Ferotec-USA” līgumprojekti u.c. Pēdējo 3 gadu kopējais finansējums aptuveni 240000 LVL, 4500 EUR un 7500 USD.

**Eiropas un pasaules kontekstā:**  
**Siltuma un masas pārnese magnētiskajos nanokoloīdos**

**Publikācijas:**

1. E. Blums, Yu. A. Mikhailov, R. Ozols. *Heat and Mass Transfer in MHD Flows*, World Scientific, Singapore, 1987, 512 p.
2. E. Blums, S. Odenbach, A. Mežulis, M. Maiorov. Soret Coefficient of Nanoparticles in Ferrofluids in the Presence of a Magnetic Field, *Physics of Fluids* 1998, **10**, No. 9, p. 2155-2163
3. E. Blums, New Problems of Particle Transfer in Ferrocolloids: Soret Effect and Thermoosmosis, *The European Physical Journal E - Soft Matter*, **15**, (November 2004) No. 3, pp. 271-276
4. A. Mežulis, E. Blums, On the microconvective instability in optically induced gratings, *Physics of Fluids*, **18**, 107101 (2006)

**Vadošais personāls:**

E. Blūms, A. Mežulis, M. Majorovs

**Finansējums:**

17 projekti, tai skaitā 1 Valsts programma, 1 LZP sadarbības projekts, 4 LZP granti, 2 Eiropas Komisijas projekti, Sorosa Fonda grants, 2 Vācijas un 1 Zviedrijas sadarbības projekti, 2 Humboldta Fonda atbalsta granti, kompānijas Ferotec-USA līgumprojekti u.c. Pēdējo 3 gadu finansējums aptuveni 240000 LVL, 4500 EUR un 7500 USD.

### **III apakšvirziens**

**Latvijas kontekstā:**  
**Degšanas procesu dinamikas izpēte.**

**Vadošais personāls:**

Vad. pētn. Dr. phys. M.Zaķe, Dr. sci. Ing. I.Barmina, Dr.sci.ing. A.Meijere

Viens no virzieniem, kurā LU Fizikas institūtu var uzskatīt par vadošo Latvijā ir degšanas procesu dinamikas izpēte ar mērķi izveidot stabili, efektīvu un ekoloģiski tīru degšanas procesu. Pētījumi apvieno liesmas dinamikas, siltuma un masas pārneses un kīmisko procesu izpēti dažādās degšanas procesa attīstības stadijās, sadedzinot gāzveida vai cieto kurināmo (dažāda sastāva un struktūras koksnes biomasu).

Degšanas procesa kontrolei un regulēšanai izmanto ārējo lauku (elektriskā, magnētiskā) un liesmas mijiedarbības efektus, kā arī vienlaicīgu gāzveida un cietā kurināmā sadedzināšanu.

Degšanas procesu pētījumi tiek veikti sadarbībā ar Valsts Koksnes Kīmijas institūtu un Valsts Mežzinību institūtu „Silava.” Sadarbībā ar VKĶI tiek veikta bioetanola ražošanas procesa atkritumu- dažāda sastāva lignīna granulu degšanas procesu kinētikas un dūmgāzu sastāva izpēte, nosakot korelācijas starp šo granulu elementārā sastāva un degšanas procesu raksturojošiem lielumu izmaiņām ar tām sekojošām saražotā siltuma daudzuma un degšanas produktu sastāva izmaiņām dažādās degšanas procesa attīstības stadijās, optimizējot granulu sastāvu, lai iegūtu efektīvu un ekoloģiski tīru degšanas procesu. Šāda tipa granulu izmantošana siltuma ražošanai būtiski palielina bioetanola ražošanas efektivitāti, samazinot izmaksu zudumus, kurus līdz šim noteica nepilnīga bioetanola ražošanas blakus produkta- lignīna izmantošana vietējai apkurei.

Sadarbībā ar VMZI „Silava” paredzēts veikt dažādu Latvijas koku sugu un sīkkoksnies degšanas procesu izpēti ar mērķi izveidot stabili degšanas procesu, kas balstās uz vietējā kurināmā apzināšanu un tā raksturojošo lielumu izpēti.

Fizikas institūtā dažāda tipa degšanas procesu izpētei ir izveidota mazas jaudas (līdz 2-3kW) eksperimentālā iekārta, kurā degšanas procesa stabilizācijai izmanto gaisa virpuļplūsmu ar pakāpenisku koksnes biomasa sadedzināšanu.

Šo pētījumu rezultātā ir izveidots eksperimentālais vietējās apkures katls ar jaudu līdz 50 kW, par kura izveidi ir sagatavots un apstiprināts patenta pieteikums, nodrošinot vienlaicīgu propāna un koksnes biomasa sadedzināšanu. Eksperimentālās iekārtas ir aprīkotas ar zondēm lokāliem liesmas temperatūras, ātruma un sastāva mērījumiem, nodrošinot arī saražotā siltuma daudzuma mērījumus dažādās degšanas procesa attīstības stadijās. Lokāliem liesmas ātruma sadalījuma mērījumiem ir iespējams izmantot Pito caurulītes un Lāzera Doplera ātruma mērītāju, bet liesmas sastāva mērījumiem izmanto gāzu analizatoru „Testo-350XL” un spektrofotometrus „Cary” un „Varian”. Visiem mērījumiem ir nodrošināta datorizēta mērījumu reģistrācija un apstrāde.

Pētījumu rezultāti ir publicēti dažāda līmeņa Starptautisko un vietējo konferenču materiālos, kā arī dažāda līmeņa zinātniskos izdevumos.

**Publikācijas:**

1. M. Zaķe, I. Barmina, M.Gedrovičs, A. Desnīckis, Effective Technique of Wood and Gaseous Fuel Co-firing for Clean Energy Production, Latvian Journal of Phys. and Techn. Sci., 2007, N2, pp. 41-56.
2. I. Barmina, A. Desnīckis, A. Meijere, M. Zake, DEVELOPMENT OF BIOMASS AND GAS CO-FIRING TECHNOLOGY TO REDUCE GREENHOUSE GASEOUS EMISSIONS, Springer- NATO publishing, 2007, pp.221.-230.
3. A. Arshanitsa, I. Barmina, T. Dizhbite, G. Telysheva, M .Zake, Co-firing of different types of biomass fuel pellets, Riga, Zinātne,2008, Renewable Energy Resources, Production and Technologies, pp.37-46.
4. I. Barmina, A. Desnīckis, M. Zake, The Influence of Electric Field on the Development of the Swirling Flame Velocity Field and Combustion Characteristics // Heat Transfer Research, 2008, Vol.39, Nr.5, pp.371-378.

**Patents:**

5. I. Barmina, M.Gedrovičs, P. Meija, A. Meijere-Līckrastiņa, M. Purmals, M. Zaķe, Atjaunojamā kurināmā un gāzveida kurināmā vienlaicīgas sadedzināšanas apkures katls- patenta pieteikums, 2008, pp.1-16 (Tiks publicēts 2009.g. 20. augustā).

**Finansējuma avoti:**

2005.-2008. g. ERAF projekts Nr. VPD1/ERAF/CFLA/05/APK/2.5.1./000001/ „Koksnes biomasas vietējo resursu racionāla izmantošana siltuma ražošanai kombinētā koksnes un gāzveida kurināmā degšanas procesā” par kopējo summu 91833Ls un LZP projekts „Siltuma un masas pārneses pētījumi kombinētā gāzveida un cietā kurināmā degšanas procesā ārējo spēku laukā” par kopējo summu 21258 Ls. 2009. gadā sadarbībā ar VKĶI un VMZI „Silava” ir sagatavots un iesniegts izskatīšanai ESF projekts „Dažādu koku sugu neapgūto sīkkoksnes resursu un to kvalitātes izpēte ekoloģiski drošu un efektīvu siltuma ražošanas procesu izveidei”.

**Latvijas Universitātes aģentūras  
„Latvijas Universitātes Fizikas institūts”  
darba plāns 2008.gadam**

Šis darba plāns ir Latvijas Universitātes (LU) un Latvijas Universitātes Fizikas institūta (LU FI) Pārvaldes līguma pielikums.

**LU FI veic savu darbību saskaņā ar savu Nolikumu, Pārvaldes līgumu un savu  
vidēja termiņa stratēģiju.**

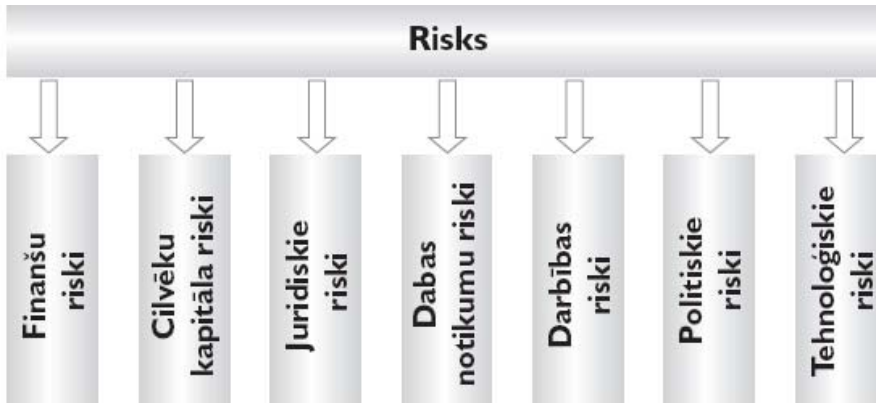
LU FI nodrošina savu pētniecisko darbību un publisko pakalpojumu sniegšanu atbilstoši zinātnieku ētikas kodeksam, starptautiski atzītiem labas prakses paraugiem un LU FI iekšējiem normatīviem dokumentiem, tādejādi nodrošinot savas darbības attiecīgos kvalitatīvos rādītājus un ceļot institūta prestižu kopumā.

**LU FI nodrošina ar 04.08.2008. Ministru Kabineta noteikumiem Nr. 623 “Bāzes finansējuma piešķiršanas kārtība valsts zinātniskajām institūcijām un valsts augstskolu zinātniskajiem institūtiem” noteiktos zinātnisko institūtu novērtēšanas rādītājus tādā mērā, lai integrētais novērtējums par 2008.gadu nav mazāks par 10.**

LU FI 2009.gadam noteiktie kvalitatīvie un kvantitatīvie rādītāji atspoguļoti nākošā tabulā.

		2009.gadā
Zinātnisko pētījumu tematiskās jomas, kurās institūtam būs nozīmīga loma, saskaņā ar stratēģiju		4
Zinātniskā personāla attīstības rādītāji (skaita pieaugums pret iepriekšējo gadu, %)		1 %
Finansējuma attīstības rādītāji (apjoma pieaugums pret iepriekšējo gadu, %)		15%
Sagatavoto zinātnisko publikāciju skaits		60
tai skaitā	SCI publikācijas (publikācijas izdevumos, kas tiek referēti starptautiski pieejamās datu bāzēs)	30
	Publikācijas starptautiski recenzētos, LZP atzītos izdevumos	19
	Publikācijas citos zinātniskajos izdevumos	8
	Populārzinātniski raksti	3
Konferenču tēzes		10
Sagatavoto un piedāvāto studiju kursu skaits		2
Sagatavotie laboratorijas darbu komplekti		2
Doktorantiem, maģistrantiem un bakalauriem piedāvāto darba vietu un/vai pētījumu tēmu skaits		6
Starptautiskās atpazīstamības rādītāji (starptautiski nozīmīgi projekti vai pasākumi kopā)		6
Eiropas Savienības 6 un 7.ietvara projektu skaits		5
Valsts pētījumu programmu projektu skaits		2
LZP finansētie sadarbības projekti		3
Latvijas Zinātnes padomes finansēto projektu skaits		4
Reģistrēto un uzturēto patentu skaits		1

LU FI nodrošina institūta darbības nepārtrauktību, balstoties uz iespējamo risku apzināšanu sekojošās sadaļās, bet jo īpašu vērību pievēršot personāla atjaunināšanai un darbinieku kvalifikācijas paaugstināšanai (cilvēku kapitāla riski), finanšu disciplīnas un likumības ievērošanai (finanšu un juridiskie riski), kā arī kvalitatīvai publisko pakalpojumu sniegšanai (darbības riski). Darbības risku pārvaldīšanai LU FI atspoguļo rīcības plānā.



LU FI nodrošina risku identificēšanu un to pārvaldību saskaņā ar sekojoš plānu.

Kārtas Nr.	Darbības raksturojums	Izpildes termiņš vai pasākuma biežums
1.	Darba grupas izveide riska faktoru identificēšanai un novērtēšanai LU FI	2. kvartāls
2.	LU FI riska pārvaldības politikas dokumenta izstrāde	2. kvartāls
3.	Pasākumu plāna izstrāde riska faktoru mazināšanai	2.kvartāls
4.	LU FI datu drošības politikas dokumenta uzlabošana	3.kvartāls
4.	Iekšējās kontroles politika dokumenta uzlabošana	3.kvartāls
5.	Riska faktoru pārvērtēšana un pasākumu plāna korekcija 2009.gadam	4.kvartāls

## LU Fizikas institūta izpildītie projekti

### 6.Ietvara programmas

Magnetic flow tomography in technology geophysics and ocean flow research MAGFLOTOM	Commission of the EC Research DG	Contract No.028670 Specific target project
<b><i>Preparation of a gallium jet limiter for testing under reactor relevant conditions</i></b>	Fixed contribution contract with EURATOM EC 6 Framework Programm-	<b>FU07-CT-2007-00047,</b>
European Isotope Separation On-Line Radiactive Ion Beam facility (EURISOL DS)	EC 6 Framework Programm	Contract 515768 (RIDS)
Virtual European Lead Laboratory (Vella)	EC 6FP: Contract type: Integrating activities implemented as integrated Infrastructure activities	Project reference 36469. NUWASTE-2005/6-3.2.3.1-1 2006.10.01-2009.09.30

### ERAF projekti

Reģistrācijas nr.	Nosaukums	Vadītājs	Īstenošan as periods
Nr.VPD1/ERAFF /CFLA/05/APK /2.5.1./000004/004	“MHD tehnoloģija svina-litija eitektiska sakausējuma iegūšanai un pielietošanai kodolsintēzes reaktoru sistēmās”.	J.Freibergs E.Platacis	2006-2008
VPD1/ERAFF /CFLA/05/APK /2.5.1./000002/002	Ferītu nanodaliņas un koloīdi termomagnētiskās dzesēšanas sistēmām un audu hipertermijai” .	E.Blūms	2006-2008
VPD1/ERAFF /CFLA/05/APK /2.5.1./000001/001	Koksnes biomasas vietējo resursu racionāla izmantošana siltuma ražošanai kombinētā koksnes un gāzveida kurināmā degšanas procesā	M.Zaķe	2006-2008
.VPD1/ERAFF/CFL A/08/NP/2.5.2./000 I/000012/038	“Latvijas Universitātes Fizikas institūta ēkas iekštelpu renovācija”	J.Freibergs	2008

**Institūtā 2008.gadā realizētas 1 valsts pētījumu programmas projekts un 3 sadarbības projekti**

<b>Reģistrācijas numurs</b>	<b>Nosaukums</b>	<b>Vadītājs</b>
Valsts pētījumu programma 1-23/49 1-23/37  Projekts 5	<p>Modernu funkcionālu 8 mikroelektronikai, nanoelektronikai, fotonikai, bi-omedicīnai un konstruktīvo kompozītu, kā arī to atbilstošo tehnoloģiju izstrāde</p> <p>Nanodaļiņu, nanostrukturālu materiālu un plāno tehnoloģiju izstrāde funkcionālo materiālu un kompozītu izveidei</p> <p style="text-align: center;"><b>1. vadītājs Dr.hab.phys. E.Blūms</b></p> <p><b>Rezultāti</b></p> <p>Veikti siltuma un masas pārneses un konvekcijas pētījumi ferrokoloīdos, noskaidrotas jaunas magnētisko nanodaļiņu pārneses parādības neizotermiskās kapilāri porainās vidēs un iegūti jauni rezultāti par magnētiskā lauka enerģijas disipāciju nanokoloīdos ar Brauna tipa relaksāciju. Publicēti 13 darbi SCI žurnālos un recenzētos rakstu krājumos, nolasīti 11 referāti starptautiskās konferencēs.</p> <p style="text-align: center;"><b>2. vadītājs Dr.hab.phys. A.Cēbers</b></p> <p>2008 g. Pirmoreiz pasaulei sintezēti lokani feromagnētiski filamenti un eksperimentāli apstiprināta teorētiski paredzētā filamentu anomālā orientācija mainīgā magnētiskā laukā (Publ. : 1.K.Ērglis, M.Belovs, A.Cēbers. Flexible ferromagnetic filaments and the interface with biology. Moscow International Symposium on Magnetism, Book of Abstracts, Moscow , P.238, 2008. 2.K.Ērglis, M.Belovs, A.Cēbers. Flexible ferromagnetic filaments and the interface with biology. Journal of Magnetism and Magnetic Materials – 2009, v.321, P.650-654.) .</p>	E.Blūms E. Cēbers
Sadarbības projekti 1.Nanomateriāli un nanotehnoloģija  2.06.0029.2.09	<p>Mīkstie magnētiskie materiāli un nanotehnoloģijas</p> <p>Difūzā un konvektīvā nanodaļiņu pārneses neizometriskos ferrokoloīdos kapilāri porainās vidēs</p> <p>MHD metodes dispersās fāzes sadalīšanai un homogenizācijai kompozītos ar metālisku matricu</p>	A.Cēbers  E.Blūms  J.Gelfgats

## Institūtā 2008.gadā īstenoti 11 Latvijas Zinātnes padomes finansētie projekti

**Bucenieks I. 05.1466 Aprēķinu metožu un izgatavošanas tehnoloģijas modernizācija elektromagnētisko sūkņu sistēmām šķidrā metāla neitronu atskaldīšanas iekārtās**

Saskaņā ar projekta uzstādītiem mērķiem un uzdevumiem projekta izpildes laika posmā 2005. – 2008. tika veikti teorētiskie un eksperimentalie pētījumi lai izstrādātu specializētas aprēķinu metodes lai modernizētu aprēķinu metodes un izgatavošanas tehnoloģijas elektromagnētisko sūkņu sistēmām šķidrā metāla neitronu atskaldīšanas iekārtās, nesmot vērā smagos specifiskos darba apstakļus, tādus kā radiācija, augstas darba temperatūras, pulsējošu (laikā mainīgu) darba režīmu ar mainīgu slodzi un plāšā elektromagnētisko indukcijas sūkņu operatīvo parametru diapazonā ažādiem šķidriem metāliem.

Konkrēti ir ir paveikti sekojoši darba uzdevumi:

- 3-fāzu elektrisko ķēžu ar nelieneāriem elementiem modelēšana;
- Magnētisko procesu modelēšana skidros metālos, sūkņu kanālu sienās, primārajā elektromagnētiskajā ķēdē (induktorā);
- Siltumpārneses dināmisko procesu modelēšana šādās sistēmās: šķidrais metāls – konstrukcijas siltumu ģenerējošie elementi – siltumu vadošie elementi, kā arī siltuma lauka noteikšana elektromagnētisko sūkņu konstruktīvos elementos;
- Mehānisko spriegumu modelēšana pie lieliem temperatūras gradientiem elektromagnētisko sūkņu konstruktīvos elementos pulsējošos/laikā mainīgos darba režīmos.

### Zinātniskā sadarbība:

Projektā realizējami pētījumi ir iekļauti LU Fizikas institūta starptautiskajos projektos un programmās, kas ir saistīti ar elektromagnētisko sūkņu sistēmu izstrādāšanu atskaldīto neitronu un transmutācijas (ADS – Acceleration Driven System) iekārtām (sadarbībā ar ENEA, Itālija), MEGAPIE sistēmā un rojekta EURISOL ietvaros (sadarbībā ar Paula Šērera Institūtu, Šveice), kā arī ar Los Alamos National Laboratory (LANL, ASV).

Robežslāņu teorija attīstās jau 100 gadus, bet līdz šim brīdim nav zaudējusi savu aktualitāti. Šis teorijas pielietošanas rezultāti dod iespēju noteikt svarīgus hidrodinamisko un magnetohidrodinamisko iekārtu parametrus: spiediena gradientu, patēriņu, berzes koeficientus u. tml. Bet katra šis teorijas uzdevuma risināšana sākas ar diezgan sarežģītu Navjē-Stoksa-Maksvela vienādojumu pārveidošanu.

Kā pieradīts prof. E. Ščerbiņina darbos, īstenībā visus robežslāņu teorijas uzdevumus var aprakstīt ar vienu vienādojumu sistēmu, kurā atkarībā no konkrētā uzdevuma nosacījumiem mainās tikai daži koeficienti. Tās nozīme, ka nav nepieciešamības veikt Navjē-Stoksa-Maksvela vienādojumu pārveidojumus katru reizi, pietiek tikai izanalizēt uzdevuma īpašības, noteikt vienādojumu koeficientus un var risināt iegūtu sistēmu. Bez tam, prof. E. Ščerbinina piedāvāta vispārējās teorijas uzbūves koncepcija ļauj noteikt dažus uzdevuma parametrus nerisinot šo sistēmu.

Iepriekšējā projekta ietvaros (projekta Nr. 01.0156) tika apskatīta vispārējās teorijas pielietošana Dekarta un polārajā koordinātu sistēmās gan parastajā hidrodinamikā, gan magnetohidrodinamikā. Arī tika izanalizēta siltuma un piesārņojuma pārnese. Iegūtie rezultāti tika publicēti gan žurnālā „Magneto hydrodynamics”, gan referēti starptautiskajos konferences. Kā projekta izpildes sasniegumu atskaite ar Latvijas Universitātes Fizikas Institūta palīdzību tika izdota monogrāfija “Automodulārā robežslāņa teorija hidrodinamikā un magnētiskā hidrodinamikā. I daļa. Plakanas plūsmas”. Šī grāmata var būt noderīga gan speciālistiem, gan attiecīgo specialitāšu augstskolu studentiem. Izstrādāto vispārējo teoriju var izmantot konstruējot dažādas MHD iekārtas, tai skaitā sūkņus, patēriņa mērītājus, maisīšanas ierīces utt..

Dotā projekta ietvaros pabeigts darbs pie vispārējas teorijas otras daļas – aksiāli simetrisko plūsmu pētīšanas.

2005. gadā pētīti eksaktie aksiāli simetriskie risinājumi hidrodinamikā. Tā kā tie ir ļoti cieši saistīti ar robežslāņa tipa risinājumiem un tāda paša veida risinājumiem magnētiskajā hidrodinamikā, tad vienlaikus tika pētīti arī šo veidu risinājumi. Tika noteikti eksakto risinājumu veidi katrā gadījuma, noteikts iespējamo uzdevumu loks atrisināšanai. Tika noteikti nosacījumi eksakto risinājumu pārveidošanai uz robežslāņa tipa atrisinājumiem un ar to saistīti efekti.

2006. gadā pabeigta 2005. gadā iegūto rezultātu noformēšana: aksiāli simetriskas plūsmas hidrodinamikā; precīzie atrisinājumi aksiāli simetriskām plūsmām hidrodinamikā. Uzsākta aksiāli simetrisko plūsmu magnetohidrodinamikā pētīšana un uzdevumu formulēšana un risināšana;

2007. gadā pabeigta 2006. gadā iegūto rezultātu noformēšana: aksiāli simetrisko plūsmu magnetohidrodinamikā izpēte un uzdevumu risināšana. Uzsākta elektrovirpuļu plūsmu un to risinājumi sfēriskajā koordinātu sistēmā izpēte, kā arī uzdevumu formulēšana un risināšana šajos sadaļās.

2008. gadā pabeigta 2007. gadā iegūto rezultātu noformēšana: elektrovirpuļu plūsmas un to risinājumi sfēriskajā koordinātu sistēmā. Pabeigta plūsmu pētīšana cilindriskajā koordinātu sistēmā, atrisināti daži uzdevumi. Pabeigti pētījumi sfēriskajā koordinātu sistēmā, noformēti iegūtie rezultāti.

Palieki pilnīgi pabeigt iegūto rezultātu noformēšanu un monogrāfijas

datorsalikumu. Šī monogrāfija varēs būt noderīga studentiem, kuri studē šķidruma un gāzu mehānikas specialitātē, lai apgūtu robežslāņu metodi, kā risināt un analizēt automodulārus uzdevumus un uzdevumus robežslāņa tuvinājumā, ka arī visiem, kas interesējas par šo nozari.

Darba gaitā daudz laika prasīja skaitliskie aprēķini un rezultātu analīze, kā arī informācijas atlase.

Monogrāfijā iekļauti materiāli, kas tika iegūti V. Kremeņecka disertācijas "Precīzi automodelāri risinājumi hidrodinamikā un magnetohidrodinamikā un to sakars ar uzdevumiem robežslāņa tuvinājumā" izstrādes gaitā. Disertāciju plānots aizstāvēt 2009. gadā.

Darba rezultāti tika pielietoti svina – litija eitektiskā sakausējuma ražošanas reaktora ar elektromagnētisko induktoru kā maisītāju, optimālas formas izveidei.

#### **Gailītis A. Sfēriska MHD Dinamo eksperimenta izveide 05.1388**

Intensīvi maisot lielu tilpumu labi elektrovadoša šķidruma (arī gāzes), tas magnētizējas. Spontāni rodas magnētiskais lauks itkā no nekā. Tā magnētizējusies Zeme, Saule, zvaigznes un galaktikas. Līdz mūsu 1999.g. 11. nov. eksperimentam šis, dabā tik plaši izplatītais process, uz Zemes virsas nebija novērots. Iemesls eksperimenta izmērā – pat no vislabākā šķidrā elektrovadītāja (Na) vajadzīgi vairāki kubikmetri un tad vēl daži simti kW jaudas tā maišanai.

Darba plāns paredzēja divus pamatdarbus. Pirmais – pilnveidojot esošo eksperimentalo iekārtu izpētīt parādību pēc iespējas sīkāk. Otrs – pētīt iespējas nākošam eksperimentam citā ģeometrijā, tuvākā tai, kas vairumā astrofizikālo objektu.

Pirmais uzdevums sekmīgi veikts. Iekārta ievērojami papildināta. Uzstādīts ar mūsu līdzdalību Francijā gatavots magnētiskais sajūgs, kas nodrošina pilnīgu ierīces hermētiskumu. Eksperiments aprīkots ar diviem manipulātoriem, kas pārvieto magnētiskā lauka trīskomponentu sensorus gan gar iekārtu un gan pa kanālu šķērsu tai. Iegādāta daudz precīzāka mēraparātūra. Iegūti detalizēti lauka gareniskie un šķērsprofilī. Iegūti detalizēti magnētiskā lauka frekvenču spektri. Novērota lauka atpakaļiedarbība uz nātrija plūsmu. Precīzēts parādības datormodelis.

Iespējamam nākošam eksperimentam izveidots samazināts ūdens modelis. Plūsmas sadalījums tajā mērīts ar lāzera-Doplera-anemometru. Atrastais ātrumu sadalījums likts lauka ģenerācijas datormodelī. Datorsimulācija vēl gan nav devusi pilnu pārliecību, ka burtiski šāds Na eksperiments būtu perspektīvākais.

Darba rezultāti publicēti 6 rakstos un izklāstīti virknē starptautisku konferenču.

Starptautiskā sabiedrība joprojām nav zaudējusi interesi par MHD dinamo problēmu. Par to, starp citu, liecina 2007.g. saņemtais Francijas Goda Legiona virsnieka ordenis.

#### **Gelfgats J. Liela apjoma šķidras elektrovadošas vides stacionāras un nestacionāras kustības ierosināšanas un slāpēšanas MHD metožu fizikālās likumsakarības 05.1378**

##### **Galvenie rezultāti.**

1. Izstrādāti oriģināli MHD ierīču konstrukcijas risinājumi izmantojot pastāvīgos cilindriskos magnētus, kuri nomagnetizēti diametrālā virzienā un inducē šķidrā metālā plūsmas ar ievērojami lielāku ātrumu. Noteikti šo plūsmu intensitātes kritēriji. Noteiktas likumsakarības starp plūsmas ātrumu un pastāvīgo cilindrisl

magnētu skaitu, attālumu starp magnētiem un blakus esošo cilindrisko magnētu magnetizācijas vektoru leņķi (J.Gelfgats, A.Bojarevičs).



Šķidra metāla kustība magnētiskā rotorā

- a)metāla virsma tālu no rotora,
- b) metāla virsma tuvu rotoram

2. Ar matemātiskās modelēšanas metodēm izpētītas plūsmu hidrodinamiskās struktūras cilindriskā bezserdes indukcijas sūkņa kanālā. Parādīts, ka izejot plūsmai no MHD iedarbības zonas, plūsmas maksimālais ātrums cilindriskā kanālā tuvojas cilindra asij (M.Abricka, J.Krūmiņš).
3. Eksperimentāli pierādīts, ka izmērot termoelektromagnētisko plūsmu ātrumu, var noteikt termoEDS lielumu šķidru metālu kausējumos. Izstrādāta ierīce un mērišanas metodika termoEDS noteikšanai dažāda sastāva kausējumos (A.Bojarevičs, I.Kaldre).

**Valdmanis J.. 04.1111** *Elektriskas un magnētiskas iedarbes procesu vadība izkausēta metāla un cietas metāliskas sieniņas robežapgabalā*

Projekta vispārīgais mērķis bija noskaidrot galvenās likumsakarības, kas nosaka cietā un šķidrā metāla robežvirsmas attīstības dinamiku ārēju iedarbību apstākļos. Ārējā iedarbe realizējās caur elektromagnētisko lauku. Iedarbes procesa izpete tika veikta ar mērķi ietekmēt attīstību vēlāmā virzienā kā arī optimizēt elektromagnētiskā lauka nepieciešamos avotus.

Veikta literatūras analīze par elektriskām un magnētiskā lauka iedarbēm, lai

vadītu metāla kristalizācijas un dažus citus fizikālus procesus divfāzu sistēmās. Izdarīts secinājums, ka īpaši aktuāli un interesanti ir plānotie eksperimenti ar noteiktā virzienā orientētas elektriskās strāvas izmantošanu, lai ietekmētu metālu sacietēšanas procesa gaitu un rezultātus.

Izprojektēta un izveidota atbilstoša eksperimentāla iekārta, kurā nelielā konteinerā ar sieniņām no elektrību nevadoša materiāla izkausē termoelektriski aktīvus metālus ( piem. bismutu ) 10 mm biezā slānī un rada apstākļus konteinerā garenvirzienā orientētai metāla cietās fāzes augšanai. Vienlaicīgi šai virzienā caur šķidro un sacietējušo metālu tiek laista līdzstrāva, pētot ar to saistītās izmaiņas kristalizācijas procesa norisē. Metāla sacietēšanas gaitu fiksē ar termopāriem, bet termoelektriskās strāvas , kas varētu veidoties metāla nehomogēnos apgabalos, ar speciāliem sensoriem, novietotiem gar cietās fāzes augšanas virzienu.

Realizēts eksperiments, novērtējot termoelektriskos efektus metāliskā (duralumīnija vai nerūsējošā tērauda) plāksnītē, kam lokālā vietā bija sabojāta struktūra – apm.  $2\text{cm}^2$  tās virsmas apgabals iepriekš bija pakļauts metināšanai. Plāksnīti uzgarsēja līdz  $300^\circ\text{C}$  un pēc tam, kad uz deformācijas robežas bija uzpilināts nedaudz ūdens, ar ātrumu  $10\text{ cm/s}$  vilka (pa sliedītēm) gar sensoru termoelektrisko strāvu magnētiskā lauka mērišanai. Tika konstatēts, ka rajonā ap metinājuma vietu veidojas palielu termoelektrisko strāvu kontūri – fiksēti asi strāvas magnētiskā lauka pīki un maksimālās lauka vērtības  $5\text{-}10\text{ mT}$ . Šāda termoelektriskā efekta cēlonis viennozīmīgi ir metāla nehomogenitāte un ar to saistītie mehāniskie spriegumi, jo plāksnītes ķīmiskais sastāvs visā tās tilpumā bija vienāds, metināšanai izmantoja to pašu materiālu ( t.i. duralumīniju vai nerūsējošo tēraudu ).

Realizēts eksperiments, novērtējot termoelektriskos efektus metāliskā (duralumīnija vai nerūsējošā tērauda) plāksnītē, kam lokālā vietā bija sabojāta struktūra – apm.  $2\text{cm}^2$  tās virsmas apgabals iepriekš bija pakļauts metināšanai. Plāksnīti uzgarsēja līdz  $300^\circ\text{C}$  un pēc tam, kad uz deformācijas robežas bija uzpilināts nedaudz ūdens, ar ātrumu  $10\text{ cm/s}$  vilka (pa sliedītēm) gar sensoru termoelektrisko strāvu magnētiskā lauka mērišanai. Tika konstatēts, ka rajonā ap metinājuma vietu veidojas palielu termoelektrisko strāvu kontūri – fiksēti asi strāvas magnētiskā lauka pīki un maksimālās lauka vērtības.

$5\text{-}10\text{ mT}$ . Šāda termoelektriskā efekta cēlonis viennozīmīgi ir metāla nehomogenitāte un ar to saistītie mehāniskie spriegumi, jo plāksnītes ķīmiskais sastāvs visā tās tilpumā bija vienāds, metināšanai izmantoja to pašu materiālu ( t.i. duralumīniju vai nerūsējošo tēraudu ).

Veikti arī eksperimenti, kuros realizēja mainīga magnētiskā lauka iedarbību uz svina-litija eitektiskā sakausējuma  $\text{Pb}15.8\text{Li}$  veidošanās procesu (šāds sakausējums vajadzīgs kodoltermiskās sintēzes reaktoru izstrādei, ar to saistītiem pētījumiem).  $\text{Pb}15.8\text{Li}$  iegūšana notika cilindriskā kristalizātorā, tanī vispirms izkausēja svinu un pēc tam šķidrā svina tilpumā ievadīja vajadzīgo litija daudzumu. Lai realizētu magnētiskā lauka iedarbību, kristalizātors bija ievietots cilindriskā trīsfāzu MHD induktoriā [1,2].

Pētīts elektromagnētiskā lauka (EM) iespaids uz kristalizējošo metālu un to sakausējumiem ar mērķi optimizēt kristalizēšanas procesa norisi. Kā eksperimentāls modelis izvēlēts bismuts, kura termoelektriskās īpašības cietā un šķidrā stāvoklī ir stingri atšķirīgas. Kā EM lauka iedarbes faktors izmantota pastāvīgas strāvas plūsma, kas pēc teorētiskiem novērtējumiem, plūstot cauri perpendikulāri kristalizācijas frontei, var izmainīt kristalizācijas ātrumu. Izgatavoti vairāki modeļi, kuros pētītas kristalizācijas ātruma izmaiņas , laižot cauri elektrisko strāvu. Konstatēta kristalizācijas ātruma atkarība no strāvas virziena. Eksperimentalī

apstiprinājās iespēja, izvēlotos noteiktu strāva stiprumu , palielinat kristalizācijas ātrumu tīra bismuta gadījumā. Svinga bismuta sakausējumam eitektiskā punkta tuvumā efekts ir mazāks , jo svinam termoelektriskās īpašības ir būtiski atšķirīgas no bismuta.

Pētījuma rezultāti apkopoti referatā, kas iesniegts konferencē ” Modelling for Material Processing 2006” Rīgā [3].

Izprojektēta un uzņemta jauna uzlabota eksperimentālā iekārta, kurā realizēs eksperimentus ar mainīga magnētiskā lauka iedarbību uz svina-litija eitektiskā sakausējuma Pb15.8Li veidošanās procesu (šāds sakausējums vajadzīgs kodoltermiskās sintēzes reaktoru izstrādei, ar to saistītiem pētījumiem). Ar jaunā iekārtu iegātas daudz lielākās porcijās eitektiskā sakausējuma (apm. 70 kg katrā). Abu komponenšu (Pb un Li) samaisīšanu realizē, izmantojot plakanu trīsfāzu MHD induktoru, īpaša vērība veltīta sistēmai, kas šķidro litiju ļoti pakāpeniski, pilienu pa pilienam, ievada izkausētā un ar elektromagnētisko lauku nepārtraukti maisītā svina tilpumā [4].

Fizikālie procesi uz šķidra - cieta metāla robežvirsmas ir daudzveidīgi i. Tie regulē jaunas fāzes daļiņu rašanos (metāla kristalizācija, adsorbcijas slāniša veidošanās uz cetas virsmas un arī pretēji procesi - kausēšana , desorbcija vai cetas virsmas šķīdināšana intensīvas kausējuma kustības rezultātā), šīs fāzes attīstību un īpašības. Pētījumi par elektriskām un magnētiskām iedarbēm radija plašāku izpratni virsmas , kristalizācijas un difūzijas parādībām un reizē lāva precīzāk apzināt iespējas, kādas šo parādību ietekmēšanai un vadībai varētu dot ārēju elektromagnētisko spēku izmantošana.

Ārējā elektromagnētiskā lauka iedarbes rezultātā izraisītās izmaiņas vielā var izmantot nosakot dzelzi saturošo konstrukciju mehāniskos spriegumus. Veikti eksperimenti, kas ļauj rast teorētisko bāzi praktisko pielietojumu izstrādei.

Ar mērķi optimizēt elektromagnētisko iedarbi, veikti pētījumi jauno metamateriālu īpašību izpausmē radiofrekvenču un zemo frekvenču diapazonā. Pētījumos noskaidrotas atsevišķu elementu, kā arī divu un vairāku elementu sadarbības izraisītie efekti. Diviem identiskiem elementiem sadarbojoties rodas divas atšķirīgas rezonances frekvences. Trīs elementiem attiecīgi trīs frekvences u.t.t. Teorētiskā ziņā rezultātus var aprakstīt ar oscilātoru sadarbības modeli. Konstatēts, ka bez pametfrekvenčēm modeļos ierosinās arī augstākie toņi, kas pēc intensitātes ir mazāk izteikti. Eksperimentāli pierādīts, ka metamateriāla atsevišķu modeli ar rezonances atbildi uz ārējo iedarbi var radīt arī 50 Hz frekveces diapazonā. Izteikta hipoteze, ka līdzīgā veidā varētu ģenerēties elektriskie potenciāli dzīvos organismos (encefalogrammas, miogrammas un t.t.). Rezultāti ziņoti vairakās konferencēs un publicēti [5-7].

Izdarīti pētījumi arī par iespējām rezonances procesus pielietot augstsprieguma radīšanai. Eksperimentāli pierādīts, ka augstsprieguma laukā var panākt situāciju, kad uz metāla elektroda izlādes procesa veidojas stabils šķidra metāla slānis. Efekti pārbaudīti gadījumos, kad elektrodi veidotī no dažādiem metāliem. Šos rezultātus paredzēts izmantot projekta pieteikumā ESF finansējumam, kas ļautu uzlabot konkrētus tehnoloģiskos procesus , pielietojot elektromagnētiskā lauka iedarbi.

**Koļesņikovs Konvektīvās un nobīdes šķidrā metāla plūsmas regulešana ar elektromagnētiskiem masas spēkiem**  
**J.**  
**05.1379**

2005. – 2008. g. tika piedāvāti pētījumi:

Dažāda veida magnētisko nevienmērību formēšana kanālā ar šķidru metālu. Parādību pētišana sarežģītas konfigurācijas magnētisko lauku iedarbībai uz šķidrā metāla plūsmu kanālā. Eksperimentālas datu bāzes iegūšana procesu skaitliskajai modelēšanai.

(Kopā ar Ilmenau Universitāti, Vācija)

Projektā galvenā uzmanība tika koncentrēta uz eksperimentāliem pētījumiem.

- Noskaidrota nehomogēna un perpendikulāri pret plūsmu orientēta magnētiskā lauka ietekme uz vadoša šķidruma plūsmu kanālā (dotajā eksperimenta prototips – šķidrā metāla plūsmu elektromagnētiskā vadīšana metalurgiskos procesos);
- Noteikti galvenie raksturojošie parametri, kas nosaka vadošā šķidruma nobīdes plūsmu veidošanos nehomogenā magnētiskā laukā.
- Tika uzbūvēta noslēgta cilpa ar elektromagnētisko sūkni šķidram metālam gālijs-indijs-alva (InGaSn) un eksperimentālais kanāls elektrisko potenciālu mērišanai.

Parametru novērtēšana rāda, ka elektriski vadošā šķidruma turbulentās strūklas veida plūsmas izplatīšanās ceļa garums samazinās šai plūsmai šķērsojot uzlikta ārējā magnētiskā lauka. Tas notiek plūsmas elektromagnētiskās bremzēšanas dēļ uz ass pateicoties Lorentza spēka rašanās rezultātā. Uzdevuma parametrs tika noteikts ar attiecību starp plūsmas ātrumu un magnētiskā lauka formu un intensitāti.

Dotajā projekta izpildē ņema dalību trīs LU fizikas specialitātes maģistranti. Tika izplānota šo maģistrantu piedalīšanās pētījumu metodikas izstrādē, fundamentālo eksperimentālo un modelējošo skaitlisko pētījumu veikšanā. Izpētīta šķidro vadošo plūsmu hidrodināmika un siltuma pārnese ārējo masas spēku iedarbības rezultātā. Studenti ir iepazīstināti ar praktiskām izstrādnēm, kurās tiek izmantota magnētiskā lauka iedarbība uz turbulentām un konvektīvām siltuma plūsmām, kas nodrošinā šo studentu redzesloka paplašināšanos un zināšanu līmeņa celšanos. Saistībā ar dotā projekta tēmu LU FI sadarbojās ar Zinātnisko centru Grenoblē.

Sadarbība ar vairākām organizācijām Latvijā un ārzemēs:

**A.** Saistībā ar dotā projekta tēmu LU FI sadarbībā ar Zinātnisko centru Grenoble (Francija), IFSW Stuttgart Universitāti (Vācija), FEP Dresden (Vācija), ALD Vacuum Technology, Hanau (Vācija), Coventry Universitāti (Anglija).

**B.** Dotā projekta vadītājs piedālās kā eksperts divās Eiropas darba grupās: the Work Group / High Magnetic Fields / within the European COST Action P17 “Magnetofluiddynamics”.

**Lielausis O. Šķidrs metāls kā darba ķermenis plazmas ierobežotājos un korpuskulāro plūsmu pārveidotājos**  
**05.1380**

[MHD mijiedarbe ir galvenais šķērslis, kas traucē plaši pielietot šķidru metālu 'okamak tipa iekārtu plazmas ierobežotājos jeb limiteros. Tieki izmēģināti varianti ar raktiski nekustīgu darba ķermenī, piemēram, kad šķidro metālu plazmai tuvina

apilārie spēki. Slikti tas, ka tādos gadījumos gan termiskā enerģija, gan iemaisījumi, kas deponējas limiterā, netiek no izlādes kameras izvadīti. Dotajā ētījumā limiteru veido ātra ( $v > 2 \text{ m/s}$ ), tieva ( $d < 3 \text{ mm}$ ) šķidra gallija strūkla. Lai iazinātu MHD mijiedarbi paredzēts, ka Releja nestabilitātes rezultātā pēc saskares ar lazmu strūkla sadalās pilienos. Pētījumā piedāvāta izteiksme strūklas relatīvā abrukšanas garuma atkarībai no Vēbera skaitļa šķidra metāla gadījumā, apkopojot iēriņumu rezultātus ar Hg, InGaSn un Ga:  $L/d = 4.2 Wb^{1/2}$ . Aprakstīts arī, kā stiprs iagnētisks šķērslauks stabilizē strūklu, palielinot tās sabrukšanas garumu:  $L/L_0 = +0,75 Ha^{0,33} Re^{-0,25}$ , kur Ha un Re ir Hartmaņa un Reinoldsa skaitļi. Atbilstošajos iēriņumos magnētiskais lauks sasniedza vērtības 5,6 T. Dots pētījums cieši saistīts r sekojošu EFDA uzdevumu Asociācijas EURATOM-LU ietvaros: *Ga strūklas mitera koncepcijas pārbaude Tokamakā ISTTOK*. Atbilstošie rezultāti apkopoti ivās publikācijās: *First results of the testing of the liquid gallium jet limiter concept on ISTTOK*, R.B.Gomes et al., AIP Conf.Proc. 875 (2006) 66-71 un *Interaction of a quid gallium jet with the Tokamak ISTTOK edge plasma*. R.B Gomes et al., Fusion Engineering and Design, 83 (2008) 102-111. Parakstīts trīspusīgs līgums par gallija mitera pārbaudi ENEA/Frascati (Itālija) Tokamakā FTU (Frascati Tokamak Upgrade). Būtiski, ka gan magnētiskais lauks, gan pirmās sienas slodzes šīnī iekārtā iu sasniedz reālam reaktoram raksturīgas vērtības.

Šķidrs metāls kā darba ķermenīs/mērkis neitronu atskaldīšanai augstas energijas orpuskulu plūsmās, tā ir viena no aktualitātēm šķidra metāla tehnoloģijās. Dotajā ētījumā tika veikta potenciālā pieprasījuma un institūta iespēju analīze. Var teikt, ka iš bija pamats nopietnam panākumam, institūta personā LU iekļauta nozīmīgā eptītās ietvarprogrammas Lielo pētniecisko kompleksu attīstības projektā- *Eiropas tskaldīto Neutronu Avots ESS*. Vairumā gadījumu (arī ESS) paredzēts protonus  $\pm$ starot smaga metāla, Hg vai PbBi, mērķī. Institūta aprīkojums un pieredze darbā ar šķidru litiju ļauj domāt arī par piedalīšanos nozīmīgajā IFMIF (International Fusion Material Irradiation Facility) programmā. Te, iestarojot ātrā ( $v > 25 \text{ m/s}$ ) litija plūsmā eitronus, paredzēts ģenerēt sintēzei raksturīgos 14 MeV neitronus ar reālam reaktoram raksturīgo intensitāti, gan nelielā, tikai aptuveni  $300 \text{ cm}^3$  tilpumā. Dotā ētījuma ietvaros sākta piedāvājuma formēšana līdzdalībai minētajā programmā.

**Grants I.  
05.1465 Nestabilitātes un pāreja uz turbulenci elektrovadošo šķidrumu plūsmās ārējos magnētiskajos laukos**

Izpētīti nosacījumi skrejoša magnētiskā lauka parametriem, kas nepieciešami, lai izmainītu kausējuma plūsmas virzienu virs ieliktas sacietēšanas frontes VGF (*Vertical gradient freeze*) kristālu audzēšanas procesos. Šāda ietekme lietderīga piemaisījumu radiālās segregācijas samazināšanai nelīela izmēra pusvadītāju monokristālu ražošanā. Pētījumi aptver plašu vadošo parametru intervālu, kas ļauj pielietot rezultātus dažādiem procesiem. Atklāts, ka dabiskā konvekcija ierosina automodulāru robežslāņa tipa plūsmu virs kristalizācijas frontes ar netriviālu atkarību no Grashofa un Prandtlā skaitļiem. Neskatotoies uz to, nepieciešamā skrejošā lauka intensitāte dabiskās plūsmas pagriešanai pretējā virzienā ir proporcionāla vienkārši Grashofa skaitļa un frontes ieliekuma dzīluma reizinājumam. Pētījumu rezultāti publicēti žurnālā *Journal of Crystal Growth*.

Turpinot augstākminētos pētījumus veikta skrejošā magnētiskā lauka ierosinātas plūsmas skaitliska stabilitātes analīze kristālaudzēšanas procesos ar VGF metodi. Noskaidrots, ka gadījumā, ja lauks tiek izmantots radiālās piemaisījumu

segregācijas samazināšanai, tad plūsma praktiski vienmēr paliek stabila. Skrejošais lauks var tikt izmantots arī cita mērķa sasniegšanai – kristalizācijas frontes ieliekuma samazināšanai. Šim nolūkam pielietojams lejup vērstīgais skrejošais magnētiskais lauks. Noskaidrots, ka izteikts šāda veida efekts ir savienojams ar plūsmas stabilitāti, ja audzējamā kristāla radiuss pārsniedz noteiktu lielumu. VGF procesam raksturīga stabila kausējuma vertikālā stratifikācija. Šāds temperatūras gradients ievērojami bremzē un stabilizē plūsmu. Stabilitātes analīze veikta plašam vadošo parametru intervālam. Novērotas vairākas interesantas parādības – zemkritiskā nestabilitāte, "stabilitātes salu" veidošanās. Skaitlisko pētījumu rezultāti daļēji pārbaudīti eksperimentā. Pētījumu rezultāti sagatavoti publikācijai žurnālā *Journal of Crystal Growth*.

Projekta pieteikumā plānotie darba uzdevumi pamatā ir izpildīti. Papildus projekta iesniegumā paredzētajam, veikti eksperimenti ar magnētisko tilpumpspēku ierosinātu virpulplūsmu šķidra metāla cilindrā. Pētījumu mērķis bija noskaidrot nosacījumus, pie kādiem veidojas intensīvs koncentrēts virpulis, kā arī šāda virpuļa raksturīgās īpašības. Eksperimentā novēroti trīs režīmi: (1) koncentrēts virpulis; (2) iekšēja kodola veidošanās; (3) meridionālās plūsmas apspiešana. Pirmajos divos režīmos novērotas vairākas līdzības ar atmosfēras virpuļiem: (1) virpuļa intensitāti nosaka meridionālās plūsmas avota intensitāte; (2) virpuļa struktūru nosaka leņķiskā momenta un meridionālās plūsmas avotu attiecība; (3) Plūsmas iekšējā kodolā meridionālā plūsma maina virzienu līdzīgi kā orkāna "acī". Magnētisko spēku izmantošana būtiski papildina iepriekš izmantotos atmosfēras virpuļu modeļus ar to, ka šie spēki principā ir neatkarīgi no plūsmas. Turklat, divu savstarpēji neatkarīgu magnētisko spēku izmantošana ļauj samērot abas virpuļa pastāvēšanai nepieciešamās komponentes – meridionālo un azimutālo. Eksperimentā parādīts, ka azimutālam spēkam ir sviras daba – salīdzinoši ļoti vājš azimutāls spēks var būtiski izmaiņt virpuļa struktūru. Pētījumu rezultāti publicēti žurnālā *Journal of Fluid Mechanics*.

**Šīško A.**

**05.1382**

***Stipra magnētiskā lauka iespaids uz elektrovadošas šķidrās un cietās vides mijiedarbības procesiem***

Institūtā tika veikti eksperimentāli pētījumi par magnētiskā lauka iespaidu uz mijiedarbību starp eutektikas Pb<sub>17</sub>Li plūsmu un EUROFER tēraudu. EUROFER tērauds tika uzskatīts kā viens no iespējamiem konstruktīviem materiāliem blanketa HCLL ITER-FEAT radīšanai. Šāda veida korozijas pētījumi tika iesākti Asociācijas kontrakta Nr. FU05-CT-2004-0078 starp EURATOM un Latvijas universitāti ietvaros, cieši sadarbojoties ar Cietvielu Fizikas Institūtu un Forschungszentrum Karlsruhe Institut fur Materialforschung.

Sie, un turpmāk veiktie eksperimenti, parādīja būtisku magnētiskā lauka iespaidu uz korozijas procesiem. Stiprā magnētiskā laukā ne tikai pieaug korozijas intensitāte, bet arī izmainās korodējošās virsmas morfoloģija. Uz paraugu virsmām tika novērotas regulāras vilņveida struktūras, orientētas eutektikas plūsmas virzienā.

Projekta ietvaros tika veikti teorētiski pētījumi par spēcīga magnētiskā lauka iespaidu uz korozijas procesiem. Uz magnētiskās hidrodinamikas un masas konvektīvās pārneses vienādojumu bāzes tika izveidots teorētiskais modelis, kas apraksta korozijas gaitu laikā un telpā. Korozija tika aprakstīta kā ar Pb<sub>17</sub>Li plūsmu kontaktējošās paraugu virsmas kvazistacionārs šķīšanas process.

Eksperimentāli iegūtie dati tika salīdzināti ar teorētiskiem rezultātiem. Tas

lāva novērtēt nezināmās fizikālās konstantes, kas raksturo EUROFER šķīšanu Pb17Li plūsmā.

No eksperimentālaiem rezultātiem iegūti parametri, kuri raksturo EUROFER korozijas intensitāti atkarībā no Pb17Li temperatūras.

Korozijas pētījumu rezultāti tika prezentēti starptautiskās konferencēs “Fundamental and Applied MHD” (PAMIR), Jūrmala – 2005.g. un Presqu’lle Giens, France, 2008.g. ; 14<sup>th</sup> International Conference on Nuclear Engineering, Miami, Florida, USA, 2006.g.; IEA Workshop on Liquid Breeder Blankets, St.Petersburg, 2006.g.

Izmantojot izstrādāto rotorveida induktoru ar moderniem spēcīgiem pastāvīgiem magnētiem lauku aprēķinu metodiku, tika veikti dažāda veida MHD sūkņu aprēķini, konstruēšana un uzbūve.

**Zaķe M.  
05.1384**

*Siltuma un masas pārneses pētījumi kombinētā gāzveida un cietā kurināmā degšanas procesā ārējo spēku laukā*

Dotais projekts apvieno fundamentālos degšanas procesa dinamikas pētījumus kombinētā degšanas procesa virpuļplūsmās, kas veidojās, vienlaicīgi sadedzinot cieto (koksnēs biomasa) un gāzveida kurināmo (propānu), izmantojot šo plūsmu kontrolei ārējo lauku (elektriskā, magnētiskā) un liesmas mijiedarbības efektus. Projekts paredz veikt arī lietīšos pētījumus, kas saistīti ar nepieciešamību izveidot ekoloģiski tīru un kontrolējamu siltuma ražošanas procesu ar ierobežotu siltumnīcas efektu un skābo lietu izraisošo CO<sub>2</sub> un NO<sub>x</sub> veidošanos degšanas procesā. Saskaņā ar projekta darba plānu laika posmā no 2005. līdz 2008. gadam tika izveidota eksperimentālā iekārta un tika izstrādāta pētījumu metodika kombinētā degšanas procesa pētījumiem ārējo lauku (elektriskā, magnētiskā) un liesmas mijiedarbības procesā. Sadarbībā ar LV Koksnes ķīmijas institūtu ir veikti dažāda tipa un sastāva koksnes biomasas granulu (bioetanola ražošanas blakus produktu) un propāna kombinētā degšanas un siltuma/masas pārneses procesu pētījumi, mainot papildus siltuma padevi koksnes biomasā un veicot regresijas analīzi, lai sasaistītu šo granulu raksturojošo parametru (augstākās un zemākās siltumspējas, elementārā sastāva, mitruma un struktūras) izmaiņas ar degšanas, siltuma/ masas pārneses un emisiju veidošanās procesu izmaiņām. Detalizēti ir pētītas arī šo procesu izmaiņas ārējo spēku un liesmas virpuļplūsmas mijiedarbības procesā. Pētījumu rezultātā ir konstatēts, ka liesmas virpuļplūsmas un aksiālā elektriskā lauka mijiedarbības process izraisa galvenokārt virpuļplūsmas dinamikas izmaiņas, intensificējot vai ierobežojot recirkulācijas plūsmu veidošanos liesmas degšanas zonā, kā arī gaisa un gaistošo savienojumu sajaukšanos, būtiski izmainot degšanas procesu kinētiku, liesmas struktūru un degšanas produktu sastāvu. Respektīvi, pētījumu rezultāti apliecina, ka ārējā elektriskā lauka mijiedarbības efektus var izmantot degšanas un siltuma/masas pārneses procesu dinamikas kontrolei. Atšķirībā no liesmas un elektriskā lauka mijiedarbības procesiem, kuru mehānismu nosaka galvenokārt pozitīvo jonu veidošanās degšanas zonā un to pārnese lauka virzienā, liesmas un magnētiskā lauka mijiedarbības mehānismu nosaka paramagnētisko (O<sub>2</sub>) un diamagnētisko (CO<sub>2</sub>, C<sub>x</sub>H<sub>y</sub>) liesmas komponenšu pārnese lauka gradiента virzienā. Liesmas un magnētiskā lauka pētījumu rezultāti apliecina, ka pamatā šī mijiedarbība reducējas uz paramagnētisko skābekļa molekulu pārnesi lauka gradienta virzienā, izraisot lokālas degšanas zonas sastāvu un degšanas procesa dinamikas izmaiņas. Projekta ietvaros veikto pētījumu rezultāti ir publicēti dažāda līmeņa zinātniskos izdevumos un ir aprobēti dažāda līmeņa Starptautiskās konferencēs. Publikāciju saraksts ir pievienots kopsavilkumam.

**Gorbunovs L.** *Liela diametra silīcija monokristālu audzēšanas procesa fizikālā modelēšana rotējošā magnētiskā laukā*  
**05.1375**

Galvenais mērķis ir izpētīt hidrodinamiku, siltuma un masas pārnesi liela diametra (300-400 mm) silīcija monokristālu audzēšanas procesā pie reāliem Prandtl skaitļiem. Šī mērķa sasniegšanai ierosinām izmantot LU Fizikas institūtā izstrādātās MHD iedarbības metodes un izmantot silīcija monokristālu audzēšanas fiziskās modelēšanas eksperimentālo stendu un InGaSn sakausējumu, kā arī datu savākšanas un apstrādes daudzkanālu sistēmu.

2005.g.-2008.g. saskaņā ar pētījumu programmu, izstrādāts un izgatavots rotējošā magnētiskā lauka induktors. Modernizēts eksperimentālais stends, kas domāts kausējuma hidrodinamikas pētišanai rotējošā magnētiskā laukā izotermiskā un neizotermiskā režīmā. Izpētīts, ka iedarbojoties uz kausējumu ar rotējošo magnētisko lauku, var aktīvi vadīt hidrodinamiskos procesus un pārveidot hidrodinamisko plūsmu struktūru. Tas rada veselu virkni pozitīvu efektu (piemēram, ļauj atteikties no tīgeļa griešanas u.c.). Tajā pat laikā, liela diametra tīgeļiem RML, ja barošanas strāvas frekvence  $f=50\text{Hz}$ , ir spilgti izteikts skinefekts. Elektromagnētiskiem spēkiem maksimālā vērtība ir pie tīgeļa sienas un krasī samazinās virzienā uz tīgeļa centru. Tas rada nevienmērīgu ātruma sadalījumu tīgeļa rādija virzienā un ātruma un temperatūras pulsāciju amplitūdas palielināšanos pie tīgeļa sienas.

Lai samazinātu šo efektu:

1. jāiedarbojas uz kausējumu ar rotējošā un skrejošā magnētiskā lauka superpozīciju. Galvenā ideja pamēģināt ar meridionālo plūsmu, ko rada skrejošais magnētiskais lauks, pārnest rotējošo kustību (kustības daudzuma momentu) kausējumā uz tīgeļa centrālo daļu.
2. iedarboties uz kausējumu, ja rotējošā magnētiskā lauka (RML) barošanas strāvas frekvence ir pazemināta (20-30Hz). Tas ļauj ievērojami samazināt skinefektu un palielināt rotējošā magnētiskā laukā iedarbības efektivitāti tīgeļa centrālajā daļā arī tajos gadījumos, ja kausējuma augstums tīgeļi ir mazs.

Salīdzinot iegūtos eksperimentālos rezultātus liela diametra (300-400mm) tīgeļos, nonākam pie slēdziena, ka šados gadījumos jāizmanto rotējošā magnētiskā laukā induktors, kura barošanas strāvas frekvence ir pazemināta (20-30Hz).

2007-2008 g.g. izstrādātas skaitliskās metodes un programmas hidrodinamisko un siltuma pārneses procesu aprēķiniem Čohrajska monokristālu audzēšanas procesam, ja uz kausējumu iedarbojas ar rotējošo magnētisko lauku. Izmantota turbulentu plūsmu aprēķināšanas tiesā skaitliskā modelēšana metode, kas ļauj izdarīt aprēķinus pie reāliem līdzības kritērijiem. Teorijas un eksperimenta saskaņa ir apmierinoša.

### **Institūta zinātnisko darbinieku publikācijas**

4. L.Gorbunov. Some Features of the Horizontal Magnetic Field Influence on the Growth of Large-Diameter Silicon Single Crystals. . Magnetohydrodynamics, No3, 97-113 , 2008

5. R.B.Gomes, H.Fernandes, C.Silva, A.Sarakovskis, T.Pareira, J.Figueiredo, B.Caravalho, A.Soares, C.Varandas, O.Lielais, A.Klyukin, E.Platacis, I.Tale. Interaction of a gallium jet with the tokamak ISTTOK edge plasma . Fusion Engineering and Design, 83 (2008)102-111
6. A.Cramer, V.Galindo, G.Gerbeth, J.Priede, A.Bojarevics, Yu.Gelfgat, O.Andersen, C.Kostmann, G.Stephani. Tailored magnetic fields in the melt extraction of metallic filaments. – In: The Minerals, Metals & Material Society and ASM International 2008, (in press).
7. Votyakov, E. V.; Zienicke, E.; Kolesnikov, Yu.: Constrained flow around a magnetic obstacle, *J. Fluid. Mech.*, Vol. 610 , pp. 131-156 (2008).
8. Andreev, O.; Kolesnikov, Yu.; Thess, A.: Application of the ultrasonic velocity profile method to the mapping of liquid metal flows under the influence of a non-uniform magnetic field. *Exp. Fluids*, 77-83 (online 30.07.2008,).
9. Platnieks I.,Freibergs J.E., Klavins J. MHD Technique For Production Of Lead-Lithium Eutectic Alloy. (Submitted for publication in journal “MagnetoHydroDynamics”)
10. Grants, G.Gerbeth, Use of a traveling magnetic field in VGF growth: Flow reversal and resulting dopant distribution, *Journal of Crystal Growth* **310**, 16, 3699 (2008)
11. Stefani, F., Gailitis, A., Gerbeth, G. *Magnetohydrodynamic experiments on cosmic magnetic fields* Z. Angew. Math. Mech. 88, 930-954 (2008); ; [arxiv.org/0807.0299](http://arxiv.org/0807.0299)
12. Gailitis, A., Gerbeth, G., Gundrum, Th., Lielais, O., Platacis, E., Stefani, F. *History and results of the Riga dynamo experiment* Comptes Rendus Physique 9 (2008), 721-728; [arxiv.org/0807.0305](http://arxiv.org/0807.0305)
13. I.Grants, C.Zhang, S.Eckert, G.Gerbeth, Experimental observation of swirl accumulation in a magnetically driven flow, *Journal of Fluid Mechanics* **616**, 135 (2008)
14. Vilnis Frishfelds; Elmars Blums, Drift of nonuniform ferrocolloid through cylindrical grid by magnetic force, *Journal of Physics: Condensed Mater*, **20** (2008) 204130 (5pp)
15. D.Zablotsky, V. Frishfelds, E. Blums. Numerical investigation of thermomagnetic convection in heated cylinder under the magnetic field of a solenoid. *Journal of Physics: Condensed Mater*, 20 (2008) 204134 (5pp).
16. E. Blums, A. Mezulis, G. Kronkalns. Magnetoconvective heat transfer from a cylinder under the effect of a non-uniform magnetic field. *Journal of Physics: Condensed Mater* **20** (2008) 204128 (5pp)

17. M.M.Maiorov, E Blums, G. Kronkalns. The heat generation by an alternating magnetic field of low frequency in a ferrofluid: the dependence of energy dissipation on temperature, *Magnetohydrodynamics*, **44** (2008), No. 1, pp. 27–32
18. G. Kronkalns, A. Dreimane, M.M. Maiorov. The effect of thermal treatment on the magnetic properties of spinel ferrite nanoparticles in magnetic fluids, *Magnetohydrodynamics*, **44** (2008), No. 1, pp. 3–10
19. E. Blums, G. Kronkalns, M. Maiorov. Thermoosmotic Transfer of Ferrocolloids through a Capillary Porous Layer in the Presence of Transversal Magnetic Field, In: *Thermal Nonequilibrium, 7th International Meeting on Thermodiffusion, Lecture notes*, Eds. S. Wiegand, W. Kohler, J.K.G. Dhont, Forschungzentrum Julich GmbH, 2008, p. 169 - 174.
20. I Segal, A. Zablotskaya, E. Lukevics, M. Maiorov, D. Zablotsky, E. Blums, I. Shestakova, I. Domracheva. Synthesis, physico-chemical and biological study of trialkylsiloxyalkyl amine coated iron oxide/oleic acid magnetic nanoparticles for the treatment of cancer, *Applied Organometallic Chemistry*, **22** (2008), 2, pp. 82 – 88.
21. L.Pauchard, F.Elias, P.Boltenhagen, A.Cebers, and J.C.Bacri. When a crack is oriented by a magnetic field. *Phys.Rev.E* – 2008,v.77-021402
22. K.Ērglis,D.Zhulenkova,A.Shapiro, and A.Cēbers. Elastic properties of DNA linked flexible magnetic filaments. *J.Phys.:Condens.Matter* – 2008, v.20, 204107
23. A.Tatulchenkov, and A.Cēbers. Magnetic fluid labyrinthine instability in Hele-Shaw cell with time dependent gap. *Physics of Fluids* – 2008, v.20, 054101.
24. I.Levental, P.A.Janmey, and A.Cēbers. Electrostatic contribution to the surface pressure of charged monolayers containing polyphosphoinositides. *Biophysical journal* – 2008, v.95,1199-1205.
25. I.Levental,A.Cēbers, and P.A.Janmey. Combined Electrostatics and Hydrogen bonding determined intermolecular interactions between polyphosphoinositides. *Journal of American Chemical Society* – 2008,v.130,9025-9030.
26. K.Ērglis, L.Alberte, A.Cēbers. Thermal fluctuations of non-motile magnetotactic bacteria in AC magnetic fields. *Magnetohydrodynamics* – 2008, v.44, P.223-236.

**Publikācijas starptautisko konferenču izdevumos – 56 referāti sagatavoti un publicēti**

**I 7th PAMIR International Conference on Fundamental and Applied MHD”,,  
Presqu`ile de Glens – France, September 8-12, 2008.**

1. Bojarevics A., Kaldre I., Gelfgat Yu., Fautrelle Y. A Sensor for Continuous Measurements of the Absolute Thermoelectric Power of Liquid Metal during Turbulent Non-Isothermal Mixing or Segregation of Multi-Component Melts. – Abstract for the Pamir 2008 Conference, Gien, 2008, France, p.109-113 .
2. Bojarevics A., Gelfgat Yu., Fautrelle Y., Etay J. Experimental Validation of a Dynamic Method to Define Thermoelectric Power of the multi-component liquid metals. – Abstract for the Pamir 2008 Conference, Gien, 2008, France, p.821-825.
3. Bucenieks I., Bojarevics A., Gelfgat Yu. On the Flows on the Liquid Metal Surface Subject to Rotating Magnetic Fields. – Abstract for the Pamir 2008 Conference, Gien, 2008, France, p.165-166
4. Abricka M. and Gelfgat Yu. On the flow hydrodynamics in the channel of a cylindrical induction pump with no core. – Abstract for the Pamir 2008 Conference, Gien, 2008, France, p.897-901.
5. S.Dementjev, F.Groeschel, S.Ivanov, “On an Electromagnetic Pump for Liquid Metal Target for Swiss Spallation Neutron Source”, 7<sup>th</sup> PAMIR Int. conf. Fundamental and applied MHD, France.
6. Mikelsons Arturs , Valdmanis Janis, Kronkalns Gunars. Pair of Rankine-type Vortices in MHD . MHD. France, MHD Conference “Pamir”, 2008., pp.405-407.
7. Valdmanis Janis, Cipiks Aleksandrs , Valdmane Rita. Transvere  $E \parallel B$  waves and their MHD aspects. MHD Conference “Pamir” 2008, France, Volume 1, pp. 501-505.
8. L.Gorbunov, A. Pedchenko. Physical modelling of large-diameter silicon single crystal growth in a rotating magnetic field. Proc.of 7<sup>th</sup> PAMIR International Conference on Fundamental and Applied MHD,649-653, 2008.
9. L.Gorbunov, A. Pedchenko. Numerical Simulation of Large-Diameter Silicon Single Crystal Growth in a Rotating Magnetic Field. Proc.of 7<sup>th</sup> PAMIR International Conference on Fundamental and Applied MHD, 873-878, 2008
10. Kolesnikov, Yu.; Karcher, Ch.; Thess, A.; Minchenya, V: Lorentz Force Velocimetry: Development and Application. Proceedings: 7th Pamir Conference, September, France, Giens, vol. 2, 537-540 (2008).
11. Minchenya, V.; Karcher, Ch.; Kolesnikov, Yu.; Thess, A.: Calibration of the Lorentz Force Velocimeter for High-Temperature Melts. Proceedings: 7th Pamir Conference, September, France, Giens, vol. 2, 785-788 (2008). J.E.Freibergs. Simulation of MHD Processes in Industrial Aluminium Electrolysis Cell. In Proceedings of the 7<sup>th</sup> International pamir Conference Fundamental and Applied MHD, Vol. 1, pp.35-38, Presqu’Île de Giens, France, September 8-12, 2008
13. I.Platnieks, J.E.Freibergs, J.Klavins. MHD Technique for Production of Lead-Lithium Eutectic Alloy. In Proceedings of the 7<sup>th</sup> International pamir Conference Fundamental and Applied MHD, Vol. 2, pp.845-849, Presqu’Île de Giens, France, September 8-12, 2008.
14. E.Platacis, R.Krishbergs, F.Muktepavela, A.Shishko. Analysis of the strong magnetic field influence on the corrosion of EUROFER steel in Pb17Li melt flows. 7<sup>th</sup> International PAMIR Conference on Fundamental and Applied MHD, Presqu’lle de Giens, France – 2008, pp. 321-325.

15. . Muktepavela F., Platacis E., Krishbergs R., Shishko A. Eksperimental studies of the strong magnetic field action on the corrosion of RAFM steels in Pb17Li melt flows. *7<sup>th</sup> International PAMIR Conference on Fundamental and Applied MHD*, Presqu'Ile de Giens, France – 2008, pp. 565-569.
16. . Ivanov S., Platacis E., Platnieks I., Krishbergs R., Flerov A., Shishko A., Zik A. Eksperimental studies of the MHD processes at the inlet elements of the liquid metal blanket. *7<sup>th</sup> International PAMIR Conference on Fundamental and Applied MHD*, Presqu'Ile de Giens, France – 2008, pp. 553-557.
17. . Bucenieks I., Kravalis K., Characteristics of disks type electromagnetic induction permanent magnet pump. *7<sup>th</sup> International PAMIR Conference on Fundamental and Applied MHD*, Presqu'Ile de Giens, France – 2008, pp. 91-95.
18. Elmars Blums, Gunars Kronkalns and Michail Maiorov, Thermoosmosis in magnetic fluids in the presence of a magnetic field, In: *Proc. 7<sup>th</sup> International PAMIR Conference on Fundamental and Applied MHD*, Presqu'Ile de Giens, France, 2008, Vol. 2, 667-272.
19. D. Zablotsky, V. Frishfelds, E. Blums, Investigation of heat transfer efficiency of thermomagnetic convection in ferrofluids, In: *Proc. 7<sup>th</sup> International PAMIR Conference on Fundamental and Applied MHD*, Presqu'Ile de Giens, France, 2008, Vol. 2, 715-720.
20. A. Mezulis, E. Blums and G. Kronkalns, Magnetoconvective intensification of heat transfer based on permanent magnets, In: Proc. 7<sup>th</sup> International PAMIR Conference on Fundamental and Applied MHD, Presqu'Ile de Giens, France, 2008, Vol. 2, 803-808.
21. M M. Maiorov, G. Kronkalns, E. Blums. Complex Magnetic Susceptibility Of Cobalt Ferrite Ferrofluid: Influence Of Carrier Viscosity And Particle Concentration, In: *Proc. 7<sup>th</sup> International Pamir Conference On Fundamental And Applied Mhd*, Presqu'ile De Giens, France, 2008, Vol. 2, 725-730.
22. I. Segal, A. Zablotskaya, E. Lukevics, M. Maiorov, D. Zablotsky, E. Blums, A. Mishnev, I. Shestakova, A. Gulbe. "Iron Oxide Based Magnetic Nanoparticles Bearing Cytotoxic Silylated Alkanolamine", In: *Proc. 7<sup>th</sup> International Pamir Conference On Fundamental And Applied Mhd*, Presqu'ile De Giens, France, 2008, Vol. 2, 691-696.
23. L.Alberte, K.Ērglis,A.Cēbers. Thermal fluctuations of magnetotactic bacteria in ac magnetic fields. *7<sup>th</sup> International Pamir Conference on Fundamental and Applied MHD*, Presqu'Ile de Giens, France, P.661-665, 2008.
24. V.Vorohobovs, A.Cēbers. Delicate milling of nonmagnetic substances by small iron oxide spherical beads.*7<sup>th</sup> International Pamir Conference on Fundamental and Applied MHD*, Presqu'Ile de Giens, France, P.455-460, 2008.

## II

25. I.Bucenieks, J.Freibergs, E.Platacis. "Evaluation of Parameters of Powerful Electromagnetic Induction Pumpson Permanent Magnets for Heavy Liquid Metals." "IV Workshop on Materials for HLM-cooled Reactors and Related Technologies". CNR, Roma, May 21-23rd, 2007
26. V. Kremeneckis, N. Kremenecka – Calculus With "Mathematica" Labs At Riga Technical University // Proceedings of the 5th WSEAS/IASME International

Conference on ENGINEERING EDUCATION, Heraklion, Crete Island, Greece, July 22-24, 2008.

27. A. Arshanitsa, I Barmina, G Telysheva, M. Zake, Combustion and emission characteristics of the wood fuel pellets, "World Bioenergy-2008", Jonkoping, Sweden, 2008, pp.244-248.
28. I. Barmina, M. Zake, Wood biomass co-firing for the clean heat energy production, "World Bioenergy-2008", Jonkoping, Sweden, 2008, pp.249-253.
29. I. Barmina, M. Zaķe, M. Purmals, The effect of wood biomass co-firing with fossil gaseous fuel on the combustion and emission characteristics, Rīga, 2008, 5<sup>th</sup> UEAA General Assembly and the associated Workshop on "Renewable Energy Resources, Production and Technologies", Zinātne, 2008, pp.54-62.
30. A. Arshanitsa, I. Barmina, T. Dizhbite, G. Telisheva, M. Zake, Combustion of Granulated Plant Biofuel, Rīga, 2008, 5<sup>th</sup> UEAA General Assembly and the associated Workshop on "Renewable Energy Resources, Production and Technologies", Zinātne, 2008, pp.37-46.
31. A. Arshanitsa, I Barmina, T.Dizhbite, G Telysheva, M. Zake, J.Rizhikov, Combustion and emission characteristics of the plant biofuel pellets 2008, Spain, Valensia, pp10.
32. M. Zaķe, I. Barmina, M. Purmals, Co-Fire of Renewable with Fossil Fuel for the Clean and Effective Heat Energy Production. Abstract for 17<sup>th</sup> European Biomass Conference, Hamburg 2009(pieņemts publicēšanai).
33. M. Zaķe, I. Barmina, Magnetic Promotion of the Swirling Combustion. Abstract for 17<sup>th</sup> European Biomass Conference, Hamburg 2009 (pieņemts publicēšanai).
34. A.Gailītis „Last results from Riga Dynamo Experiment” nolasīts seminārā „Magnetic field generation in experiments, geophysics and astrophysics”, Santa Barbara, Kalifornija, ASV, 15-18.07.2008
35. Janis Valdmanis, Aleksandrs Cipiks, Electromagnetic metamaterials and new aspects of electricity, XVI International Congress on Electricity applications in modern world, Krakow, Poland, 2008, pp.79-80.
36. Janis Valdmanis, Aleksandrs Cipiks. On the mechanism of low frequency bioelectromagnetism. 14th Nordic-Baltic Conference on Biomedical Engineering and Medical Physics. Riga,2008. p.69 , pilns teksts IFMBE Proceedings , Volume 20, Springer
37. Gelfgat Yu., Tiselsky S. ELECTROMAGNETIC METHOD AND DEVICE FOR MIXING UP FINE SCRAP AND ALLOYING ADDITIONS INTO MOLTEN METAL. – Proc. 4<sup>th</sup> International „Aluminium Recycling” Conference and Exhibition, St.-Petersburg, Russia, April 1-5 2008,p.124-136.
38. Bojarevics A., Bucenieks I., Gelfgat Yu. Tests and optimization of a permanent magnetic device for driving the flow at the free surface of liquid metal. – International Scientific Colloquium “Modelling for Electromagnetic Processing, Hannover, Germany, 2008, (in press).
39. E. Blums, G. Kronkalns, M. M. Maiorov, The heater with cobalt ferrite nanoparticles utilizing a low frequency magnetic field, , In: *International Baltic Sea Region conference “Functional materials and nanotechnologies-2007*, Institute of Solid State Physics, University of Latvia, April 2-4, Riga 2007, p. 108.

40. E. Blums, G. Kronkalns, M. Maiorov. Thermoosmotic transfer of ferrocolloids through a capillary porous layer in the presence of transversal magnetic field. Abstracts, *7th International Meeting on Thermodiffusion*, Bonn, June 2008, p. 56 – 57.
41. D. Zablockis, V. Frishfelds, E. Blums. Numerical Investigation of Heat Transfer in Magnetic Nanocolloids under Inhomogeneous Magnetic Field, Abstracts, *International Baltic Sea Region conference “Functional materials and nanotechnologies”*, Institute of Solid State Physics, April 1 – 3, 2008, Riga.
42. M. Maiorov, G. Kronkalns, E. Blums. The Magnetic Susceptibility Spectrum of Cobalt Ferrite Ferrofluid, Abstracts, *International Baltic Sea Region conference “Functional materials and nanotechnologies”*, Institute of Solid State Physics, April 1 – 3, 2008, Riga.
43. Kolesnikov, Y.: Flow around a magnetic obstacle: Experimental illustrations. Conference 11<sup>th</sup> MHD Days, Ilmenau, Dec. 1–3, Germany (2008).
44. Kolesnikov, Yu.; Karcher, Ch.; Thess, A.: Magnetic field application in metallurgy; Flow control and measurements. The 1<sup>st</sup> Intern. Engineering Science Conf. – IESC’2008, Aleppo, Syria Nov. 2–4, 21-28 (2008).
45. Kolesnikov, Yu.; Karcher, Ch.; Thess, A., Minchenya, V.: Development of Lorentz Force Velocimetry and Applications. Workshop Elektroprozesstechnik, Technische Universität Ilmenau, 28.-29. Aug. (2008).
46. Minchenya, V.; Karcher, Ch.; Kolesnikov, Yu.; Thess, A.: Calibration of the Lorentz Force Flowmeter. International Scientific Colloquium Modelling for Electromagnetic Processing Hannover, October 27-29 (2008).
47. Kolesnikov, Yu. Lecture: Electromagnetic breaking of turbulent MFD channel flow. SINO-German summer School on Fundamental and applied Thermofluidynamics, Northeastern University, Shenyang, PR China, Sept. 13–27, 20 p. (2008).
48. Kolesnikov, Yu. Lecture: Magnetic obstacles in turbulent MFD flow. SINO-German summer School on Fundamental and applied Thermofluidynamics, Northeastern University, Shenyang, PR China, Sept. 13–27, 25 p. (2008).
49. Kolesnikov, Yu. Lecture: Electromagnetic control of industrial fluid-flow. SINO-German summer School on Fundamental and applied Thermofluidynamics, Northeastern University, Shenyang, PR China, Sept. 13–27, 23p. (2008).
50. E.Platacis, I.Platnieks, J.E.Freibergs, R.Križbergs, J.Kļaviņš, F.Muktepāvela, A.Šiško. MHD tehnoloģija svina-litija sakausējuma iegūšanai un izmantošanai. 24.zinātniskās konferences, veltītas LU CFI 30 gadu jubilejai, referātu tēzes. 2008. gada 20-22 februāris. lpp. 30.
51. I.Bucenieks, S.Ivanovs, R.Križbergs, E.Platacis, I.Platnieks, A.Romančuks, A.Šiško, A.Ziks. Eksperimentālie pētījumi par MHD procesiem Pb-Li eutektikas blanketa ieejas elementos supravadoša magnēta laukā. 24.zinātniskās konferences, veltītas LU CFI 30 gadu jubilejai, referātu tēzes. 2008. gada 20-22 februāris, 31 lpp.
52. A.Cēbers,K.Ērglis. Elasticity of Cytoskeleton and Motion of Magnetotactic bacteria in AC magnetic Field. In: The Joint Biophysical Society 52<sup>nd</sup> Annual Meeting, 16<sup>th</sup> IUPAB International Biophysics Congress, Long Beach, California, 3243-Pos.,2008.

53. K. Ērglis, A. Cēbers. Magnetic field sensing by magnetotactic bacteria and elasticity of cytoskeleton. Third International Conference Smart Materials, Structures&Systems, Acireale, Sicily, Italy, E-3.1:L03, P.78, 2008.
54. K. Ērglis, M. Belovs, A. Cēbers. Flexible ferromagnetic filaments and the interface with biology. Moscow International Symposium on Magnetism, Book of Abstracts, Moscow , P.238, 2008
55. M. Belovs, A. Cēbers. Properties of twisted ferromagnetic filaments. 11<sup>th</sup> International Conference on Electrorheological Fluids and Magnetorheological Suspensions, Dresden, P.123, 2008
56. K. Ērglis, A. Cēbers. Dynamics of flexible ferromagnetic filaments. 11<sup>th</sup> International Conference on Electrorheological Fluids and Magnetorheological Suspensions ,Dresden, P.129, 2008.

#### Citi izdevumi

6. M. Zaķe, Co-firing of renewable with fossil fuel for the clean and effective heat energy production, reklāmas katalogs "High Tech in Latvia", 2008, pp. 31.

#### **Reģistrēto un uzturēts patents** Patenti

1. "Verfahren und Anordnung zur Berührungslosen Inspektion elektrisch leitfähiger Materialien", 10 2006 025 542.9 (Deutschland, USA), 2007, /Thess A., Kolesnikov Y., Karcher Ch./
2. Latvijas patents Nr.13575, 20.07.07. Universāls kompleks aluminijs sakausējumu iegūšanai un liešanai. Autori: J.Gelfgats, V.Foliforovs, S.Tiseļskis.
3. Latvijas patents Nr.13571, 20.07.07. Ierīce šķīdru metālu vai sakausējumu maisīšanai metalurgiskos agregātos. Autori: J.Gelfgats, V.Foliforovs, S.Tiseļskis.
4. Latvijas patents Nr.13580, 20.07.07. Magnētiskā skrejlauka lineārs inductors metalurgiskiem agregātiem. Autori: J.Gelfgats, V.Foliforovs, S.Tiseļskis.
5. W.v.Ammon, Yu.Gelfgat, L. Gorbunov , E.Tomzig, J.Virbulis. Verfahren und Vorrichtung zum Herstellen eines Einkristalls aus Silicium." Wanderfeld". EP122525581, DE502015950, 2005.
6. US Patent 7,335,256, 2008. Silicon single crystal and process for producing it. Authors: W.von Ammon, H. Schmidt, J. Virbulis, Yu. Gelfgat et .al.
7. European Patent (Application No.08016830.5-2209) "Vervahren und Anordnung zur Messung des Durchflusses elektrisch leitfähiger medien" (2008). Autori: G.Gerbeth, ... A.Bojarevics, J.Gelfgats.
8. Karcher, Ch., Kolesnikov, Y., Thess, A.: German Patent DE 10 2007 038 685 (2008).
9. I. Barmina, M.Gedrovičs, P. Meija, A. Meijere-Līckrastiņa, M. Purmals, M. Zaķe, Atjaunojamā kurināmā un gāzveida kurināmā vienlaicīgas sadedzināšanas apkures katls- patenta pieteikums, 2008, pp.1-16.

**Institūta (augstskolas) 2008.gadā īstenoto līgumdarbu kopā ar Latvijas un  
ārvalstu uzņēmējiem**

<i>Paul Scherer Institute</i>	<i>Switzerland</i>	<i>Modification of an electromagnetic pumps</i>
<i>Corus Research, Development and Technology</i>	<i>The Netherlands</i>	<i>Design, manufacture, test and delivery of a permanent magnet system</i>
<i>SIEMENS, Grenobles Politehniskais institūts CNRS, INPG</i>	<i>Germany France</i>	<i>Feasible study for the MHD facility with permanent magnets for the glass technology</i>
<i>Center for Automatics R&amp;D CIDAUT Foundation for R&amp;D in Automotive Sector</i>	<i>Spain</i>	<i>A research project for liquid aluminium pumps on rotating permanent magnets</i>
<i>Commissariat à l'énergie atomique, Département de technologie nucléaire</i>	<i>France</i>	<i>Assesment of possibility to design and develop pfEM pump related to m3 irradiation devices</i>
<i>Los Alamos National Laboratory (LANL)</i>	<i>ASV</i>	<i>System of electromagnetic pumps</i>
<i>Oak Ridge National Laboratory (ORNL)</i>	<i>ASV</i>	<i>Design, manufacture, test and delivery 2 electromagnetic pumps</i>

**Institūta (augstskolas) 2008.gadā īstenoto tirgus orientēto pētījumu vai  
pašvaldību pasūtījumu skaits un nosaukums: 1 līgums**

<i>IZM TOP08-17</i>	<i>Titāna ražošanas tehnoloģijas izstrādāšana, bāzējoties uz savstarpēju titāna tetrahlorida un metāliskā magnija tvaiku savstarpēju mijiedarbību”</i>	<i>E.Platacis</i>
---------------------	--	-------------------

LU Fizikas institūta doktoranti – 3

K.Kravalis – vadītājs dr.fiz. Imants Bucenieks

G.Lipsbergs – vadītājs dr.fiz. Agris Gailītis

A.Desnickis – vadītāja dr.fiz. Maija Zaķe

D.Zablockis- vad, dr.hab.fiz. Elmars Blūms

Asistents Vl. Kremeņeckiis pabeidzis promocijas darbu “ Precīzi automodulārie risinājumi hidrodinamikā un magnētiskajā hidrodinamikā un to sakars ar uzdevumiem robežslāņu tuvinājumā” fizikas doktora grāda iegūšanai.

Asistenta v.i. I.Kaldre izstrādājis maģistra darbu “termoelektrisko strāvu un magnētiskā lauka mijiedarbības izraisītas šķidra metāla plūsmas eksperimentāla izpēte adatveida režģa apkārtnē”

Asistenta v.i. T. Beinerts izstrādājis bakalaura darbu „Magnētisku dipolu rotācijas inducēta šķidra metāla kustības eksperimentāla izpēte”

## **I apakšvirziens**

Zinātniskās pētniecības apakšvirziens, kurā LUFI ir vadošo institūciju vidū pasaулē:

**Šķidru metālu magnetohidrodinamika un hidrodinamika,  
fundamentālie un pielietojumie pētījumi.**

# **EU Project MAGFLOTOM**

Magnetic flow tomography  
in technology, geophysics, and ocean flow research

Contract number 028670

Sixth Framework Programme  
New and Emerging Science and Technology (NEST)

## **Mid-term Progress Report October 2008**

### **Annex 6**

**Report:**      **Report on Riga dynamo experiment**

Authors:      A. Gailitis, E. Platacis (IPUL), Th. Gundrum, F. Stefani, G. Gerbeth (FZD)

Report nature:      Public

## 1. Introduction

The Riga dynamo experiment was worldwide the first liquid metal experiment in which magnetic field self-excitation was ever observed [1]. Between 1999 and 2005, seven experimental campaigns have been carried out that have brought about a wealth of data on the kinematic and on the saturated regime [2,3,4,5,6,7]. Since the Karlsruhe dynamo experiment [8] was disassembled in 2004, the Riga dynamo experiment is presently the only homogeneous dynamo in the world that is really running. The VKS (von Karman sodium) experiment in Cadarache (France) has provided many interesting results [9,10], but only with the use of iron propellers with high permeability, which disqualifies it as a real homogeneous dynamo.

Within the MAGFLOTOM project, the unique Riga dynamo experiment was expected to be further exploited. According to the specific character of MAGFLOTOM, one of the main focuses was on the inverse problem of inferring velocity structures of the liquid sodium flow from measured magnetic field information. This is still a most interesting task since direct flow measurements in the facility have turned out to be very difficult.

In accordance with the project plan, one experimental campaign has been carried out in July 2007. Since the old dry face seal was worn out, a completely new seal in form of a magnetic coupler had been installed for this campaign. Therefore, the first goal of the experiments with this important technical modification was to test the new sealing concept. In the first part of this report, we will describe the main results of this experimental campaign.

In the second part, we report on the progress that was made in the numerical understanding of the saturation regime. This understanding relies on a hybrid forward/inverse approach, in which a simple one-dimensional back-reaction model is used in order to predict the modification of the velocity structure in the saturation regime, which then, in turn, can be evaluated by comparison with the growth rate, the frequency and the spatial structure of the measured magnetic eigenmode, and with the Joule power resulting from it. While in former approaches the coupling between induction equation and back-reaction model was realized with only a single step of an iteration [5,6], we have actualized a full time-dependent coupling of both effects which yields indeed an improved agreement with the measurements [7].

## 2. The experimental campaign of 2007

After intensive preparatory work, the experimental campaign took place on 23 and 24 July 2007. The main focus was on the integrity and the correct functioning of the new magnetic coupler. The latter is shown in Figure 1.

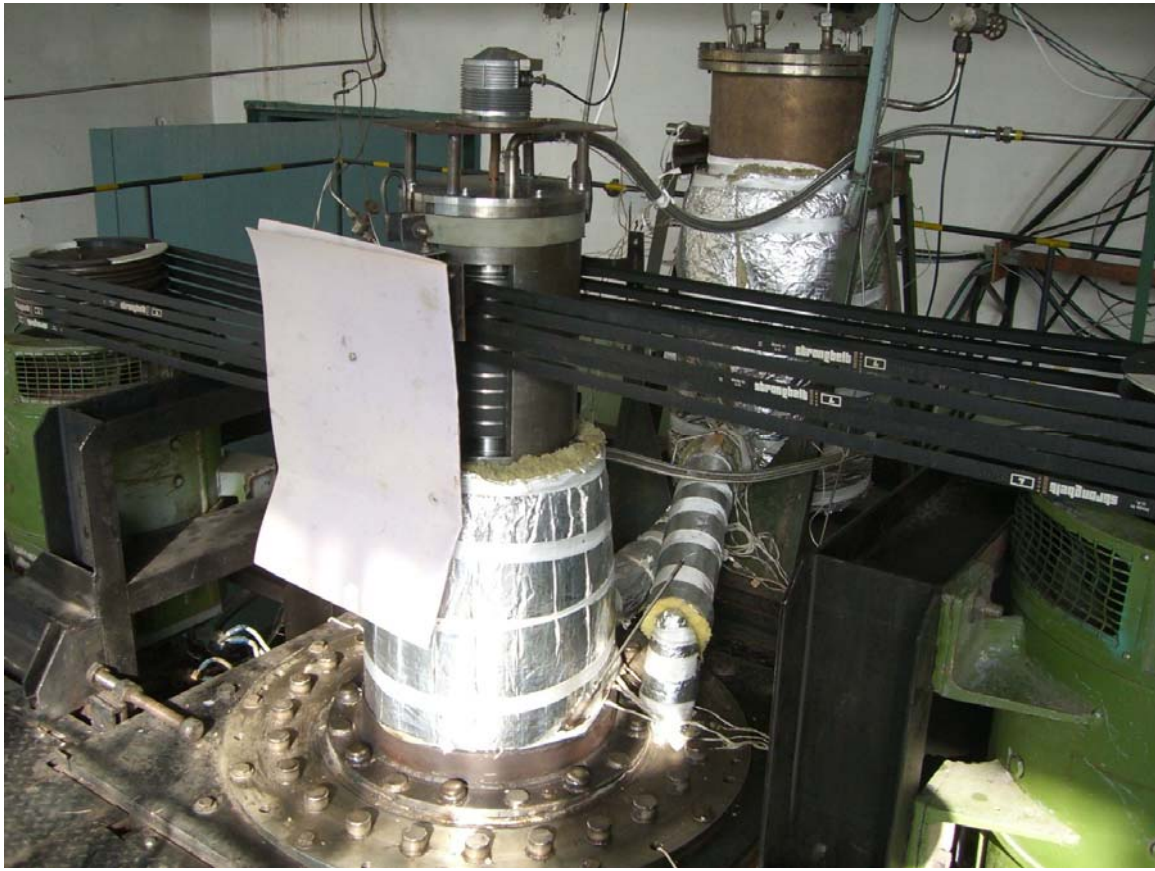


Fig. 1: The newly installed magnetic coupler, connected by 2x5 belts to the two 100 kW motors.

In total, four experimental runs where carried out. Since there was some problem with data acquisition in the first run, we document here only the runs 2, 3 and 4. An overview of these three runs is given in Fig.2.

The interesting point in run 2 was that, after some intermediate stop at 2000 rpm where the dynamo started self-excitation, the next rotation rate of 2100 rpm was kept for around 12 minutes during which the temperature of the sodium increased significantly, leading to a noticeable decrease of the electrical conductivity, so that the magnetic field dies away at the end of this period.

In run 3, the propeller rotation rate was driven to 2200 rpm, without any noticeable problem with the magnetic coupler.

In run 4, the rotation rate was increased in steps of 100 until 2200, at which, however, one of the belts was broken and forced us to stop the experiment.

In principle, it can be stated that the magnetic coupler has been tested successfully until rotation rates of 2200, which is, however, still below the value of 2500 rpm that was

achieved in previous campaigns. Such a test of larger rotation rate, therefore, left for the next campaign that is envisioned for the end of 2008.

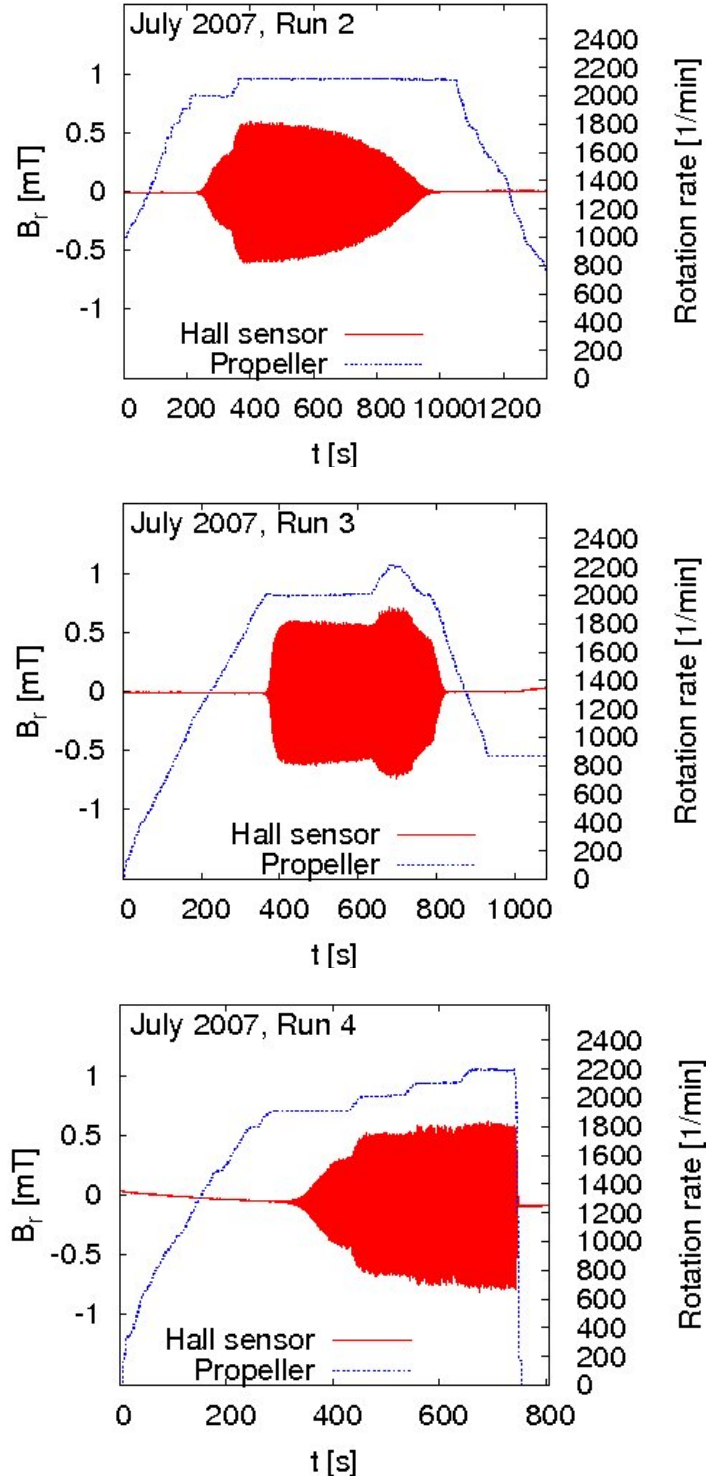


Fig 2: Three of the four runs in the 2007 campaign. The blue lines show the propeller rotation rate, the red line shows the signal of one external Hall sensor, both in dependence on time.

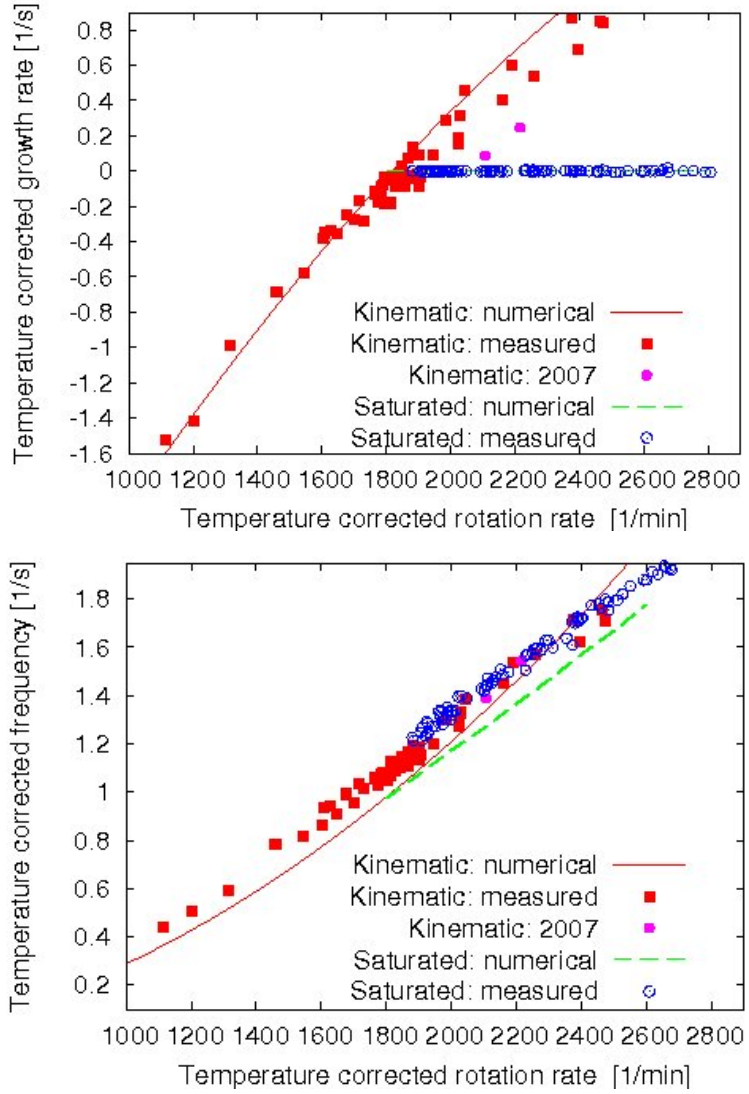


Fig. 3. Growth rate and frequency of the eigenmode of the Riga dynamo experiment. The red squares are the values in the kinematic regime that had been observed between 1999 and 2005. The two pink squares are two corresponding values of the 2007 campaign.

An interesting point in connection with the magnetic coupler concept is whether the dynamo works as good as in former campaigns. A significant criterion in order to evaluate the “quality” of the dynamo is the growth rate and the frequency of the magnetic field eigenmode in the kinematic regime (where the back-reaction of the magnetic field can be neglected). Figure 3 shows both quantities in dependence on the rotation rate, which has been, as usually, corrected by the temperature effect. We have distinguished the two points from the new campaign (pink circles) from all the other points from

previous campaigns (red squares). Obviously, the growth rates for the 2007 campaign are significantly lower than usually. In terms of the critical rotation rate, which was around 1840 rpm in former runs, we can extrapolate the 2007 one to approximately 2040 rpm.

The reason for this underperformance of the dynamo is not yet clear. One possibility could be that during the long resting time between 2005 and 2007 oxides have stuck to the inner walls, hence increasing the electrical resistance between the different tubes. Another possibility might have to do with the effect of a lower filling level of the liquid sodium, which is a necessity for the magnetic coupler to function properly. This lower filling, in turn, could be responsible for more argon entry into the sodium in the propeller region which could lead to a deteriorated pumping efficiency. This would mean that, although the magnetic coupler works in principle well, it has unintended consequences for the dynamo. This point will be clarified in the next campaign.

Another new aspect of the campaign was the use of modified version of the permanent magnet probe (PMP) for the determination of the sodium velocity in the inner cylinder. This probe was already tested in the February 2005 campaign, but now the wiring was changed in order to get a better distinction between the axial and the azimuthal velocity component. The probe is shown in Figure 4

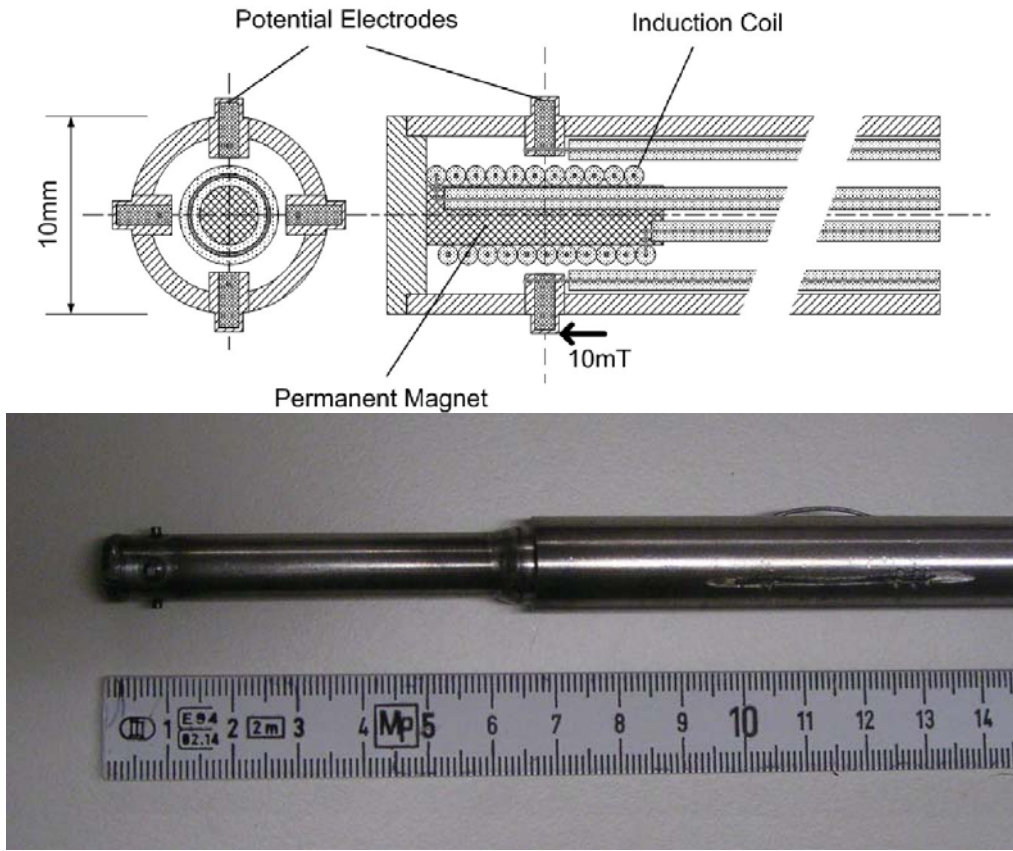


Fig. 4: Scheme and photograph of the permanent magnet probe used for the determination of the sodium flow velocity in the innermost channel.

The measuring principle is shown in Fig. 5. The permanent magnet in the middle produces a dipolar magnetic field. The interaction of the velocity with this dipolar magnetic field induces voltage that is basically proportional to the velocity component that is perpendicular to both the magnetic field and the connecting line between the electrodes.

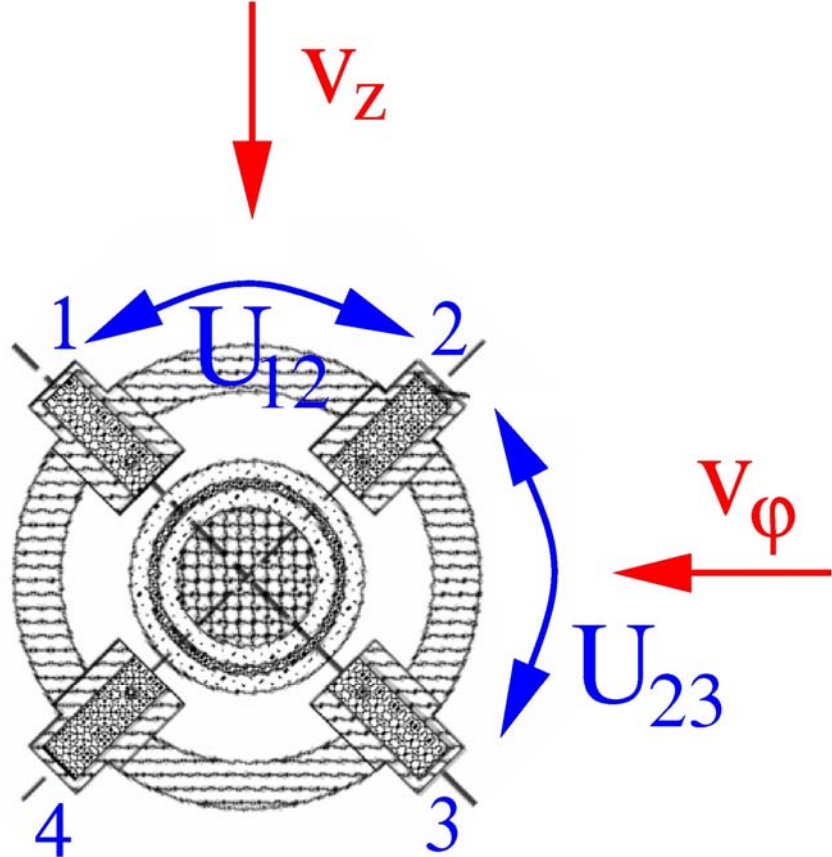


Fig. 5: Illustration of the measuring principle. The induced voltage between the electrodes 1 and 2 is basically proportional to the axial velocity, the voltage between electrodes 2 and 3 is basically proportional to the azimuthal velocity.

Figure 6 shows now the results from this probe. The blue curves show again the propeller rotation rates, the red and green curves show the measured voltages indicating the axial and the azimuthal velocity components. At each instant, the voltages are averaged over 10 seconds in order to average out the effect of the oscillating magnetic eigenfield which adds to the field of the PMP. Although the different amplitudes (by a factor around 2) of the two velocity components are in rough agreement with the earlier water dummy measurements, it should be noticed that the probe has not been calibrated yet and that the precise attribution of the axial velocity to  $U_{12}$  and of the azimuthal component to  $U_{23}$  has still to be validated.

Further work will also be needed to check the numerical predictions of the saturation model with respect to the saturated velocity.

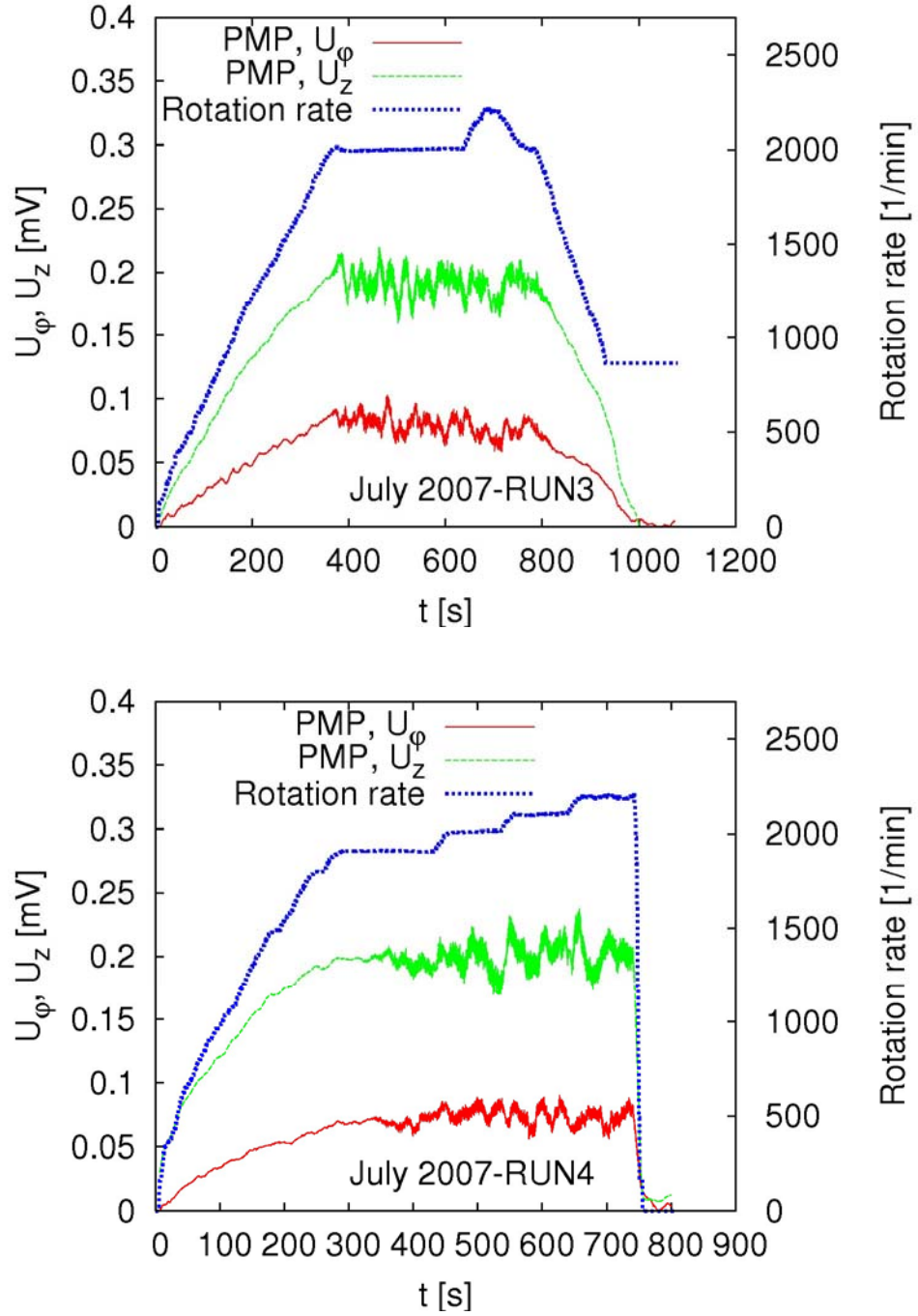


Fig. 6: Measured voltages at the PMP, indicating the axial and azimuthal velocity components. At each instant, the voltages are averaged over 10 seconds in order to average out the effect of the oscillating magnetic eigenfield which adds to the field of the PMP.

### 3. An improved saturation model

In our simple saturation model of the Riga dynamo, we try to implement the most important back-reaction effect. While the axial velocity component has to be more or less constant from top to bottom due to mass conservation, the azimuthal velocity component is susceptible to be braked by the Lorentz forces without producing a significant pressure (and hence power) increase. In the inviscid approximation, and taking only into account the axi-symmetric component of the Lorentz force, we end up with the ordinary differential equation for the Lorentz force induced perturbation of the azimuthal velocity component  $\delta v_\varphi(r, z)$ :

$$\bar{v}_z(r, z) \frac{\partial}{\partial z} \delta v_\varphi(r, z) = \frac{1}{\mu_0 \sigma} [(\nabla \times \mathbf{B}) \times \mathbf{B}]_\varphi(r, z)$$

where  $\bar{v}_z(r, z)$  represents the mean axial velocity. Differing from the procedure describes in [5,6] where we had used the measured excess Joule power at a given super-criticality to calibrate the Lorentz force term on the r.h.s. of this equation, we have now solved the equation simultaneously with the induction equation. This is done both in the innermost channel where  $\delta v_\varphi(r, z)$  is decelerated downward and in the back-flow channel where it is accelerated upward. Both effects together decrease the differential rotation, which leads to saturation simply by a deteriorated dynamo capability if the flow, in particular in the lower part.

The validity of this self-consistent saturation model (which automatically gives a zero growth rate) can be judged from the behaviour of the frequency curve in the lower panel of Fig. 3. Actually, we see a good correspondence with the measured frequencies in the saturated regime, in particular concerning the slope of the curve.

For more details, we refer to the attached recent publication [7] where this new improved model has been discussed.

### References:

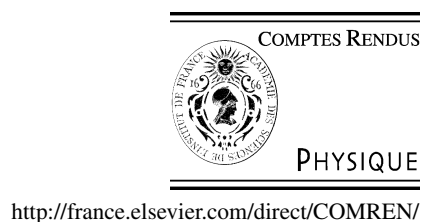
- [1] A. Gailitis et al. (2000): Detection of a flow induced magnetic field eigenmode in the Riga dynamo facility, Phys. Rev. Lett. 84, 4365
- [2] A. Gailitis et al. (2001): Magnetic Field Saturation in the Riga Dynamo Experiment, Phys. Rev. Lett. 86, 3024
- [3] A. Gailitis et al. (2003) : The Riga dynamo experiment, Surv. Geophys. 24, 247
- [4] A. Gailitis et al. (2002) : Laboratory experiments on hydromagnetic dynamos, Rev. Mod. Phys. 74, 973
- [5] A. Gailitis et al. (2004): Riga dynamo experiment and its theoretical background, Phys. Plasmas 11, 2838

- [6] S. Kenjeres et al. (2006) : Coupled fluid-flow and magnetic-field simulation of the Riga dynamo experiment, Phys. Plasmas 13, 122308
- [7] A. Gailitis et al. (2008): History and results of the Riga dynamo experiments, Comptes Rendus Phys. 9, 721-728
- [8] R. Stieglitz and U. Müller (2001): Experimental demonstration of a homogeneous two-scale dynamo, Phys. Fluids 13, 561
- [9] R. Monchaux et al. (2007): Generation of a magnetic field by dynamo action in a turbulent flow of liquid sodium, Phys. Rev. Lett. 98, 044502
- [10] M. Berhanu et al. (2007) : Magnetic field reversals in an experimental turbulent dynamo, EPL 77, 59001

Available online at [www.sciencedirect.com](http://www.sciencedirect.com)

ScienceDirect

C. R. Physique 9 (2008) 721–728

<http://france.elsevier.com/direct/COMREN/>

## The dynamo effect/L'effet dynamo

## History and results of the Riga dynamo experiments

Agris Gailitis<sup>a</sup>, Gunter Gerbeth<sup>b</sup>, Thomas Gundrum<sup>b</sup>, Olgerts Lielausis<sup>a</sup>,  
Ernests Platacis<sup>a</sup>, Frank Stefani<sup>b,\*</sup>

<sup>a</sup> Institute of Physics, University of Latvia, LV-2169 Salaspils 1, Latvia

<sup>b</sup> Forschungszentrum Dresden-Rossendorf, P.O. Box 510119, 01314 Dresden, Germany

Available online 29 August 2008

**Abstract**

On 11 November 1999, a self-exciting magnetic eigenfield was detected for the first time in the Riga liquid sodium dynamo experiment. We report on the long history leading to this event, and on the subsequent experimental campaigns which provided a wealth of data on the kinematic and the saturated regime of this dynamo. The present state of the theoretical understanding of both regimes is delineated, and some comparisons with other laboratory dynamo experiments are made. **To cite this article:** A. Gailitis et al., *C. R. Physique* 9 (2008).

© 2008 Académie des sciences. Published by Elsevier Masson SAS. All rights reserved.

**Résumé**

**Historique et résultats des expériences dynamo de Riga.** Le 11 novembre 1999, un mode propre magnétique auto-excité était détecté pour la première fois dans l'expérience dynamo au sodium liquide de Riga. Nous relatons le long historique qui a conduit à cet événement et présentons les campagnes expérimentales qui ont suivi et qui ont produit de très nombreuses données sur les régimes cinématique et saturé de cette dynamo. L'état actuel de compréhension théorique des deux régimes est esquissée et des comparaisons avec d'autres expériences dynamo sont fournies. **Pour citer cet article :** A. Gailitis et al., *C. R. Physique* 9 (2008).  
© 2008 Académie des sciences. Published by Elsevier Masson SAS. All rights reserved.

**Keywords:** Dynamo; Magnetic field; Liquid sodium

**Mots-clés :** Dynamo ; Champ magnétique ; Sodium liquide

**1. Introduction**

It is widely believed that almost any flow of a conducting liquid will give rise to self-excitation of a magnetic field provided that, first, the flow topology is not too simple (e.g. a flow in one direction or a purely rotational flow) and, second, the so-called magnetic Reynolds number is large enough. This dimensionless number  $Rm = \mu_0\sigma LV$ , which is defined as the product of the magnetic permeability  $\mu_0$  and the electrical conductivity  $\sigma$  of the fluid and the typical

\* Corresponding author.

E-mail addresses: [gailitis@sal.lv](mailto:gailitis@sal.lv) (A. Gailitis), [G.Gerbeth@fzd.de](mailto:G.Gerbeth@fzd.de) (G. Gerbeth), [Th.Gundrum@fzd.de](mailto:Th.Gundrum@fzd.de) (T. Gundrum), [mbroka@sal.lv](mailto:mbroka@sal.lv) (O. Lielausis), [platacis@sal.lv](mailto:platacis@sal.lv) (E. Platacis), [F.Stefani@fzd.de](mailto:F.Stefani@fzd.de) (F. Stefani).

length scale  $L$  and the typical velocity scale  $V$  of its flow, measures the ratio of diffusive time scale to kinematic time scale in the induction equation for the magnetic field  $\mathbf{B}$ :

$$\frac{\partial \mathbf{B}}{\partial t} = \nabla \times (\mathbf{v} \times \mathbf{B}) + \frac{1}{\mu_0 \sigma} \nabla^2 \mathbf{B} \quad (1)$$

While this number is large in many astrophysically relevant flows, simply due to their huge spatial extension, it requires significant effort to produce a flow with  $Rm \sim 10, \dots, 100$  in the laboratory. The simple reason for this is that the electrical conductivity of liquid metals, even in the optimum case of liquid sodium, does not exceed a value of  $10^7$  S/m, which leads to a product  $\mu_0 \sigma \sim 10$  s/m<sup>2</sup>. Hence, in order to get an  $Rm \sim 10$ , it requires a product of fluid dimension and flow velocity of  $VL \sim 1$  m<sup>2</sup>/s. It is this large number, in connection with the precautions that are indispensable for the safe handling of sodium, which had prevented dynamo experiments for a long time.

There are many possibilities to organize a dynamo-active flow in a vessel, and quite a number of them have been tried in experiment. By now, experimental dynamo science is completely international with strong activities in Latvia, Germany, France, US, and Russia. These attempts, only three of which were successful in showing dynamo action, have been summarized in a number of recent review papers [1–6], and some of them are also described in the present special issue. Therefore, in this paper we will restrict our attention to the Riga dynamo experiment, with only a few comparative side-views on other experiments.

## 2. The history of the Riga dynamo experiment

The idea of the Riga dynamo experiment originates from one of the simplest dynamo concepts that was investigated by Ponomarenko in 1973 [7]. The Ponomarenko dynamo consists of one conducting rigid rod which undergoes a spiral motion within – and in gliding contact with – a medium of the same conductivity that extends infinitely in the radial and axial directions. People working on planetary, stellar, or galactic dynamos might be sceptical about the physical relevance of such a system. The first answer to them is that this dynamo represents an “elementary cell” of a number of more complicated dynamos, and in this function it deserves particular attention in its own right. The second answer is that possibly some natural systems work in a similar manner as the Ponomarenko dynamo. One promising candidate is the “double helix nebula” which was detected recently in the outflow from the galactic centre [8]. The basic idea that cosmic jets could work as a Ponomarenko-like dynamo was already discussed in an early paper by Shukurov and Sokoloff [9].

Soon after its invention by Ponomarenko, the dynamo was further analyzed by Gailitis and Freibergs [10] who found a remarkably low critical magnetic Reynolds number for the convective instability of 17.7 (with the radius taken as the defining length scale). An essential step towards an experimental realization was the consideration of a straight back-flow concentric to the inner helical flow, which converts the convective instability into an absolute one [11].

Based on this early analytical and numerical work, a first experimental attempt was undertaken in 1986 by Gailitis et al. [12]. In contrast to the later Riga dynamo experiment, the central helical flow in this experiment was actualized by a spiral flow guide (the “helical labyrinth”) at the entrance of the flow. The main experimental result was the observation of a significant amplification of an externally applied magnetic field. Unfortunately, the experiment had to be stopped due to some construction problems leading to strong mechanical vibrations, and so it is not known if this dynamo would have been able to show self-excitation.

With this experience in mind, it was decided to change slightly the concept of the experiment by replacing the “helical labyrinth” by a propeller and some guiding blades, restricted to the inlet of the central tube. Later we will see that the lack of mechanical constraints along the 3 m distance from the propeller region to the bottom qualifies this dynamo as a markedly *fluid* dynamo, in which the saturation mechanism of the magnetic field strongly relies on the deformability of the velocity field. In addition to the concentric back-flow channel, a third cylinder with sodium at rest was attached in order to further reduce the critical  $Rm$  due to improved boundary conditions for the electric currents.

A good deal of work was devoted to the optimization of the geometry and the details of the flow structure. The main dimensions, i.e. length and the radii of the three cylinders were optimized in [13]. A further idea of optimization relied on the expectation that a flow with maximum helicity (at fixed kinetic energy) should represent a sort of optimum for dynamo action to occur. The calculus of variation for the corresponding problem in cylindrical geometry leads to Bessel functions of the zero and first order for the axial and the azimuthal velocities, respectively. It turned out that

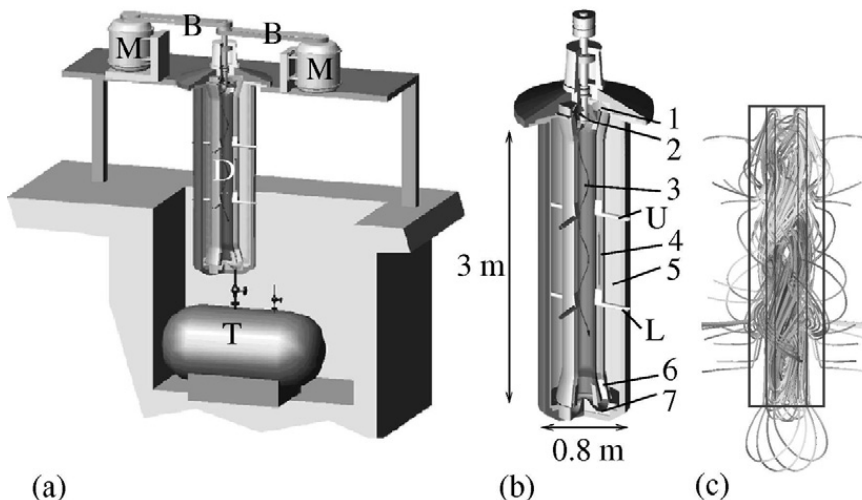


Fig. 1. The Riga dynamo experiment and its eigenfield. (a) Sketch of the Riga dynamo facility. M – Two 100 kW motors. B – Belts from the motors to the propeller shaft. D – Central dynamo module. T – Sodium tank. (b) Details of the central dynamo module. 1 – Upper bending region; 2 – Propeller; 3 – Central helical flow region; 4 – Return-flow region; 5 – Outer sodium region; 6 – Guiding vanes for straightening the flow in the return flow. 7 – Lower bending region. At approximately 1/3 (L) and 2/3 (U) of the dynamo height there are four ports for various magnetic field, pressure and velocity probes. (c) Simulated structure of the magnetic eigenfield in the kinematic regime.

radial flow profiles of this kind lead indeed to a minimum for the critical magnetic Reynolds number [14]. For people familiar with Taylor relaxation and the reversed field pinch [15], in which a turbulent plasma produces a magnetic field of the same Bessel function shape, this might appear as an intriguing duality of velocity optimization and magnetic-field self-organization.

Besides the general problems in setting up a large scale liquid sodium facility, the realization of the desired flow structure was a time-consuming process in particular. Most of the work was done by G. Will, M. Christen and H. Hänel at the Technical University of Dresden, where a 1:2 water dummy model of the Riga sodium facility was built and utilized for flow measurements and optimization [16]. While the propeller geometry was fixed at an early stage, much numerical and experimental effort was needed to find a configuration of pre- and post-propeller vanes suitable to shape the flow as close as possible to the desired Bessel function profiles.

Between 1995 and 1999, the dynamo facility was installed at the Institute of Physics in Salaspils, Latvia (actually, the name “Riga dynamo experiment”, which has been chosen for a better recognizability, is not fully correct, since Salaspils is an independent town 25 km eastward of Riga). The main components of the facility and the structure of the simulated (and experimentally widely confirmed) magnetic eigenfield are shown in Fig. 1.

After all preparations had been done, a first experimental campaign took place on 10–11 November 1999. Before an experiment starts, sodium is usually heated up to 300 °C and pumped slowly through the central module for about 24 hours in order to achieve good electrical contact between sodium and the internal stainless steel walls. It was planned to decrease the temperature to approximately 150 °C since the electrical conductivity and hence the magnetic Reynolds number increase with decreasing temperature. During this cooling-down process, some measurements of the amplification of an externally applied magnetic field were carried out [17,19,20]. Amplification factors up to 25 were identified, with a distinct resonance behaviour at such propeller rotation rates where the frequency of the applied field corresponds to the eigenfrequency of the dynamo. For almost all rotation rates the measured signal had only a single component with the frequency of the applied field. However, at the highest achieved propeller rotation rate of 2150 rpm, an additional exponentially increasing mode was identified with a frequency different from that of the externally applied field (see Fig. 2).

Due to some technical problems arising with the seal, this highest rotation rate had soon to be reduced to 1980 rpm, at which the external field was switched off. This allowed the observation of a pure eigenstate, which was already slowly decaying at this lowered rotation rate [17,18,20]. In hindsight it can be stated that the eigenfrequencies and growth rates measured at these two events fit perfectly into the many other data that were taken in later experimental campaigns. Hence 11 November 1999 marks the first observation of an exponentially growing eigenmode in a liquid metal dynamo experiment.

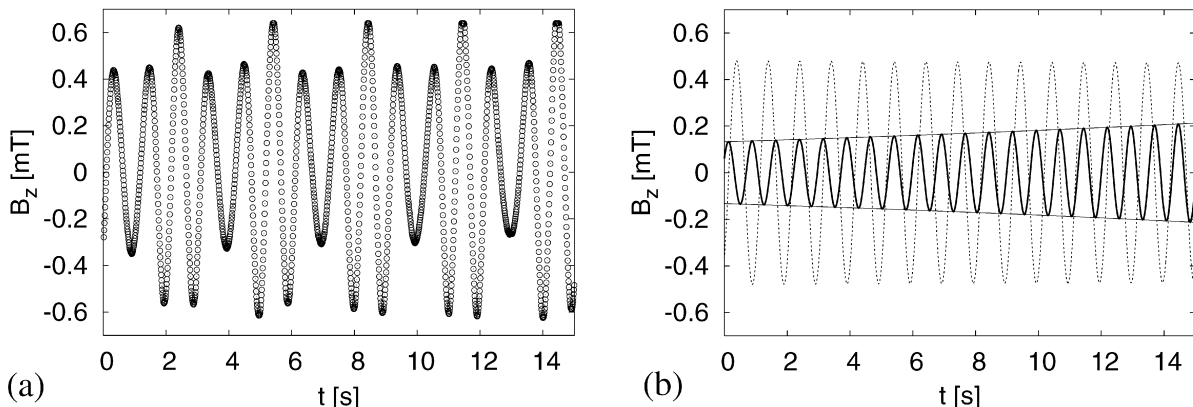


Fig. 2. (a) Axial magnetic field measured by a fluxgate sensor (situated close to the innermost wall) at the highest propeller rotation of 2150 rpm on 11 November 1999. (b) Decomposition of this signal into the amplified externally applied field (dotted line) and the exponentially increasing self-excited dynamo eigenmode (full line).

What was, however, not achieved in this first experimental campaign was the saturated regime of the dynamo in which the Lorentz forces resulting from the self-excited magnetic field reduce the amplitude and modify the structure of the flow velocity in such a way that the growth rate drops down to zero. To observe this saturated state took another 8 months in which a new seal had to be installed. Then, in July 2000, four runs were carried out, partly with, partly without externally applied magnetic fields, which provided a first stock of growth rate, frequency, and spatial structure data of the magnetic eigenfield [21].

A further step towards the detailed determination of the magnetic eigenfield was done in June 2002, when several lances with radially spaced Hall sensors were inserted into the dynamo module.

A somehow frustrating story was the attempt to measure flow velocities in a direct manner. This was, for the first time, tried in February 2003 and reiterated in the July 2003 and May 2004 campaigns, when three ultrasonic transducers were installed at the outer wall in order to measure the velocity in the outermost cylinder of the dynamo. Note that there is no mechanical forcing of the sodium in this outer cylinder, and any significant flow there can only result from the Lorentz forces due to the magnetic eigenfield. This flow structure was numerically estimated to be a main rotation with a velocity of the order of 1 m/s, and a poloidal flow in the form of a double vortex. This flow structure was experimentally confirmed during some runs in the May 2004 campaign, while we failed to study it in more details in further runs. The reason for this failure is not completely clear: it seems that, after some short initial phase in which data can be collected, the Lorentz force induced flow stirs up a lot of oxides in the outer cylinder which then accumulate at the interfaces of the ultrasonic transducers that may act as cold traps.

Another novelty of the May 2004 campaign was the measurements of pressure data in the inner dynamo channel by a piezoelectric sensor that was flash mounted at the innermost wall. These measurements provided not only the expected  $f^{-7/3}$  behaviour of the pressure fluctuations [22], but also the velocity modes at the double and the quadruple of the eigenfrequency of the dynamo which result from the non-axisymmetric parts of the Lorentz forces.

Another attempt to measure velocities in a direct way was undertaken in February/March 2005 when a stainless-steel permanent magnet probe for the determination of flow induced electric potentials was installed. In principle, this probe has provided data on the velocity. However, it was not trivial to disentangle the axial and the azimuthal velocity components from the obtained signals. What was also new in the February/March 2005 campaign was the installation of two traversing rails with Hall sensors moving in axial direction outside the dynamo and induction coils moving in radial direction within the dynamo module. These traversing sensor rails allowed for the detailed determination of the spatial structure of the magnetic eigenfield, the results of which will be published elsewhere.

Fig. 3 shows the axial magnetic field measured by induction coils inside the upper and the lower port close to the innermost wall during the last run on 1 March 2005. This figure might serve as an example on how the magnetic field can be switched on and off at will, and on how its amplitude depends on the propeller rotation rate. Comparing Figs. 3(a) and 3(b), a peculiarity of this dependence becomes visible. Whereas at the upper sensor (Fig. 3(b)) the field amplitude increases from 27 mT for 2000 rpm to 120 mT for 2500 rpm, at the lower sensor (Fig. 3(a)) the corresponding increase is only from 24 mT to 65 mT. This is a clear indication for a drastic change of the field

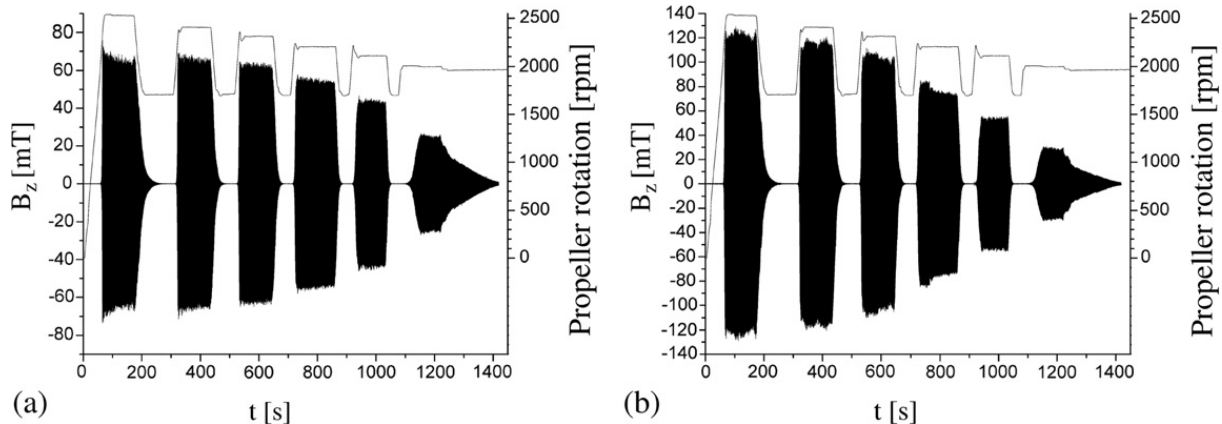


Fig. 3. Axial magnetic field and propeller rotation rate during the run 6 of the February/March 2005 campaign, measured by induction coils within the lower (a) and upper (b) port, close to the innermost wall where the axial magnetic field has its maximum.

dependence in axial direction with increasing supercriticality of the dynamo, which in turn mirrors a significant change of the axial dependence of the flow.

The most recent campaign was undertaken in July 2007, after which the outworn gliding ring seal for the propeller shaft was replaced by a magnetic coupler which had been designed and produced by SERAS-CNRS in Grenoble. After a few successful runs had been done with this magnetic coupler, the experiment had to be stopped due to fact that the belts between the motors and the propeller shaft were broken.

### 3. Summary of main results

The most significant number for the qualification of a dynamo is the growth rate of the magnetic field eigenmode. In the subcritical regime, this negative number can either be obtained after switching off an externally applied magnetic field or by lowering the propeller rotation rate from supercritical to subcritical and tracing again the following exponential decay of the eigenfield. When the dynamo is driven into the supercritical state, there are typically a few seconds during which the field is still weak enough so that the dynamo can be considered as a kinematic one. Since the Riga dynamo has a complex eigenvalue, there is also a rotation frequency of the eigenfield which can easily be determined both in the kinematic and in the saturated regime.

During the eight experimental campaigns, plenty of growth rate and frequency measurements were carried out. When scaled appropriately by the temperature dependent conductivity of sodium, both quantities turned out to be reproducible over the years. Only a slight change appeared, starting with the June 2002 campaign when a lance with sensors was inserted into the central helical flow leading to a slight additional braking of the flow and a corresponding slight decrease of the growth rate.

In Fig. 4, the temperature corrected measurements for the growth rate (Fig. 4(a)) and the frequency (Fig. 4(b)) are shown in comparison with the corresponding numerical results. The numerical curves in the kinematic regime were obtained with the 2D solver [14,27] and were corrected for the slight effect of the lower conductivity of the stainless steel walls that was estimated separately by a 1D solver. As for the saturation regime we have tried to identify the most important back-reaction effect within a simple one-dimensional model [19,26]. While the axial velocity component has to be rather constant from top to bottom due to mass conservation, the azimuthal component  $v_\phi$  can be easily braked by the Lorentz forces without any significant pressure increase. In the inviscid approximation, and considering only the  $m = 0$  mode of the Lorentz force, we end up with the ordinary differential equation for the Lorentz force induced perturbation  $\delta v_\phi(r, z)$  of the azimuthal velocity component:

$$\bar{v}_z(r, z) \frac{\partial}{\partial z} \delta v_\phi(r, z) = \frac{1}{\mu_0 \rho} [(\nabla \times \mathbf{B}) \times \mathbf{B}]_\phi(r, z) \quad (2)$$

In contrast to the procedure described in [19,27] where we had utilized the measured Joule power at a given supercriticality to calibrate the Lorentz force on the r.h.s of Eq. (2), here we solve Eq. (2) simultaneously with the induction equation. Note that Eq. (2) is solved both in the innermost channel where it describes the downward braking of  $v_\phi$ , as well as in the back-flow channel where it describes the upward acceleration of  $v_\phi$ . Both effects lead to a reduction

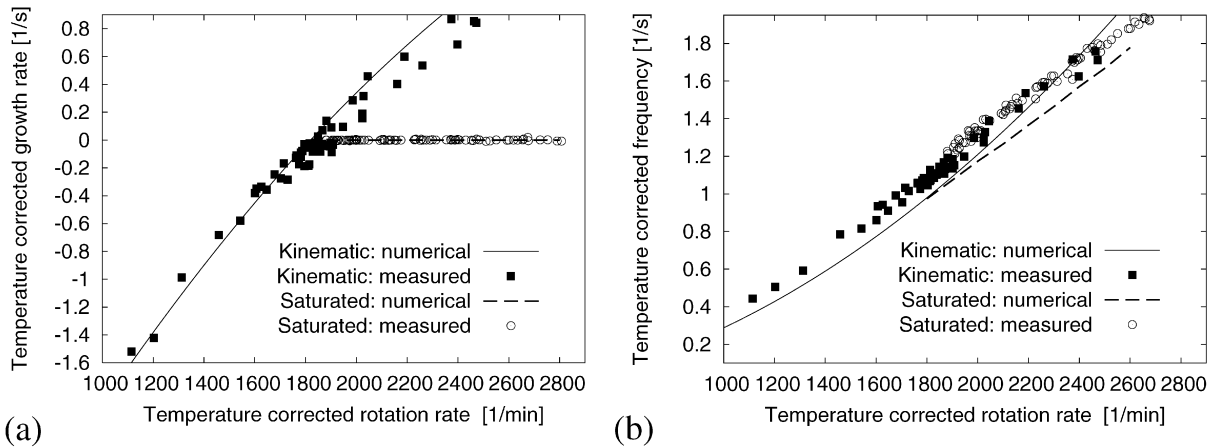


Fig. 4. Measured and computed growth rates (a) and frequencies (b) in the kinematic and saturated regime.

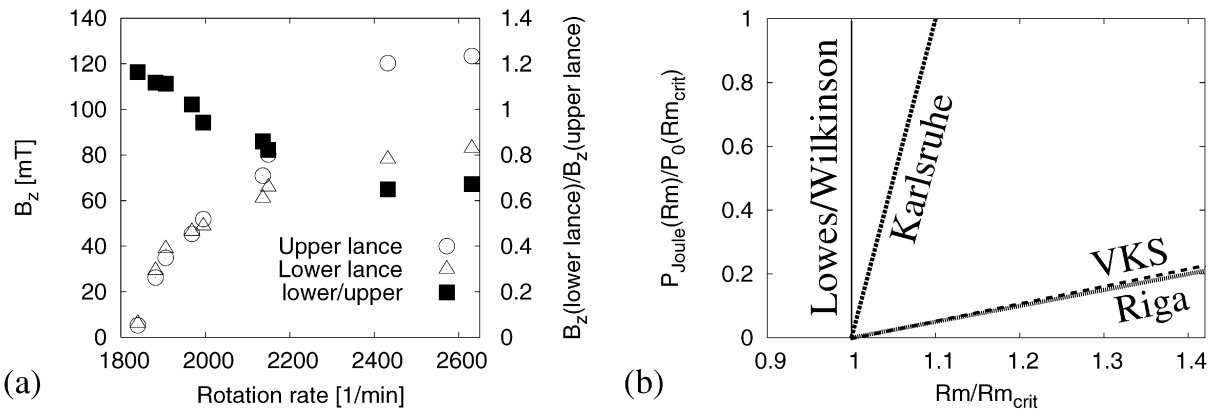


Fig. 5. (a) Decreasing ratio of fields at magnetic field sensors at the lower and upper lances. (b) The difference between experimental dynamos manifests itself in the steepness of the Joule power curve beyond the critical  $Rm_c$ . The more flexible a dynamo is, the easier it can refrain from producing more magnetic field.

of the differential rotation and hence to a deterioration of the dynamo capability of the flow. The validity of this self-consistent back-reaction model, which gives automatically a zero growth rate, can be judged from the dependence of the resulting eigenfrequency in Fig. 4(b). Actually, we see a quite reasonable correspondence with the measured data, in particular with respect to the slope of the curve. A slight jump of the measured eigenfrequencies between the kinematic and the saturated regime could be attributed to the arising fluid rotation in the outermost cylinder, which is not described by the back-reaction model according to Eq. (2). Other criteria for the quality of the back-reaction models are the correspondence of the resulting amplitude and shape of the eigenfield which also turned out to be quite satisfactory.

The braking of the azimuthal velocity component, which accumulates downstream from the propeller, results in a deteriorated self-excitation capability of the flow in the lower parts of the dynamo and therefore in an upward shift of the magnetic field structure. This is visible in Fig. 5(a) which shows the measured axial magnetic field amplitudes (from the June 2002 campaign) at the upper and lower ports and their ratio in dependence on the supercriticality. Corresponding dependencies for the outer Hall sensors were already documented in Fig. 12 of [20].

This deformation of the flow field under the influence of the Lorentz force of the self-excited magnetic field has a strong impact on the dependence of dissipated Joule power on the supercriticality. In Fig. 5(b) we try to compare the corresponding curves for the Lowes and Wilkinson experiment [23], the Karlsruhe experiment [24], the VKS experiment [25], and the Riga experiment. Deliberately, we have given only a schematic plot of these dependencies since all four curves are not very accurately known. For the Lowes and Wilkinson case we refer to their paper [23], for the Karlsruhe results we rely on the pressure increase shown in the inset of Fig. 4 in [24], for VKS we took the mean value between the estimates 15 and 20 per cent for a supercriticality of 30 per cent [25], for Riga we took the

fit  $P_{\text{Joule}} = (\Omega - 1840 \text{ rpm})/(1840 \text{ rpm}) \times 48.4 \text{ kW}$  of the motor power measurements published in [27]. In stark contrast to the sharp rise for the Lowes and Wilkinson experiment, but also strongly differing from the steep increase in the Karlsruhe experiment, the Joule power dependence on supercriticality in both the VKS and the Riga experiment is very flat. For the latter we had already seen that, quite different to the back-reaction of a rigid body, the sodium flow deforms under the influence of the Lorentz forces, and the resulting deterioration of the dynamo condition makes the growth rate drop down to zero.

#### 4. Conclusions

The Riga dynamo experiment, which relies on the concept of the Ponomarenko dynamo, was the first successful liquid metal experiment in which the critical magnetic Reynolds number had been exceeded. Its kinematic regime has been simulated by a 2D-dimensional finite-difference solver with an accuracy of a few percent, and its saturated regime is qualitatively well understood by means of a simplified one-dimensional back-reaction model that accounts for the downward braking of the azimuthal component of the flow. The detailed measurements of the spatial structure of the magnetic eigenfield in dependence on the supercriticality make the Riga dynamo an ideal test-field for validating various MHD-turbulence models in a contemporary three-dimensional RANS model [28–30].

Contrary to what is sometimes written in the literature, the Riga dynamo has a highly unconstrained flow: the volume fraction in which the fluid flow is directly imposed by the propeller or by guiding blades is only 10 percent of the free flow volume behind the propeller. Interestingly, this is the same 10 per cent ratio as in the VKS experiment, hence it is not surprising that the slope of the Joule power curve is approximately the same in both experiments (see Fig. 5(b)). In contrast to the VKS experiment, the turbulence level in the Riga experiment is rather low (approximately 8%, depending on the position). The good correspondence of numerical predictions (based on the mean flow) with experimental data indicates that fluctuations of this level do not play a significant role in the dynamo mechanism.

A drawback of the Riga dynamo could be seen in the fact that it is definitely not suited for any investigation of field reversals since it is an oscillatory dynamo from the very outset. By virtue of its flow topology (a s1t1 in the terminology of Dudley and James [31]) there is no chance to observe any reversal process which, we believe, is connected with a transition between steady and oscillatory eigenvalues of the non-selfadjoint dynamo operator [32]. Such reversal studies have to be left to dynamo experiments with other flow topologies, e.g. of the s2t2 type as in the VKS experiment, in which reversals were actually observed [33].

The Riga dynamo is still operating. Further improvements of the velocity and magnetic field measuring techniques are planned and will possibly help to constrain turbulence models of flows under the influence of a self-excited magnetic field.

#### Acknowledgements

A significant number of people were involved in the construction of the facility and in carrying out the experimental campaigns. In particular, we are grateful to Arnis Cifersons, Sergej Dement'ev, Janis Zandarts, Anatolii Zik, Michael Christen, Heiko Hänel, and Gotthard Will.

We thank the Latvian Science Council for support under Grants Nos. 96.0276 and 01.0502, the Deutsche Forschungsgemeinschaft for support under INK 18/A1-1 and SFB 609, and the European Commission for support under HPRI-CT-2001-50027 and 028679.

#### References

- [1] P. Chossat, D. Armbruster, I. Oprea (Eds.), *Dynamo and Dynamics, A Mathematical Challenge*, Springer, Berlin, 2001.
- [2] K.-H. Rädler, *Magnetohydrodynamics* 38 (1–2) (2002).
- [3] A. Gailitis, O. Lielausis, E. Platacis, G. Gerbeth, F. Stefani, *Rev. Mod. Phys.* 74 (2002) 973–990.
- [4] A. Tilgner, *Astron. Nachr.* 323 (2002) 407–410.
- [5] A. Gailitis, O. Lielausis, G. Gerbeth, F. Stefani, *Dynamo experiments*, in: S. Molokov, et al. (Eds.), *Magnetohydrodynamics – Historical Evolution and Trends*, Springer, Berlin, 2007, pp. 37–54.
- [6] F. Pétrélis, N. Mordant, S. Fauve, *Geophys. Astrophys. Fluid Dyn.* 101 (2007) 289–323.
- [7] Yu.B. Ponomarenko, *J. Appl. Mech. Tech. Phys.* 14 (1973) 775–779.
- [8] M. Morris, K. Uchida, T. Do, *Nature* 440 (2006) 308–310.

- [9] A. Shukurov, D.D. Sokoloff, Hydromagnetic dynamo in astrophysical jets, in: Cosmic Dynamo, in: IAU Symposia, vol. 157, Kluwer, Dordrecht, 1993, pp. 367–371.
- [10] A. Gailitis, Ya. Freibergs, Magnetohydrodynamics 12 (1976) 127–129.
- [11] A. Gailitis, Ya. Freibergs, Magnetohydrodynamics 16 (1980) 116–121.
- [12] A. Gailitis, B.G. Karasev, I.R. Kirillov, O.A. Lielausis, S.M. Luhanskii, A.P. Ogorodnikov, G.V. Preslitskii, Magnetohydrodynamics 23 (1987) 349–353.
- [13] A. Gailitis, Magnetohydrodynamics 32 (1996) 58–62.
- [14] F. Stefani, G. Gerbeth, A. Gailitis, Velocity profile optimization for the Riga dynamo experiment, in: A. Alemany, Ph. Marty, J.P. Thibault (Eds.), Transfer Phenomena in Magnetohydrodynamic and Electroconducting Flows, Kluwer, Dordrecht, 1999, pp. 31–44.
- [15] J.B. Taylor, Rev. Mod. Phys. 58 (1986) 741–763.
- [16] M. Christen, H. Hänel, G. Will, Entwicklung der Pumpe für den hydrodynamischen Kreislauf des Rigaer “Zylinderexperimentes”, in: W.H. Faragallah, G. Grabow (Eds.), Beiträge zu Fluidenergiemaschinen 4, Faragallah-Verlag und Bildarchiv, Sulzbach/Ts., 1998, pp. 111–119.
- [17] A. Gailitis, O. Lielausis, S. Dement'ev, E. Platacis, A. Cifersons, G. Gerbeth, Th. Gundrum, F. Stefani, M. Christen, H. Hänel, G. Will, Phys. Rev. Lett. 84 (2000) 4365–4368.
- [18] A. Gailitis, O. Lielausis, E. Platacis, G. Gerbeth, F. Stefani, Magnetohydrodynamics 37 (2001) 71–79.
- [19] A. Gailitis, O. Lielausis, E. Platacis, S. Dement'ev, A. Cifersons, G. Gerbeth, Th. Gundrum, F. Stefani, M. Christen, G. Will, Magnetohydrodynamics 38 (2002) 5–14.
- [20] A. Gailitis, O. Lielausis, E. Platacis, G. Gerbeth, F. Stefani, Surv. Geophys. 24 (2003) 247–267.
- [21] A. Gailitis, O. Lielausis, E. Platacis, S. Dement'ev, A. Cifersons, G. Gerbeth, Th. Gundrum, F. Stefani, M. Christen, G. Will, Phys. Rev. Lett. 86 (2001) 3024–3027.
- [22] A. Gailitis, O. Lielausis, E. Platacis, F. Stefani, G. Gerbeth, Laboratory astrophysics as exemplified by the Riga dynamo experiment, in: R. Rosner, G. Rüdiger, A. Bonanno (Eds.), MHD Couette flows – Experiments and Models, in: AIP Conference Proceedings, vol. 733, AIP, Melville, NY, 2004, pp. 35–44.
- [23] I. Wilkinson, Geophys. Surveys 7 (1984) 107–122.
- [24] R. Stieglitz, U. Müller, Magnetohydrodynamics 38 (2002) 27–33.
- [25] R. Monchaux, et al., Phys. Rev. Lett. 98 (2007) 044502.
- [26] A. Gailitis, O. Lielausis, E. Platacis, G. Gerbeth, F. Stefani, Magnetohydrodynamics 38 (2002) 15–26.
- [27] A. Gailitis, O. Lielausis, E. Platacis, G. Gerbeth, F. Stefani, Phys. Plasmas 11 (2004) 2838–2843.
- [28] S. Kenjereš, K. Hanjalić, S. Renaudier, F. Stefani, G. Gerbeth, A. Gailitis, Phys. Plasmas 13 (2006) 122308.
- [29] S. Kenjereš, K. Hanjalić, Phys. Rev. Lett. 98 (2007) 104501.
- [30] S. Kenjereš, K. Hanjalić, New J. Phys. 9 (2007) 306.
- [31] M.L. Dudley, R.W. James, Proc. R. Soc. Lond. A 425 (1989) 407–429.
- [32] F. Stefani, G. Gerbeth, Phys. Rev. Lett. 94 (2005) 184506.
- [33] M. Berhanu, Europhys. Lett. 77 (2007) 59001.

# Magnetohydrodynamic experiments on cosmic magnetic fields

Frank Stefani<sup>1,\*</sup>, Agris Gailitis<sup>2\*\*</sup>, and Gunter Gerbeth<sup>1\*\*\*</sup>

<sup>1</sup> Forschungszentrum Dresden-Rossendorf, P.O. Box 510119 Dresden, Germany

<sup>2</sup> Institute of Physics, University of Latvia, LV-2169 Salaspils 1, Latvia

Received XXXX, revised XXXX, accepted XXXX

Published online XXXX

**Key words** Magnetohydrodynamics, Dynamo, Magnetorotational instability

**MSC (2000)** 04A25

It is widely known that cosmic magnetic fields, i.e. the fields of planets, stars, and galaxies, are produced by the hydromagnetic dynamo effect in moving electrically conducting fluids. It is less well known that cosmic magnetic fields play also an active role in cosmic structure formation by enabling outward transport of angular momentum in accretion disks via the magnetorotational instability (MRI). Considerable theoretical and computational progress has been made in understanding both processes. In addition to this, the last ten years have seen tremendous efforts in studying both effects in liquid metal experiments. In 1999, magnetic field self-excitation was observed in the large scale liquid sodium facilities in Riga and Karlsruhe. Recently, self-excitation was also obtained in the French "von Kármán sodium" (VKS) experiment. An MRI-like mode was found on the background of a turbulent spherical Couette flow at the University of Maryland. Evidence for MRI as the first instability of an hydrodynamically stable flow was obtained in the "Potsdam Rossendorf Magnetic Instability Experiment" (PROMISE). In this review, the history of dynamo and MRI related experiments is delineated, and some directions of future work are discussed.

Copyright line will be provided by the publisher

## 1 Once upon a time...

Magnetism has been known for approximately 3000 years. There is some evidence that a hematite bar, found close to Veracruz (now Mexico), had served the Olmecs as a simple compass [29]. In any case, the Chinese have built, probably in the first century B.C., a compass in the form of a lodestone spoon that was freely turnable on a polished bronze plate [155]. The old Greek philosophers, starting with Thales of Miletus [2], were well aware of the attracting forces of lodestone, and the Roman philosopher Lucretius (95?-55 B.C.) described its action in an atomistic way [140]: "First, stream there must from off the lode-stone seeds. Innumerable, a very tide, which smites by blows that air asunder lying betwixt the stone and iron. And when is emptied out this space, and a large place between the two is made a void, forthwith the primal germs of iron, headlong slipping, fall conjoined into the vacuum, and the ring itself by reason thereof doth follow after and go thuswise with all its body."

As early as 1269, a first systematic experimental study of the attracting and repelling forces of lodestone was published by Petrus Peregrinus in his "Epistola de magnete" [169]. For the first time, he defined the concept of polarity and distinguished the north and south poles of the magnet. He was the first to formulate the law that poles of opposite polarity attract while poles of the same polarity repel each other (cf. Figure 1a). Besides the construction of several compasses (cf. Figure 1b), he also proposed a magnetic perpetuum mobile.

Three centuries later, Peregrinus' work inspired William Gilbert to make his own experiments with small spheres of lodestone ("terrellae"), which led him, in 1600, to the conclusion that "...that the terrestrial globe is magnetic and is a lodestone [79]"

However, this lodestone theory soon ran into trouble when the westward drift of the Earth's magnetic field declination was described by Gellibrand in 1635 [76], and the detection of abrupt polarity reversals by David and Brunhes in 1904/05 [21] has dealt it the ultimate deathblow.

Interestingly, it was not the well-studied magnetic field of the Earth, but the observation of magnetic fields in sunspots [87], that put Larmor on the right track speculating [127] that it could be "...possible for the internal cyclic motion to act after the manner of the cycle of a *self-exciting dynamo*, and maintain a permanent magnetic field from insignificant

---

\* Corresponding author, e-mail: F.Stefani@fzd.de, Phone: +49 351 260 3069, Fax: +49 351 260 2007

\*\* gailitis@sal.lv

\*\*\* G.Gerbeth@fzd.de

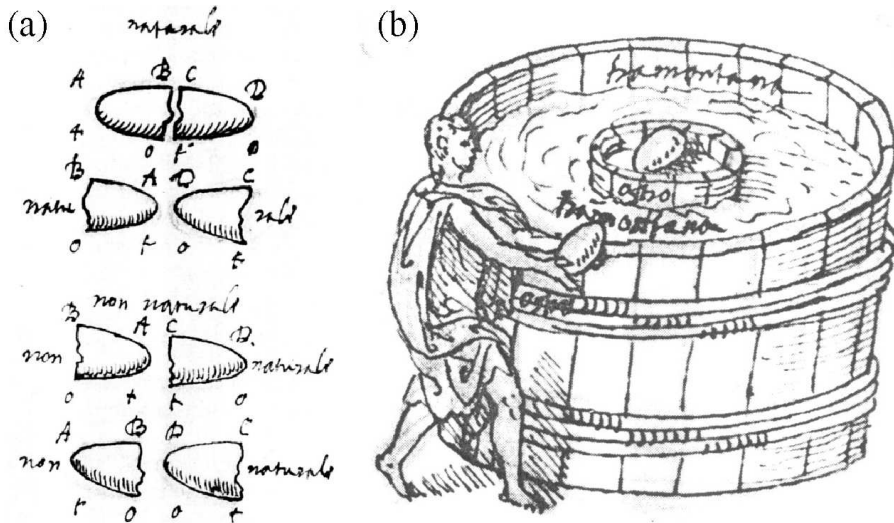


**Fig. 1** Lodestone experiments of Petrus Peregrinus. (a) Experiments showing the attracting and repelling forces of broken piece of loadstone. Upper configuration: "naturale", lower configuration: "non naturale". (b) A simple compass. Figures from [169].

beginnings, at the expense of some of the energy of the internal circulation." This one-page communication, in which a natural process was explained in terms of a technical device [208, 209, 257], was the birth certificate of the modern hydromagnetic theory of cosmic magnetic fields.

## 2 Cosmic magnetism

Wherever in the cosmos a large quantity of an electrically conducting fluid is found in convection, one can also expect a magnetic field to be around.

The Earth is not the only planet in the solar system with a magnetic field [144, 233]. Fields are produced inside the gas giants Jupiter, Saturn and the ice giants Uranus, and Neptune. Possibly, a dynamo had worked inside Mars in the ancient past [41]. The Mariner 10 mission in 1974-75 had revealed the magnetic field of Mercury [156] and there remain many puzzles as to how it can be produced [212, 35, 81, 82]. The detection of the magnetic field of Ganymede, the largest Jupiter moon, was one of the major discoveries of NASA's Galileo spacecraft mission in 1996 [114]. The fact that Venus does not have a dynamo generated magnetic field has been attributed to the very slow rotation [144], but also to the stably stratified liquid core [232] of this planet.

The magnetic fields of sunspots were discovered by Hale (1908) at Mt. Wilson observatory, thus proving evidence that natural magnetism is not a phenomenon restricted to the Earth. With view on the tight relation of sunspots and magnetic fields, sunspot observation turns into a perfect test field for any theory of solar magnetism. Still today, the 11 year periodicity of sunspots, their migration towards the equator (the "butterfly diagram"), and the occurrence of grand minima which are superimposed upon the main periodicity are the subject of intensive investigations [160].

Some main-sequence stars of spectral type A have remarkable magnetic field strengths on the order of 1 T which are hardly explainable by dynamo action and which have been claimed to be remnants of the star's formation, i.e. "fossil fields" [17]. However, this magnetic field strength is rather moderate compared with that of other stars. The field of some white dwarfs can easily reach values of 100 T, and even fields of  $10^{11}$  T have been ascribed to some anomalous X-ray emitting pulsars [117].

Large-scale magnetic fields of the order of  $10^{-9}$  T are observed in many spiral galaxies [11]. Usually there is a close correlation of the magnetic field structure with the spiral pattern that indicates the relevance of dynamo action, although by far not all problems with the origin and amplitude of galactic seed fields are solved [85, 123, 48].

Fascinating phenomena appear close to the centers of galaxies which are usually occupied by supermassive black holes. These are fed by so-called accretion disks [9], a process which results typically in two oppositely directed jets of high-energetic particles that can fill vast volumes with magnetic field energy [120]. In our galaxy, these jets are rather weak but show a particularly interesting feature. Morris et al. recently reported the detection of a double-helix nebula in this outflow,

not far from the galactic center, which they described as an Alfvén wave [148]. However, we will see later that this might well be connected with a typical dynamo action.

The working principle of accretion disks, which are the most efficient "powerhouses" in the universe [88] supplying energy for systems such as X-ray binaries, active galactic nuclei, and quasars through the release of gravitational potential energy, had been a puzzle for a long time. The problem is that matter, before it can be accreted by the central object, has to get rid off its angular momentum. The molecular viscosity of such gas disks is much to small to explain the observed accretion rates of stars and black holes, so that turbulent viscosity has to be assumed [204]. The point is only: why accretion disks are turbulent at all? Since they obey Kepler's third law, i.e., their angular velocity decays as  $r^{-3/2}$  with the radius, while the angular momentum increases as  $r^{1/2}$ , Rayleigh's criterion must be applied stating that rotating flows with radially increasing angular momentum are linearly stable for all Reynolds numbers [184]. In principle, the solution to this puzzle was already given in papers by Velikhov in 1959 [247] and Chandrasekhar in 1960 [30], who had detected that a Taylor-Couette flow in the hydrodynamically stable regime could be destabilized by an axially applied magnetic field. The astrophysical importance of this "magnetorotational instability" was, however, noticed by Balbus and Hawley in their seminal paper of 1991 [7].

Going beyond the galactic scale, we find randomly tangled magnetic fields also in galaxy clusters [84] which brings us to the topic of *fluctuation dynamos* (or *small-scale dynamos*) which have attracted much interest recently [198, 199].

### 3 Some mathematical basics

The temporal evolution of the velocity field  $\mathbf{v}$  under the influence of a magnetic field  $\mathbf{B}$  is governed by the Navier-Stokes equation

$$\frac{\partial \mathbf{v}}{\partial t} + (\mathbf{v} \cdot \nabla) \mathbf{v} = -\frac{\nabla p}{\rho} + \frac{1}{\mu_0 \rho} (\nabla \times \mathbf{B}) \times \mathbf{B} + \nu \Delta \mathbf{v} + \mathbf{f}_d , \quad (1)$$

where  $\rho$  and  $\nu$  denote the density and the kinematic viscosity of the fluid,  $p$  is the pressure,  $\mu_0$  the magnetic permeability of the vacuum, and  $\mathbf{f}_d$  symbolizes driving forces as, e.g., buoyancy in cosmic bodies or mechanical forcing by propellers in liquid metal experiments. The magnetic field  $\mathbf{B}$  in equation (1) is in general the sum of an externally applied magnetic field and the flow induced or self-excited magnetic field.

In order to derive the temporal evolution for  $\mathbf{B}$  in a fluid of electrical conductivity  $\sigma$ , we start with Ampère's law, Faraday's law, the divergence-free condition for the magnetic field, and Ohm's law in moving conductors:

$$\nabla \times \mathbf{B} = \mu_0 \mathbf{j} \quad (2)$$

$$\nabla \times \mathbf{E} = -\dot{\mathbf{B}} \quad (3)$$

$$\nabla \cdot \mathbf{B} = 0 \quad (4)$$

$$\mathbf{j} = \sigma(\mathbf{E} + \mathbf{v} \times \mathbf{B}) . \quad (5)$$

Here,  $\mathbf{E}$  denotes the electric field and  $\mathbf{j}$  denotes the electric current density. We have skipped the displacement current in equation (2) as in most relevant cases the quasistationary approximation holds. Taking the *curl* of equations (2) and (5), inserting equation (3), and assuming  $\sigma$  to be constant in the considered region, one readily arrives at the *induction equation* for the magnetic field:

$$\frac{\partial \mathbf{B}}{\partial t} = \nabla \times (\mathbf{v} \times \mathbf{B}) + \frac{1}{\mu_0 \sigma} \Delta \mathbf{B} . \quad (6)$$

Obviously, the right hand side of equation (6) describes the competition between the diffusion and the advection of the field. For  $\mathbf{v} = 0$  equation (6) reduces to a vector heat equation and the field will decay within a typical time  $t_d = \mu_0 \sigma l^2$ , with  $l$  being a typical length scale of the considered system. Switching on the advection term, it can lead to an increase of  $\mathbf{B}$  within a kinematic time  $t_k = l/v$ , where  $v$  is a typical velocity of the flow. If the kinematic time is smaller than the diffusion time, the net effect can become positive, and the field will grow. Comparing the diffusion time-scale with the kinematic time-scale we get a dimensionless number that governs the "fate" of the magnetic field which is called magnetic Reynolds number  $Rm$ :

$$Rm := \mu_0 \sigma l v . \quad (7)$$

Depending on the flow pattern, the values of the critical  $Rm$ , at which the field starts to grow, are usually in the range of  $10^1 \dots 10^3$ . Most flows in cosmic bodies, in which  $Rm$  is large enough, will act as dynamos, although there are a number of anti-dynamo theorems excluding too simple structures of the velocity field or the self-excited magnetic field [42, 51, 189, 97, 104].

The competition between field dissipation and production can also be understood in terms of the energy balance. Taking the scalar product of the induction equation with  $\mathbf{B}/\mu_0$ , and performing an integration by parts, we find for the time evolution of the magnetic energy

$$\frac{d}{dt} \int_V \frac{\mathbf{B}^2}{2\mu_0} dV = - \int_V \mathbf{v} \cdot (\mathbf{j} \times \mathbf{B}) dV - \int_V \frac{\mathbf{j}^2}{\sigma} dV - \frac{1}{\mu_0} \oint_S (\mathbf{E} \times \mathbf{B}) \cdot d\mathbf{S}. \quad (8)$$

In this form, the dynamo action can be interpreted in a convenient way: the time derivative of the magnetic field energy equals the difference between the work done (per time) by the Lorentz forces on one side and the Ohmic and Poynting flux losses on the other side. The Lorentz force converts kinetic energy into magnetic energy, the Ohmic dissipation converts magnetic energy into heat, the Poynting flux transports electromagnetic energy across the surface  $S$  of the considered volume  $V$ .

Besides the magnetic Reynolds number  $Rm$ , the coupled system of Eqs. (1) and (6) is governed by some more dimensionless numbers: first of all the well known Reynolds number  $Re := lv/\nu$ , second the Hartmann number  $Ha := Bl\sqrt{\sigma/\nu\rho}$  which describes the square root of the ratio of magnetic to viscous forces. In some cases, the system behaviour is better described by the interaction parameter (Stuart number)  $N = \sigma B^2 l / (v\rho) = Ha^2/Re$  or the Lundquist number  $S := Bl\sigma\sqrt{\mu_0/\rho} = Ha\sqrt{Pm}$ , wherein the magnetic Prandtl number is defined as the ratio of kinematic viscosity to magnetic diffusivity:  $Pm := \nu\mu_0\sigma$ . Of course, more dimensionless numbers will enter the scene when a particular forcing and/or global rotation of the system is taken into account.

The coupled system of equations (1) and (6) can be treated with varying complexity. For many technologically relevant cases, but also for the "helical MRI" to be discussed later, with  $Rm \ll 1$ , it will suffice to use the so-called inductionless approximation [173]. On the other extreme, one can study "kinematic dynamo models" by just solving equation (6) while supposing  $\mathbf{v}$  to be fixed. In general, however, the treatment of most magnetic instabilities and of dynamically consistent dynamos requires the simultaneous solution of equations (1) and (6).

The numerical costs of the simulations are strongly governed by the relevant spatial dimension of the considered system. In some cases, including long cylindrical dynamos with axially invariant flows or long MRI experiments based on Taylor-Couette flows, it is appropriate to start with an analysis of normal modes in axial and azimuthal directions giving an eigenvalue problem in  $r$  direction only. For dynamo or MRI experiments in finite cylinders, 2D models in  $r, z$  will be appropriate. Most expensive are, of course, fully coupled 3D simulations of Eqs. (1) and (6).

Dynamo relevant flows are in general turbulent, the question is only about the turbulence level and its role in the dynamo process. Commonly, one distinguishes between so-called *laminar* and *mean-field* dynamo models. Laminar models are described by the unchanged equation (6) with neglected turbulence. The self-excited magnetic field varies on the same length scale as the velocity field does. Mean-field dynamo models, on the other hand, are relevant for highly turbulent flows. In this case the velocity and the magnetic field are considered as superpositions of mean and fluctuating parts,  $\mathbf{v} = \bar{\mathbf{v}} + \mathbf{v}'$  and  $\mathbf{B} = \bar{\mathbf{B}} + \mathbf{B}'$ . From equation (6) we get the equation for the mean part  $\bar{\mathbf{B}}$ ,

$$\frac{\partial \bar{\mathbf{B}}}{\partial t} = \nabla \times (\bar{\mathbf{v}} \times \bar{\mathbf{B}} + \mathcal{E}) + \frac{1}{\mu_0\sigma} \Delta \bar{\mathbf{B}}. \quad (9)$$

This equation for the mean field is identical to equation (6) for the original field, except for one additional term

$$\mathcal{E} = \overline{\mathbf{v}' \times \mathbf{B}'}, \quad (10)$$

that represents the mean electromagnetic force (emf) due to the fluctuations of the velocity and the magnetic field. The elaboration of mean-field dynamo models in the sixties by Steenbeck, Krause and Rädler [216] was a breakthrough in dynamo theory (cf. [119, 180]). They had shown that, for homogeneous isotropic turbulence, the mean electromotive force takes on the form

$$\mathcal{E} = \alpha \bar{\mathbf{B}} - \beta \nabla \times \bar{\mathbf{B}}, \quad (11)$$

with a parameter  $\alpha$  that is non-zero only for non-mirrorsymmetric velocity fluctuations  $\mathbf{v}'$  ("cyclonic motion" [161]) and a parameter  $\beta$  that describes the enhancement of the electrical resistivity due to turbulence. The fact that helical fluid motion can induce an emf that is *parallel* to the magnetic field is now commonly known as the  $\alpha$ -effect. Dynamo models based on the  $\alpha$ -effect have played an enormous role in the study of solar and galactic magnetic fields, and we will later explain the physics of the Karlsruhe experiment in terms of a mean-field model with the  $\alpha$ -effect.

A promising way to combine the credibility of direct numerical simulations with the convenience (and robustness) of mean-field models is to carry out global 3D simulations at affordable spatial resolution, and to extract then the mean-field coefficients by means of a test-field method [202, 203, 77, 19].

## 4 Why doing liquid metal experiments?

During recent decades tremendous progress has been made in the analytical understanding and the numerical treatment of flows with high  $Rm$ , including dynamos, which has been reported in dozens of monographs and review articles [24, 145, 119, 95, 190, 191, 31, 91, 144, 50, 192, 25, 26, 193, 18].

As for the geodynamo, to take one example, recent numerical simulations [83, 103, 122, 27, 33, 36, 254, 230, 89, 4, 231] share their main results with features of the Earth's magnetic field, including the dominance of the axial dipolar component, weak non-dipolar structures, and, in some cases, full polarity reversals, a behaviour that is well known from paleomagnetic measurements (for a recent overview, see [116]).

Despite those successes, a number of unsolved problems remain. The simulations of the Earth's dynamo, to remain in this picture for the moment, are carried out in parameter regions far from the real one. This concerns, in particular, the Ekman number  $E$  (the ratio of the rotation time scale to the viscous time scale) and the magnetic Prandtl number  $Pm$  (the ratio of the magnetic diffusion time to the viscous diffusion time). The Ekman number of the Earth is of the order  $10^{-15}$ , the magnetic Prandtl number is of the order  $10^{-6}$ . Present numerical simulations are carried out for values as small as  $E \sim 10^{-5}$  and  $Pm \sim 0.1$ . The wide gap between real and numerically tractable parameters is, of course, a continuing source of uncertainty about the physical reliability of those simulations. The usual way in fluid dynamics to deal with parameter discrepancies of this sort, namely to apply sophisticated turbulence models, is presently hampered by the lack of validated turbulence models for fluids that are both fast rotating and strongly interacting with a magnetic field. Here is the crucial point where laboratory experiments are unavoidable in order to collect knowledge about the turbulence structure in the (rotating or not) dynamo regime.

With this critical attitude towards simulations, one must likewise admit that none of the real cosmic bodies can be put into a *Bonsai form* to be studied in laboratory. Taking again the geodynamo as a (striking) example, it is not possible to actualize all of the dimensionless numbers in an equivalent experimental set-up. A liquid sodium experiment of 1 m radius would have to rotate with  $10^8$  (!) rotations per second in order to reach the Ekman number of the Earth, which amounts to twice the speed of light at the rim of the vessel.

So what, then, can we actually learn from liquid metal experiments ?

*First*, it is worthwhile to verify experimentally that hydromagnetic dynamos work at all. In theory and numerics, kinematic dynamo action has been proved for a large variety of more or less smooth velocity fields or pre-described distributions of turbulence parameters. However, liquid metal flows, at the necessary  $Rm$ , will be highly turbulent. Further, most dynamo simulations have been carried out in spherical geometry. What happens when we are using cylindrical vessels instead of spheres? How important is the correct implementation of the non-local boundary conditions for the magnetic field, which is trivial for spherical geometry but requires sophisticated methods in other, e.g. cylindrical, geometry [220, 259, 260, 96, 86, 80, 78]? Later, when discussing the VKS dynamo, we will see that even slight modifications of the experimental design can teach a lot about the role of turbulence, boundary conditions, and the distribution of different dynamo sources.

*Second*, if one was lucky to make a hydromagnetic dynamo running, how can the exponential field growth be stopped, how does the dynamo saturate? Roughly speaking, dynamo saturation is nothing than an application of Lenz's rule stating that an induced current acts against the source of its own generation. How this saturation works in detail, depends strongly on the mechanical constraints the flow is experiencing. All of the present laboratory dynamos comprise mechanical installations to drive and guide the flow (propellers, guiding blades, etc.). Obviously, the fewer installations are present in the fluid, the more freedom has the flow to be modified and re-organized by the Lorentz forces. It would be most interesting to drive the flow purely by convection, as in the Earth's outer core. However, it seems to be impossible to reach velocities sufficient for dynamo action in a purely convective way in laboratory experiments, as discussed, e.g. in [240]. Hence, all present laboratory experiments have to find a compromise between a mechanical forcing of the flow and the degree of freedom of the flow for the magnetic field back-reaction.

This brings us to the *third* point: Besides its influence on the large scale flow, the magnetic field back-reaction may also change the turbulence properties of the flow. Sometimes this effect is considered the most important one that dynamo experiments may help to understand, as they provide an interesting test-case for MHD turbulence models (a summary of the latter can be found in [249]). Those models, once validated, could gain reliability when applied to such hard problems as magnetic field generation in the Earth's core . But "turbulence model validation" sounds much easier as it is in reality. Even the simple flow measurement in liquid sodium is a problem in its own right, let alone the measurements of all sorts of correlation functions which might be important for the validation of turbulence models.

A *fourth* topic, which is intimately connected with the issue of turbulence modification, is the destabilizing role magnetic fields can have on flows. Typically dynamo experiments and experiments on the magnetorotational instability are of a similar size, making it worth to hunt for new instabilities in the presence of (self-excited or externally applied) magnetic fields. In addition to this, there is a large variety of wave phenomena to be studied in rotating magnetized flows.

A *fifth* issue that could possibly be addressed by dynamo experiments has to do with the distinction between steady and oscillatory dynamo states. Typically, these transitions occur at so-called exceptional points of the spectrum of the non-selfadjoint dynamo operator, and polarity reversals have been described as noise triggered relaxation oscillations in the vicinity of such points [221, 222, 224]. However, reversals can occur for a wide variety of bistable systems [94], and experiments can be helpful to distinguish between different reversal scenarios.

## 5 The experiments in detail

In the following we will concentrate on the most important experimental efforts related to the understanding of the origin and the action of cosmic magnetic fields. We will start with the four experiments that have already shown homogeneous dynamo action, and then move to experiments devoted to wave phenomena and magnetic instabilities in liquid metals. For the sake of shortness, we have to skip some very interesting older experiments like those of Lehnert [130] (cf. [131] for a very amuzing account of these experiments in Stockholm) and Gans [74], but also the impressive series of liquid metal experiments on Alfvén waves which have been summarized by Gekelmann [75]. Another topic omitted is the search for self-excitation phenomena in fast breeder reactors [13, 171, 111, 1, 170], although this close connection was occasionally used as a political argument to motivate dynamo experiments (see [218]). Slightly focusing on some newer experimental activities, we advise the reader to consult some former reviews on earlier experiments [190, 25, 128, 69, 70, 39, 240, 49, 168, 72].

For decades, hydromagnetic dynamo experiments seemed to be at the edge of technical feasibility. The problem to achieve self-excitation is that values of the critical  $Rm$  for different flow geometries are of the order of 100. For the best liquid metal conductor, sodium, the product of conductivity and magnetic permeability is approximately  $10 \text{ s/m}^2$ . Hence, to get an  $Rm$  of 100, the product of length and velocity has to be  $10 \text{ m}^2/\text{s}$ . To reach this value one should have more than  $1 \text{ m}^3$  sodium and use at least 100 kW of mechanical power to move it. Another possibility is of course to increase  $Rm$  by simply using materials with a high magnetic permeability. This brings us directly to the first experiment on homogeneous, though not hydromagnetic, dynamo action.

### 5.1 The dynamo experiments of Lowes and Wilkinson

In the sixties of the 20 century, Lowes and Wilkinson have carried out a long-term series of homogeneous dynamo experiments [138, 139, 255] at the University of Newcastle upon Tyne. The main idea of their experiments was already laid down in a 1958 paper by Herzenberg [90] who had given the first rigorous existence prove for a homogeneous dynamo consisting of two rotating small spheres embedded in a large sphere (Figure 2a). Thus motivated, Lowes and Wilkinson started with the first homogeneous dynamo using two rotating cylinders in a “house-shaped” surrounding conductor (Figure 2b). The key point for the success of this and the following experiments was the utilization of various ferromagnetic materials (perminvar, mild steel, electrical iron) making the magnetic Reynolds number large, simply by a high relative magnetic permeability  $\mu_r$  (between 150 and 250).

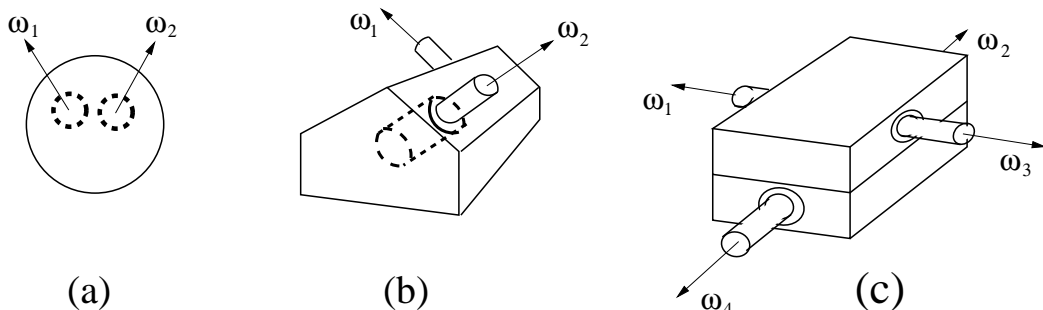


**Fig. 2** (a) The Herzenberg dynamo. Two spheres rotate around non-parallel axes. (b) The first dynamo of Lowes and Wilkinson. Two cylinders rotate in a “house-shaped” block. (c) The fifth dynamo with four independent rotors.

The history of these experiments is impressive, not only for their step-by-step improvements but also for the continuing comparison of the resulting field with geomagnetic features [255]. Starting with a simple geometry of the rotating cylinders (Figure 2b), which produced steady and oscillating magnetic fields, the design was made more sophisticated (Figure 2c) so that finally it permitted the observation of field reversals. That way it was shown that a complex field structure and behaviour can result from comparatively simple patterns of motion.

Needless to say, the experiments were flawed by the use of ferromagnetic materials and the nonlinear field behaviour which is inevitably connected with these materials. One attempt to get self-excitation with rotating non-magnetic copper

cylinders failed. And, although homogeneous, these dynamos were not suited to study the nontrivial back-reaction of the magnetic field on the fluid motion, and there was no chance to learn something about MHD turbulence.

### 5.2 The dynamo experiments in Riga

There is a long tradition at the Institute of Physics Riga, Latvia, to carry out dynamo related experiments.

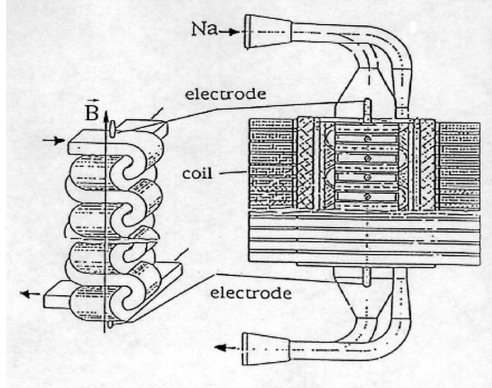


**Fig. 3** The “ $\alpha$ -box,” the first dynamo-related experiment in Riga. The sodium flow through the helically interlaced channels produces an emf parallel to the applied magnetic field.

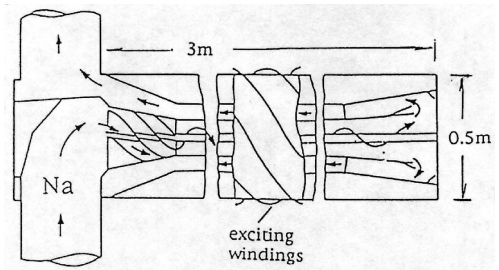


**Fig. 4** The dynamo module of the 1987 experiment. Significant amplifications of externally applied magnetic fields were measured, before the experiment had to be stopped due to mechanical vibrations.

The first one, actually proposed by Max Steenbeck, was intended to prove experimentally the  $\alpha$  effect, i.e. the induction of an electromotive force parallel to an applied magnetic field. This experiment, the “ $\alpha$ -box” (Figure 3), consisted of two orthogonally interlaced copper channels through which sodium was pumped with velocities up to 11 m/s. Interestingly, although the very flow helicity  $\mathbf{v} \cdot (\nabla \times \mathbf{v})$  is zero everywhere in this set-up, an  $\alpha$  effect results from the non-mirrorsymmetry of the flow. The main result of this experiment was that the induced voltage between the electrodes (cf. Figure 3) is proportional to  $v^2$ , i.e., it is independent of the flow direction, and that it reverses if the applied magnetic field is reversed. The  $\alpha$ -effect was therefore validated [217]. Interestingly, the induced current was shown to increase slower than linearly with the applied magnetic field, a result which points to some quenching of  $\alpha$  with increasing interaction parameter.

A second experiment was also prepared in Riga but actually carried out in St. Petersburg in 1986 [62] (Figure 4). The principle idea of this, as well as of the later Riga dynamo experiment, traces back to Ponomarenko [172] who had proved that a helically moving, electrically conducting cylinder embedded in an infinite stationary conductor can show dynamo action. This simple configuration was analyzed in more detail by Gailitis and Freibergs [60] who found a remarkably low critical magnetic Reynolds number of 17.7 for the convective instability. By adding a back-flow, this convective instability can be transformed into an absolute instability [61].

All this early numerical work, including the optimization [59] of the main geometric relations which led to the design of the Riga dynamo (Figure 5a,b), was done with a one-dimensional eigenvalue solver. For refined kinematic simulations a two-dimensional finite difference code (in radial and axial direction) was written whose main advantage is the possibility to treat velocity structures varying in axial direction, which is indeed of relevance for the Riga dynamo [71]. The magnetic field structure as it comes out of this code is illustrated in Figure 5c.

Much effort has been spent to fine-tune the whole facility. The first step was to optimize the main geometric relations, in particular the relations of the three radii to each other and to the length of the system [59]. The resulting shape of the central module of the dynamo is shown in Figure 5b. In a water dummy facility at the Dresden Technical University, many tests have been carried out to optimize the velocity profiles [32] and to ensure the mechanical integrity of the system. All the experimental preparations were accompanied by extensive numerical simulations. One main result of these simulations was the optimization of the velocity profile with regard to the limited motor power resources of around 200 kW. For helicity maximizing profiles (“Bessel function profiles”) a critical  $R_m$  as low as 12.0 (for the convective instability) and 14.7 (for the absolute instability) has been found, while the corresponding numbers for the measured (as far as possible optimized) profiles were 14.3 and 17.6, respectively [219]. Another result was the prediction of the main features of the expected magnetic field, i.e., its growth rate, frequency, and spatial structure, and the dependence of these features on the rotation rate of the propeller.

At the present facility, eight experimental campaigns have been carried out between November 1999 and July 2007. In the first campaign in November 1999, a self-exciting field was documented for the first time in a liquid metal dynamo

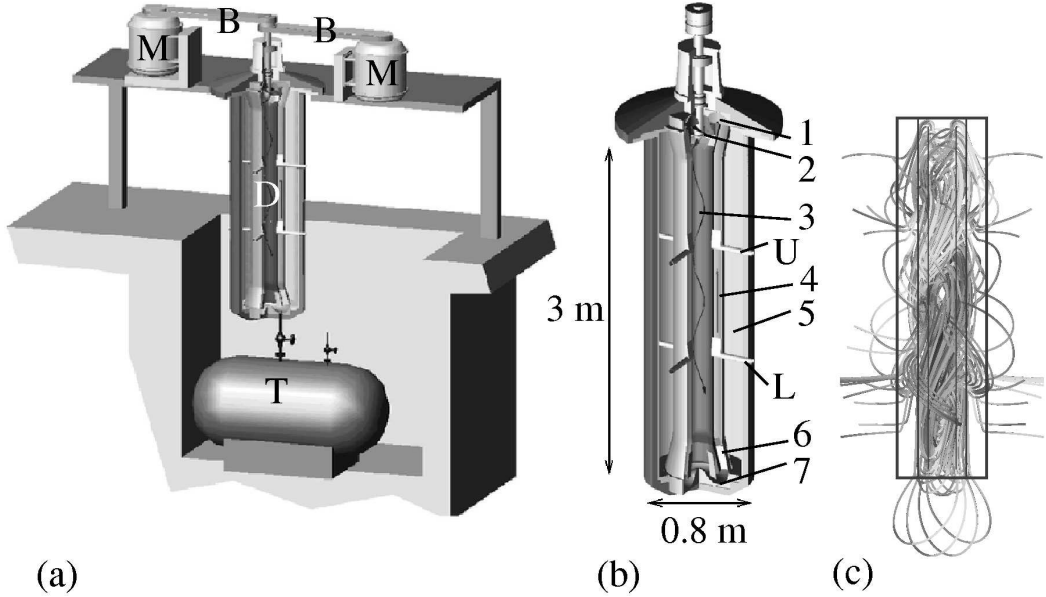


**Fig. 5** The Riga dynamo experiment and its eigenfield. (a) Sketch of the facility. M - Motors. B - Belts. D - Central dynamo module. T - Sodium tank. (b) Sketch of the central module. 1 - Guiding blades. 2 - Propeller. 3 - Helical flow region without any flow-guides, flow rotation is maintained by inertia only. 4 - Back-flow region. 5 - Sodium at rest. 6 - Guiding blades. 7 - Flow bending region. (c) Simulated magnetic eigenfield. The gray scale indicates the vertical component of the field.

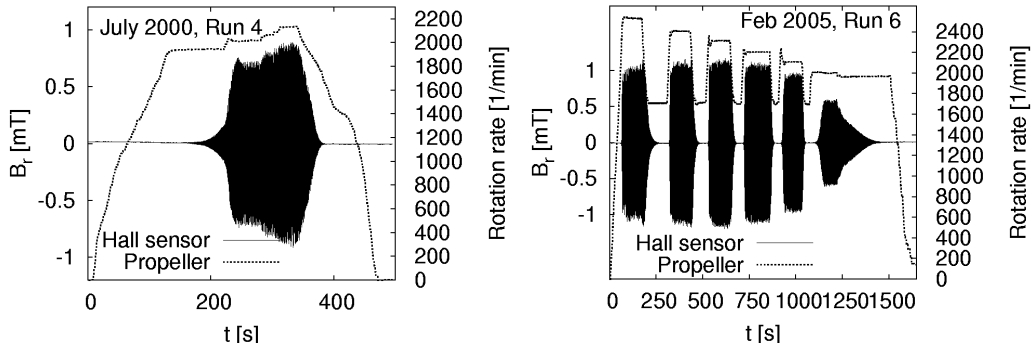


**Fig. 6** Two experimental runs carried out in July 2000 and in February 2005. Rotation rate of the motors, and magnetic field measured at one Hall external sensor plotted vs. time. After the exponential increase of the magnetic field in the kinematic dynamo regime, the dependence of the field level on the rotation rate has been studied in the saturation regime.

experiment, although the saturated regime could not be reached at that time [64]. This had to be left until the July 2000 experiment [65]. In June 2002, the radial dependence of the magnetic field was determined by the use of Hall sensors and induction coils situated on "lances" going throughout the whole dynamo module. In February and June 2003, first attempts were made to measure the Lorentz force induced motion in the outermost cylinder. A novelty of the May 2004 campaign was the measurements of pressure in the inner channel by a piezoelectric sensor that was flash mounted at the innermost wall. In February/March 2005, a newly developed permanent magnet probe was inserted into the innermost cylinder in order to get information about the velocity there, and two traversing rails with induction coils and Hall sensors were installed to get continues field information along the  $z$ -axis and across the whole diameter of the dynamo. In July 2007, a newly developed magnetic coupler was installed to replace the outworn gliding ring seal. More details about these results can be found in Refs. [69, 71, 68, 66, 67, 70], and will also be published elsewhere.

In Figure 6 we document two experimental runs carried out in July 2000 and in February 2005. It is clearly visible that the magnetic field switches on and off when a critical value of the propeller rotation rate is crossed from below or above, respectively.

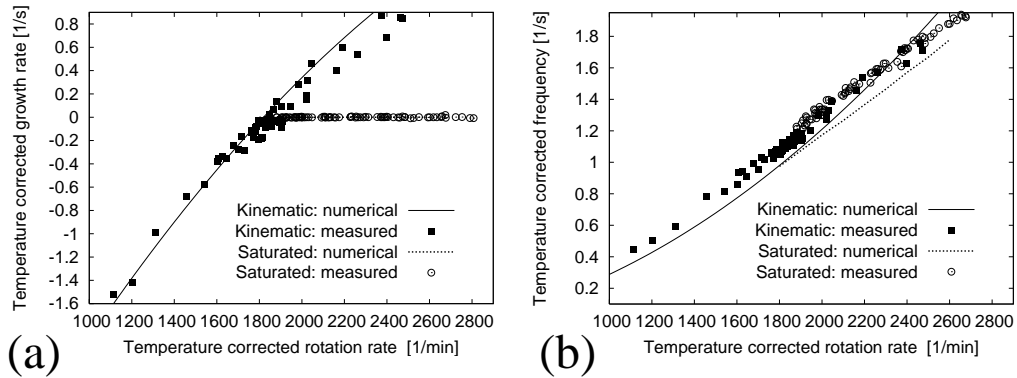


**Fig. 7** Measured growth rates and frequencies of the magnetic eigenfield for different rotation rates  $\Omega$  in the kinematic and the saturation regime, compared with the numerical predictions.  $\Omega$ ,  $p$ , and  $f$  at the temperature  $T$  were scaled to  $(\Omega_s, p_s, f_s) = \sigma(T)/\sigma(157^\circ C)$  ( $\Omega(T), p(T), f(T)$ ) as required by the scaling properties of equation (6).

In Figure 7 the temperature corrected measurement data for the growth rate (Fig. 7a) and the frequency (Fig. 7b) are shown in comparison with the corresponding numerical results. The numerical curves in the kinematic regime were obtained with the 2D solver [219, 71] and were slightly corrected by the effect of the lower conductivity of the stainless steel walls that was estimated separately by a 1D solver.

As for the saturation regime we have modelled the most important back-reaction effect within a simple one-dimensional model [68, 71]. This relies on the fact that, while the axial velocity component has to be rather constant from top to bottom due to mass conservation, the azimuthal component  $v_\phi$  can be easily braked by the Lorentz forces without any significant pressure increase. In the inviscid approximation, and considering only the  $m = 0$  mode of the Lorentz force, we end up with the ordinary differential equation for the Lorentz force induced perturbation  $\delta v_\phi(r, z)$  of the azimuthal velocity component:

$$\bar{v}_z(r, z) \frac{\partial}{\partial z} \delta v_\phi(r, z) = \frac{1}{\mu_0 \rho} [(\nabla \times \mathbf{B}) \times \mathbf{B}]_\phi(r, z) . \quad (12)$$

This equation is now solved simultaneously with the induction equation, both in the innermost channel where it describes the downward braking of  $v_\phi$ , and in the back-flow channel where it describes the upward acceleration of  $v_\phi$ . Both effects together lead to a reduction of the differential rotation and hence to a deterioration of the dynamo capability of the flow. The validity of this self-consistent back-reaction model, which gives automatically a zero growth rate, can be judged from the dependence of the resulting eigenfrequency in Figure 7b. Actually, we see a quite reasonable correspondence with the measured data, in particular with respect to the slope of the curve.

Only recently, a sophisticated T-RANS (transient Reynolds average Navier-Stokes equation) model of the Riga dynamo experiment has been developed at the Delft Technical University [105, 106, 107]. This model, which incorporates the state of the art of hydrodynamic turbulence modelling under the influence of magnetic fields, has basically confirmed, and slightly improved, the main predictions of our simple one-dimensional back-reaction model.

### 5.3 The Karlsruhe dynamo experiment

Historically it is interesting that not only the basic idea and the geophysical motivation, but also a final formula for the critical flow-rates for a sort of Karlsruhe experiment can already be found in a paper of 1967 [58]. The idea was to substitute real helical ("gyrotropic") turbulence by "pseudo-turbulence" actualized by a large (but finite) number of parallel channels with a helical flow inside. Later, in 1975, Busse considered a similar kind of dynamo [23] which prompted him to initiate the Karlsruhe dynamo experiment which was then designed and carried out by R. Stieglitz and U. Müller.

In 1972, Roberts had proved dynamo action for a velocity pattern periodic in  $x$  and  $y$  that comprises both a rotational flow and an axial flow [188]. The  $\alpha$ -part of the electromotive force for this flow type can be written in the form  $\mathcal{E} = -\alpha_\perp (\bar{\mathbf{B}} - (\mathbf{e}_z \cdot \bar{\mathbf{B}}) \mathbf{e}_z)$ , which represents an extremely anisotropic  $\alpha$ -effect that produces only electromotive forces in the  $x$ - and  $y$ -directions, but not in the  $z$ -direction [175].

In the specific realization of the Karlsruhe experiment (Figure 8), the Roberts flow in each cell is replaced by a flow through two concentric channels. In the central channel the flow is straight, in the outer channel it is forced by a "spiral staircase" on a helical path (Figure 9). This design principle of the Karlsruhe dynamo being given, a fine tuning of the

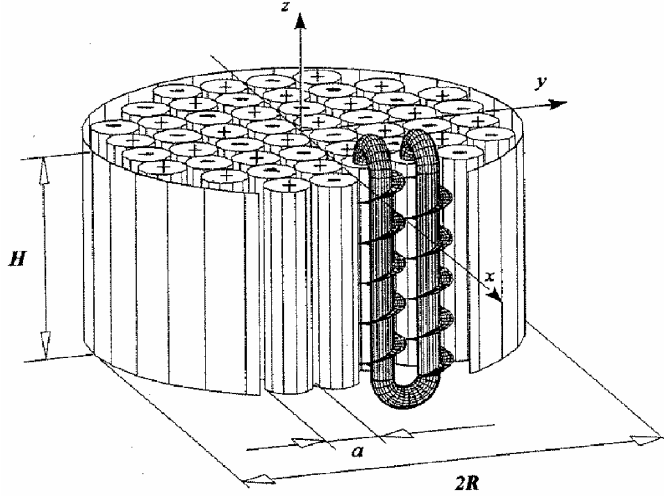
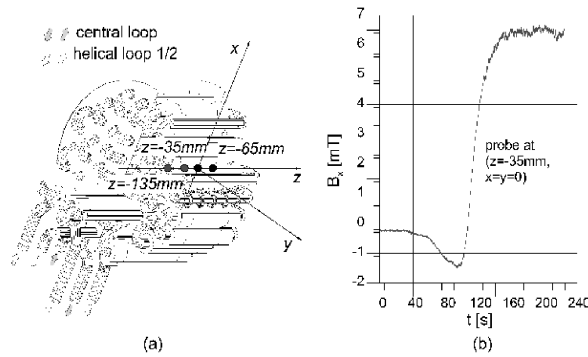


**Fig. 8** Central part of the Karlsruhe dynamo facility. The module consists of 52 spin-generators, each containing a central tube with non-rotating flow and an outer tube where the flow is forced on a helical path. Figure courtesy of R. Stieglitz.

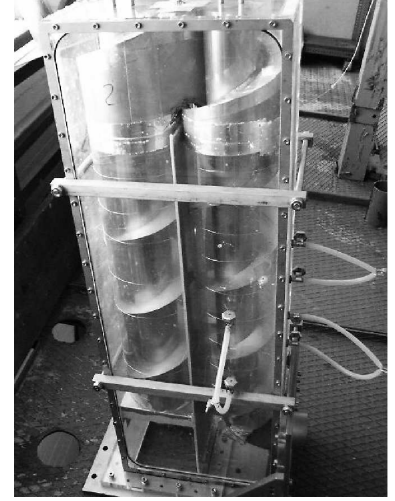
geometric relations was carried out with the aim to achieve a maximum  $\alpha$  effect for a given power of the pumps. Such an optimization led to a number of 52 spin generators, a radius of 0.85 m and a height of 0.7 m for the dynamo module.

Figure 10 documents the experiment carried out in December 1999 [149, 234]. The scheme in Figure 10a depicts again the central dynamo module with the 52 spin-generators, and defines the coordinate system for the location and direction of the Hall probes. Figure 10b shows the measured  $x$ -component of the magnetic field. This signal was recorded after the central flow rate  $\dot{V}_C$  was set to a constant value of 115 m<sup>3</sup>/h and the flow rate  $\dot{V}_H$  in the helical ducts was increased from 95 m<sup>3</sup>/h to 107 m<sup>3</sup>/h at a time 30 s from the start of the experiment. After approximately 120 s the field starts to saturate at a approximately 7 mT.

For the experimentally interesting region, the isolines of the quantity  $C = \mu_0 \sigma \alpha_{\perp} R$ , which is a dimensionless measure of the  $\alpha$ -effect, and the experimentally obtained curves, are plotted in Figure 11. The experimentally determined neutral line, separating dynamo and non-dynamo regions, corresponds to values of  $C^{crit}$  in the region of 8.4...9.3. Hence, the numerical prediction,  $C^{crit} = 8.12$ , resulting from mean-field theory [176], was quite reasonable.



**Fig. 10** Self-excitation and saturation in the Karlsruhe dynamo experiment. (a) The dynamo module with the connections between the spin-generators and the supply pipes. (b) Hall sensor signals of  $B_x$  in the inner bore of the module. Figure courtesy of R. Stieglitz.



**Fig. 9** A model of a spin-generator. Figure courtesy of R. Stieglitz and Th. Gundrum.

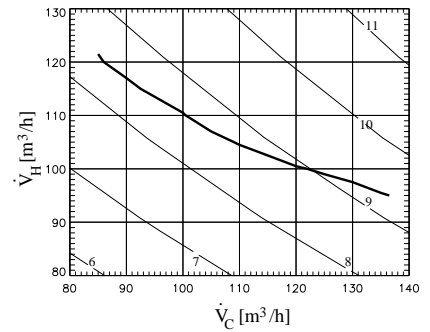


**Fig. 11** Isolines of the dimensionless number  $C = \mu_0 \sigma \alpha_{\perp} R$  in the  $\dot{V}_C - \dot{V}_H$ -plane. In a certain approximation, dynamo action should occur beyond the isoline with  $C^{crit} = 8.12$  [176]. The experimentally determined neutral line (bold), separating regions with and without dynamo action, slightly deviates from the theoretical line. Figure courtesy of K.-H. Rädler.

During its comparably short lifetime, the Karlsruhe dynamo experiment has brought about many results on its imperfect bifurcation behaviour and on MHD turbulence which are documented in [150, 151, 152]. Much work has also been done in order to predict the kinematic dynamo behaviour [238, 239, 176, 243] and to understand quantitatively the saturated regime

[241, 177, 178]. It should be mentioned that data from the Karlsruhe experiment have been used in an attempt to distinguish between two different scaling laws of the geodynamo, with interesting consequences for its power consumption [34].

A last remark: There is growing evidence that the disassembling of the Karlsruhe dynamo facility was too rash. Recent numerical simulations have shown [5] that just a very slight decrease of the aspect ratio of the dynamo module would have changed the dominant dipole direction from equatorial to axial. It suggests itself that in the vicinity of this point one could have expected quite interesting flip-flop phenomena between equatorial and axial dipoles in the non-linear regime of the dynamo. A similar point concerns transitions between steady and oscillatory dynamo regimes which typically occur at so-called exceptional points of the spectrum of the non-selfadjoint dynamo operator. Those transitions have been made responsible for the polarity reversals of the Earth's magnetic field [221, 222, 224]. In technical terms, an appropriate sign change of  $\alpha$  along the radius of the module would have been sufficient for such a transition to occur. In any case, with modifying slightly the central module of the Karlsruhe dynamo, keeping all other parts of the installation unchanged, there would have been a good chance to investigate very interesting effects. Unfortunately, this opportunity has been missed.

#### 5.4 The VKS experiment in Cadarache

At the CEA research center in Cadarache (France), a group lead by J.-F. Pinton (ENS Lyon), S. Fauve (ENS Paris) and F. Daviaud (CEA Saclay) has built a dynamo experiment under the acronym VKS ("von Kármán sodium"). Here, "von Kármán" stands for the flow between two rotating disks [262].

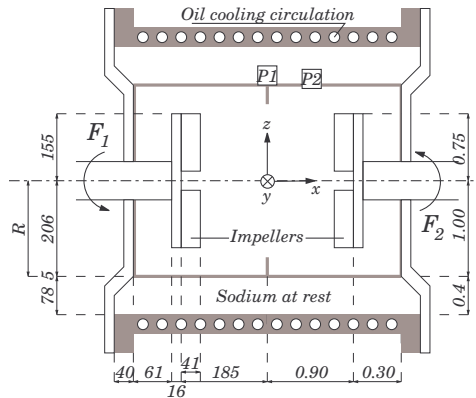


**Fig. 12** Design of the VKS experiment with two disks counter-rotating in the cylinder driving two poloidal and two toroidal eddies ( $s2^+t2$ ). The numbers on the l.h.s are the dimension in mm, the numbers on the r.h.s are the dimensions normalized by the radius. Figure courtesy of the VKS team.

In a first version of the experiment (VKS 1), the flow was produced inside a cylindrical vessel with equal diameter and height,  $2R = H = 0.4$  m, driven by two 75 kW motors at rotation rates up to 1500 rpm. The von Kármán flow geometry has been chosen as it represents a convenient realization of the so-called  $s2^+t2$  flow that consists of two poloidal eddies ( $s2$ ) which are inward directed in the equatorial plane (+), and two counter-rotating toroidal eddies ( $t2$ ). Such a flow is known to yield self-excitation at comparably low values of  $Rm$  [47, 154]. One problem of such flows is that the counter-rotation in the equatorial plane is a powerful source of turbulence. Although significant induction effects were measured in this first experiment [141, 15, 166, 167], no self-excitation was observed.

Based on this experience, a new version of the experiment (VKS 2) had been constructed (Figure 12). The total sodium volume was extended from 50 l to 150 l, the available motor power from 75 kW to 300 kW, and great effort was spent in order to optimize the shape of the blades of the impellers [142, 181, 143]. Further, a side layer with sodium at rest was attached which reduces the critical  $Rm$  drastically. In spite of this thorough optimization, this experiment failed to show self-excitation [183], and the induced magnetic fields turned out to be significantly weaker than numerically predicted [182]. The reason for this general under-performance was controversially discussed. One "school" attributed it to (large scale) fluctuations [129], another one attributed it to the existence of "lid layers" behind the impellers, and in particular to the sodium rotation therein [223, 261, 124].

In an attempt to mitigate this detrimental effect of lid layers, it was decided to change the axial magnetic boundary conditions by replacing the stainless steel impellers by those made of soft-iron. This modification led ultimately to the observation of self-excitation in fall 2006 [146]. In some parameter regions, characterized by asymmetric forcing with different rotation rates of the two impellers, impressive magnetic field reversals (cf. Figure 13) were recorded [12].

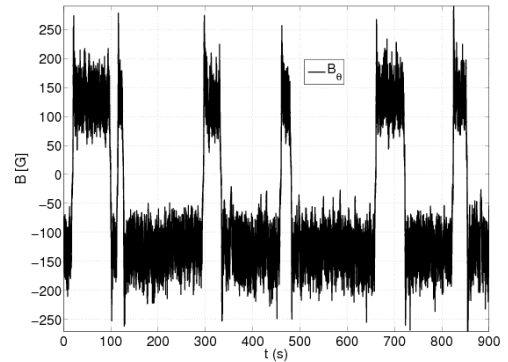


**Fig. 13** A reversal of the azimuthal magnetic field occurring when the rotation rate of one propeller was 16 Hz and that of the other propeller was 22 Hz. Figure courtesy of the VKS team.

The critical  $Rm$  of the VKS 2 experiment with soft iron propellers was determined to be  $\approx 31\ldots 35$ , in contrast to the numerical predictions between 48 and 133 (the latter depending mainly on the flow details in the lid layers). The really surprising thing was, however, that the self-excited eigenfield turned out to be basically an axisymmetric one, in contradiction to the non-axisymmetric equatorial dipole that was predicted by numerics. This axisymmetric field is apparently at odds with Cowling's theorem [42] which forbids non-decaying axisymmetric eigenfields to be excited by large-scale flows.

Hence, numerical work is going on to understand better the functioning of the VKS dynamo [80, 78], in particular the role of the iron propellers and the possible influence of helicity in the propeller region [125]. A final explanation of the axisymmetric eigenmode and its comparably low critical  $Rm$  is, however, still missing.

### 5.5 The Bullard-von Kármán experiment in Lyon

A simple mechanical dynamo model, that had been proposed by Bullard in 1955, is the homopolar disk dynamo [22]: Imagine a metallic disk rotating with an angular velocity  $\omega$  in a magnetic field  $\mathbf{B}$ . The emf  $\mathbf{v} \times \mathbf{B}$  points from the axis to the rim of the disk and drives a current  $I$  through a wire that is wound around the axis of the disk. The orientation of the wire is such that the external magnetic field is amplified. At a critical value of  $\omega$ , the amplification becomes infinite: self-excitation sets in. With growing magnetic field, the Lorentz force  $\mathbf{j} \times \mathbf{B}$  acts against the driving torque, which will ultimately lead to saturation. The feasibility of such an experiment was recently discussed in a paper by Rädler and Rheinhardt [179].

Inspired by this disk dynamo, a team in Lyon has investigated an interesting experimental arrangement which generates a magnetic field by a simple trick [16]. Basically, it comprises a flow of the same  $s2^+t2$  type as the VKS flow. The working fluid is, however, gallium instead of sodium ("von Kármán gallium" experiment, [250]). The magnetic Reynolds number reaches only values of 5 which is clearly not sufficient for dynamo action to occur. The trick is now that a part of the amplification process is taken over by an external electrical amplifier which takes as input the azimuthal field component measured by a Hall sensor and feeds a coil which produces an axial magnetic field. Roughly speaking, the  $\Omega$  effect (i.e. the generation of a toroidal from a poloidal field by means of differential rotation) is produced by the flow, while the  $\alpha$  effect is mimicked by the external amplifier. Very interesting results have been obtained with this machine, including intermittent reversals of the dipole field, as well as excursions [16].

### 5.6 Madison

At the University of Wisconsin, Madison, C. Forest and his colleagues have undertaken the "Madison dynamo experiment" (MDX) which is, in many respects, quite similar to the VKS dynamo. The flow topology is of the same  $s2^+t2$  type with two counter-rotating toroidal eddies and two poloidal eddies which are pointing inward in the equatorial plane. Historically it is noteworthy that Winterberg had proposed exactly this propeller configuration as early as 1963 [256].

The difference to VKS is that MDX works not in a cylinder but in a 1 m diameter sphere (Figure 14) and that the flow is driven by two impellers with Kört nozzles instead of two disks (with blades) as in VKS. A lot of effort had been spent in the hydrodynamic and numerical optimization of the precise geometry of the  $s2^+t2$  flow [54].

The MDX dynamo has not shown self-excitation up to present. It was a surprise, however, that the measured *induced* magnetic field turned out to be dominated by an axial dipole component (Figure 15), since such an induced axial dipole cannot be produced by a large scale axisymmetric flow [213].

Evidently, this puzzle has a striking resemblance with the self-excitation of the axisymmetric field in the VKS experiment. The most plausible explanation comes from assuming some sort of  $\alpha$  effect in the flow. And again one has to bear in mind the extreme sensitivity of the mode selection to minor amounts of helical turbulence (i.e.  $\alpha$ ) in the impeller region that was identified (for VKS) in [125].

Further results have been published on intermittent bursts of dynamo action [157], the detailed measurement of the magnetic field structure [158], and its interpretation in terms of possible dynamo sources [214]. In the latter paper, the induction of an axial dipole has been interpreted as a sort of "turbulent diamagnetism", which is not necessarily in contradiction with the interpretation given in [125]. Present activities at MDX point on further optimizing the flow by installing various types of baffles.

Another focus of the Madison group is on replacing liquid metal experiments by plasma experiments. A main step in this direction is to confine the plasma and to drive a rotating flow by means of crossed magnetic and electric fields at the boundary [55, 40]. Interestingly, this is a configuration which had been used in many flow control experiments with low conducting fluids [63, 252]. The big advantage of plasma experiments is, of course, that  $Pm$  is not a constant of the material but can be adjusted in a wide range [251]. By controlling the poloidal profile of the toroidal rotation, high  $Rm$  flows will be generated that can result in MRI or dynamo action.

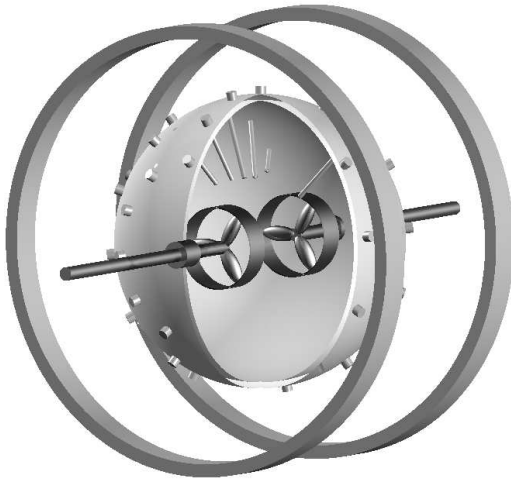


**Fig. 14** Schematic plot of the Madison Dynamo experiment (MDX). The flow topology is of the same  $s2^+t2$  type as in the VKS experiment. The two rings symbolize the Helmholtz coil for producing an axial magnetic field. The lances for internal magnetic field sensors are also shown. Figure courtesy of E. Spence.

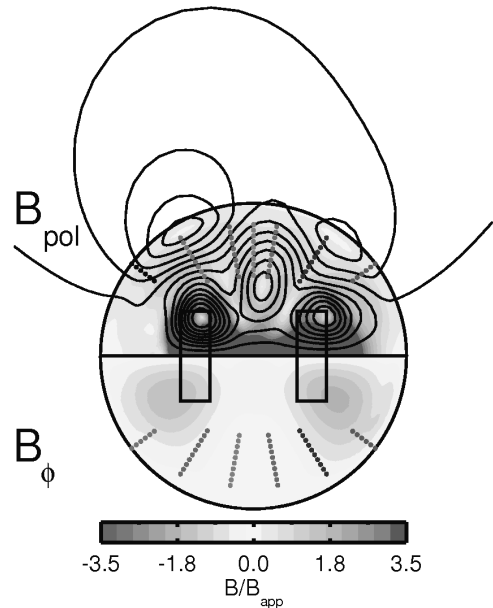


**Fig. 15** Induced magnetic field structure measured in the MDX, including a significant axial dipole component. Figure courtesy of E. Spence.

### 5.7 The rotating torus experiment in Perm

An ingenious idea to circumvent the large driving power that is usually needed to do dynamo experiments has been pursued by the group of P. Frick at the Institute of Continuous Media Mechanics in Perm, Russia [56, 228, 43]. The idea relies on the fact that a helical flow of the Ponomarenko type can be produced within a torus when its rotation is abruptly braked and a fixed diverter forces the inertially continuing flow on a helical path. While this concept is very attractive not only with respect to the low motor power that is necessary to slowly accelerate the torus, but also with respect to the fact that the sodium can be perfectly confined in the torus without any need for complicated sealing, a less attractive feature is the non-stationarity of the flow allowing only the study of a transient growth and decay of a magnetic field.

Extensive water pre-experiments and numerical simulations [44] have been carried out to optimize and predict magnetic self-excitation in such a non-stationary dynamo. Figure (16) gives an impression of the flow that appears shortly after the braking of the torus. The major radius of the water-filled torus is 10 cm, the minor radius is 2.7 cm. The photograph was taken 1.5 s after the full stop.

Based on these preparations a sodium experiment has been build with the following dimensions: major radius of the torus 40 cm, minor radius of the torus 12 cm, mass of sodium 115 kg, rotation rate 3000 rpm, maximal velocity 140 m/s, effective magnetic Reynolds number 40, minimal braking time 0.1 s. The main problem for such an experiments is connected with the tremendous mechanical stresses that appear in the short braking period. A special bronze alloy has been used for of the torus. First water experiments have been carried out, but for a sodium experiment more safety tests will be necessary.

In the preparatory phase of this experiment, important results on mean-field turbulence parameter have been obtained with a smaller gallium experiment [228, 43]. The importance of these parameters results from the question whether highly turbulent flows with high  $Rm$  lead to an effective reduction of the conductivity of the liquid. This reduction has been described in the context of mean-field dynamo theory as  $\beta$  effect (cf. equation (11)). While a significant reduction by a factor  $10^4 \dots 10^5$  can be well justified for the solar dynamo [113], the corresponding value for the geodynamo is not safely known. Recent studies of reversal sequences and their statistical properties suggest that the effective conductivity of the Earth's outer core might be reduced by a factor 3, when compared to the molecular conductivity of the material [52, 53]. Interestingly, this value is not that far from the factor 10 that was indicated by recent numerical simulations of mean-field coefficients in the geodynamo [203].

While neither the Riga nor the Karlsruhe dynamo experiment have shown any measurable  $\beta$  effect, there was only one experiment in which the measurement of an  $\beta$  effect had been claimed [185]. Now, the Perm group has identified, by means

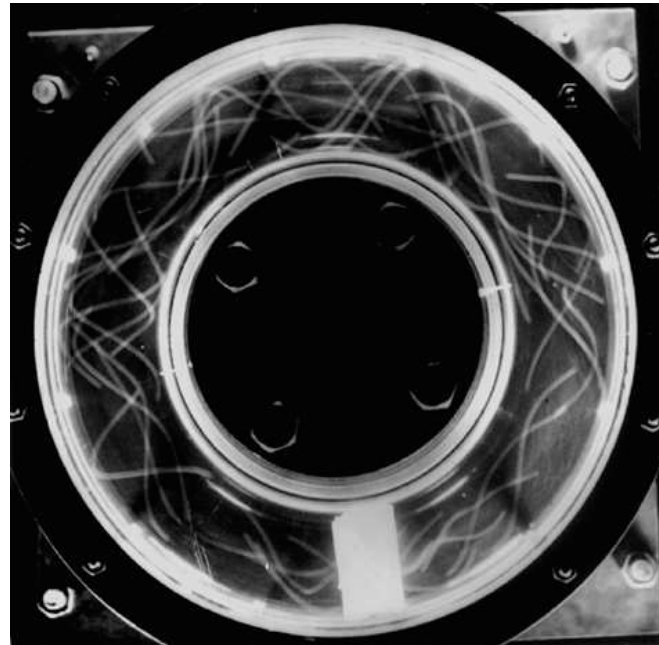


**Fig. 16** Helical flow that develops after the abrupt brake of the torus in the Perm water test experiment, visualized by polystyrene particles. The white bar at the bottom of the picture represents the diverter. Figure courtesy of P. Frick.

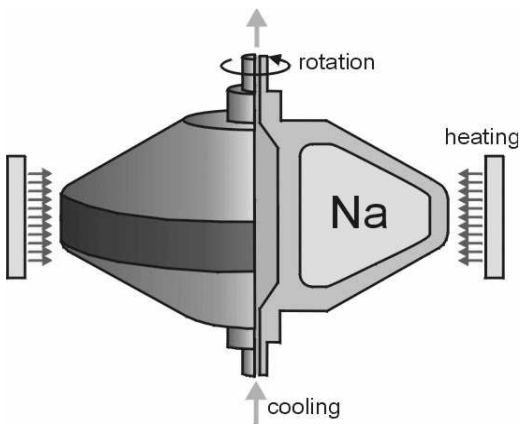


**Fig. 17** The first dynamo experiment in Maryland. A rapidly rotating torus is heated at the rim and cooled at the axis. Figure courtesy of D. Lathrop.

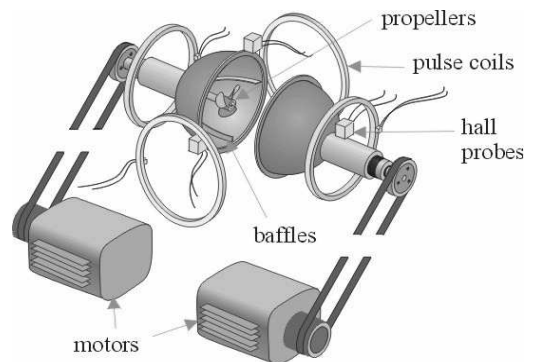


**Fig. 18** The second dynamo experiment in Maryland. In a 0.3 m diameter sphere different flows have been produced by propellers. This configuration, but with the propellers replaced by an inner sphere, was used for the MRI experiment. Figure courtesy of D. Lathrop.

of a very thorough measurement technique, a conductivity reduction in the order of 1 per cent for a comparably low  $Rm$  of  $\approx 1$  [43]. This sounds not very much, but since the dependence of  $\beta$  on  $Rm$  starts to be quadratic (in the low-conductivity limit) one could well imagine a significant  $\beta$  effect in planetary core flows characterized by much higher values of  $Rm$ .

### 5.8 Sodium experiments in Maryland

A variety of liquid sodium experiments have been carried out under the guidance of D. Lathrop at the University of Maryland [162, 163, 128, 205, 210, 211, 206].

In the first experiment (Dynamo I, see Figure 17), a 0.2 m diameter titanium vessel containing 1.5 l of liquid sodium was heated on the outer side and cooled at the axis. The fast rotation (up to 25000 rpm!) was intended to induce centrifugally driven convection, with the centrifugal force as a substitute for gravitation in the planetary case. Self-excitation was not observed.

The second device (Dynamo II, see Figure 18) consisted of a 0.3 m diameter sphere made of steel. A total of 15 l of sodium was stirred by two counter-rotating propellers, each powered by 7.4 kW motors. Note that the flow is again of the  $s^2+t^2$  topology as in VKS and MDX. The most interesting result of this experiment was obtained by carefully analyzing

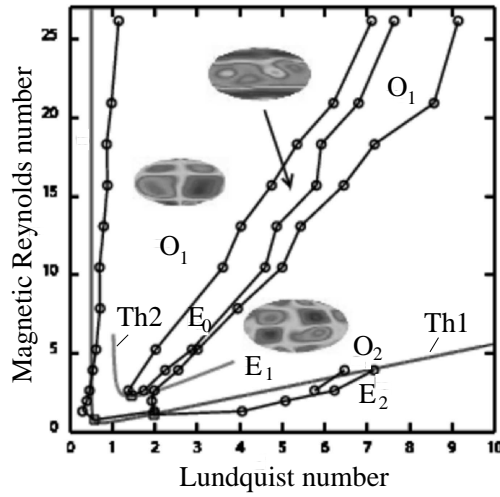


**Fig. 19** Phase diagram of the spherical Couette experiment in dependence on the Lundquist number and the magnetic Reynolds number. O<sub>1</sub> E<sub>1</sub> O<sub>2</sub> AND e<sub>2</sub> are different modes. Th1 and Th2 are the theoretical stability boundary curves from the dispersion relation for the longest (Th1) and second longest wavelength. Figure courtesy of D. Lathrop.



**Fig. 20** The rotating 3m sphere in Maryland. An impressive video is available under [www.youtube.com](http://www.youtube.com). Figure courtesy of D. Lathrop.

the decay rates of different modes. The decay of an axisymmetric applied field turned out to be more slowly as  $Rm$  was increased, while the decay of a non-axisymmetric field even accelerated with increasing  $Rm$ . Actually the decrease of the decay rate of the axisymmetric magnetic field was by about 30 per cent compared to the un-stirred fluid, at a magnetic Reynolds number of about 65. Naively, a simple extrapolation of this trend would point to a critical  $Rm$  of around 200. Although we know from Cowling's theorem how problematic an interpolation of decay rates of an axisymmetric mode towards zero is [242], one might ask again if not a similar mechanism as in VKS (and MDX) could provide a positive growth rate of an axisymmetric field.

Maybe the most important result of the Maryland group was obtained with a modification of this Dynamo II. By replacing the two propellers by one 5 cm diameter sphere, one arrives at a classical spherical Couette configuration. Applying, as before, an axial magnetic field to this flow, new modes of correlated magnetic field and velocity perturbation appeared [211] in certain parameter regions of  $Rm$  and  $S$  (see Figure 19). On closer inspection the dependence of these modes on  $Rm$  and  $S$  turned out to be in amazingly accurate correspondence with predictions of the MRI based on the dispersion relations. Running in an already strongly turbulent regime, this experiment was certainly not able to show MRI as the *first instability of a stable flow*. Nevertheless, it is tempting to speculate (in the spirit of [134]) that the fine-grained background turbulence just gives some renormalized viscosity, without terribly affecting the basic mechanism of MRI that seems robust enough to show up as an "coherent structure" as long as only  $Rm$  and  $S$  are in the right range.

The most recent project of the Maryland group is the construction of a giant rotating sphere with 3 m diameter (Figure 20), for future studies of MHD instabilities and (hopefully) the dynamo effect in rotating systems.

## 5.9 Grenoble

Continuing the tradition of former geophysically inspired experiments [20, 3], a group in Grenoble has prepared the so-called DTS ("Derviche Tourneur Sodium") experiment which is quite similar to the MRI experiment in Maryland. The distinguishing feature is a permanent magnet in the inner sphere in order to study the magnetostrophic regime [28] even when self-excitation is expectedly not achieved (Figure 21).

One of the most important results of the DTS experiment was the experimental observation of strong super-rotation of the liquid sodium in the equatorial region [153], which had been predicted by Dormy et al. in 1998 [45]. This was made possible by inferring velocity profiles from electric potentials measurements at the rim of the spherical container. While the observed latitudinal variation of the electric potentials in the experiments differs markedly from the predictions of a numerical model similar to that of Dormy, recent numerical results show a better agreement with the measurements [93].

A further focus of the DTS experiment is the investigation of various wave phenomena in magnetized rotating flows [201].

### 5.10 Princeton

A group at Princeton Plasma Physics Laboratory, headed by H. Ji, has a long tradition in doing plasma experiments with relevance to astrophysical processes, in particular to magnetic reconnection [98] and the  $\alpha$  effect [99] (which is, in the laboratory fusion plasma community, sometimes denoted as "dynamo effect" [14]).

At present an experiment is under preparation that is intended to show MRI in a Taylor-Couette cell filled with liquid gallium, at Reynolds numbers of several millions [100]. The basic question for such an experiment is, of course, under which conditions the underlying flow can really be considered laminar. Although Rayleigh's criterion predicts linear stability for the ratio of rotation rates of outer to inner cylinder being larger than the squared ratio of inner to outer radius, it has long been thought that the effect of boundaries together with non-linear instabilities will make the flow ultimately turbulent. Actually, in the linear stable regime turbulence had been reported by a number of authors [253, 200, 46].

After a long optimization process [102], the Princeton group has finally succeeded to find such a configuration of differentially rotating end rings that preserves the Taylor-Couette profile of the angular velocity. The measured torques, fluctuation levels and Reynolds stresses suggest that the flow is indeed laminar up to Reynolds numbers of about  $2 \times 10^6$  [101]. Experiments with liquid gallium are presently under preparation. Recent numerical simulations suggest that the MRI should indeed be identifiable in such an experiment, in particular by its linear growth and the increased torque [137].

However, as usual for such experiments, some uncertainties remain. They concern, in particular, the not well understood role of the rotating rings in the end-caps. Actually, the rotation rates which have been chosen in the experiment in order to restore the Taylor-Couette flow profile are different from the numerically optimized ones. To explain this discrepancy, even cylinder wobbling has been invoked, which may point to a quite complicated process involved in restoring the Taylor-Couette profile [187, 137].

On the other hand, the Maryland experiment has shown that MRI seems to be a quite robust phenomenon that appears quite independently on other flow features as long as only the necessary combination of  $Rm$  and  $S$  is reached.

However this might be, the Princeton gallium experiment will certainly teach us a lot about hydromagnetic instabilities in Taylor-Couette flows at high  $Rm$ .

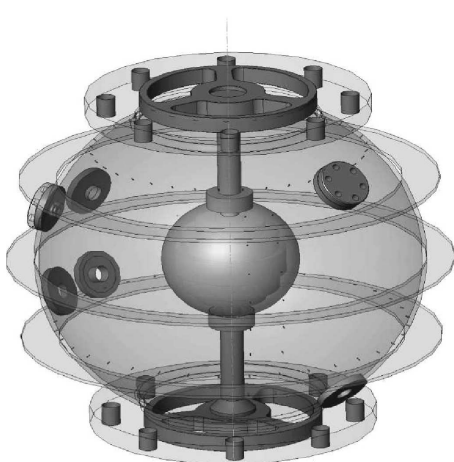


**Fig. 21** The DTS experiment in Grenoble. Forty liters of liquid sodium are contained between a 7.4 cm inner sphere and a 21 cm radius outer sphere. The copper inner sphere contains a magnet which produces a nearly dipolar field with a maximum of 0.345 T in fluid close to the poles. Figure courtesy of D. Schmitt and the DTS team.

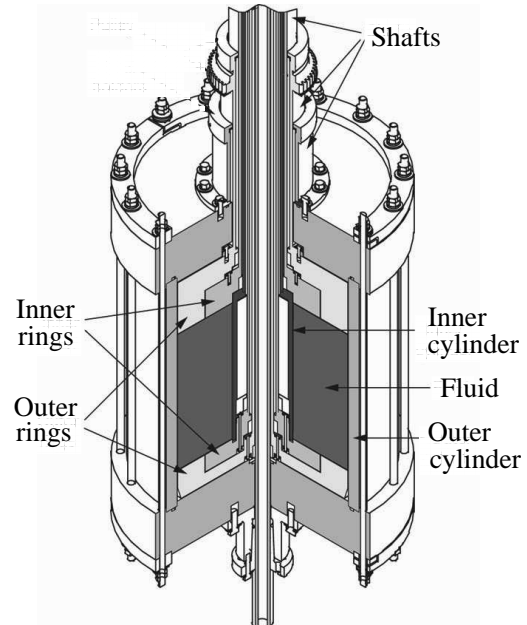


**Fig. 22** The Princeton MRI experiment. The rotating gallium of height 27.86 cm is contained between two differentially rotating concentric cylinders of radii 7.06 cm and 20.30 cm. Figure courtesy of H. Ji.

### 5.11 The sodium experiment in New Mexico

Since a couple of years, a sodium experiment is under construction at the New Mexico Institute of Mining and Technology (NMIMT) in Socorro [37, 38]. The title of the project is "The  $\alpha - \Omega$  accretion disk dynamo that powers active galactic nuclei (AGN) and creates the magnetic field of the universe."

At the present stage, the experiment is a Taylor-Couette experiment (Figure 23), quite similar to the Princeton experiment. It is planned to produce an  $\alpha$  effect by means of "plumes" that are driven by pulsed jets. The envisioned  $Rm$ , based on the rotation alone, is 130, the corresponding  $Rm$  for the plumes is 15 [37]. The water experiments have already revealed that the differential rotation of the Couette flow speeds up the anticyclonic rotation of the plumes. This anticyclonic rotation will form the basis for the  $\alpha$ -effect of the  $\alpha$ - $\Omega$ -dynamo.

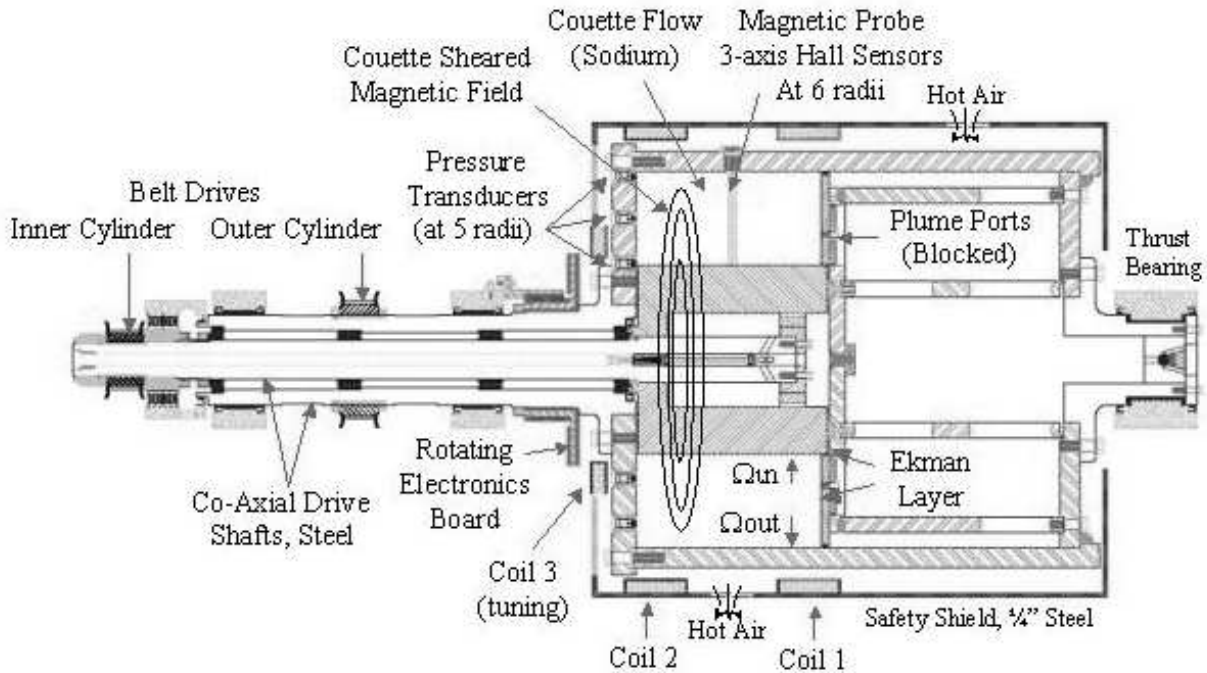


**Fig. 23** The NMIMT  $\alpha - \Omega$  experiment, at the present stage without the pulsed jet. Figure courtesy of S. Colgate.

### 5.12 The MRI experiment in Obninsk

An MRI experiment with liquid sodium, proposed by E.P. Velikhov, is under preparation at the Institute of Physics and Power Engineering in Obninsk (Russia), in collaboration with the Kurchatov Institute in Moscow. The basic idea is to drive a flow in a torus of rectangular cross-section by a Lorentz force due to an applied vertical field and an applied radial current [248, 108, 109]. The hope is that in the bulk of the volume one gets an angular velocity dependence  $\sim r^{-2}$  which would exactly correspond to the Rayleigh line. A similar experiment had been proposed in [229], although as a Taylor-Dean flow to have the angular momentum increasing at all radii. While experimental results are not available from those experiments an interesting claim has been made on a re-interpretation of the Moresco-Alboussiere experiment [147, 118] on the stability of the Hartmann flow in terms of MRI [110].

### 5.13 The PROMISE experiment in Dresden-Rossendorf

In this last subsection we leave the realm of high  $Rm$  flows and discuss an experiment on a particular type of MRI which has been coined "inductionless MRI" [173] or "helical MRI" (HMRI) [136].

The background for this is the following: We have seen, in connection with "standard MRI" (SMRI) experiments with an axially applied magnetic field, that it is extremely difficult to keep those high  $Re$  flows laminar. However, those high  $Re$  are not a genuine necessity for MRI, but just a consequence of the need for  $Rm$  in the order of one or larger.

The reason for this is that the azimuthal magnetic field (which is an unavoidable ingredient for MRI) must be *induced* from the applied axial field by the rotation of the flow, and such induction effects are just proportional to  $Rm$ . This being said, one could ask why not to replace the induction process by just *externally applying* the azimuthal magnetic field as well? This question was addressed in a 2005 paper by Hollerbach and Rüdiger [92], who showed that the MRI is then possible with dramatically reduced experimental effort. Actually, the scaling characteristics of this HMRI are completely

different from those of SMRI. While the latter needs  $Rm$  and  $S$  of the order of 1, the former depends on  $Re$  and  $Ha$  (or the interaction parameter  $N$ ).

HMRI is currently the subject of intense discussions in the literature [165, 194, 135, 136, 173, 235, 236, 126], the roots of which trace back to an early dispute between Knobloch [115] and Hawley and Balbus [8].

A remarkable property of HMRI, which has been clearly worked out in [173], is the apparent paradox that a magnetic field triggers an instability though the dissipation is larger than without magnetic fields. This is not so surprising when put in the context of other *dissipation induced instabilities* which are quite common in many areas [121, 112].

Another, and not completely resolved, issue concerns the relevance of HMRI for astrophysical flows. On first glance, HMRI seems well capable to work in cold regions of accretion disks characterized by small  $Pm$  where SMRI cannot work. This scenario might indeed be important for the "dead zones" of protoplanetary disks [245] as well as for the outer parts of accretion disks around black holes [10].

However, before entering such a discussion in detail, one has to check whether HMRI works at all for Keplerian rotation profiles  $\Omega(r) \sim r^{-3/2}$ . While the answer resulting from the dispersion relation was negative [135], the solution of the eigenvalue equation gave an affirmative answer, as long as at least the outer or the inner radial boundary is conducting [195].

Unfortunately, even this is not the end of the story. Since HMRI appears in the form of a travelling wave, one has to be quite careful with the interpretation of the instability of a single monochromatic wave. Actually, one has to look for wave packet solutions with vanishing group velocity. Typically, the regions in parameter space for this *absolute instability* are only a subset of those for the *convective instability*. A comprehensive analysis of this topic is under preparation [174].

Notwithstanding this ongoing discussion, the dramatic decrease of the critical  $Re$  and  $Ha$  for the onset of the MRI in helical magnetic fields, as compared with the case of a purely axial field, made this new type of MRI very attractive for experimental studies.

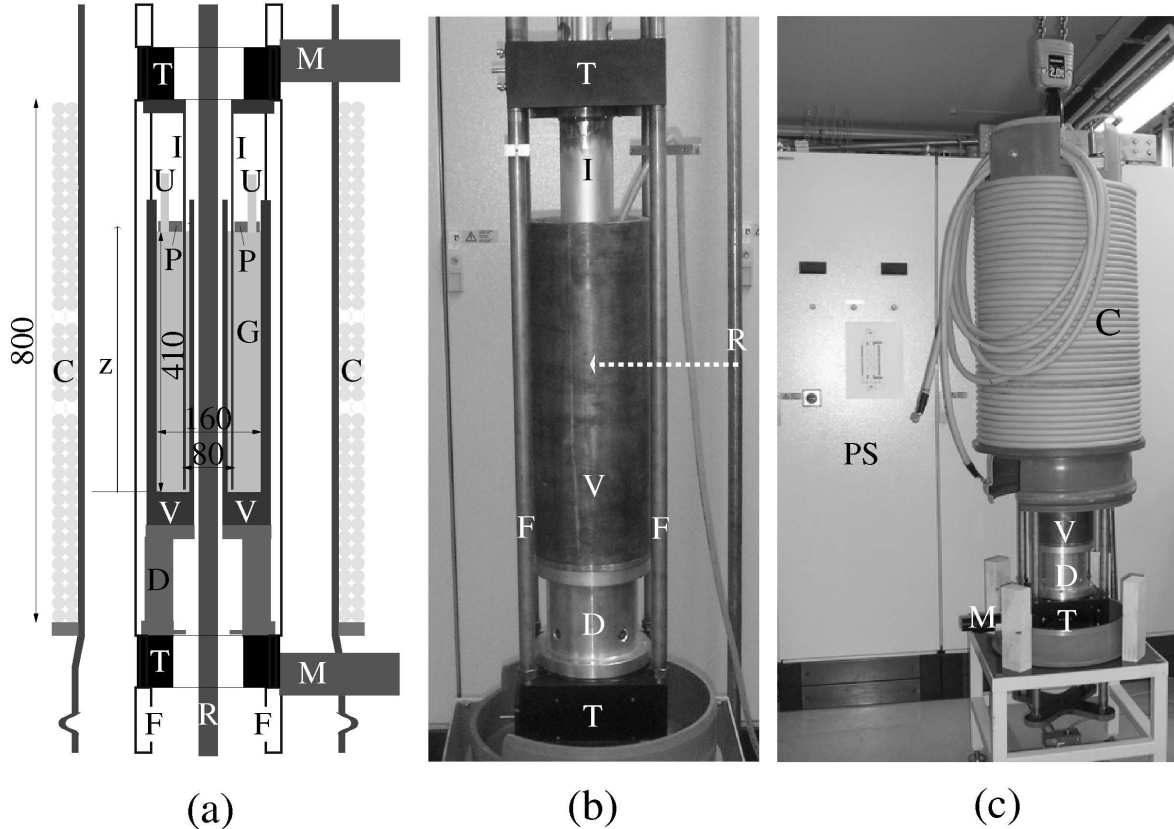


**Fig. 24** The PROMISE experiment. (a) Sketch. (b) - Photograph of the central part. (c) - Total view with the coil being installed. V - Copper vessel, I - Inner cylinder, G - GaInSn, U - Two ultrasonic transducers, P - Plexiglas lid, T - High precision turntables, M - Motors, F - Frame, C - Coil, R - Copper rod, PS - Power supply for currents up to 8000 A. The indicated dimensions are in mm.

The PROMISE facility (*Potsdam ROssendorf Magnetic InStability Experiment*), shown in Figure 24, is basically a cylindrical Taylor-Couette cell with externally imposed axial and azimuthal magnetic fields. Its primary component is a

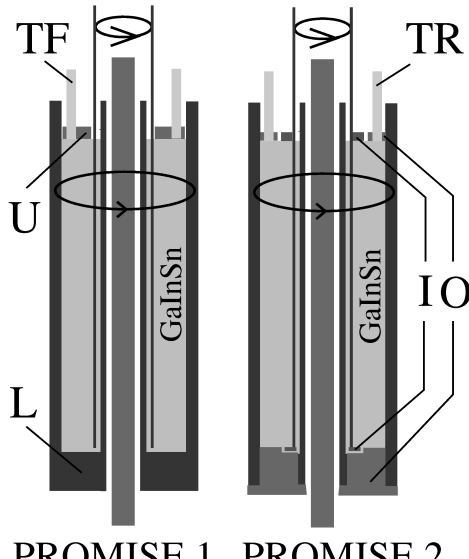


**Fig. 25** The asymmetric end cap configuration in PROMISE 1 is replaced by a symmetric one in PROMISE 2. U - Upper end cap fixed in the laboratory frame, L - Lower end cap, made of copper, rotating with the outer cylinder, I - Inner plastic rings, O - Outer plastic rings, TF - Fixed ultrasonic transducer, TR - Rotating ultrasonic transducer.

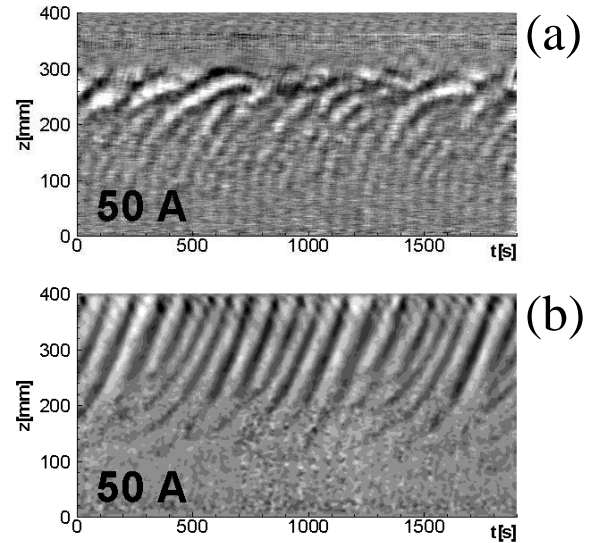


**Fig. 26** The measured axial velocity perturbation for  $Re = 2975$  and  $I_{coil} = 50$  A, showing the appearance of MRI as a travelling wave. (a) PROMISE 1 experiment with  $I_{rod} = 6000$  A. (b) PROMISE 2 experiment with  $I_{rod} = 7000$  A.

cylindrical copper vessel V, fixed on a precision turntable T via an aluminum spacer D. The inner wall of this vessel is 10 mm thick, extending in radius from 22 to 32 mm; the outer wall is 15 mm thick, extending from 80 to 95 mm. The outer wall of this vessel forms the outer cylinder of the TC cell. The inner cylinder I, also made of copper, is fixed on an upper turntable, and is then immersed into the liquid metal from above. It is 4 mm thick, extending in radius from 36 to 40 mm, leaving a 4 mm gap between it and the inner wall of the containment vessel V. The actual TC cell therefore extends in radius from 40 to 80 mm, for a gap width  $d = r_o - r_i = 40$  mm. This amounts to a radius ratio of  $\eta := r_i/r_o = 0.5$ . The fluid is filled to a height of 400 mm, for an aspect ratio of  $\sim 10$ . Axial fields of the order of 10 mT are produced by a coil C, and azimuthal fields of the same order are produced by currents of up to 8000 A in a water cooled copper rod R going through the center of the facility.

First results of PROMISE were published recently [225, 197, 226]. The most important result was the appearance of MRI in form of a travelling wave in a limited window of  $Ha$  (which is proportional to the coil current  $I_{coil}$ ). The frequency of this wave turned out to be in good agreement with numerical predictions.

The intricacies of this PROMISE 1 experiment, as we call it now, trace back to the two points discussed above. First, HMRI only slightly extends beyond the Rayleigh line and, second, the small unstable region for the convective instability is further reduced when considering the absolute instability. From this high sensitivity of the instability with respect to  $\mu := \Omega_o/\Omega_i$  one has to be careful with Ekman/Hartmann pumping and a possible change of the profiles by short circuited currents which can drive a Dean flow [236]. Another point is the critical role of the radial jet approximately at mid-height of the Taylor-Couette cell at which the MRI wave is typically stopped [227]. This radial jet results from the Ekman pumping at the lower and upper end caps.

For all those reasons, some changes of the axial boundary conditions have been implemented in a modified experiment which is called now PROMISE 2. As suggested by a thorough analysis of Szklarski [236], the Ekman pumping can be minimized by using split rings, the inner one rotating with the inner cylinder and the outer rotating with the outer cylinder, with a splitting position at 0.4 of the gap width (Figure 25). Both upper and lower rings are now made of insulating material. Since the ultrasonic transducers are rotating with the outer ring (i.e. with the slow rotation rate of the outer cylinder) their signal must be transmitted by slip rings to the computer.

Without going into the detailed results of the PROMISE 2 experiment, which will be published elsewhere, we can state that these modifications bring about a drastic improvement of the MRI wave and a significant sharpening of the transitions between stable and unstable regimes. In Figure 26 we see that for PROMISE 2 the MRI wave goes through the entire volume while it was stopped at the radial jet position in PROMISE 1.

## 6 Conclusions and prospects

The last ten years have seen tremendous progress in liquid metal experiments on the origin and the action of cosmic magnetic fields. With the success of the complementary sodium experiments in Riga and Karlsruhe in 1999 it was shown that self-excitation works not only in computer programs on the basis of rather smooth flows, but also in real-world turbulent flows. Kinematic dynamo theory has been shown to be robust with respect to low levels of turbulence and complicated boundary and interface conditions. The saturation mechanism in the Riga experiment is non-trivial as it results not only from a global pressure increase but also from a significant redistribution of the flow.

While the Riga and Karlsruhe dynamos are characterized by an amazing predictability, in some respect one can learn even more from the efforts to make the VKS dynamo (and also the MDX dynamo) running. After some modifications of the original concept, the VKS experiment was eventually successful in self-exciting a magnetic field. The fact that the observed eigenfield in VKS is essentially an axisymmetric dipole, in contrast to the original prediction of an equatorial dipole, is an inspiring challenge to understand better the intricate field amplification loop the dynamo mechanism relies on. The "little brother" of the VKS experiment, the VKG experiment in Lyon, has yielded fascinating field reversals when complemented by an external amplification loop that mimics a sort of  $\alpha$  effect.

On the way to the final rotating torus experiment, the Perm group has obtained important results concerning the mean-field coefficients in turbulent flows.

After dynamo action has thus been proven, one observes presently some tendency to take a breath and turn back to somewhat smaller machines in order to study MHD instabilities and wave phenomena. The identification of the MRI is only one aspect in this direction, though an important one due to the enormous astrophysical implications of this instability. Apart from standard MRI (Maryland, Princeton, New Mexico) and helical MRI (Dresden-Rossendorf) there are other magnetic instabilities that are capable of destabilizing hydrodynamically stable flows or even fluids at rest. Among them we have to note the Taylor-Vandakurov instability (with a current flowing through the liquid) [246, 237, 215] and the "azimuthal MRI" (AMRI) [196] based on an purely azimuthal field. Future experiments on those instabilities are very desireable.

There are many wave phenomena in rotating fluids under the influence of (externally applied or self-excited) magnetic fields which still deserve a deeper understanding. At this point we observe a revival of the activities in the sixties on Alfvén wave studies with liquid metals. In this respect, it might also be interesting that presently magnetic fields are available [258] which are so strong that for potassium and sodium the Alfvén velocity exceeds the sound velocity. The small scale experiments in Maryland and Grenoble have provided a wealth of data, and the 3 m sphere in Maryland will be a fascinating tool for extending those investigations into extreme parameter regions.

An interesting direction of future research could be the experimental investigation of precession driven dynamos, for which a water test experiment had been carried out by Léorat et al. [132, 133]. Numerical work by Tilgner [244] points to a critical  $Rm$  of around 200 which makes a laboratory experiments not unrealistic. Of course, much more optimization would be necessary before such an experiment could be designed.

If one had a wish for free, one could think of constructing a huge self-sustaining nonlinear dynamo [186] (or "self-creating dynamo" [57]). One could start, for example, in the hydrodynamic stable regime of a Taylor-Couette flow (mimicking a Keplerian flow) which could be destabilized, via MRI, by an externally applied magnetic field. Suppose now that the resulting flow would act as a dynamo, the resulting eigenfield could possibly replace the initially applied magnetic field as a trigger for the instability.

Having another wish for free, one could also think about the experimental realization of a fluctuation dynamo, based on more or less homogeneous isotropic turbulence [199]. For those flows, critical  $Rm$  around 200 have been found in recent simulations. However, simple Kolmogorov scaling arguments tell us that such a "James-Bond-dynamo" ("...shaken, not stirred...") is only possible with a giant input power of many Megawatts.

In spite of the fact that liquid metal experiments should not be expected to be perfect Bonsai models of any real astrophysical systems, experimental work has already started to change some views on those natural systems. Maybe that the Riga dynamo will once become a model of the double helix nebula close to the galactic center [148, 207], maybe that the partitioning of  $\alpha$  and  $\Omega$  effects in the VKS dynamo will re-animate the old Babcock-Leighton theory of the solar dynamo [6], maybe that the PROMISE experiment will illuminate the possible action of helical MRI in cold parts of accretion disks were standard MRI cannot work.

**Acknowledgements** Support from Deutsche Forschungsgemeinschaft in the framework of SFB 609, from European Commission under contract 028679, and from Leibniz-Gemeinschaft in the framework of the SAW project PROMISE is gratefully acknowledged. We are indebted to Raul Avalos-Zuñiga, Michael Christen, André Giesecke, Thomas Gundrum, Uwe Günther, Rainer Hollerbach, Saša Kenjereš, Jacques Léorat, Olgerts Lielausis, Ernests Platacis, Jānis Priede, Karl-Heinz Rädler, Günther Rüdiger, Luca Sorriso-Valvo, Jacek Szklarski, and Mingtian Xu for the fruitful collaboration over the course of many years.

## References

- [1] A. Alemany, Ph. Marty, F. Plunian, and J. Soto, *J. Fluid Mech.* **403**, 262–276 (2000).
- [2] Aristotle, *De anima* (On the soul) (Penguin, Harmondsworth, 1986), pp. 135–136.
- [3] J. Aubert, D. Brito, H.-C. Nataf, P. Cardin, and J.-P. Masson, *Phys. Earth Planet. Inter.* **128**, 51–74 (2001).
- [4] J. Aubert, J. Aurnou, and J. Wicht, *Geophys. J. Int.* **172**, 945–956 (2008).
- [5] R. Avalos-Zuñiga, M. Xu, F. Stefani, G. Gerbeth, and F. Plunian, *Geophys. Astrophys. Fluid Dyn.* **101**, 389–403 (2007).
- [6] H.W. Babcock, *Astrophys. J.* **133**, 572 (1961).
- [7] S.A. Balbus and J. F. Hawley, *Astrophys. J.* **376**, 214–222 (1991).
- [8] J.F. Hawley and S.A. Balbus, *Astrophys. J.* **400**, 595–609 (1992).
- [9] S.A. Balbus and J. F. Hawley, *Rev. Mod. Phys.* **70**, 1–53 (1998).
- [10] S.A. Balbus and P. Henri, *Astrophys. J.* **674**, 408–414 (2008).
- [11] R. Beck, A. Brandenburg, D. Moss, A. Shukurov, and D. Sokoloff, *Ann. Rev. Astron. Astrophys.* **34**, 155–206 (1996).
- [12] M. Berhanu et al., *EPL* **77**, 59001 (2007).
- [13] M.K. Bevir, *J. Br. Nucl. Energy Soc.* **12**, 455–458 (1973).
- [14] E.G. Blackman and H. Ji, *Mon. Not. R. Astron. Soc.* **369**, 1837–1848 (2006).
- [15] M. Bourgoin et al., *Phys. Fluids* **14**, 3046–3058 (2001).
- [16] M. Bourgoin et al., *New J. Phys.* **8**, 329 (2006).
- [17] J. Braithwaite and H.C. Spruit, *Nature* **431**, 819–821 (2004).
- [18] A. Brandenburg and K. Subramanian, *Phys. Rep.* **417**, 1–209 (2005).
- [19] A. Brandenburg, K.-H. Rädler, and M. Schrinner, *Astron. Astrophys.* **482**, 739–746 (2008).
- [20] D. Brito, P. Cardin, H.-C. Nataf, and G. Marolleau, *Phys. Earth Planet. Int.* **91**, 77–98 (1995).
- [21] B. Brunhes, *J. Phys.* **5**, 705–724 (1906).
- [22] E.C. Bullard, *Proc. Camb. Phil. Soc.* **51**, 744–760 (1955).
- [23] F.H. Busse, *Geophys. J. R. Astr. Soc.* **42**, 437–459 (1975).
- [24] F.H. Busse, *Ann. Rev. Fluid Mech.* **10**, 435–462 (1978).
- [25] F.H. Busse, *Annu. Rev. Fluid Mech.* **31**, 383–408 (2000).
- [26] F.H. Busse, *Phys. Fluids* **14**, 1301–1314 (2002).
- [27] F.H. Busse, E. Grote, and A. Tilgner, *Stud. Geophys. Geod.* **42**, 1–6 (1998).
- [28] P. Cardin, D. Brito, D. Jault, H.-C. Nataf, and J.-P. Masson, *Magnetohydrodynamics* **38**, 177–189 (2002).
- [29] J.B. Carlson, *Science* **189**, 753–760 (1975).
- [30] S. Chandrasekhar, *Proc. Nat. Acad. Sci.* **46**, 253–257 (1960).
- [31] S. Childress, and A. D. Gilbert, *Stretch, Twist, Fold: The Fast Dynamo* (Springer, Berlin/Heidelberg/New York, 1995).
- [32] M. Christen, H. Hänel, and G. Will, in *Beiträge zu Fluidenergiemaschinen 4*, edited by W. H. Faragallah and G. Grabow (Faragallah-Verlag und Bildarchiv, Sulzbach/Ts., 1998), pp. 111–119.
- [33] U.R. Christensen, P. Olson, and G. A. Glatzmaier, *Geophys. J. Int.* **138**, 393–409 (1999).
- [34] U.R. Christensen and A. Tilgner, *Nature* **429**, 169–171 (2004).
- [35] U.R. Christensen, *Nature* **444**, 1056–1058 (2006).
- [36] U.R. Christensen and J. Aubert, *Geophys. J. Int.* **166**, 97–114 (2006).
- [37] S.A. Colgate, H. Li, and V. Pariev, *Phys. Plasmas* **8**, 2425–2431 (2001).
- [38] S.A. Colgate et al., *Magnetohydrodynamics* **38**, 129–142 (2002).
- [39] S.A. Colgate, *Astron. Nachr.* **327**, 456–460 (2006).
- [40] C. Collins, C.B. Forest, R. Kendrick, and A. Seltzman, *Bull. Amer. Phys. Soc.* **52**, No. 11, BP8.00113 (2007).
- [41] J.E.P. Connerney, M. H. Acuña, P. J. Wasilewski, G. Kletetschka, N. F. Ness, H. Rème, R. P. Lin, and D. L. Mitchell, *Geophys. Res. Lett.* **28**, 4015–4018 (2001).
- [42] T.G. Cowling, *Mon. Not. Roy. Astr. Soc.* **140**, 39–48 (1934).
- [43] S.A. Denisov, V.I. Noskov, V.A. Stepanov, and P.G. Frick, *JETP Letters* **88**, 167–171 (2008).
- [44] W. Dobler, P. Frick, and R. Stepanov, *Phys. Rev. E* **67**, 056309 (2003).
- [45] E. Dormy, P. Cardin, and D. Jault, *Earth Planet. Sci. Lett.* **160**, 15–30 (1998).
- [46] B. Dubrulle et al., *Phys. Fluids* **17**, 095103 (2005).
- [47] M.L. Dudley and R. W. James, *Proc. R. Soc. Lond. A* **425**, 407–429 (1989).
- [48] N. Dziourkevitch, D. Elstner, and G. Rüdiger, *Astron. Astrophys.* **423**, L29–L32 (2004).
- [49] S. Fauve and F. Petrelis, *C.R. Phys.* **8**, 87–92 (2007).
- [50] D.R. Fearn, *Rep. Prog. Phys.* **61**, 175–235 (1998).
- [51] D.R. Fearn, P.H. Roberts, and A.M. Soward, in *Energy, Stability, and Convection*, edited by G. P. Galdi and B. Straughan (Longmans, New York, 1988), pp. 60–324.
- [52] M. Fischer, F. Stefani, and G. Gerbeth, *Eur. J. Phys. B*, in press (2008); arxiv.org/0709.3932.
- [53] M. Fischer, G. Gerbeth, A. Giesecke, and F. Stefani, *Inverse Problems*, submitted (2008); arxiv.org/0808.3310.
- [54] C.B. Forest et al., *Magnetohydrodynamics* **38**, 107–120 (2002).
- [55] C.B. Forest et al., *Bull. Amer. Phys. Soc.* **52**, No. 11, BP8.00114 (2007).
- [56] P. Frick et al., *Magnetohydrodynamics* **38**, 143–162 (2002).
- [57] H. Fuchs, K.-H. Rädler, M. Rheinhardt, *Astron. Nachr.* **320**, 129–133 (1999).
- [58] A. Gailitis, *Magnetohydrodynamics* **3**, No. 3, 23–29 (1967).
- [59] A. Gailitis, *Magnetohydrodynamics* **32**, 58–62 (1996).
- [60] A. Gailitis and Ya. Freibergs, *Magnetohydrodynamics* **12**, 127–129 (1976).

- [61] A. Gailitis and Ya. Freibergs, Magnetohydrodynamics **16**, 116–121 (1980).
- [62] A.K. Gailitis et al., Magnetohydrodynamics **23**, 349–353 (1987).
- [63] A. Gailitis, Appl. Magnetohydrodyn. **12**, 143 (1961).
- [64] A. Gailitis et al., Phys. Rev. Lett. **84**, 4365–4368 (2000).
- [65] A. Gailitis et al., Phys. Rev. Lett. **86**, 3024–3027 (2001).
- [66] A. Gailitis, O. Lielausis, E. Platacis, G. Gerbeth, and F. Stefani, Magnetohydrodynamics **37**, No. 1/2, 71–79 (2001).
- [67] A. Gailitis et al., Magnetohydrodynamics **38**, 5–14 (2002).
- [68] A. Gailitis, O. Lielausis, E. Platacis, G. Gerbeth, and F. Stefani, Magnetohydrodynamics **38**, 15–26 (2002).
- [69] A. Gailitis, O. Lielausis, E. Platacis, G. Gerbeth, and F. Stefani, Rev. Mod. Phys. **74**, 973–990 (2002).
- [70] A. Gailitis, O. Lielausis, E. Platacis, G. Gerbeth, and F. Stefani, Surv Geophys. **24**, 247–267 (2003).
- [71] A. Gailitis, O. Lielausis, E. Platacis, G. Gerbeth, and F. Stefani, Phys. Plasmas **11**, 2838–2843 (2004).
- [72] A. Gailitis, O. Lielausis, G. Gerbeth, and F. Stefani, in: *Magnetohydrodynamics: Historical Evolution and Trends*, edited by S. Molokov, R. Moreau, H.K. Moffatt (Springer, Dordrecht, 2007), pp. 37–54.
- [73] A. Gailitis, G. Gerbeth, Th. Gundrum, O. Lielausis, E. Platacis, and F. Stefani, C.R. Phys. **9**, 721–728 (2008).
- [74] R.F. Gans, J. Fluid Mech. **45**, 111–130 (1970).
- [75] W. Gekelman, J. Geophys. Res. **104** 14417–14435 (1999).
- [76] H. Gellibrand, H., *A discourse mathematical on the variation of the magneticall needle*, reprint edited by G. Hellmann (A. Asher, Berlin, 1887).
- [77] A. Giesecke, U. Ziegler, and G. Rüdiger, Phys. Earth Planet. Inter. **152**, 90–102 (2005).
- [78] A. Giesecke, F. Stefani, and G. Gerbeth, Magnetohydrodynamics, in press (2008); arXiv:0803.3261.
- [79] W. Gilbert, *De Magnete*, translated by P. F. Mottelay, (Dover, New York, 1958).
- [80] C. Gissinger, A. Iskakov, S. Fauve, and E. Dormy, EPL **82**, 29001 (2008).
- [81] K.-H. Glassmeier et al., Space Sci. Rev. **132**, 511–527 (2007).
- [82] K.-H. Glassmeier, H.U. Auster, and U. Motschmann, Geophys. Res. Lett. **34**, L22201 (2007).
- [83] G.A. Glatzmaier and P. H. Roberts, Nature **377**, 203–209 (1995).
- [84] F. Govoni and L. Feretti, Int. J. Mod. Phys. D **13**, 1549–1594 (2004).
- [85] D. Grasso and H. R. Rubinsteiin, Phys. Rep. **348**, 163–266 (2001).
- [86] J.-L. Guermond, R. Laguerre, J. Léorat, and C. Nore, J. Comp. Phys. **221**, 349–369 (2007).
- [87] G.E. Hale, Astrophys. J. **28**, 315–345 (1908).
- [88] J.F. Hawley, Phys. Plasmas **10**, 1946–1953 (2003).
- [89] H. Harder and U. Hansen, Geophys. J. Intern. **161**, 522–532 (2005).
- [90] A. Herzenberg, Philos. Trans. R. Soc. London **A250**, 543–585 (1958).
- [91] R. Hollerbach, Phys. Earth Planet. Int. **98**, 163–185 (1996).
- [92] R. Hollerbach and G. Rüdiger, Phys. Rev. Lett. **95**, 124502 (2005).
- [93] R. Hollerbach, E. Canet, and A. Fournier, Eur. J. Mech. B/Fluids **26**, 729–737 (2007).
- [94] P. Hoyng and J.J. Duistermaat, EPL **68**, 177–183 (2004).
- [95] D. R. Inglis, Rev. Mod. Phys. **53**, 481–496 (1981).
- [96] A.B. Iskakov, S. Descombes, and E. Dormy, J. Comp. Phys. **197**, 540–554 (2004).
- [97] D.J. Ivers and R.W. James, Geophys. Astrophys. Fluid Dyn. **44**, 271–278 (1988).
- [98] H. Ji, M. Yamada, S. Hsu, and R. Kulsrud, Phys. Rev. Lett. **80**, 3256–3259 (1998).
- [99] H. Ji et al., Phys. Plasmas **3**, 1935–1942 (1996).
- [100] H. Ji, J. Goodman, and A. Kageyama, Mon. Not. Roy. Astr. Soc. **325**, L1–L5 (2001).
- [101] H. Ji, M. Burin, E. Schartman, and J. Goodman, Nature **444**, 343–346 (2006).
- [102] H. Ji, J. Goodman, and A. Kageyama, Mon. Not. Roy. Astron. Soc. **325**, L1–L5 (2001).
- [103] A. Kageyama, M. M. Ochi, and T. Sato, Phys. Rev. Lett. **82**, 5409–5412 (1999).
- [104] R. Kaiser, Geophys. Astrophys. Fluid Dyn. **101**, 185–197 (2007).
- [105] S. Kenjereš, K. Hanjalić, S. Renaudier, F. Stefani, G. Gerbeth, and A. Gailitis, Phys. Plasmas **13**, 122308 (2006).
- [106] S. Kenjereš and K. Hanjalić, Phys. Rev. Lett. **98**, 104501 (2007).
- [107] S. Kenjereš and K. Hanjalić, New J. Phys. **9**, 306 (2007).
- [108] I.V. Khalzov, Tech. Phys. **76**, 26 (2006).
- [109] I.V. Khalzov, V.I. Ilgisonis, A.I. Smolyakov, and E.P. Velikhov, Phys. Fluids **18**, 124107 (2006).
- [110] I.V. Khalzov, A.I. Smolyakov, and V.I. Ilgisonis, arxiv:0711.2818 (2007).
- [111] I.M. Kirko, G.E. Kirko, A.G. Sheinkman, and M.T. Telichko, Dokl. Akad. Nauk. SSSR, **266**, 854–856 (1982).
- [112] O.N. Kirillov, Int. Journ. Non-Lin. Mech. **42**, 71–87 (2007).
- [113] L.I. Kitchatinov and G. Rüdiger, Astron. **329**, 372–375 (2008).
- [114] M.G. Kivelson et al., Nature **384**, 537–541 (1996).
- [115] E. Knobloch, Mon. Not. R. Astron. Soc. **255**, P25–P28 (1992).
- [116] M. Kono and P.H. Roberts, Rev. Geophys. **40**, 1013 (2002).
- [117] C. Kouveliotou et al., Nature **393**, 235–237 (1998).
- [118] D.S. Krasnov, E. Zienicke, O. Zikanov, T. Boeck, and A. Thess, J. Fluid Mech. **504**, 183–211 (2004).
- [119] F. Krause and K.-H. Rädler, *Mean-field magnetohydrodynamics and dynamo theory* (Akademie, Berlin, 1980).
- [120] P.P. Kronberg, Q.W. Dufton, H. Li, and S.A. Colgate, Astrophys. J. **560**, 178–186 (2001).
- [121] R. Krechetnikov and J.E. Marsden, Rev. Mod. Phys. **79**, 519–553 (2007).
- [122] W. Kuang and J. Bloxham, Nature **389**, 371–374 (1997).
- [123] R.M. Kulsrud and E.G. Zweibel, Rep. Progr. Phys. **71**, 046901 (2008).

- [124] R. Laguerre, C. Nore, J. Léorat, J.L. Guermond, C.R. Mec. **334**, 593-598 (2006).
- [125] R. Laguerre et al., Phys. Rev. Lett. **101**, 104501 (2008).
- [126] V.P. Lakhin and E.P. Velikhov, Phys. Lett. A **369** 98-106 (2007).
- [127] J. Larmor, Rep. Brit. Assoc. Adv. Sci., 159–160 (1919).
- [128] D.P. Lathrop, W.L. Shew, and D.R. Sisan, Plasma Phys. Contr. Fusion **43**, A151-A160 (2001).
- [129] J.-P. Laval, P. Blaizeau, N. Leprovost, B. Dubrulle, F. Daviaud, Phys. Rev. Lett. **96**, 204503 (2006).
- [130] B. Lehnert, Arkiv för Fysik **13**, 10, 109–116 (1958).
- [131] B. Lehnert, in: *Magnetohydrodynamics: Historical Evolution and Trends*, edited by S. Molokov, R. Moreau, H.K. Moffatt (Springer, Dordrecht, 2007), pp. 27-36.
- [132] J. Léorat, F. Rigaud, R. Vitry and G. Herpe, Magnetohydrodynamics **39**, 321-326 (2003).
- [133] J. Léorat, Magnetohydrodynamics **42**, 143-151 (2006).
- [134] J.T.C. Liu, Ann. Rev. Fluid Mech. **21**, 285-315 (1988).
- [135] W. Liu, J. Goodman, I. Herron, and H.T. Ji, Phys. Rev. E **74**, 056302 (2006).
- [136] W. Liu, J. Goodman, and H. Ji, Phys. Rev. E **76**, 016310 (2007).
- [137] W. Liu, Astrophys. J. **684**, 515-524 (2008).
- [138] F.J. Lowes and I. Wilkinson, Nature **198**, 1158–1160 (1963).
- [139] F.J. Lowes and I. Wilkinson, Nature **219**, 717–718 (1968).
- [140] Lucretius Carus, Titus, On the nature of things, Project Gutenberg Etext ([www.gutenberg.org/etext/785](http://www.gutenberg.org/etext/785)), translated by William Ellery Leonard
- [141] L. Marié et al., in *Dynamo and Dynamics, a Mathematical Challenge*, edited by P. Chossat, D. Armbruster, and I. Oprea (Kluwer, Dordrecht/Boston/London, 2001), pp. 35–50.
- [142] L. Marié, J. Burguete, F. Daviaud, and J. Léorat, Eur. Phys. J. B **33m** 469-485 (2003).
- [143] L. Marié, C. Normand, and F. Daviaud, Phys. Fluids **18**, 017102 (2006).
- [144] R.T. Merrill, R. T., M. W. McElhinny, and Ph. L. McFadden, *The magnetic field of the earth : paleomagnetism, the core, and the deep mantle* (Academic, San Diego, 1998).
- [145] H.K. Moffatt, *Magnetic field generation in electrically conducting fluids* (Cambridge University, Cambridge, 1978).
- [146] R. Monchaux et al., Phys. Rev. Lett. **98**, 044502 (2007).
- [147] P. Moresco and T. Alboussiere, J. Fluid Mech. **504**, 167-181 (2004).
- [148] M. Morris, K. Uchida, and T. Do, Nature **440**, 308-310 (2006).
- [149] U. Müller and R. Stieglitz, Naturwissenschaften **87**, 381–390 (2000).
- [150] U. Müller and R. Stieglitz, Nonl. Proc. Geophys. **9**, 165-170 (2002).
- [151] U. Müller, R. Stieglitz, and S. Horanyi, J. Fluid Mech. **498**, 31-71 (2004).
- [152] U. Müller, R. Stieglitz, and S. Horanyi, J. Fluid Mech. **552**, 419-440 (2006).
- [153] H.-C. Nataf et al., Geophys. Astrophys. Fluid Dyn. **100**, 281-298 (2006).
- [154] T. Nakajima and M. Kono, Geophys. Astrophys. Fluid Dynamics **60**, 177–209 (1991).
- [155] J. Needham, Science and Civilisation in China, (Cambridge University, Cambridge, 1962), vol. 4, part 1.
- [156] N.F. Ness, K. W. Behannon, R. P. Lepping, and Y. C. Whang, Nature **255**, 204–205 (1975).
- [157] M.D. Nornberg, E.J. Spence, R.D. Kendrick, C.M. Jacobson, and C.B. Forest, Phys. Rev. Lett. **97**, 044503 (2006).
- [158] M.D. Nornberg, E.J. Spence, R.D. Kendrick, C.M. Jacobson, and C.B. Forest, Phys. Plasmas **13**, 055901 (2006).
- [159] G.I. Ogilvie and A.T. Potter, Phys. Rev. Lett. **100**, 074503 (2008).
- [160] M. Ossendrijver, Astron. Astrophys. Rev. **11**, 287-367 (2003).
- [161] E.N. Parker, Astrophys. J. **122**, 293-314 (1955).
- [162] N.L. Peffley, A.B. Cawthorne, and D.P. Lathrop, Phys. Rev. E. **61**, 5287–5294 (2000).
- [163] N.L. Peffley, A. G. Goumievski, A. B. Cawthorne, and D. P. Lathrop, Geophys. J. Int. **141**, 52–58 (2000).
- [164] C.L. Pekeris, Y. Accad, and B Shkoller, Phil. Trans. R. Soc. Lond. **A275**, 425–461 (1973).
- [165] M.E. Pessah and D. Psaltis, Astrophys. J. **628**, 879-901 (2005).
- [166] F. Pétrélis, M. Bourgoin, L. Marié, J. Burguete, A. Chiffaudel, F. Daviaud, S. Fauve, P. Odier, and J.-F. Pinton, Magnetohydrodynamics **38**, 163-176 (2002).
- [167] F. Pétrélis et al., Phys. Rev. Lett. **90**, 174501 (2003).
- [168] F. Pétrélis, N. Mordant, and S. Fauve, Geophys. Astrophys. Fluid Dyn. **101**, 289-323 (2007).
- [169] Petrus Peregrinus de Maricourt, *Opera* (Scuola normale superiore, Pisa, 1995).
- [170] F. Plunian, P. Marty P, and A. Alemany, J. Fluid Mech. **382**, 137–154 (1999).
- [171] E.S. Pierson, E. S., Nucl. Sci. Eng. **57**, 155–163 (1975).
- [172] Yu.B. Ponomarenko, J. Appl. Mech. Tech. Phys. **14**, 775–779 (1973).
- [173] J. Priede, I. Grants, and G. Gerbeth, Phys. Rev. E **75**, 047303 (2007).
- [174] J. Priede and G. Gerbeth, in preparation
- [175] K.-H. Rädler, E. Apstein, M. Rheinhardt, and M. Schüler, Studia geoph. et geod. **42**, 1–9 (1998).
- [176] K.-H. Rädler, M. Rheinhardt, E. Apstein, and H. Fuchs, Magnetohydrodynamics **38**, 41-71 (2002).
- [177] K.-H. Rädler, M. Rheinhardt, E. Apstein, and H. Fuchs, Magnetohydrodynamics **38**, 73-94 (2002).
- [178] K.-H. Rädler, M. Rheinhardt, E. Apstein, and H. Fuchs, Nonl. Proc. Geophys. **9**, 171-187 (2002).
- [179] K.-H. Rädler and M. Rheinhardt, Magnetohydrodynamics **38**, 211-217 (2002).
- [180] K.-H. Rädler and M. Rheinhardt, Geophys. Astrophys. Fluid Dyn. **101**, 117-154 (2007).
- [181] F. Ravelet, A. Chiffaudel, F. Daviaud, J. Léorat, Phys. Fluids **17**, 117104 (2005).
- [182] F. Ravelet, *Von Karman flow and the dynamo effect*, Thesis (Ecole Polytechnique, 2005), <http://tel.archives-ouvertes.fr/tel-00011016/en/>.

- [183] F. Ravelet et al., arXiv:0704.2565
- [184] Rayleigh Lord, *On the dynamics of revolving fluids* Scientific papers **6**, 447-453 (1929).
- [185] A.B. Reighard and M. R. Brown, Phys. Rev. Lett. **86**, 2794–2797 (2001).
- [186] F. Rincon, G.I. Ogilvie, and M.R.E. Proctor, Phys. Rev. Lett. **98**, 254502 (2007).
- [187] A. Roach, H. Ji, W. Liu, and J. Goodman, Bull. Amer. Phys. Soc. **52**, No. 11, BP8.00084 (2007).
- [188] G.O. Roberts, Philos. Trans. R. Soc. London, **A271**, 411–454 (1972).
- [189] P.H. Roberts, P. H., in *Lectures on Solar and Planetary Dynamos*, edited by M. R. E. Proctor and A. D. Gilbert, (Cambridge University, Cambridge, 1994), pp. 1–58.
- [190] P.H. Roberts and T. H. Jensen, Phys. Fluids B **7**, 2657–2662 (1992).
- [191] P.H. Roberts and A. M. Soward, Annu. Rev. Fluid Mech. **24**, 459–512 (1992).
- [192] P.H. Roberts and G. A. Glatzmaier, Rev. Mod. Phys. **72**, 1081–1123 (2002).
- [193] G. Rüdiger and R. Hollerbach, *The Magnetic Universe* (Wiley, Berlin, 2004).
- [194] G. Rüdiger, R. Hollerbach, M. Schultz, and D.A. Shalybkov, Astron. Nachr. **326**, 409-413 (2005).
- [195] G. Rüdiger and R. Hollerbach, Phys. Rev. E **76**, 068301 (2007).
- [196] G. Rüdiger, R. Hollerbach, M. Schultz, and D. Elstner, Mon. Not. R. Astron. Soc. **377**, 1481-1487 (2007).
- [197] G. Rüdiger et al., Astrophys. J. **649**, L145-L147 (2006).
- [198] A.A. Schekochihin and S.C. Cowley, Phys. Plasmas **13**, 056501 (2006).
- [199] A.A. Schekochihin et al., New J. Phys. **9**, 3000 (2007).
- [200] F. Schultz-Grunow, ZAMM **39**, 101-110 (1959).
- [201] D. Schmitt et al., J. Fluid Mech. **604**, 175-197 (2008).
- [202] M. Schrinner, K.-H. Rädler, D. Schmitt, M. Rheinhardt, and U. Christensen, Astron. Nachr. **326**, 245-249 (2005).
- [203] M. Schrinner, K.-H. Rädler, D. Schmitt, M. Rheinhardt, and U. Christensen, Geophys. Astrophys. Fluid Dyn. **101**, 81-116 (2007).
- [204] N.I. Shakura and R.A. Sunyaev, Astron. Astrophys. **24**, 337-355 (1973).
- [205] W.L. Shew, W. L., D. R. Sisan, and D. P. Lathrop, in *Dynamo and Dynamics, a Mathematical Challenge*, edited by P. Chossat, D. Armbruster, and I. Oprea (Kluwer, Dordrecht/Boston/London, 2001), pp. 83–92.
- [206] W.L. Shew and D.P. Lathrop, Phys. Earth Planet. Inter. **153**, 136-149 (2005).
- [207] A. Shukurov and D.D. Sokoloff, in *The Cosmic Dynamo*, edited by F. Krause et al. (IAU, 1993), pp. 367-371.
- [208] C.W. Siemens, Proc. R. Soc. London **15**, 367 (1867).
- [209] Simonyi, K., *Kulturgeschichte der Physik*, (Urania, Leipzig/Jena/Berlin, 1990), p. 343.
- [210] D.R. Sisan, W.L Shew, and D.P. Lathrop, Phys. Earth Planet. Inter. **135**, 137-159 (2003).
- [211] D.R. Sisan et al., Phys. Rev. Lett. **93**, 114502 (2004).
- [212] D.J. Southwood, Planet. Space Sci. **45**, 113–117 (1997).
- [213] E.J. Spence, M.D. Nornberg, C.M. Jacobson, R.D. Kendrick, and C.B. Forest, Phys. Rev. Lett. **96**, 055002 (2006).
- [214] E.J. Spence et al., Phys. Rev. Lett. **98**, 164503 (2007).
- [215] H.C. Spruit, Astron. Astrophys. **381**, 923-932 (2002).
- [216] M. Steenbeck, F. Krause, and K.-H. Rädler, Z. Naturforsch. **21a**, 369–376 (1966).
- [217] M. Steenbeck, I. M. Kirko, A. Gailitis, A. P. Klawina, F. Krause, I. J. Laumanis, and O. A. Lielausis, Mber. Dt. Ak. Wiss. **9**, 714–719 (1967).
- [218] M. Steenbeck, Letter to H. Klare, President of the Academy of Sciences of the GDR (1975).
- [219] F. Stefani, G. Gerbeth, and A. Gailitis, in *Transfer Phenomena in Magnetohydrodynamic and Electroconducting Flows*, edited by A. Alemany, Ph. Marty, J. P. Thibault (Kluwer, Dordrecht/Boston/London, 1999) pp. 31–44.
- [220] F. Stefani, G. Gerbeth, and K.-H. Rädler, Astron Nachr. **321**, 65-73 (2000).
- [221] F. Stefani and G. Gerbeth, Phys. Rev. Lett. **94**, 184506 (2005).
- [222] F. Stefani, G. Gerbeth, U. Günther, and M. Xu, Earth Planet. Sci. Lett. **243**, 828-840 (2006).
- [223] F. Stefani et al., Eur. J. Mech. B/Fluids **25**, 894-908 (2006).
- [224] F. Stefani, M. Xu, L. Sorriso-Valvo, G. Gerbeth, and U. Günther, Geophys. Astrophys. Fluid Dyn. **101**, 227-248 (2007).
- [225] F. Stefani et al., Phys. Rev. Lett. **97**, 184502 (2006).
- [226] F. Stefani et al., New J. Phys. **9**, 295 (2007).
- [227] F. Stefani et al., Astron. Nachr. **329**, 652 (2008).
- [228] R. Stepanov et al., Phys. Rev. E **73**, 046310 (2006).
- [229] F. Stefani and G. Gerbeth, in MHD Couette Flows. Experiments and Methods, edited by A. Bonanno, R. Rosner and G. Rüdiger (AIP Conference Proceedings 733, 2004), pp. 100-113.
- [230] S. Stellmach and U. Hansen, Phys. Rev. E **70**, 056312 (2004).
- [231] S. Stellmach and U. Hansen, Geochem. Geophys. Geosyst. **9**, Q05003 (2008).
- [232] D.J. Stevenson, Rep. Progr. Phys. **46**, 555-620 (1983).
- [233] D.J. Stevenson, Earth Planet. Sci. Lett. **208**, 1-11 (2003).
- [234] R. Stieglitz and U. Müller, Phys. Fluids **13**, 561–564 (2001).
- [235] J. Szklarski and G. Rüdiger, Astron Nachr. **327**, 844-849 (2006).
- [236] J. Szklarski, Astron Nachr. **328**, 499-506 (2007).
- [237] R. J. Tayler, Mon. Not. R. Astron. Soc. **161**, 365-380 (1973).
- [238] A. Tilgner, Acta Astron. et Geophys. Univ. Comenianae **XIX**, 51–62 (1997).
- [239] A. Tilgner, Phys. Lett. A **226**, 75–79 (1997).
- [240] A. Tilgner, Phys. Earth Planet. Inter. **117**, 171–177 (2000).
- [241] A. Tilgner and F. H. Busse, in *Dynamo and Dynamics, a Mathematical Challenge*, edited by P. Chossat, D. Armbruster, and I. Oprea (Kluwer, Dordrecht/Boston/London, 2001), pp. 109–116.

- [242] A. Tilgner, Phys. Rev E **66**, 017304 (2002).
- [243] A. Tilgner, Phys. Fluids **14**, 4092-4094 (2002).
- [244] A. Tilgner, Phys. Fluids **17**, 034104 (2005).
- [245] N.J. Turner, T. Sano, and N. Dziourkevitch, Astrophys. J. **659**, 729-737 (2007).
- [246] Y.V. Vandakurov, Soviet Astron. **16**, 265 (1972).
- [247] E.P. Velikhov, Sov. Phys. JETP **36** 995-998 (1959).
- [248] E.P. Velikhov, Phys. Lett. A. **358**, 216-221 (2006).
- [249] M.K. Verma, Phys. Rep. **401**, 229-380 (2004).
- [250] R. Volk, P. Odier, and J.-F. Pinton, Phys. Fluids **18**, 085105 (2006).
- [251] Z. Wang, V.I. Pariev, C.W. Barnes, and D.C. Barnes, Phys. Plasmas **9**, 1491-1494 (2002).
- [252] T. Weier, V. Shatrov, and G. Gerbeth, in: *Magnetohydrodynamics: Historical Evolution and Trends*, edited by S. Molokov, R. Moreau, H.K. Moffatt (Springer, Dordrecht, 2007), pp. 295-312.
- [253] G. Wendt, Ing.-Arch. **4**, 577-595 (1933).
- [254] J. Wicht and P. Olson, Geochem. Geophys. Geosyst. **5**, Q03H10 (2004).
- [255] I. Wilkinson, Geophys. Surveys **7**, 107-122 (1984).
- [256] F. Winterberg, Phys. Rev. **131**, 29-37 (1963).
- [257] C. Wheatstone, Proc. R. Soc. London **15**, 369 (1867).
- [258] J. Wosnitza et al., J. Mag. Magn. Mat. **310**, 2728-2730 (2007).
- [259] M. Xu, F. Stefani, and G. Gerbeth, J. Comp. Phys. **196** 102-125 (2004).
- [260] M. Xu, F. Stefani, and G. Gerbeth, Phys. Rev. E **70**, 056305 (2004).
- [261] M. Xu, F. Stefani, and G. Gerbeth, J. Comp. Phys. **227**, 8130-8144 (2008).
- [262] P.J. Zandbergen and D. Dijkstra, Ann. Rev. Fluid Mech. **19**, 465-491 (1987).

## Pb-Li eutektikas ražošana (J.Freibergs, I.Platnieks, E.Platacis, J.Kļaviņš)

Izstrādāta metodika un izgatavota iekārta, lietojot magnetohidrodinamisku maisīšanu, svina--litija 15.7at% rūpnieciskai ražošanai. Ar šīs iekārtas saražotas 5 tonnas augstas tīrības Pb-15.7at%Li eutektikas, kas nodotas Itāliem (ENEA Fusion and Nuclear Technologies Department, Frascati) kodolsintēzes reaktora dzesēšanas sistēmas pētījumiem.



### 1) Starting materials.

The lead is supplied by firma CFM Oskar Tropitzsch and firma DOMA as the mediator. The lithium is supplied by firma Chemetall GmbH through the same mediator. The data given by suppliers are in the Appendix 1.

### 2) Melting process, crucible material, heating, gained experience.

The alloyage process is going in reactor made of stainless steel. The liquid components and the product have contact only with stainless steel. The description of the process, regimes and the gained experience are given in the Appendix 2 and Appendix 3.

### 3) Information about batches.

In following table dates about each batch are concentrated. The weight of a batch is given as the sum of all ingots weight. The batches were weighted regularly after first 14 casts and later selectively only when by-flow at mould filling was fixed. The weight of recasted batches was carefully fixed because the mould filling interruption was done by hand following the level detector signal. In common cases the weight

was estimated as exceeding 75 kg. The characteristic weight of a normal batch is 75.5 kg.

The solidification temperature on the crystallization front was fixed by thermocouple. The restricted accuracy of the used thermocouple (2.5%) and the intensive heat flux near the tip of the thermocouple do not allow qualifying the measurement as exact solidification point temperature measurement. The equality between the fixed temperatures through all the casts at identical conditions was used as a criterion of stability of all the production process. The temperature not shown in table because for all batches was fixed the quantity:  $233.7 \pm 0.5$  °C.

For batches 7, 11, 28, 34, 35 as minimum one of the Lithium analyses result is out of the range requested in the Technical Specification. However, the cast average Li content based on the all of the performed Li analyses is in the specified range.



Fig. 1. The ingots

acquiring the process, the description of the design of the equipment for producing 75 kg in one batch, the description of operations during the run of the process, the safety measures in handling with lead and lithium, the operation instruction to control the process and the chemical content fixation of the produced alloy.

**Introduction.** The most important problems which must be solved by designing of the equipment are:

- It is necessary to ensure very effective mixing because the very large difference in densities of the alloy components results in considerable tendency to stratification.
- It is necessary to minimize the formation of intermetalites which happens in result of the chemical reactions between lead and lithium. They have high melting temperatures ( $\text{Li}_4\text{Pb} - 648$  °C,  $\text{Li}_7\text{Pb}_2 - 726$  °C,  $\text{Li}_3\text{Pb} - 658$  °C,  $\text{Li}_5\text{Pb}_2 - 642$  °C,  $\text{LiPb} - 482$  °C) and suspend in the Pb-Li alloy when it temperature is lower.

The solution of the first problem was finding by using MHD-mixing. The running magnetic field was used to stir up the two-component melt.

The way to minimize the quantity of intermetalites was found by resuming the experience of different castings, watching the pouring-out difficulties. The quantity of the reactions products, believably, depends from the character the injected lithium fronts lead and the temperature of the components. The experience shows that slow injection at temperature which does not essentially exceed the lead melting temperature results in increased quantity of intermetalites. A good result was achieved

when lead in the reactor was heated up to 390 °C and injection was performed using high pressure (10 bars) through a nozzle which ensures dispersive spray

**Design of the equipment and description of operations during the process.** The composition of main units of the equipment are shown on fig. 1.

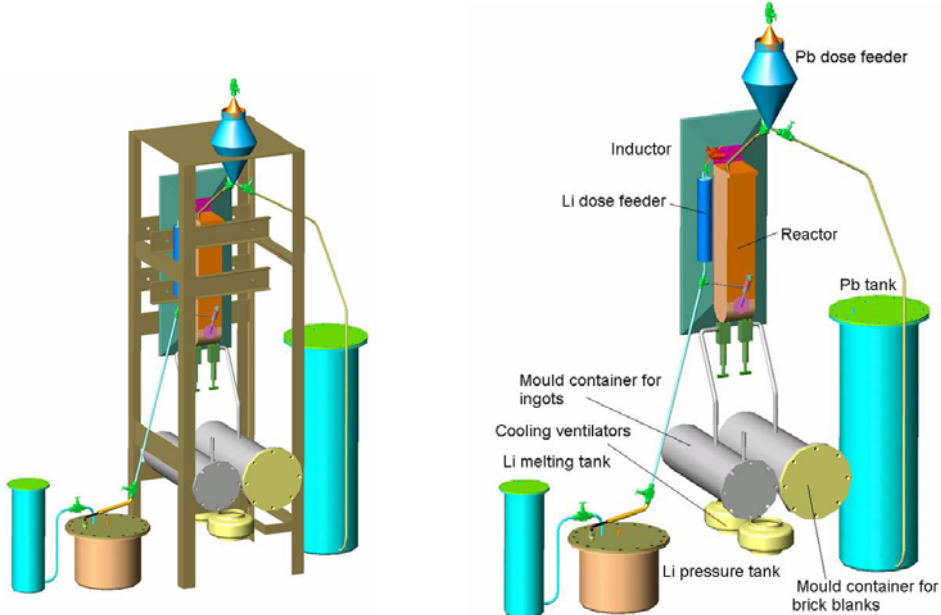


Fig. 1. Composition of the main units of the equipment.

The alloyage and the reaction between the lead and the lithium goes in the reactor which is designed as a vertically orientated elongated box tacking by one side the electro-magnetic inductor. The inductor creates the running magnetic field induction lines of which are closed through the liquid metal. It creates up-orientated force in the metal. The decay of the local strength of the force by increasing the distance from inductor is the reason the rotating velocity structure in the liquid metal arises.

The preparation of the lead goes in the lead tank by putting the pieces of solid lead in, vacuum-treatment of closed tank and electrical heating of the tank to melt the metal. For the preparation of lithium 100 g pieces of metal are put in a special melting tank under argon atmosphere, melted by electrical heating and transfused in the pressure tank. There is possibility to fix the height of levels in Pb tank and in Li pressure tank by electrical contact sounds.

At the beginning of the process the for-vacuum is ensured in all containers of the equipment; the temperature predicted for different containers, pipes and valves is maintained by special automatized system controlled by computer (390°C , 280°C and 300°C for units containing lead, lithium and the alloy). To obtain the necessary quantity of lead for one alloyage cycle the vacuum-treated Pb-dose feeder is filled by argon pressure created in lead tank. It must be high enough to raise the liquid metal to the top point of the feeder. The dose of lead is canalized to the reactor by closing valve to the lead tank and opening the other to the reactor. The dose feeder is designed to feed the stated quantity of lead in the reactor. The mixing of the lead is started and goes 15 minutes admitting that some solution of remnants from the previous batch would take place in the lead heated up to 390\* C.

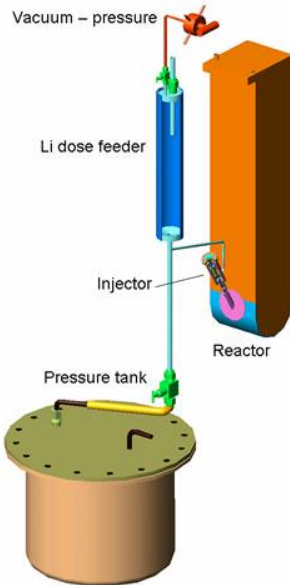


Fig. 2.Lithium feeding system.

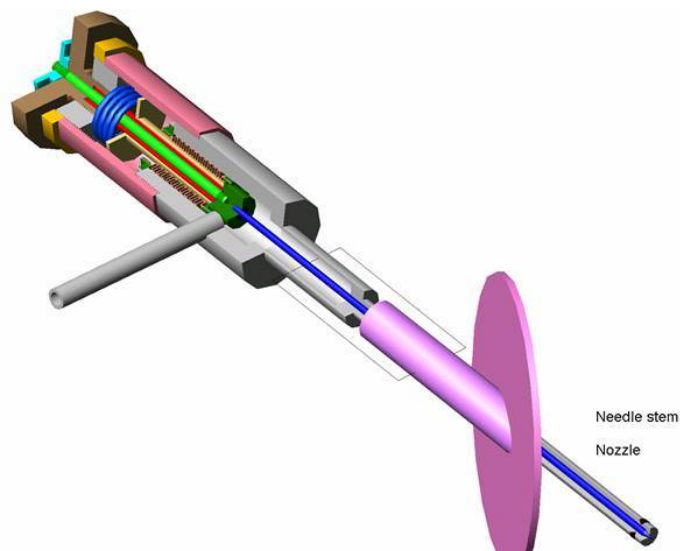


Fig. 3. Injector.

The lithium system must ensure feeding the dose of lithium in the matching lead dose which is subject of stirring during the injection. To fill the calibrated dose feeder pressure of argon is created in the lithium pressure tank. To prepare the Li dose for the injection the vacuum treatment of the dose feeder goes through the 4-way valve. When the feeder is disconnected from the vacuum and connected to the Li pressure tank the Li fills the feeder. To run the injection the dose feeder is disconnected from the Li pressure tank and connected to 10 bars pressure trough the 4-way valve before the injection valve is opened.

The injector (Fig. 3) is designed to form disperse spray of the lithium in the lead. The 10 bars pressure which drives the injection must ensure the effect. The injection of 0.95 liter of Li takes about 30 seconds. The end of the injection is fixed by pressure measurement in the reactor – spoiled vacuum indicates the end of injection.

The mixing continues at least 40 minutes after the end of the injection. Then without interruption of the mixing the valve to the mould container is opened to empty the reactor. Two ways to two mould containers are put in the design (Fig. 1). For the two mould containers two valves with the 15.9 mm orifices is welded to the reactor bottom to pour the alloy in the sequent mould container through  $\frac{3}{4}$ " pipes. Use of the second container doubles the productivity of the process when the batches follow one after another. We have the possibility to perform the 75 kg cycle one in each hour. This process demands quick cooling of filled mould container and changing the filled sectioned mould by prepared next one during this hour. In one of the containers casting of brick blanks take place; in another the 10 kg ingots for melts to supply liquid metal loops are produced. Two sectioned moulds for each container are used to cast the brick blanks and the

ingots are in use. It ensures the quick renewing the start position for the following cycle. The sectioned moulds of the containers are shown in the Fig. 4.

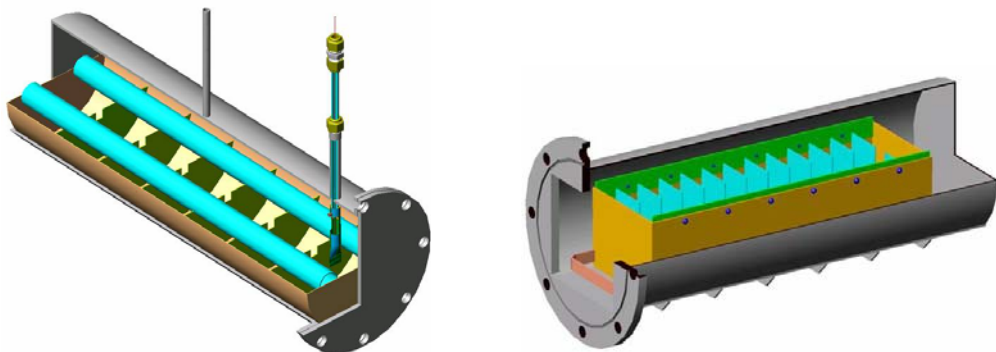
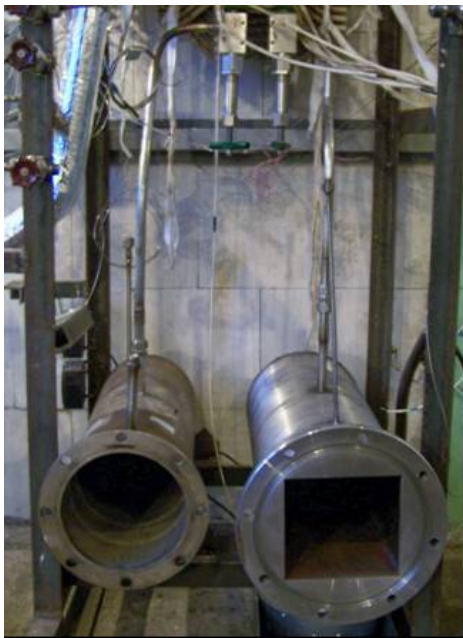


Fig. 4. Mould containers.

The produced ingots are shown in the photo (fig. 5).



Fig. 5. Ingots

During the solidification the temperature measurements and record are performed to fix the solidification point. A special unit for this purpose is designed. A slide able sealed pipe gives possibility to draw a little amount of liquid alloy in a dipper and take it up out of level. A thermocouple is placed in the dipper. The temperature during the cooling is recorded and analyzed by computer (fig. 6). The temperature at which the solidification heat stop the reduction of temperature is fixed as the solidification point.

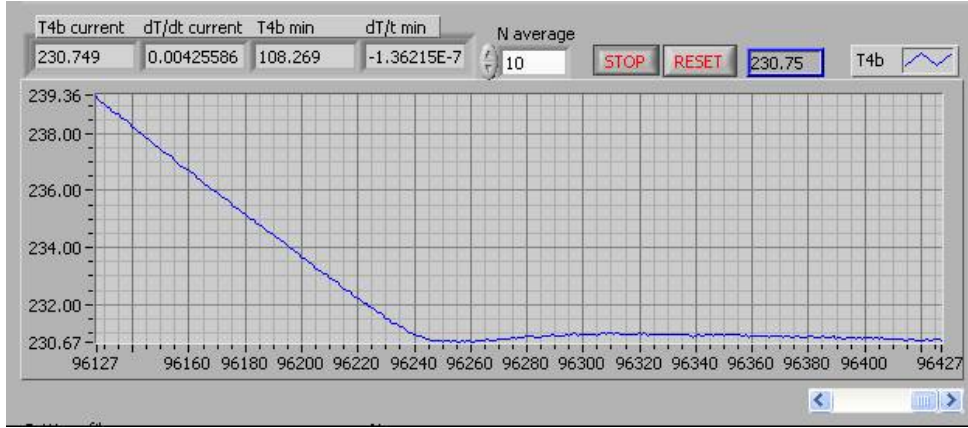


Fig.6. Temperature record during the cooling of alloy.

The ELTHERM heating cables is used for heating of all units of the equipment. The power is supplied through CRYDOM power controllers. The controllers are connected to an automatic temperature maintenance system controlled by computer program worked out in LABVIEW (fig.7). The program gains the temperature measurements by certified NiCr-Ni (K) type thermocouples from TEMPERATUR MESSELEMENTE HETTSTEDT GmbH.

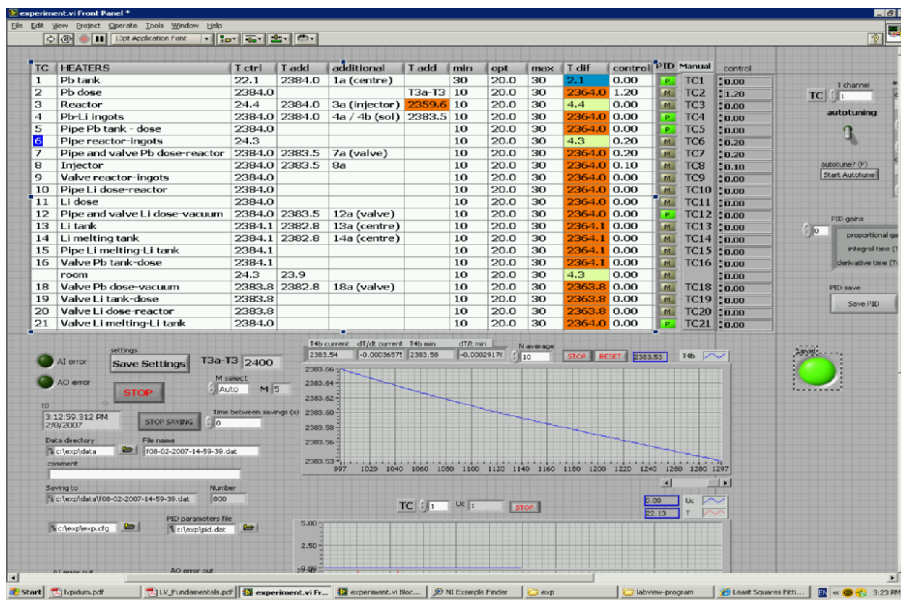


Fig. 7. Computer control of the process

**Chemical analyses.** The specimens are cut of the ingots to analyze the content of gained alloy. The addresses of location of specimens are determined as shown in picture (fig. 8).

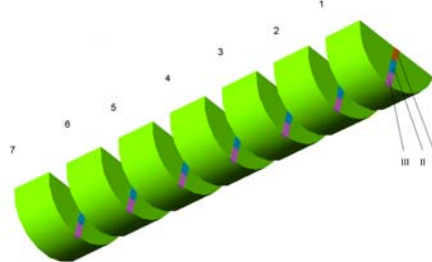


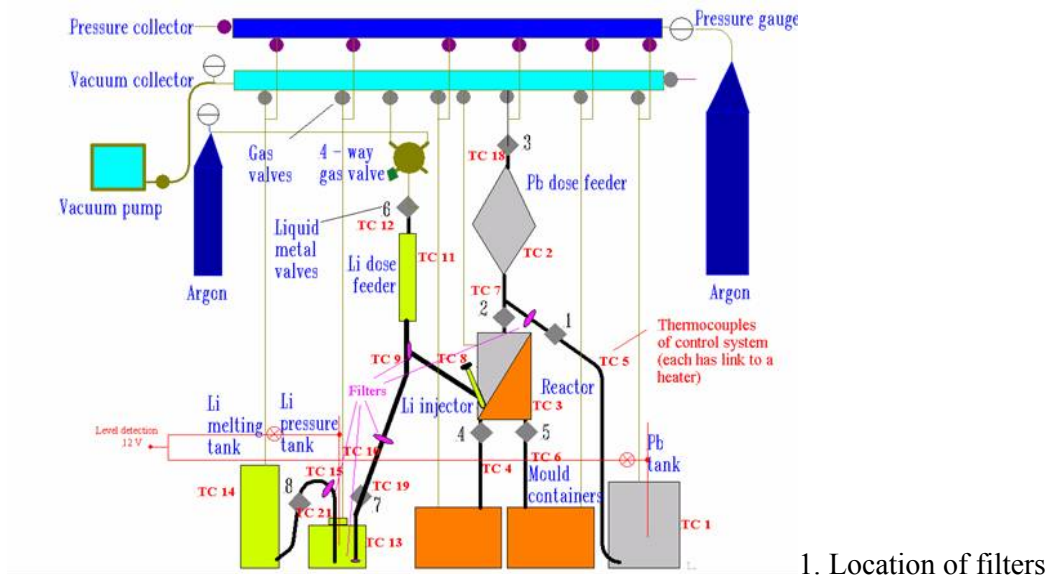
Fig. 8. The location of specimens on ingots.

**Safety measures.** For the staff safety the measures related to handling with lead and with lithium are respected.

1) The lead is kept in hermetic closed packing to avoid inhalation of the lead dust. For the same reason vacuum cleaning of rooms where cleaning of surface of ingots or machine works goes take place. At continuous works a special respirator recommended by specialists is used. The persons for which the working place is defined near the equipment are under custody of the Department of Occupational and Environmental Medicine of Institute of Labour and Environmental Health of Stradins University. Regular health checking take place.

2) The safety requirements regarding works with lithium are kept up by minimizing contact with lithium in the working place. During the filling the melting tank by pieces of lithium the tank is filled by overflowing argon.

The rule about maximum of amount of liquid lithium (10 litres) in rooms of such type is kept. The room is provided with powerful and effective ventilation system. It is ensured that in case of emergency, when the lithium flows out it will be localized in stainless steel pans. Isolating oxygen masks for two persons will be ready-to-wear for the case of necessity to enter the room when the lithium runs out.



## LU Fizikas institūtā dažādu izstrādāto un izgatavoto reālo elektromagnētisko indukcijas sūkņu uz pastāvīgiem magnētiem piemēri

Kā piemērus var minēt vairākus dažādas konstrukcijas un jaudas MHD indukcijas sūkņus uz pastāvīgiem magnētiem, kuri tika izprojektēti un izgatavoti LU Fizikas Institūtā un pārbaudīti darbībā reālajās iekārtās sadarbībā ar dažādiem ārvalstu zinātnisko pētījumu centriem risinot dažādus zinātnisko pētījumu uzdevumus saistītus ar minēto neutrōnu atskaldīšanas avotu realizēšanu.

Pirmais reālais MHD cilindriska tipa indukcijas sūknis uz pastāvīgiem magnētiem eutēktiskā sakausējuma svins-bismuts (Pb-Bi) pārsūknēšanai pie darba temperatūras  $350^{\circ}\text{C}$  tika izgatavots Fizikas institūtā 2000. gadā pēc sadarbības līguma ar Itālijas enerģētisko problēmu pētīšanas aģentūru ENEA. Sūknis tajā pašā 2000. gadā tika pārbaudīts un sekmīgi darbojās ENEA zinātnisko pētījumu centrā Brasimone eksperimentālajā šķidrā metāla (Pb-Bi) divu cilpu cirkulācijas iekārtā CHEOPE-1, zīm. 1.

Sūkņa testēšanas experimentālie rezultāti reālajos apstākļos parādija ļoti labu sakritību ar sukņa novērtētiem galveniem parametriem balstoties uz teorētiskiem aprēķiniem un modelējošo eksperimentu rezultātiem [3]. Tā, piemēram, kļūda starp novērtētām sūkpa attīstāmā spiediena un radītās caurteces raksturlīknēm un experimentāli nomērītām nepārsniedza  $5 \div 7$  procentu robežas. Tie ir ļoti vērtīgi rezultāti, kas ļauj novērtēt lielāko gabarītu un daudz jaudīgāko sūkņu parametrus un ražotspēju.

Nākošais reālais MHD disku konstrukcijas sūknis uz pastāvīgiem magnētiem tā paša eutēktiskā sakausējuma svins-bismuts (Pb-Bi) pārsūknēšanai pie darba temperatūras līdz  $400^{\circ}\text{C}$  tika izgatavots Fizikas institūtā 2001. gadā pēc sadarbības līguma ar Paula Šērera institūtu (PSI, Šveice), zīm. 2, zīm. 3. Sūknis ilgstoši vairākus gadus veiksmīgi tika darbināts radiācijas apstākļos eksperimentālajā PSI iekārtā LiSoR, kurā tika pētītas dažādu materiālu īpašību izmaiņas radiācijas ietekmē.



Zīm. 1. Cilindriska tipa MHD indukcijas sūknis uz pastāvīgiem magnētiem svina-bismuta sakausējuma pārsūknēšanai pie temperatūras  $350^{\circ}\text{C}$ . Maksimālais attīstāmais spiediens  $P = 6$  atmosfēras, caurceļ līdz  $Q = 1,2$  litriem sekundē (jeb  $4.3 \text{ m}^3$  stundā). Sūkņa piedziņas elektriskā motora jauda  $10,0 \text{ kW}$ . Sūknis bija uzstādīts un pārbaudīts 2000. gadā šķidrā metāla iekārtā CHEOPE-1 (ENEA, Brasimone, Itālija).



Zīm. 2. Disku tipo MHD indukcijas sūknis uz pastāvīgiem magnētiem svina-bismuta sakausējuma pārsūknēšanai pie temperatūras  $400^{\circ}\text{C}$ . Maksimālais attīstāmais spiediens  $P = 1,7$  atmosfēras, caurceļe  $Q = 1.0$  litrs sekundē (jeb  $3.6 \text{ m}^3$  stundā). Sūknā piedziņas elektriskā motora jauda  $5.0 \text{ kW}$ , lietderības koeficients  $10\%$ . Sūknis uzstādīts 2001. gadā šķidrā metāla iekārtā LiSoR (PSI, Šveice).



Zīm. 3. LiSoR iekārtā (PSI, Šveice), kurā tika pētītas dažādu materiālu īpašību izmaiņas šķidrā metāla plūsmā radiācijas ietekmē [4].

Vēlāk līdzīgi šādi diskveidīgie MHD indukcijas sūknji uz pastāvīgiem magnētiem tika izprojektēti un izgatavoti LU Fizikas institūtā un uzstādīti un veiksmīgi darbojas arī citās iekārtās, piemēram: tur pat PSI (Šveice), zīm. 4 [5]; Rossendorfas pētniecības centrā (Vācija), zīm. 5; Stokholmas Karaliskajā Tehnoloģijas institūtā (Zviedrija), zīm. 6, kā arī LU Fizikas institūtā ilgstošos (trīs sesijās, katra no tām 2000 stundas gara) eksperimentos pētot šķidrā metāla plūsmas magnētiskajā laukā ietekmi uz tērauda EUROFER-97 korozijas procesiem, zīm. 7 [6].



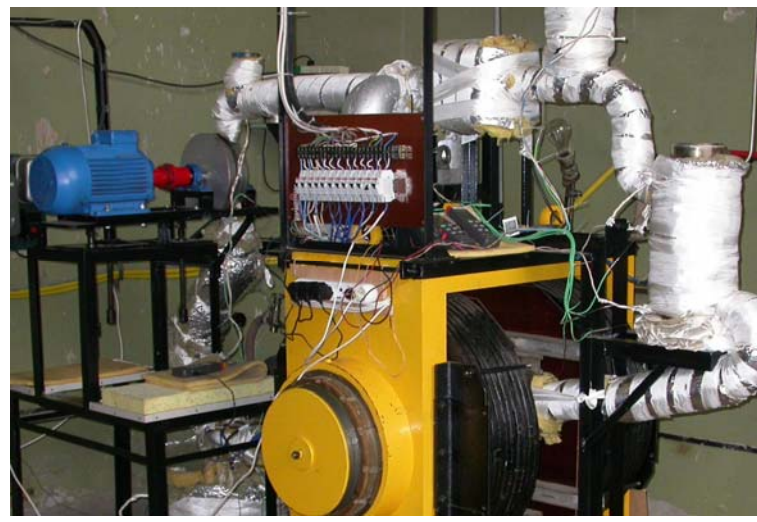
Zīm. 4. Dubults (divu pāru disku) sūknis uzstādīts šķidrā metāla (Pb-Bi) divu cilpu cirkulācijas iekārtā (PSI, Šveice) termohidrauliskiem pētījumiem neitronu atskaldīšanas mērķu modeļos.



Zīm. 5. Diskveidīgais sūknis tīra svina (darba temperatūra līdz  $500^{\circ}\text{C}$ ) cirkulācijas cilpā ELEFANT (Rossendorfas pētniecības centrā, Vācija) foto-neitronu avota pētījumiem izmantojot jaudīgā elektronu kūļa starojuma absorbēšanu tīrā šķidrā svinā.



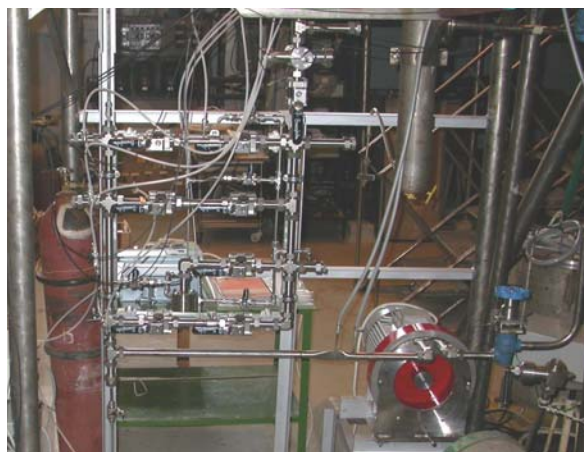
Zīm. 6. Diskveidīgais sūknis svina-bismuta vertikālajā cirkulācijas cīlpā TALL termohidrauliskiem pētījumiem Stokholmas Karaliskajā Tehnoloģijas Institūtā (Zviedrija).



Zīm. 7. LU Fizikas institūtā ilgstošos (trīs sesijās, katra no tām 2000 stundas gara) eksperimentos pētot šķidrā metāla plūsmas magnētiskajā laukā ietekmi uz tērauda EUROFER-97 korozijas procesiem arī tika izmantots MHD diskveidīgais indukcijas sūknis uz pastāvīgiem magnētiem.

Speciālas konstrukcijas cilindriska tipa MHD indukcijas sūknis dzīvsudraba pārsūknēšanai, zīm. 8. uz pastāvīgiem magnētiem izprojektēts, izgatavots un izmantots LU Fizikas institūtā kopīgos eksperimentos ar Juelihas pētniecības centru (Vācija) gāzes burbuļu iešprīcei dzīvsudraba plūsmā un šo burbuļu dzīves ilguma mērījumos atkarība no to izmēriem. Šie pētījumi ir svarīgi sakarā ar gāzes burbuļu izmantošanu (iešpricēšanu) šķidrajā metālā neutronu atskaldīšanas iekārtas ar mērķi lai apslāpētu augsta spiediena impulsus mērķa bombardēšanas laikā.

Dzīvsudraba cirkulācijas cilpa ar cilindriska tipa sūkni uz pastāvīgiem magnētiem (kā arī ar elektromagnētisko kondukcijas caurteces mērītāju) izgatavota LU Fizikas institūtā pēc sadarbības līguma priekš ORNL (Oakridge National Lab., ASV), zīm. 9. Iēkārta izmantota kā gāzes burbuļu dināmikas pētīšanai dzīvsudraba plūsmā, tā arī neutronu atskaldīšanas ikārtu kandidātu materiālu izturības pētījumos radiācijas apstākļos un minēto spiediena impulsu iedarbības rezultātā, kuri tiek veikti LANL (Los Alamos National Lab., ASV).



Zīm. 8. Speciālas konstrukcijas cilindriska tipa MHD indukcijas sūknis dzīvsudraba pārsūknēšanai uz pastāvīgiem magnētiem (ar abpusējiem aktīviem koncentriskiem cilindriskiem induktoriem un gregzenveidīgo kanalu spraugā starp tiem) relatīvi mazām caurtecēm ( $250 \text{ cm}^3/\text{s}$ ), bet lieliem spiedieniem – līdz 8.0 atmosfēram.



Zīm. 9. Dzīvsudraba cirkulācijas cilpa ar cilindriska tipa sūkni uz pastāvīgiem magnētiem izgatavota LU Fizikas institūtā pēc sadarbības līguma priekš ORNL (Oakridge National Lab., ASV).

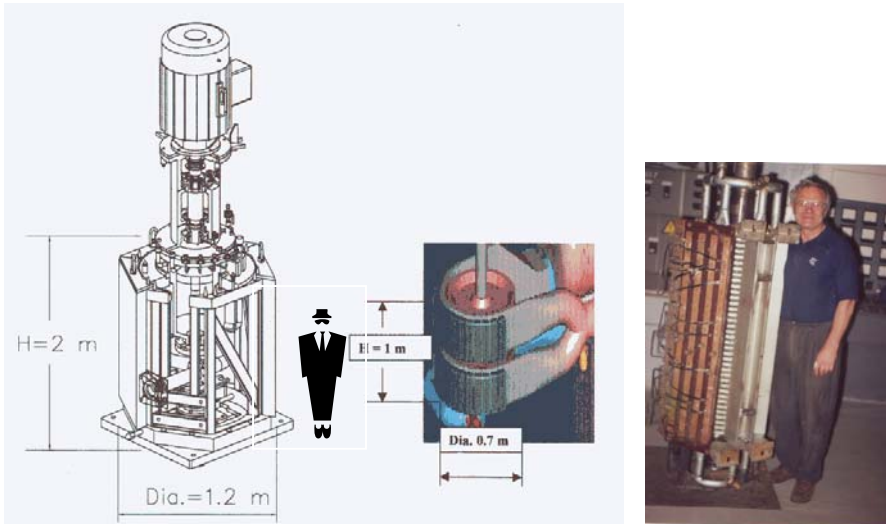
## **Jaudīgi elektromagnētiskie indukcijas sūknī uz pastāvīgiem magnētiem neutronu atskaldišanas iekārtām**

Pēc sadarbības līguma ar Juelihas pētniecības centru (Vācija) 2003. gadā LU Fizikas institūtā tika izprojektēts, izgatavots un noteztēts jaudīgs sūknis dzīvsudrabam, zīm. 10. Šis sūknis nogādāts Vācijā un bija paredzēts izmantošanai bijušā ESS projektā.



Zīm. 10. Jaudīgs indukcijas sūknis uz pastāvīgiem magnētiem dzīvsudrabam.  
Spiediens 6 atm., caurtece 13 L/s (170 kg/s), sūkņa piedziņas motora jauda 90 kW.

Iegūtā LU Fizikas institūtā pieredze ļauj aprēķināt parametrus vēl jaudīgākiem indukcijas sūknīem smagiem šķidriem metāliem (Pb, Pb-Bi, Hg) uz pastāvīgiem magnētiem – spiedienam līdz 10 atm., caurteci līdz 20 L/s, zīm. 11b, kuriem ir lielas priekšrocības salīdzinājumā ar tradicionāliem MHD lineāriem 3-fāžu induktoru sūknīem, zīm. 11c, jo tiem ir vienkāršāka konstrukcija, mazāki gabarīti un lielāks lieterības koeficients. Sūknīem uz pastāvīgiem magnētiem arī ir daudz vienkāršaka konstrukcija un nesalīdzināmi lielāka drošība, kā arī mazāki gabarīti, salīdzinājumā ar mehāniskiem sūknīem



Zīm. 11. Mehāniskais sūknis (a), indukcijas sūknis uz pastāvīgiem magnētiem (b)  
un tradicionālais lineārais cilindriskais 3-fāžu indukcijas sūknis (c).

## Literatūra

1. *I.Bucenieks*, Perspectives of using rotating permanent magnets for electromagnetic induction pump design. *Magnetohydrodynamics*. - 2000. - # 2. - p.p.181 - 187.
2. *I.Bucenieks*, High pressure and high flowrate induction pumps with permanent magnets, *Magnetohydrodynamics*. - 2003. - # 4. - p.p.411 - 417.
3. *Bucenieks I., Platacis E., Turroni P., Agostini P., Bertacci G.* Electromagnetic induction pump on permanent magnets for Pb/Bi melt. // Proceed. of 4<sup>th</sup> International PAMIR conference on *MagnetoHydroDynamics at Dawn of Third Millennium*, Presqu'ile de Giens, France, September 18 – 22, 2000, p.p. 651 – 655.
4. *Bucenieks I., Dementjev S., Viol D., Zik A., Glasbrenner H., Kirchner T., Heinrich F., Platacis E., Pozdnjaks A., Krysko S.* Lead-bismuth eutectic loop for LiSoR facility. Design and experience of operation./ 5<sup>th</sup> International PAMIR conference on Fundamental and Applied MHD, Ramatuelle, France, 2002, vol. 2, p.p. 201 – 206.
5. *J.A.Patorski, F.Barbagallo, I.Bucenieks, I.Platnieks, A.Bollhalder, R.Kaech, F.Groeschel*, Commissioning of the Liquid Lead Bithmuth Eutectic Double-Circuit-Loop at PSI, Paul Sherrer Institute annual Report, vol. 3, 2005.
6. *Bucenieks I., Platacis E., Muktupavel F., Shishko A.* Corrosion Phenomena of EUROFER steel in Pb-17Li stationary flow at magnetic field. Proceedings of 14<sup>th</sup> International Conference on Nuclear Engineering Miami, Florida, USA, July 17 - 20, 2006, paper 89195.
7. *Bucenieks I. Butzek M.*, Proposed Mercury Pump for ESS./ Proceedings of ICANS-XVI – 16<sup>th</sup> Meeting of the International Collaboration on Advanced Neutrons Sources, May 12 – 15, 2003, Dusseldorf-Neuss, Germany.
8. *I.Bucenieks*, Perspectives of increasing efficiency and productivity of Electromagnetic Induction Pumps for mercury basing on Permanent Magnets. Proceedings of 14<sup>th</sup> International Conference on Nuclear Engineering Miami, Florida, USA, July 17 - 20, 2006, paper 89193.

## Fixed contribution contract with EURATOM

### EC 6 Framework Programm-

***Preparation of a gallium jet limiter for testing under reactor relevant conditions***

**FU07-CT-2007-00047,**

### **Preparation of a gallium jet limiter for testing under reactor relevant conditions.**

In 2008 a paper [1] was published summarizing the results of the work with a liquid gallium jet limiter on the tokamak ISTTOK. These results can be characterized by a following citation from the abstract “*... It was stated that ISTTOK has been successfully operated with the gallium jet without degradation of the discharge or a significant plasma contamination by liquid metal. This observation is supported by spectroscopic measurements showing that gallium radiation is limited to the region around the jet. Furthermore, the power deposited on the jet has been evaluated at different radial locations and its temperature increase estimated*” . An additional practical achievement should also be underlined - the fully new technology of preparation and introduction of liquid gallium in the vacuum of the discharge chamber was mastered. But ISTTOK is a typically small size tokamak {*major radius R=0.46m, minor radius r=0.085 m, toroidal magnetic field B\_t=0.45T, center electron temperature T\_e(0)=150 eV, centre electron density n\_e(0)=5x10<sup>18</sup>m<sup>-3</sup>, plasma current I\_p~6kA, loop voltage V\_p~3V*}

. It means that in the sense of all the critical to the process loads the mentioned results are giving not so much. To make a step towards more reactor relevant conditions in 2007 a collaboration agreement among three associations (ENEA, Frascati- IST, Lisbon – Univ.of Latvia) on the development of liquid metal systems for protection of plasma facing components was signed. A high magnetic field, high plasma density, high current tokamak, the Frascati Tokamak Upgrade FTU {*R=0.93m, r = 0.28m, B=8T, I=1.6 MA*}

, was chosen for potential next step experiments. On FTU, due to reduced dimension, the power per unit would be comparable even with that of ITER.

On Fig.1 two schemes have been compared how such an experiment on FTU could look like. The geometry of ISTTOK practically allowed only for one version when the jet is introduced through the upper port and evacuated trough the opposite lower one. On Fig.1a it is shown that in principle such a directly downward directed jet could be incorporated also in the cross section of FTU. However, at such a version the clearance inside the design becomes very limited, no more than a few centimeters remain free from the jet up to the outer wall and the internal corner of the lower port, it is difficult to find a place free for installation of some additional units, etc. But the cross section of FTU allows also for other versions when the jet is touching upon the plasma under a definite angle and in the same time all the constructive elements remain placed outside the scrape-off layer. One of such examples is shown on Fig.1b. In such a case the jet can be backed by some droplet trapping sub-channel drained into the main receiver installed in the lower port. It is essential since it is necessary to give a definite space for some deflection of the jet by the plasma which was detected on ISTTOK. A full exclusion of any interaction of the plasma with the liquid metal will be newer achieved, however, on ISTTOK the outward displacement of the jet was essentially higher then expected and the corresponding forces are still waiting for explanation. An experiment on FTU with gradually deepened into plasma jets would be very helpful also for answering this question. By some horizontal replacement of the nozzle this deepening could be started with a very low initial level. It can be seen on the figure that jets of the length L ~0.4m are needed, the loads are requiring the velocities on the level v~ 10m/s. Break-up in droplets remains as one of the tools for minimization of the MHD interaction, however, it requires a very exact relation between the velocity, length and diameter. More flexible would be the version when

the continuity of the jet would be broken by means of targeting it against a ceramic stopper. In any case, the geometry of the receiver should be investigated rather carefully, to avoid back-splashing etc. The possibility to transfer to a multi-jet version, able to scrape-off already a noticeable layer of plasma, should also be remembered.

Fig.1 gives also an idea how the liquid Ga stand linked up with FTU could look like. This sketch was prepared in a very easy way, simply by joining the scheme of ISTTOK Ga stand together with the scheme of the cross section of FTU. It is worth mentioning this circumstance since it means that the main liquid metal technologies mastered on ISTTOK could be used also on FTU, that a definite number of design units could be directly transferred, that new in essence procedures and tools will not be necessary.

### **Stability of long liquid metal jets.**

The working length of the jet  $L$  will always be roughly proportional to the small radius of the plasma. In the case of ISTTOK  $r = 85$  mm and in the experiments the length of the jet was kept on the level  $L \sim 10$  cm. After a great number of measurements with different metals (Hg, InGaSn and Ga) a dimensionless dependence, characterizing the stability of the jet, was constructed:  $L/d = 4.2 Wb^{1/2}$ , where  $L$  stays for the break-up length,  $d$  for the diameter of the jet and  $Wb$  for the Weber number. In the case of FTU  $r = 300$  mm, it means, the working lengths of the jet will be approx. equal to  $L \sim 35$  cm. It can be checked also on Fig.1. It was not fully clear what will the behavior of a liquid metal jet at such high values of the relative length ( $L/d > 100$ ). A corresponding experiment was performed on our Ga stand. In the test section a 50cm long glass cylinder was installed, instead of the previous model of ISTTOK's chamber (Fig.2a,b). It was stated that the  $d = 3$  mm InGaSn jet remains stable over all the length of the cylinder. As an example on Fig.2c a photo of the length interval 30cm-40cm is presented. It should be underlined that also the break-up length of such long jets remains depending on the same mentioned above relation. A conclusion can be drawn that generation of long enough Ga jets should not cause essential problems. Additionally, to generate such long jets the equipment and methods tested on ISTTOK and at IPUL could be directly applied.

### **Liquid metal jets in strong magnetic fields.**

It is MHD-interaction, that makes the promotion of any proposal about the application of liquid metal to fusion difficult. To overcome this obstacle experiments under conditions as close as possible to the reality are required. In the case of FTU specific are very high values of the main magnetic field, theoretically up to 8T. Therefore the question about the behavior of jets in strong fields remains topical, in spite of the fact that the general tendency was cleared already in the previous years - an orthogonal field enhances, and essentially, the stability of the jet. Basing on experiments with Hg and InGaSn jets in an up to 3.4 T field (electromagnet with permendure field concentrators) for the break-up length  $L$  a following empiric dependence was developed:  $L/L_0 = 1 + 0.75 Ha^{0.33} Re^{-0.25}$  where  $L_0$  stays for the BUL without a field,  $Ha$  and  $Re$  for Hartman and Reynolds numbers. In a 5.6 T field the enhanced stability of a system of ten parallel InGaSn jets was demonstrated. In these previous experiments an ordinary N/He cooled superconducting magnet was used. Last year a modern cryogen-less superconducting magnet with 6T in a D=30cm and L=967cm bore was acquired, mainly for fusion related MHD investigations. In the very first set of experiments the stable behavior of a InGaSn jet in high fields was demonstrated. Our many times used InGaSn stand was connected to the magnet by a parallel hydraulic

arm adapted for proper feeding and draining of the test section (Fig.3). The test section was based on a glass cylinder with a  $d=3\text{mm}$  nozzle in the centre of the upper lid (Fig.4). In the lower lid an opening for draining was foreseen, rather simple by configuration, newer the less, working surprisingly well, especially in the presence of strong fields. Without the field the behavior of the liquid metal jet was familiar, typical to any liquid jet, with definite fluctuations, splashing, etc. Already in a 1T field the jet was like a string in view, without any remarkable by eye fluctuations and outlet splashing. This picture remained practically unchanged also at values of the field 2, 3, 4 and 5 T.

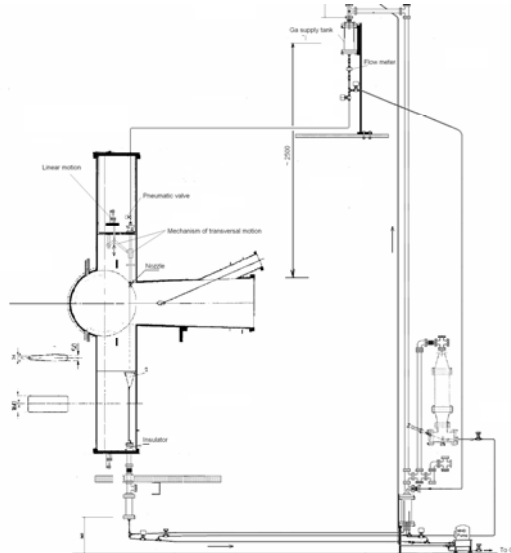


Fig.1a

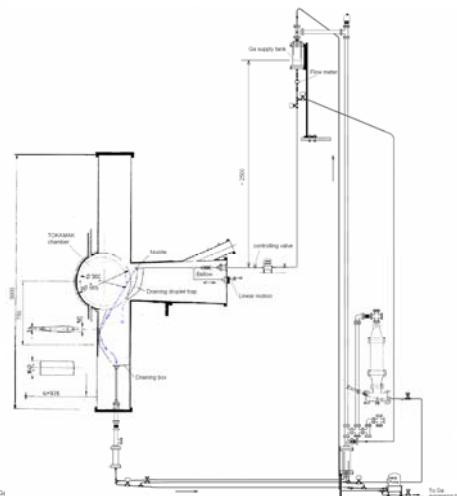
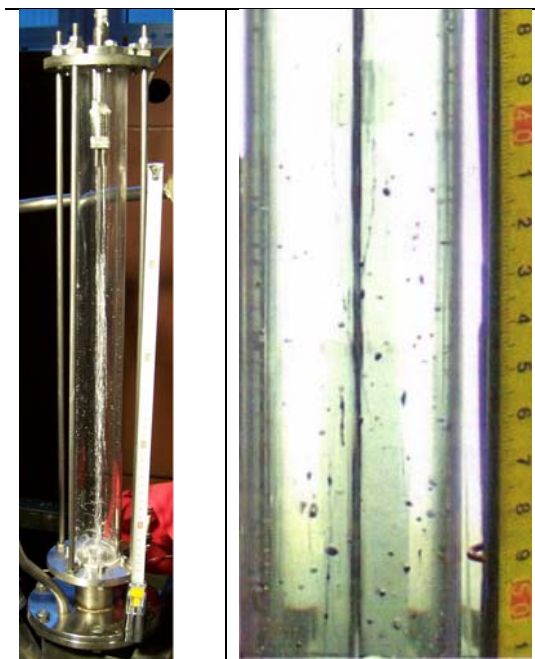
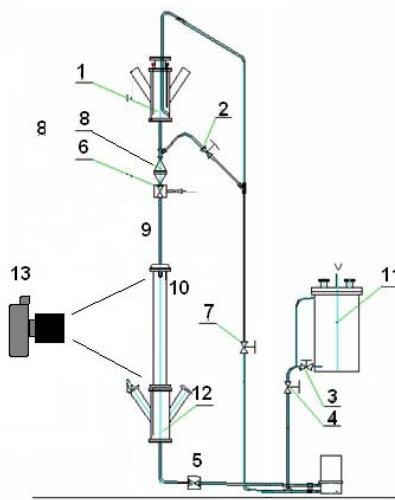


Fig.1b



1 - upper tank; 2-7 - valves; 8 - flow meter; 9 - tube; 10 - glass tube D45mm;  
11 - hot tank; 12 - supply tank; 13 - photo camera.

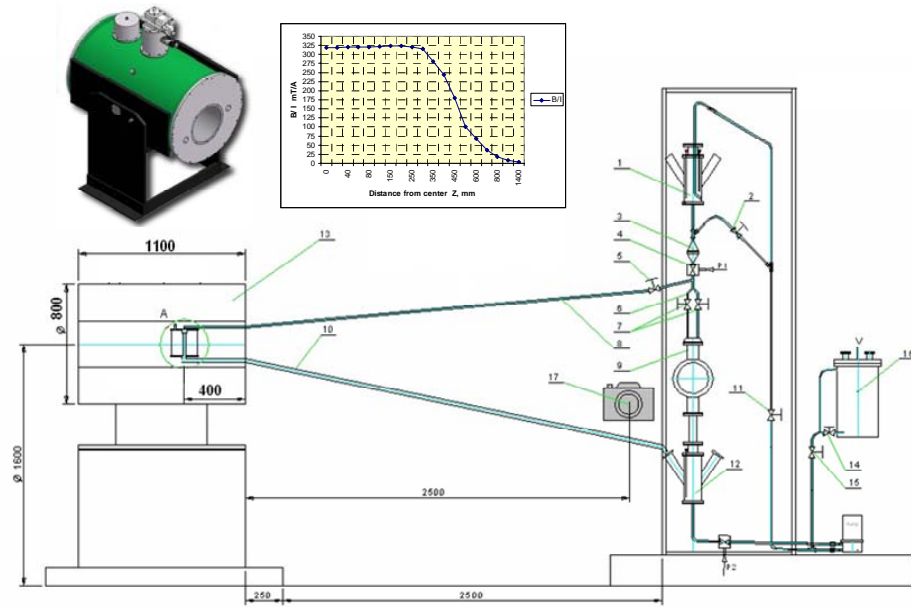
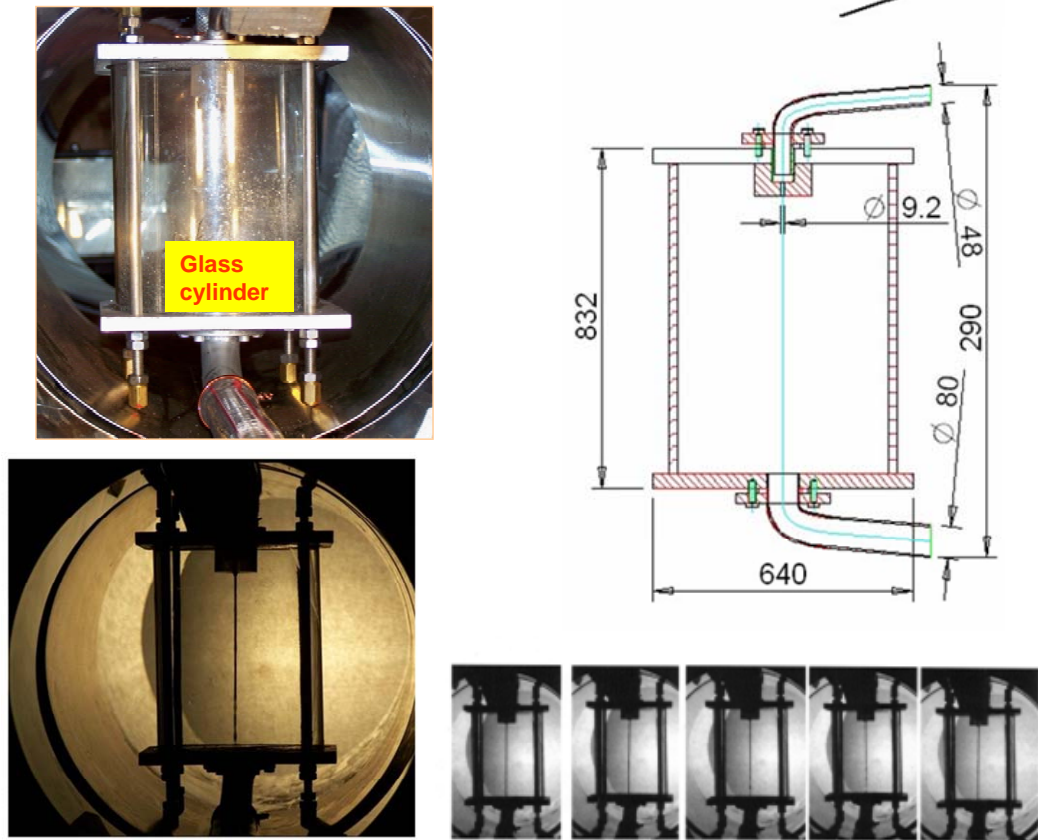


Fig.3

D



B=1 T

1T

2T

3T

4T

5T

Fig.4

**EURISOL DS** (European Isotope Separation On-Line  
Radiactive Ion Beam facility)  
**RIDS**  
**Contract number 515768**

**EURISOL DS, TASK# 2- MULTI-MW TARGET STATION**

*Participants to the Task and total human effort deployed*

<b>Participant number 1)</b>	4	18	19
<b>Participant short name 2)</b>	CERN	PSI	IPUL

The Task has progressed towards its objectives in a satisfactory way. The conceptual design of the Multi-MW target station (D1) has been consolidated by means of detailed coupled neutronics and computational fluid dynamics simulations. A first target station layout (D5) has been proposed which includes the building, hot cells, service and storage areas. A beam dump capable of handling a 4 MW proton beam has been designed and integrated. A risk register has been drawn up and the corresponding risk analysis launched. The conceptual design of the Multi-MW target station has been reviewed by an international expert panel.

**Sub-task#1: Engineering Study of the liquid metal converter**

The conceptual design of the Multi-MW target station (D1) has been consolidated by means of detailed coupled neutronics and 3D computational fluid dynamics simulations. The goal is to deliver predictions for METEX-1 useful in terms of safety and test correlations, but also for planning a second experiment for which the instrumentation must be established.

Broadly we obtain the same results as in 2D, that is:

- stable flow, no oscillations or large recirculation zones.
- cavitation at around  $P = -2.5$  bar.
- Total pressure loss of  $P = 0.6$  bar.

There is a negative impact from the three supports of the fins which is not so significant

## Basic parameters:

Length of the loop – 13 m

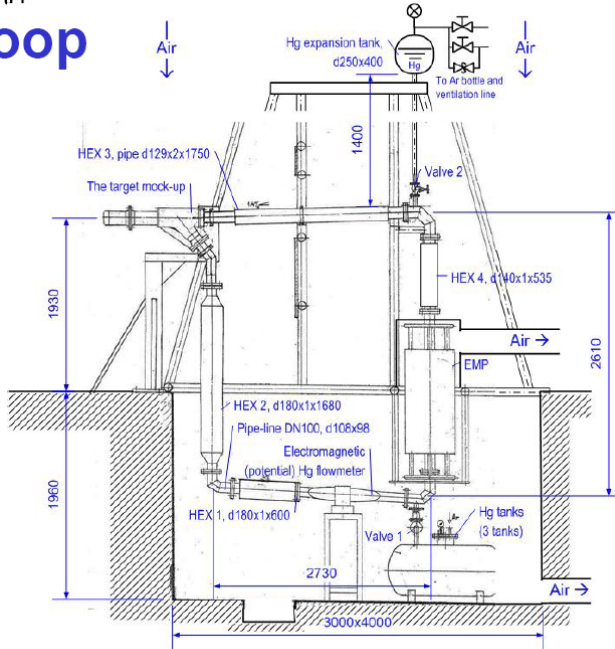
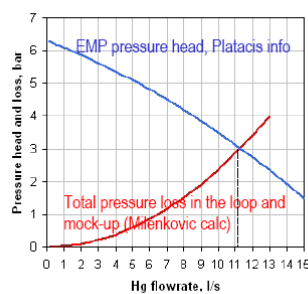
Hg volume – 127 liters

Max flowrate with the mock-up – ca. 11 l/s

Max Hg velocity in the pipes – 1.6 m/s

Max Hg temperature – ca. 88°C (S.Joray)

Cover gas (Ar) pressure - 0.5bar



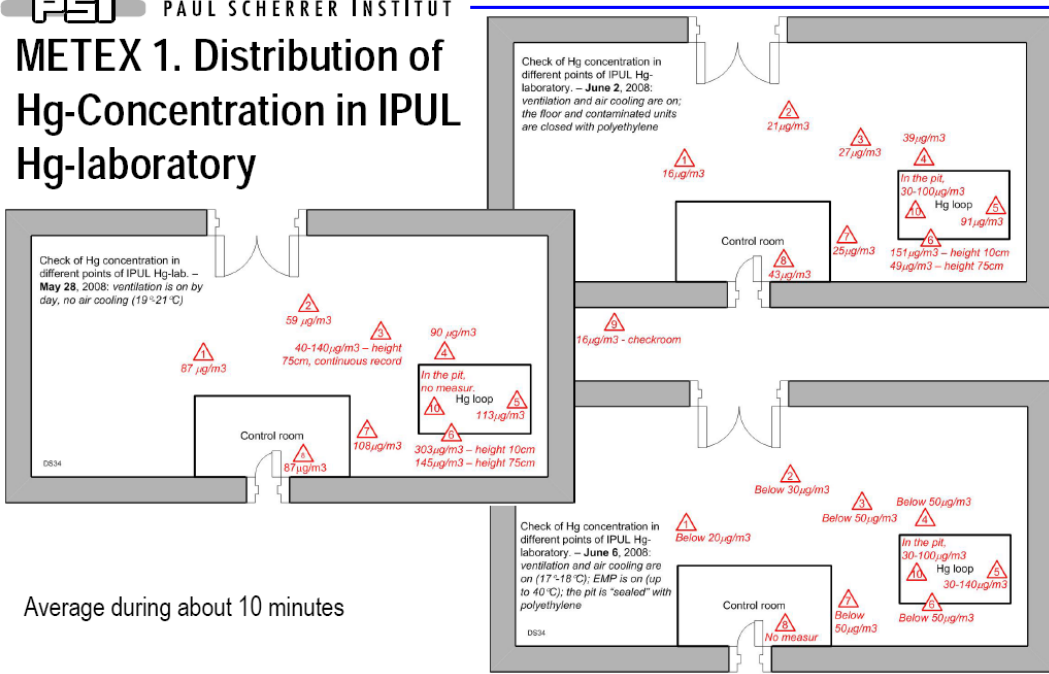
Paul Scherrer Institut • 5232 Villigen PSI

PSI. EURISOL converter target. METEX status. Technical meeting. PSI June 17 2008 DS34

In the beginning of the June, the **180° bend coaxial flow target** was installed on the loop. All engineering parameters were successfully checked, and the loop was pressurized to 6 bars. A first check of the filling system of the loop, serviceability and, stability of the hydraulic parameters (pressure drop, flow rate , temperature and so on) was planned, however mercury vapours exceeded allowable level in the experimental hall and it was decided to postpone the tests to late autumn.



# METEX 1. Distribution of Hg-Concentration in IPUL Hg-laboratory



Paul Scherrer Institut • 5232 Villigen PSI

PSI. EURISOL converter target. METEX status. Technical meeting. PSI June 17 2008 DS34

In parallel, a mock-up of the **transverse flow film windowless target** having a length of 300mm and a width of 16mm (injector with parallel separator inner structure) was designed, fabricated and installed on the Hg – loop,



According to the theoretical estimations, in order to constrain the liquid metal film in the beam direction well – shaped solid walls were incorporated in the injector body. This ensures an almost flat free surface in the transverse plane. The following parameters were achieved: flow rate in the loop – 6 L/s; velocity of mercury in the film – 1.8 m/s; temperature of Hg during experiment – 16 – 18°C; pressure drop in the loop – 0,7 – 0,9 bars.



Following a request from EURISOL-DS MB, a visit to the EURISOL mercury target experiment at IPUL (Institute of Physics of University of Latvia) outside Riga in Latvia was organized for 17th September 2008 with J.Gulley (CERN Safety Commission, chemical safety expert) accompanied by K. Samec (CERN, AB Department) and K.Thomsen (Paul Scherrer Institute, PSI). The aim of the visit was to provide general recommendations to IPUL on health and safety issues related to the use of mercury, with the objective being to reduce exposure to acceptable levels, so far as is reasonably practicable. An in-depth process safety study using a systematic risk assessment/hazard identification technique was outside the scope of the study.

The concentrations measured on the day of the visit, at the approximate height of the breathing zone of operators were, for comparison, below the occupational exposure limits referenced by Suva and INRS. However the operating parameters of the target loop were not fully representative of the real EURISOL test conditions and further continuous readings should be taken during the next planned operation of the loop. Measures to improve the situation have been outlined. The measures should not be considered as exhaustive, but are based on the observations made on the day of the visit. Certain specific measures relating to PPE (4.1.1) and health surveillance (4.1.6) are to be observed by CERN staff, other remarks are addressed to IPUL and/or the Consortium IPUL-CERN-PSI for implementation.

It is very important that the appointed person responsible for the safe operation of the test facility, E. Platacis, is given the authority to stop (and restart) any activity and to call on, if necessary, additional experts/outside help in dealing with any emergency. As part of his duties E. Platacis should ensure that a log book is compiled, recording all normal operations (e.g. filling/draining the loop, start of pump) and all abnormal situations (e.g. leak of mercury, power failure) as well as regular entries reporting the concentration of mercury in the air at selected sampling point

#### **Sub-task#4: Off-line testing and validation of the thermal hydraulics and fluid dynamics**

Following the visit of CERN's Safety commission to IPUL, which reviewed the safety conditions in the mercury laboratory and provided important recommendations on safety issues related to the use of mercury, considerable efforts were carried out to bring the Hg loop up to standard enabling therefore to re-schedule the offline tests (D4) to December 2008.

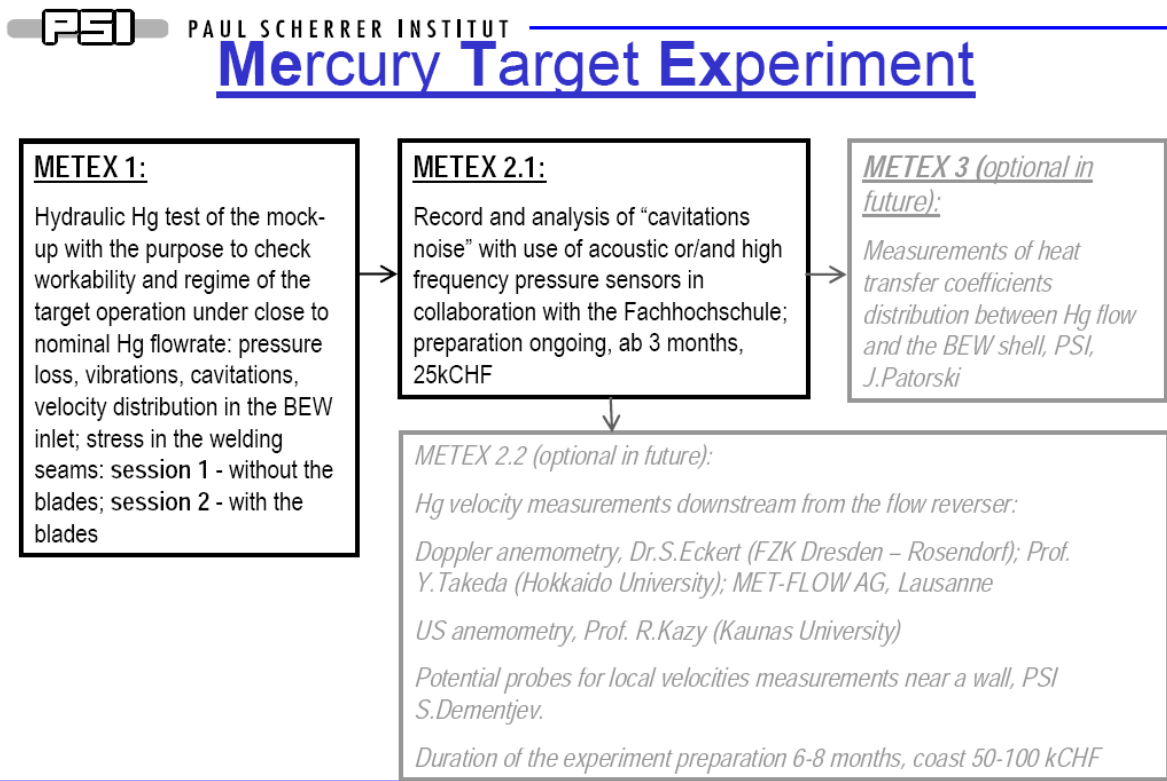
We propose to split the experimental program into three phases, provided the results of the first one are satisfactory. Since the experiment will explore up to now unexperienced flow rates and velocities in a liquid metal target, Phase 1 shall be a proof of principle experiment. In this experiment, the overall behaviour of the target will be assessed. The main variables will be the flow rate and the static pressure as well as the effectiveness of the guiding fins. The parameters explored will be the

- Pressure drop in the target
- Flow velocity and distribution in the target downcomer
- Vibrations
- Cavitation
- Deformation

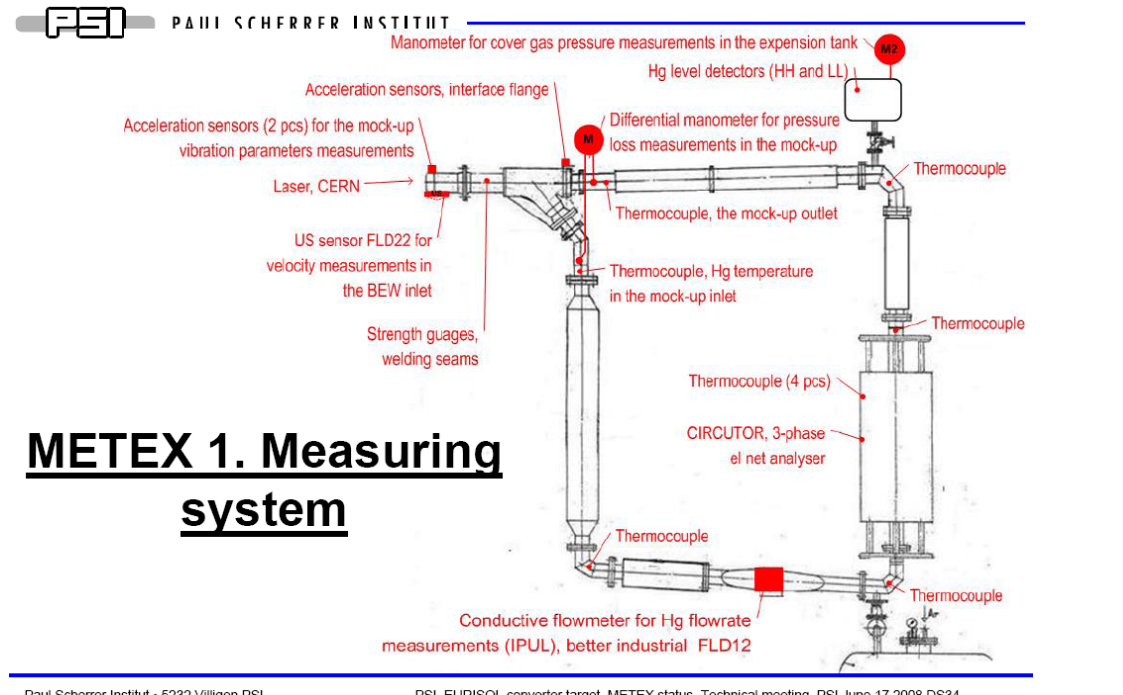
If the performance of the target is successful, a second phase is envisaged, in which

- the local flow velocity field in the beam window area using UDV
- the local heat transfer coefficient in the beam window using Infrared Thermography

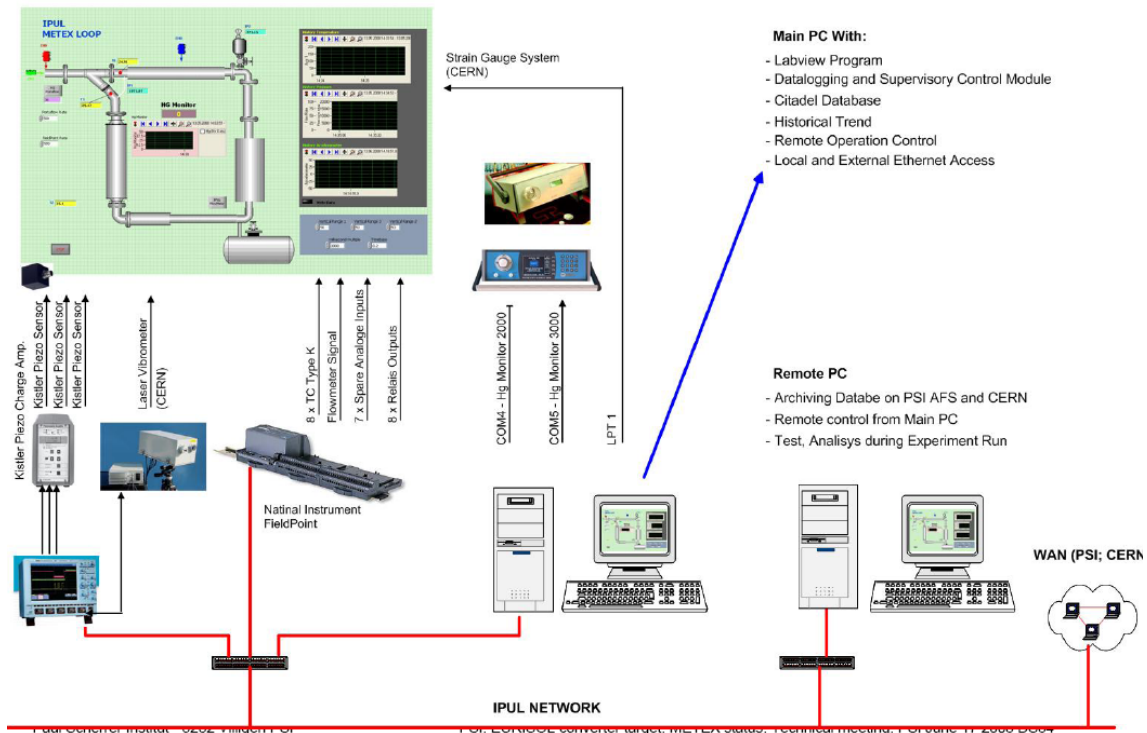
could be measured to validate the CFD calculation.



The instrumentation of the target is shown below.



### METEX0 MEASUREMENT AND DATA AQUISITION SYSTEM



# Start-up of the loop and the test matrix

The following steps will be carried out to start the experiment:

- Purge the target-loop system by filling with Ar of 6 bar and evacuating to 1 mbar three times
- Maintain the system at 1 mbar for several hours and check pressure evolution during 12 hours (the leakrate above should be confirmed)
- Check the measuring system including the Hg-analyzers.
- Start and check the loop water cooling (no leakage, flowrate if possible)
- Fill the target with Hg by pressurizing the storage vessel up to the indication of the level detector in the expansion vessel. The filling pressure is < 10 bar. The volume of the target loop system is 80 l.
- Adjust cover gas pressure 4 bar. Observe the loop during 1 hour. Check the pressure evolution (no leakage). Check Hg analyzer indications (no rise of the Hg-content in air). Check level of Hg in the expansion tank.
- Start circulating the EMP at low velocity (2 l/s) for 30 min. Observe the indications of the signals. Check Hg flow direction.
- Stop circulation for 30 min to let impurities swim up
- Check for leakage by sniffing with the mobile Hg vapor monitor along the loop (gas masks are obligatory)
- Check for vibrations by manual verifications
- Resume circulation for another 30 min (2 l/s)
- Drain the Hg from the loop into the storage vessel, observe loop pressure. Adjust cover gas pressure in the storage vessel >1 bar.
- Let settle for at least 2 hours
- Repeat the filling operation as described above
- Condition the loop until stable operation is achieved: 1 l/s; 2 l/s; 3 l/s; 4 l/s; 5 l/s. Observe the Hg temperature and Hg-analyzers indications.

AN-34-08-01/1

Session No.1 – without the blades; No.2 – with the blades

GG Pressure [bar]	Mercury Flowrate [l/s]												
	1	2	3	4	5	6	7	8	9	10	11	12	13
5													
4													
3													
2													
1													

Measurements of mercury velocity distribution in the target BEW inlet

Measurements of: cover gas pressure in the expansion tank; mercury flowrate in the loop; hydraulic pressure loss in the mock-up; vibrations parameters; stress in the welding seams

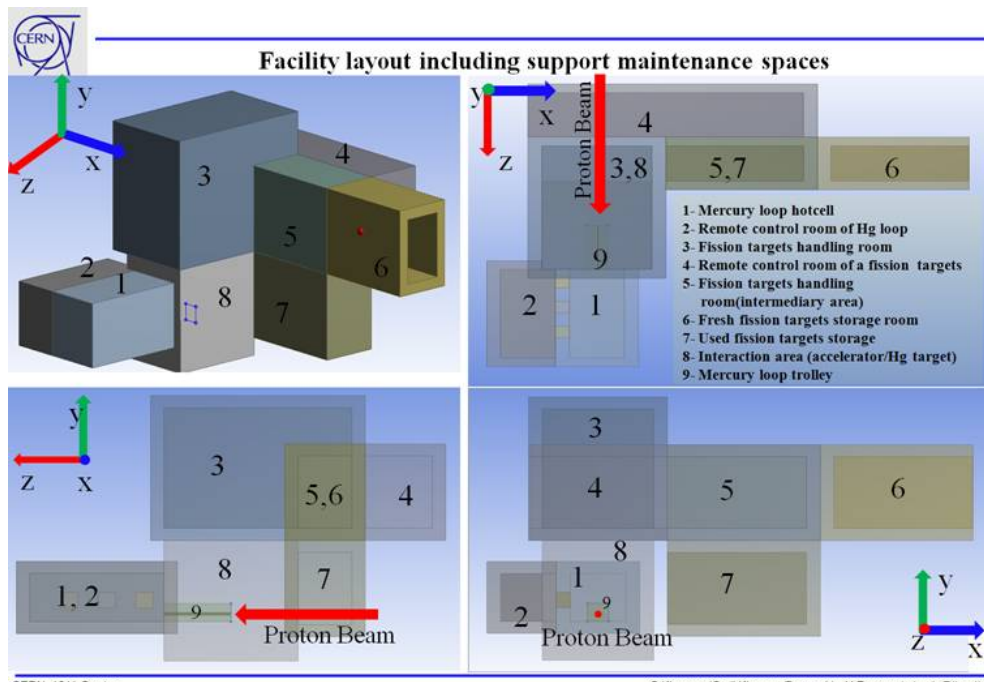
EURISOL-MR34-005

Paul Scherrer Institut • 5232 Villigen PSI

PSI. EURISOL converter target. METEX status. Technical meeting. PSI June 17 2008 DS34

## Sub-task#5: Engineering design of the entire target station

A first target station layout (D5) has been proposed which includes the building, hot cells, service and storage areas. A beam dump capable of handling a 4 MW proton beam has been designed and integrated.



A risk register has been drawn up and the corresponding risk analysis launched. The conceptual design of the Multi-MW target station has been reviewed by an international expert panel.

The requirements for radiation protection of the multi-MW power target station and propose options for the minimization of dose rates, activation, during and after operation are being studied in collaboration with **Task#5 and ITN**.

Optimisation of the target design and integration of the secondary fission target designed by **Task#4** has been performed.

Investigation of the safe handling of the liquid Hg target (remote handling, target interchange, etc...) in collaboration with **ORNL-C5** is in progress.

***Protonu mērķu salīdzinoša izpēte programmā  
EIROPAS ATSKALDĪTO NEITRONU AVOTS.***

**ESS – nākošās paaudzes neutronu avots Eiropai.**

**Situācijas raksturojums**

Neitrons – neitrāla elementārdalīja ar spinu  $\frac{1}{2}$  un masu, ļoti tuvu protona masai. Kā kodola sastāvdaļas neutronu un protonu var uzskatīt arī kā vienu daļiņu – nuklonu – divos dažādos stāvokļos, kas atšķiras tikai ar elektriskā lādiņa klātbūtni. Neutronam nav lādiņa, tādēļ tas var bez grūtībām šķērsot atoma ārejo ektronu mākonī un „trāpīt” tieši kodolā. Brīvā veidā neutroni var eksistēt tikai īslaicīgi, blīvos materiālos šis laiks mērojams desmitos mikrosekunžu. Jebkurš neutroni tiek galu galā absorbēts kādā kodolā, izsaucot to vai citu kodolreakciju. Neutronam raksturīgi visi šobrīd zināmie daļiņu mijiedarbības veidi – gravitācijas, vājā, stiprā un elektromagnētiskā. Tieši bagātais mijiedarbību arsenāls nosaka neutrona kā pētniecības līdzekļa vērtību, salīdzinot to ar citām elementārdalīņām. Šobrīd dažādas enerģijas un blīvuma neutronu plūsmas tiek uzskatītas par vienu no spēcīgākajie pētniecības ieročiem ne tikai tādos tradicionālos virzienos kā kodolfizika, cietvielu fizika utt., bet arī veselā rindā citu zinātņu, kuras īsi norādīsim zemāk. Jāatceras arī, ka neutroni ir arī galvenā darba darītājs kodolenerģētikā.

Līdz mūsu dienām pētniecības nolūkiem neutronus ģenerē galvenokārt dalīšanās reaktoros ar jaudu starp 10 un 100 MW. Pēdējās desmitgadēs aizvien lielāka vērība tiek pievērsta citai alternatīvai – ģenerēt neutronus tā saucamajā „atskaldīšanas” procesā. Līdz 1-2 GeV enerģijām paātrinātu protonu kūlis tiek iestarots „mērķī” (target), veidotā no kāda materiāla (metāla) ar augstu Z-skaitli.. Atbilstošie atomu kodoli tiek tādā mērā ierosināti, ka viena sadursme rezultē lielā skaitā atskaldīto neutronu (tieki minēti skaitļi līdz 50). Tilpumā ar ūdeņradi saturošu vielu tie tiek palēnināti līdz termiskām (vai tuvu tam) enerģijām un pa neutronu vadiem piegādati patēriņtajam (eksperimentiem ar neutronu difraktometriem, spektrometriem, reflektometriem utt). Jāatceras, ka tradicionālajā kodolu dalīšanās reakcijā katrs elementārais process producē tikai vienu neutronu. Tas pats sakāms arī par nākotnē gaidāmo kodolu sintēzes reakciju. Tieši sagaidāmais lielais producēto neutronu blīvums ir viens no galvenajiem parametriem, kas nosaka paaugstināto interesu par neutronu „atskaldīšanas” procesu. Sevišķi jāatzīmē prognozētā iespēja rūpnieciski pārstrādāt dalīšanās reaktoru „atkritumus”.

Uzdevums veidot Eiropas Atskaldīto Neutronu Avotu ESS (European Spallation Source) ar 5 MW „mērķa” jaudu tika formulēts 1997.gadā ( „ESS.A Next Generation Neutron Source for Europe”, Vol.II „The Scientific Case”, Vol.III „The ESS Technical Study” ISBN 090 237 6 500, Vol.II 090 237 6 608, Vol.III 090 237 6 659, March 1997). ESS „idejiskā”, kā arī principiālā shēma redzama zemāk zīmējumos. Lineārais paātrinātājs (LINAC) „uzdzēn” partikulas līdz 1,33 GeV enerģijai, nodrošinot 5 MW lielu kopējo stara jaudu 1.2 ms impulsos ar 50 Hz frekvenci. Divos paralēli saslēgtos cirkulāros akumulātoros/kompresoros šie impulsi tiek „saspiesti” līdz 1μs. Sādi

protonu impulsi tiek iestaroti divos ar dzīvsudrabu pildītos mērķos, vienā ar 50Hz, otrā ar 10 Hz frekvenci. Redzams arī interesantākais no iecerētajiem rezultātiem – apmēram 25  $\mu$ s gari impulsi ar stāvu priekšējo fronti un, galvenais, ar  $2 \times 10^{17}$  cm $^{-2}$  s $^{-1}$  lielu termālo neitrronu plūsmu maksimumā. Parādīta arī šķidrā metāla mērķa shēma – tas orientēts horizontāli. Mērķim jāspēj uzņemt 100 kJ, pie tam lielākā daļa šīs jaudas realizējas triecienvilņu veidā. Tas nozīmē, ka mērķis pakļauts kombinētai augsta starojuma, termisko spriegumu un triecienvilņu iedarbei. Bet tieši protonu kūla mērķis ir paredzamais FI pētījumu objekts. Interesanti redzēt, kā mērķis „kotējas” salīdzinājumā ar pārējām ESS komponentēm. Pēc sākotnējām 1997.gada aplēsēm projekts kopā izmaksās 806 M Eiro, tanī skaitā paātrinātājs 206 M, dubultais akumulātors 129 M un abi Hg mērķi 116 M. Tātad Hg mērķi, mūsu paredzamo pētījumu objekti, tiek minēti izdevumu galvgalī. Tika paredzēts projektu realizēt 10 gados - trīs gadi R&D, divi gadi projektēšanai un pieci gadi celtniecībai. Bet reāls starta signāls Sestā Ietvara rāmjos tā arī netika dots.

Sepītais Ietvars sākas cerīgi. ESS paredzēts sadaļā par Lielajām Pētnieciskajām Infrastruktūrām. Ar 01.01.08. sākta divgadīga projekta sagatavošanas fāzes. Starp „labuma guvējiem”(beneficiary) minēta arī „Latvijas Universitātei”. Pievienotā lappuse „sakombinēta” no atbilstošajiem dokumententiem, redzami formālie projekta „tituli”, redzami izpildītāji, redzami arī kritiskie jautājumi, kuri gaida atbildes sagatavošanas fāzē. Kā jau minēts, LU līdzdarbība saistīta ar šķidrā metāla mērķa izveidi. Norādīts, ka fāzes ietvaros „tehniskais darbs” centrēsies mērķa materiāla izvēlē (praktiski runa ir par Hg vai PbBi). Tas var būt saistīts pat ar vietas izvēli ESS celtniecībai. Bet tieši šī izvēle ir viens no galvenajiem sagatavošanas fāzes uzdevumiem. Kā pretendenti startē Zviedrija, Spānija un Ungārija.

### **Iepriekšējos gados izdarītais (FI līdzdalība)**

Šodienas optimisma pamatā ir iepriekšējos gados izpildītā pētnieciskā darba lielais apjoms. Zemāk pievienotajā tabulā norādīti visi līdz 1996. gada beigām publicētie ESS-Zinojumi (ar burtu „T” atzīmēti materiāli, kas attiecas uz „target”). Saraksta ievadā norādīti šobrīd galvenie Atskaites Sējumi (Reference Volumes), kā arī to adrese. Nākošajā pielikumā parādīta pieminētā Vol.II (1997) tituļlapa, kurā iekopēta daļa no šī sējuma satura rādītāja – uzskaitītas tās zinātnes nozares, uz kuru „apkalpošanu” pretendē ESS. Pašā sējumā attieksme pret katru no šīm nozarēm definēta sīkāk, aptuveni uz 2 lappusēm (šis materiāls pieietams FI). Vispār jāatzīmē, ka ESS sagatavošanas processā potenciālo pielietojumu „propogandai” veltīta ļoti liela uzmanība. Neitrona specifisko īpašību dēļ tāds avots kā ESS tiešām var kļūt par unikālu, plaši pielietojamu pētniecisku rīku. No viena cita avota ļemts nākošais pievienotais materiāls – prognoze, kā palielināsies patērētāju loks, pieaugot piejamo neitronu plūsmu blīvumam.

Turpinot apskatīt iepriekšējos gados paveikto, atgādināsim par Latvijas zinātnieku līdzdalību. Līdz šim galvenokārt te darbojies LU Fizikas institūts (FI), IPUL atšifrējas kā Institute of Physics of University of Latvia. Tam pamatā FI specifiskā, daļēji unikālā pieredze darbā ar dažādiem šķidriem metāliem. Piemēri izvēloti no augšminētajām atskaitēm, tātad tā būs tikai tā līdzdalības daļa, kas fiksēta ESS dokumentos. Vairums no tā aprakstīts arī dažādās citādās publikācijās, daudz kas palicis arī aiz kadra. Šī materiāla ievadlappusē parādīta ESS 5 MW mērķa shēma. Kā darba ķermenis kalpo dzīvsudrabs. Protonu kūlis vērstīs horizontāli un tiek iestarots tilpumā ar horizontālu turp/atpakaļ Hg kustību (par kustības detaļām turpmāk sīkāk). Nākošajā lappusē uzskaitītas galvenās uzdevumu klases, norādīts, kādu uzdevumu

izpildē IPUL piedalījies, kāda atskaitē tas publicēts. Par darba raksturu spriest ļauj sekojošās piecas pielikuma lappuses, arī izkopētas no konkrētām ESS atskaitēm

Informatīvs ir arī nākošais zīmējums, kurā aprakstīts SNS protonu starā mērķis. Oak Ridge(ASV) laborotorijā uzstādītajā atskaldīto neutronu avotā SNS (Spallation Neutron Source) mērķis veidots līdzīgi( tiek akcentēts, aizņemoties pieredzi no ESS). SNS projektētā jauda būtiski mazāka, konkrēti, 2MW. Bet svarīgi tas, ka SNS darbību jau sācis, gan tikai ar jaudu zem 1MW. Konstatēta vesela rinda problēmu, saistītu arī ar procesiem Hg sistēmā. Bet neutronu atskaldīšanas efektivitāte tika nodemonstrēta, praktiski vienlaicīgi kā MEGAPIE projektā, par kuru runāsim vēlāk. Var atzīmēt, ka arī SNS izveidē FI var pretendēt uz mazu daļiju dalības – pirmais Hg stends, paredzēts ievietošanai protonu starā „iekš” Oak Ridge, tika projektēts un izgatavots Salaspilī. Bez tam SNS pārstāvji apmeklēja FI dzīvsudraba laboratoriju, lai pārliecinatos, ka iespējama lielas jaudas Hg stendu izveide un darbināšana.

Japānā tiek realizēts JAERI / KEK projekts. Zemāk vispirms redzams aksiālais izdalītās jaudas sadalījums Hg mērķī, tas raksturīgs arī visiem pārējiem apskatāmajiem projektiem. ESS un SNS mērķa variantus japāni dēvē par „atgriezeniskās plūsmas mērķiem, ( return-flow targets)” – protoni tiek iestaroti atpakaļejošajā Hg plūsmas daļā. Arī paši sviņi šādu variantu nēm pamatā, tomēr paralēli tam apskata arī „šķērsplūsmas mērķi (cross-flow target)”. Ar iekšēja vadaparāta palīdzību Hg plūsma tiek orientēta perpendikulāri staram, pie tam panākts optimāls šķērsplūsmas ātruma sadalījums gar mērķa „asi” – ātruma perpendikulārā komponente pēc lieluma atbilst izdalītās jaudas līmenim. Tas panākts, pakāpeniski izpētot četrus dažadus vadaparāta modeļus.Lieliska mācību stunda!

### **MEGAPIE projekts**

„*MEGAPIE ir starptautisks „ceļa laušanas” eksperiments Paula Šerera institūtā (PSI) Šveicē, kura mērķis ir producēt neutronus šķidra metāla mērķī. Pirmoreiz pasaulei lielas jaudas protonu kūlis tiek producēts ar vienu megavatu ieejā. Augstas enerģijas neutroni tiek izmantoti dažādos pētniecības virzienos un teorētiski varētu tikt izmantoti kodolatkritumu pārstrādei. Eksperimenta pirmā fāze nesen tika pabeigta un , par lielu apmierinājumu starptautiskajai zinātniskajai sabiedrībai, rezultāti pārspēja cerības”*

„*tika pierādīta iespēja ilglaicīgi darbināt 920 kg svina-bismuta mērķi protonu starā, ko ģenerē PSI cirkulārais ciklotrons ar vienu megavatu izejā.”....*

„*Ilgī dzīvojošie aktinidi ir galvenās komponentes, kas nosaka kodolatkritumu radioaktivitāti. To transmutācija īslaicīgi dzīvojošos vai stabilos elementos ir teorētiski iespējama zemkritiskos ar paātrinātāju vadāmos reaktoros (Accelerator Driven Systems ADS), apgādātos ar iekšēju neutronu avotu, kuru ierosina ar lielas jaudas protonu staru. Lielas jaudas atskaldīto neutronu avots, veidots no šķidra metāla (svina-bismuta eutektika) un vērts uz nepieciešamo neutronu plūsmas blīvumu, tas tiek uzskatīts par principiālu soli ceļā uz ADS.”.*

„*Pēc intensīvas pamatproblēmu izpētes 2000. un 2001.gados tāds mērķis un tā palīgsistēms tika izprojektēts un izgatavots Francijā, Itālijā, Latvijā un Šveicē. Mērķis satur 920 kg.svina-bismuta eutektikas, ietvertas tērauda apvalkā. No iestaratā 800 kW protonu kūla 580 kW deponējas mērķa materiālā kā siltums, kurš tiek aizvadīts, sūknējot PbBi caur ārēju siltummaini. Protonu kūlis, iestarots svinā-bismutā, ģenerē  $10^{17}$  augstas enerģijas atskaldītos neutronus sekundē”*

Par MEGAPIE projektu ir tīcīs un tiek daudz rakstīts. Augstāk tiek citēti fragmenti no PSI primārās Preses informācijas (Media release) 31.01.2007., tātad no paša kompaktākā, rezumējošā materiāla. Atkal varam ar prieku konstatēt, ka Latvijas

līdzdalība šīnī fundamentālajā eksperimentā tiek „dokumentāli” apstiprināta. Šīs atskaites atsevišķā nodalījā aprakstīts svarīgais PSI un IPUL sadarbība sākuma posms. Te ne vārdos, bet reālās darbībās tika reaģēts uz apstākli, ka visvairāk slogots un apdraudēts ir tieši protonu kūļa iestarošanas logs. Tika pierādīta nepieciešamība veidot divplūsmu loga dzesēšanas sistēmu, ievedot pamatplūsmai paralēlu strūklu tiešai loga dzesēšanai. Zemāk dotajos pielikumos ilustrēta mūsu sadarbība jau inženiertehniskā līmeni. Redzama MEGAPIE eksperimenta shēma. Protonu kūlis ar magnetu palīdzību tiek pavērsts vertikāli augšup un iestaroši cilindriskā, aptuveni 2m garā ķermenī/mērķī, pildītā ar PbBi. Nepieciešamās divkomponentu plūsmas radīšanai virs paša mērķa, ļoti ierobežotā telpā iebūvēti divi cilindriski elektromagnetiskie sūknji. Tiem jāiztur gan pieklājīga temperatūra, gan iepriekš faktiski nezināmā radiācija, ko nosaka mērķī ģenerētie neitroni. Fakts, ka FI taisītā iekārta tādos apstākļos izrādījas darba spējīga, jāuzskata par šobrīd atraktīvāko apliecinājumu mūsu tehniskajam potenciālam. Pirms uzstādīšanas Šveicē iekārta tika testēta un trenēta speciālā PbBi stendā Salaspilī. Bet kā nākošais pielikumā parādīts cits stends, arī projektēts un būvets Salaspilī – kontūrs LiSoR eksperimentam. Tas bija pirmais eksperiments, kura laikā PbBi saturošs kontūrs tika pakļauts augstam starojumam. Par šī eksperimenta „dramatisko” gaitu liecina pielikuma nākošā lappuse (šīnī eksperimentā formāli FI pārstāvji gan nepiedalījās). Cikliski vadot kūli gar parauga virsmu, izveidojās pora un šķidrais metāls visiem par briesmām parādījās ārpusē. Pēc tam tika konstatēts, ka pora veidojusies parauga mehāniska defekta rezultātā.

### **Ar paātrinātu vadītu kodolu dalīšanās reaktors (ADS)**

Var droši teikt, ka ESS tiek balstīts ne tikai aiz tūras zinātnes mīlestības. Kā jau minēts, neitronu atskaldīšanas process ļauj runāt jau par tādiem parametriem, kad iespējama klūst radioaktīvo atkritumu rūpnieciska pārstrāde. Ar to tiktu likvidēts fundamentāls šķērslis kodolenerģētikas attīstībai, kā tehnisks, tā morāls. Viens no etapiem ceļā uz šo mērķi saistīts ar „zemkritisku”, ar paātrinātu vadāmu reaktoru (ADS) izveidi. Parastā „virskritiskā” reaktorā katrs neitrons, kas tiek absorbēts kodolā, dalīšanās rezultātā nodrošina vismaz viena jauna neutrona izstarošanu (teorētiski, praktiski aptuveni 2.5 reiz vairāk). Tā reaktora aktīvajā zonā tiek nodrošināts nepārtraukts kodolu dalīšanās process. Paredzamajā ADS reaktora aktīvajā zonā neitroni tiks ģenerēti atskaldīšanas procesa rezultātā, iestarojot augstas enerģijas protonus materiālā ar augstu Z-skaitli (atskaldīto neitronu skaits tieši korelē ar Z-skaitli un iestaroto protonu enerģiju). Zemāk aprakstīto ADS shēmu („Rubiatronu”) ieteica kolektīvs Nobela prēmijas laureāta C.Rubia vadībā

( .Carminati,R.Klapisch, J.P.Revol, Ch.Roche, J.A.Rubia, C.Rubia. *An enargy amplifier for cleaner and inexhaustible nuclear energy production driven by a particle beam accelerator*. Report

CERN / AT / 93-47 (ET). Genf, Nov.1993., C.Rubia et al., *Conceptual design of a fast neutron operated high power energy amplifier*. CERN / AT / 95-44 (ET), 1995.). Zemāk dotās ilustrācijas ļemtas no: *Energy amplifier demonstration facility reference configuration*. ANSALDO,

EA B0.00 1 200, Revision 0.

Pirmajā zīmējumā redzama reaktora kopējā shēma. Tālāk seko divi iespējamie protonu mērķa varianti – mērķis ar „karsto” logu un „bezloga” mērķis. Citēsim fragmentu no „Conclusions”:

„Viens no galvenajiem uzdevumiem ir atrisināt jautājumu par Mērķa Loga izveidi, tas ir, par pārejas virsmu starp protonu kūli aptverošo vacuuma cauruli un pašu mērķa materiālu....Karstais logs veido mehanisku barjeru, veidotu no materiāla, pēc iespējas caurspīdīga neitronu un protonu starojumam, tam jāiztur spiediena un mehāniskās

slodzes, raksturīgas mērķa darba režīmam. Bezloga mērķī protonu kūlis no paātrinātaja tiek iestaroši tieši mērķa materiālā....”

Autoritātes tik gari citējam tādēļ, ka sakarā ar daudz perespektīvāko „bezloga” mērķi nozīmīgs eksperiments tika veikts Salaspilī. Ideja principā vienkārša – ar speciāla vadaparāta palīdzību augšupejoša plūsma jāpavērš atpakaļ tā, lai veidotos pietiekoši liels brīvs šķidrā metāla „logs” ar pietiekoši stabīlu virsmu. Tāda iespēja iepriekš tika pētīta kā skaitliski, tā ūdens eksperimentos. Eksperimentā, kas atspoguļots zemāk, šī iespēja tika nodemonstrēta darbā ar blīvu materiālu, konkrēti Hg , pie tam mērogā 1:1 gan pēc izmēriem, gan ātruma.

U

Direction de l'énergie nucléaire  
Le Directeur

CEA/DEN/DSOE/DIR

DO 69 29/07/08



08MBX000069

diffusé le : 29/07/08



**Prof. Janis Ernests FREIBERGS**  
Institute of Physics of University of Latvia,  
32 Miera Str., Salaspils, LV-2169  
LATVIA

Saclay, 29<sup>th</sup> July 2008

Dear Prof. Freibergs,

I have the pleasure of informing you that at the 2<sup>nd</sup> Governing Board meeting held in Prague on May 29th 2008, the application of IPUL to become a member of the *Sustainable Nuclear Energy Technology Platform* was approved. The document explaining organization and rules of the SNE-TP was also approved at the Governing Board meeting [http://www.snetp.eu/home/liblocal/docs/SNETP\\_Organisation\\_version7.5.pdf](http://www.snetp.eu/home/liblocal/docs/SNETP_Organisation_version7.5.pdf), and I refer you to this document for questions you may have concerning the governance of the platform.

IPUL may now participate fully and officially in the different Working Groups (Strategic Research Agenda, Deployment Strategy, Education, Training and Knowledge Management). You may also be interested in the preparation of a European Industrial Initiative for sustainable fission (Generation IV technologies) in the context of the European Energy Research Plan. You may find more details on the status of the platform's activities in the recently released Newsletter (available on the website) or by contacting the secretariat at [secretariat@snetp.eu](mailto:secretariat@snetp.eu).

I look forward to IPUL's active participation in the platform's work, and to welcoming you to our first General Assembly, which will take place in Brussels on the 26<sup>th</sup> November 2008. Details and registration for this event may be found on the website, [www.snetp.eu](http://www.snetp.eu).

With my very best regards,

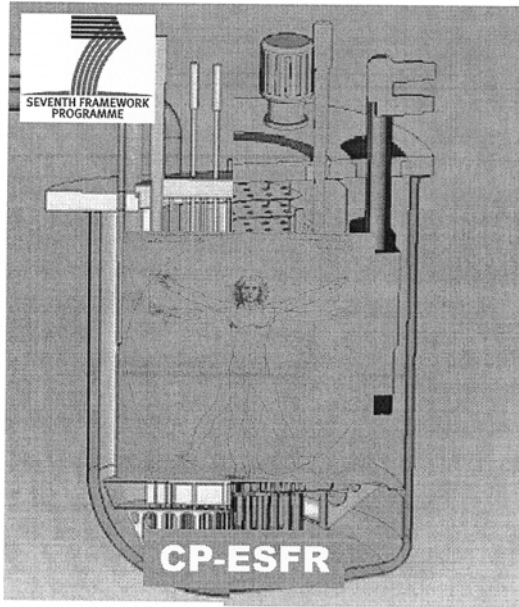
Philippe PRADEL  
Chair of SNE-TP



Copy: Mr. Bernd Güthoff (E.ON Kernkraft), Mr. Frantisek Pazdera (UJV).

Commissariat à l'énergie atomique  
Centre de Saclay - Bâtiment 121 - 91191 Gif-sur-Yvette cedex  
Tél : 33 - 1 69 08 61 90 - Fax : 33 - 1 69 08 61 95 - [philippe.padel@cea.fr](mailto:philippe.padel@cea.fr)  
Etablissement public à caractère industriel et commercial  
R.C.S. PARIS B 775 685 019

2.



"Part B"  
**Collaborative Project for an  
European Sodium Fast Reactor**

Proposal acronym:  
**CP-ESFR**

Type of funding scheme:

**Large-scale integrating (CP-IP)**

Work programme topics addressed:

**FP7 – Fission 2008-01-24 - Nuclear Fission and Radiation Protection**

**Advanced nuclear systems : Fission-2.2 - Fission-2008-2.2.1: Innovative reactor systems**

Other addressed topics: *Partitioning and transmutation: Fission-1.2- Fission-2008-1.2.2; Transmutation fuels and targets and their reprocessing*

Name of the coordinating person:

*Gian Luigi FIORINI*

*Chargé de Mission "Generation IV"*

*Nuclear Energy Division/ Reactor Studies Department/ Innovative System Section*

*CEA/CADARACHE - Bt 212*

*13108 Saint Paul Lez Durance cedex*

*Tel Cadarache : 33 (0)4 42 25 46 02; Cell phone : 33 (0) 6 78 09 77 96; Secrétariat : 33 (0)4 42 25 38 77;*

*Fax : 33 (0)4 42 25 48 58*

*Mail address: [gian-luigi.fiorini@cea.fr](mailto:gian-luigi.fiorini@cea.fr)*

## **Contribution of IPUL to ESFR project**

**Introduction of IPUL Partner:** In the field of Magneto hydrodynamics, the Institute of Physics of the University of Latvia (IPUL) is widely recognized by the MHD research community as a world-class facility and one of the world's leading research institutes, both in fundamental and applied MHD studies. Activities of IPUL deals with various liquid metals such as Hg, Na, Li, Ga, Pb-Li, Pb-Bi, In-Ga-Sn,... Thanks to its capabilities, IPUL has provided innovative electro-magnetic pumps and flow-meters for various nuclear systems i.e. MEGAPIE spallation target, investigated MHD effects in PHENIX Sodium Fast Reactor, and contributes more recently to the development of irradiation devices for the Reactor Jules Horowitz reactor, or lithium loop for IFMIF. IPUL operates three sodium loops in the Alkali metal laboratory" (157 m<sup>2</sup> dedicated to Na) which has been fully renovated, recently: a d=100mm (diameter o the main part) loop with minimized hydraulic resistance for high velocity experiments (corrosion, cavitation, local resistances and heat-sinkers, etc.), a loop stand for precise calibration of different type Na flow-meters, as well multi loop stand for testing multi channel innovative electromagnetic pumps.

### **Task 1:: High performance electromagnetic pumps and instrumentation for various electrically conducting Liquids.**

Due to the future development of SFRs, it is necessary to update the liquid sodium technologies. One of the key technologies to be optimized are the induction electromagnetic pumps for the generation of flows in the primary liquid sodium circuit, and the electromagnetic flow-meters. One of the major advantages of those types of pumps or flow-meters is the absence of any contact with the liquid metal.

IPUL will perform an assessment of the existing technologies for the sodium applications and also for potential intermediate coolants, in order to have the feedback from previous developments. IPUL will also investigate the criteria on flow-rates for the selection of the most appropriate options, identify the needs for EMP developments, particularly for very large flow-rates and achieve recommendations for future R&D. IPUL will investigate particularly permanent magnet systems.

#### **Deliverable**

#### **No Deliverable title Delivery**

<b>month</b>	<b>Nature</b>	<b>Task</b>
--------------	---------------	-------------

Month 12 : D-WPxxx Synthesis of the existing technologies for the sodium applications and also for potential intermediate coolants

Month 24 : D-WPyyy Criteria on flow-rates and local conditions with regards identification of innovative EMP and instrumentation.

Dr. Kurt Clausen  
Paul Sherer Institut PSI  
52323 Vilingen,  
Switzerland

Confirmation of participation

This is to confirm that in the *Preparatory Phase* of the European Spallation Source (ESS) the University of Latvia is willing to act as a partner of the consortium for the 7th Framework Programme project proposal INFRA-2007-2.2.1.23: ESS (European Spallation Source). The Institute of Physics (IPUL) as a subsidiary of the University of Latvia will be involved in implementing the tasks under WP9. All documents necessary for participation at the project consortium will be signed by the University of Latvia.

Prof. Indrikis Muiznieks,  
Prorector for science

# LATVIJAS UNIVERSITĀTS ZINĀTNU PROREKTORS

Raiņa bulv. 19, Rīga, LV – 1586 tālr. 7034401; fakss 7034302; e-pasts: Indrikis.Muižnieks@lu.lv

24. 05. 2007. Nr. \_\_\_\_\_

LU Fizikas institūta direktoram Dr. J. Freibergam  
LU FMF Fizikas nodaļas vadītājam Dr. L. Buliginam  
LU Akadēmiskā departamenta direktora vietniekam A. Pujātam

## Par LU līdzdalību ESS projektā

Godājamie kolēģi!

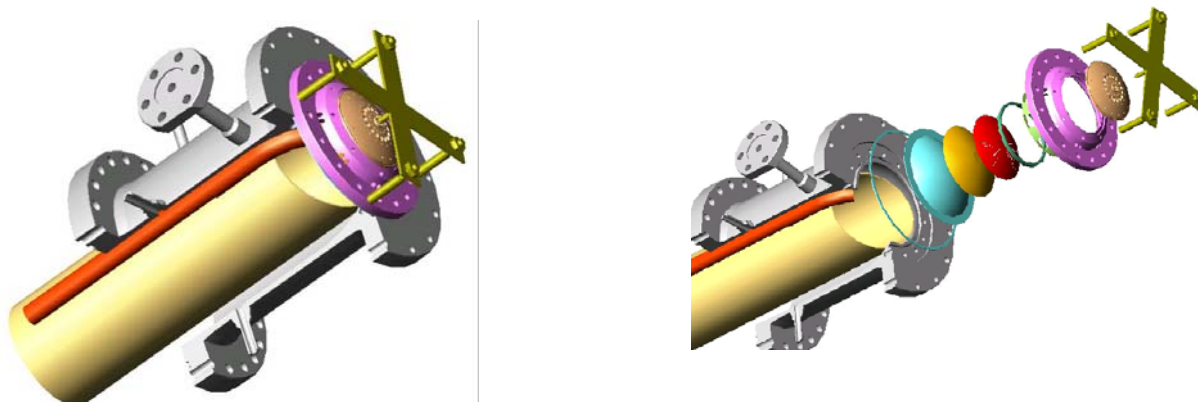
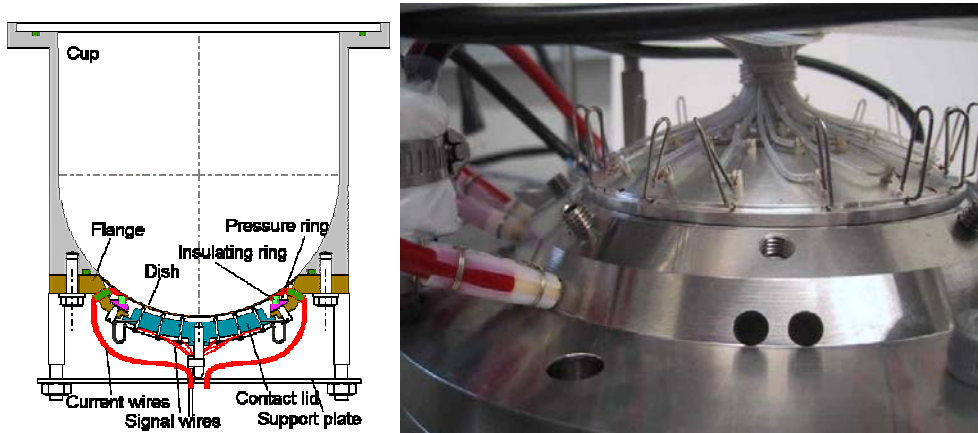
Piedāvāju tālāk aprakstīto shēmu un nosacījumus LU līdzdalībai Eiropas Savienībā ietvarprogrammas (ES7FP) lielās infrastruktūras projektā *European Spallation Source* sagatavošanas aktivitātēs:

- 1) Tiek izveidota LU ESS projekta Vadības Padome (VP), kuras sastāvā ir trīs pārstāvji no fakultātēm un divi - no LU Fizikas institūta (LU FI), kā arī LU Akadēmiskā departamenta (I) pārstāvis.  
Padomes darba uzdevumi: -
  - apstiprināt ar ESS projekta konsorciiju saskaņotu darbu plānu ESS sagatavošanas aktivitāte
  - apstiprināt aktivitāšu plānu, tai skaitā: neutronu mērķa konstruēšanas iestrādei, studiju izveidei, studentu un doktorantu piesaistei, un meklēt papildu finansējuma avotus šīm aktivitātēm LU, IZM un EM resursiem, lai sagatavotos pilna apjoma līdzdalībai ESS
  - nodrošināt ES7FP projekta sasaisti ar LU, pirmkārt Fizikas nodaļas studijām, apkopojo tēmu piedāvājumu un sekmējot studentu iesaisti projektā, lai pēc 2 – 5 gadiem mūsu jaunie sāču spējīgi darboties ESS;
  - iniciēt diskusiju, lai novērtētu Latvijas iespēju iesaistīties ESS Zviedrijas konsorcijā ar savu līdzfinansējumu.
- 2) LU Fizikas nodaļa deleģē projekta administratoru, kura pienākums ir arī nodrošināt oficiālo ar projekta konsorciija koordinatoru, Paula Šērera institūtu (PSI), par projekta administrāciju jautājumiem.
- 3) Projekta pārraudzību veic LU AD, kurā tiek nozīmēta par projektu atbildīgā persona.
- 4) ES7FP ESS sagatavošanas aktivitātes finansējums tiek apsaimniekots LU grāmatvedībā. dokumentācijas sagatavošanu un saskaņošanu ar PSI veic projekta administratora sadarbībā a tos apstiprina LU AD atbildīgā persona. Atkarībā no ES7FP projekta finansēšanas mehāniķos apmaksā LU FI projekta plānā paredzēto uzdevumu veikšanu kopumā vai arī LU FI pētnieki uz īstenošanas laiku slēdz uzņēmuma līgumus ar LU. Projekta administratora darbs jāiekļauj projekta izmaksās.
- 5) No LU zinātniskās infrastruktūras attīstības līdzekļiem tiek piešķirts līdzfinansējums ESS sagatavošanai Ls 6000 apmērā pēc ar PSI saskaņota darba plāna, pārējā pieprasījuma daļes nesniegtā pieprasījuma tiek vērtēta kopējā LU infrastruktūras projektu konkursā.  
Ja ieinteresētās puses (šīs vēstules adresāti) piekrīt iepriekšminētajiem nosacījumiem, LU parakstīt atbalsta vēstuli un iesaistīties ESS iesaistīties sagatavošanas aktivitātēs kā universitātē

I. Muižnieks

Viena no atskaldīto neutronu avotu pamatīpašībām ir netipiski lielais neutronu plūsmas blīvums, līdz  $10^{17}$  neutroni/cm<sup>2</sup> sek. Salīdzinājumam var minēt tradicionālo neutronus ģenerācijas avotu kodolu dalīšanās reaktoru- kur attiecīgā plūsma pēc kārtas nepārsniedz līmeni  $10^{14}$ . Tieks sagaidīts, ka lielā plūsmas intensitāte un specifiskais enerģētiskais sadalījums pavērs principiāli jaunas iespējas neitronikai kā pētniecības līdzeklim dažādās zinātnes nozarēs, fizikā, bioloģijā, u.c. Sevišķi jāatzīmē iespēja atskaldīto neutronu avotos pārstrādāt atomelektrostaciju "atkritumus", pārvērst ilgi sabrūkošos izotopus ātrāk sabrūkošos.

Neutronu atskaldīšanas procesā kāda blīvā materiāla "mērķī" tiek iestaroti protoni, paātrināti līdz tik augstām enerģijām, ka vienā sadursmes aktā ar kodolu tiek "atskaldīts" liels skaits (līdz divdesmit) neutronu. Būtiska daļa šīs energijas transformējas siltumā, tādēļ lielas jaudas mērķus veido no šķidra metāla (Hg vai PbBi), kas dod iespēju izdalīto siltumu atvadīt. LU Fizikas institūts, specializējies dažādās šķidra metāla tehnoloģijās, iesaistīts praktiski visu šobrīd eksistējošo šķidra metāla protonu mērķu izveidē. Kā piemērs zemāk apskatīts MEGAPIE (MW Pilot Exp.) projekts Šveicē, Paula Šerera Institūtā (PSI), kura ietvaros 2006.gada nogalē pirmo reizi tika ģenerēti neutroni ar prognozēto augsto pūsmas blīvumu. Institūtā pētījumu rezultātā tika izstrādāta protonu iestarošanas "loga" dzesēšanas metodika. Zīm.1 ilustrē atbilstošo izmantoto aparātu. Tika izveidots un PSI uzstādīts stends, lai pirmo reizi reālu augstas energijas protonu kūli iestarotu sienā, dzesētā ar PbBi. Beidzot, tika izstrādāts, izgatavots un MEGAPIE kompleksā uzstādīts sapārots elektromagnētiskais sūknis, ar kuru veiksmīgi tika realizēta Institūta ieteiktā divplūsmu shēma protonu mērķa dzesēšanai (Zīm.2).



# **Electromagnetic metamaterials and new aspects of electricity**

Janis Valdmanis, Aleksandrs Cipiks

## I.INTRODUCTION

There are old and good theory of electromagnetic ( EM) field - classical electrodynamics. It looks that all aspects of theory is realized. But recently the new branch of electrodynamics have rapid growth – it is electrodynamics of materials with negative index-of-refraction [1, 2]. Such materials are called Left-handed materials, Metamaterials or Backwaid wave materials.

In general, materials have two EM parameters, permeability and permittivity, that are positive. Left-handed material is a material whose permeability and permittivity are both negative. Such materials are artificially created and their unique electromagnetic properties were investigated. Because an index-of-refraction is negative light that enters a left-handed material from a right-handed medium will undergo refraction, but opposite to that usually observed. Another unique are that in left-handed medium light propagates in opposite direction as energy flow and such materials have reversal Doppler shift and Cherenkov radiation. Optic lens made from left-handed materials that could be conversing if made from conventional material, will be diverging, and vice-versa . There is also some situation than left-handed material attracts EM radiation.

Historically first theoretical work were done by Victor Veselago (1967), then long calm period and first experimental activities , that confirmed many theoretically predicted interesting results ( see: The Research group of David Smith, Novel Electromagnetic Materials, [http://www.ee.duke.edu/~drsmith/smith\\_pubs.htm](http://www.ee.duke.edu/~drsmith/smith_pubs.htm)) in the microwave region of EM field.

Really metamaterials have periodic composite material structure. Separate element of such structure consist of part that resonate on electrical field and one that resonate on magnetic field. One of the requirements is that EM wave lengths need to be much larger than that characteristic dimension of structure elements. That is because in optic region elements need to be in atomic or molecular dimension. That is one of the problem the are not progress made metamaterials in optical region. Characteristic element of metamaterials have small copper wire (electrical) and ring (magnetic) resonator and have metamaterials properties in micro wave region.

From physical point of view it is interest to made metamaterials in MHz, kHz and low frequency region including 50-60 Hz. There are some advantages and also disadvantages. First, it is easy to fulfill requirement that wave length is much larger then elements dimension.

Second we can investigate and optimize separate structure element. Disadvantages are to maid line, plane and space structure in cases when structure elements dimension is large.

In microwave region metamaterials element electrical and magnetic part are separated. More compatible is element that resonates at EM field at the same time. It is shown that in above-mentioned frequency region it is possible realize.

## II. EXPERIMENTAL INVESTIGATIONS

Main characteristics of metamaterials are: periodic structure, separate elements that responded to EM field, elements dimension and distance between them are smaller

than EM wave length, there are essential dispersion effects. Last one is because EM energy density needs to be positive

$$W = \frac{\partial(\mu\omega)}{\partial\omega} H^2 + \frac{\partial(\epsilon\omega)}{\partial\omega} E^2 > 0 , \quad (1)$$

where  $\mu$  – permeability,  $\epsilon$  – permittivity,  $f = \omega/2\pi$  - frequency, H and E – magnetic and electric intensity. (1) is positive if  $\frac{\partial(\mu\omega)}{\partial\omega} \text{ and } \frac{\partial(\epsilon\omega)}{\partial\omega} > 0$

We instigated EM waves at range from 50 Hz to hundreds MHz where the waves length are long enough to be larger than elements as well as distances between them. Next step where unite element that response to E and H components. In microwave region there are thin wire (E elements) and split ring resonator (H elements). On fig. 1 unite element that response to E and H field at 520 kHz are given. Such element response is active with resonant character fig. 2. The voltage of generator was 2.2 volt and maximal intensification  $\sim 70$ . Really there are also some higher modes but we concentrated on the main one because intensification in that case is larger. For the mode1 fig. 1 next mode is  $\sim 2.38$  MHz with intensification  $\sim 3$ . Result fig. 2 was received when generator is connected to element but the some results are if we excite it electrically or by magnetic induction without straight contacting. Typical situation

is in plasma physics where  $\epsilon = \epsilon_0(1 - \frac{\omega_L^2}{\omega^2})$ ,  $\omega_L$  - plasma (Longmuir) frequency.

In that cases  $\frac{\partial(\epsilon\omega)}{\partial\omega} = \epsilon_0(1 + \frac{\omega_L^2}{\omega^2}) > 0$



Fig. 1. element , that resonates at 520 kHz

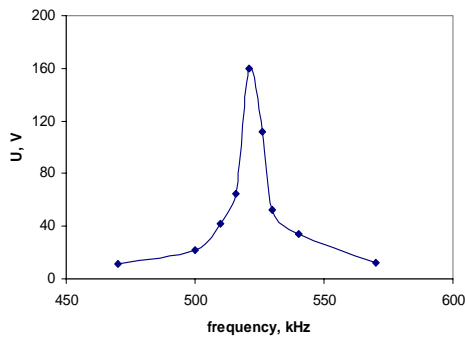


Fig. 2. Voltage- frequency characteristic for element fig.1.



Fig. 3 . Two interacting elements at characteristic distance.

On fig. 3, two identical element are given at characteristic distance. In that cases we have two resonance frequencies. One when both elements are in phase ( frequency 510 kHz ), another when phase are opposite ( 472 kHz ). Generator is connected to one element, no straight contact with other. The element can be excited also without straight contact, it is by electric or magnetic induction. Due to interaction the symmetrical mode resonances frequency is larger than asymmetric one. Compare with one element cases ( fig. 1 ) the maximal intensification for symmetrical mode is smaller but for asymmetrical mode due to apposite character give intensifications increase. Physically situation is the same as in two interacting oscillators.

On fig. 4 results of interacting are shown when one element is excited by EM impulse. At first one element is excited, than excitation go to second and vice versa. Process repeat many times. The higher frequency on fig. 4 is 510 kHz, oscillation between elements 90 kHz. If distances between elements increase the oscillation period also increase ( fig. 5 ). It is necessary to emphasize the influence of measuring process. There are used HAMEG type oscilloscope with resistance 10 MW and C=12 pF. Fig. 2 and fig. 4 - 5 results were received when oscilloscope contacted to electrode. If measuring procedure is without contacting the resonate frequency is larger. On fig. 6 are situation when impulse excitation are realized without oscilloscope straight contact. Higher resonant frequency is 800 kHz , oscillation between element 200 kHz. It is easy to realize situation discussed in [3 ]. Lets take case when the resonance frequency of element excited by generator is smaller or larger than that one of neighbour element. If excited frequency is near the neighbours element resonance the voltage and excitation increase and the passive element is pumped up. Light diode in generators element go out and in neighbour (passive) catch fire [3]. On fig. 7 such situation are shown. In generator element we have 2 volts but in neighbour 14 volts. There are also situation when passive elements volts are 10 or more time larger.

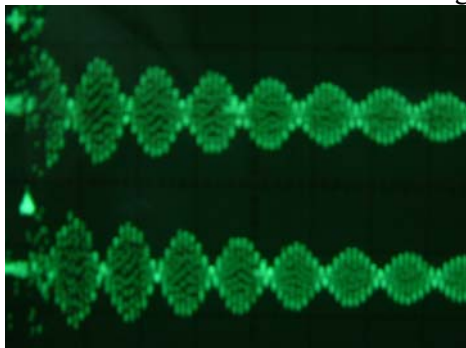


Fig. 4. Two-element interaction process dynamic. Distance between elements 2 cm.

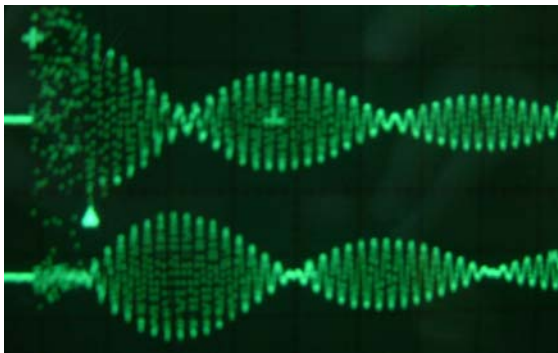


Fig. 5. Distance between interactive elements 30 cm.

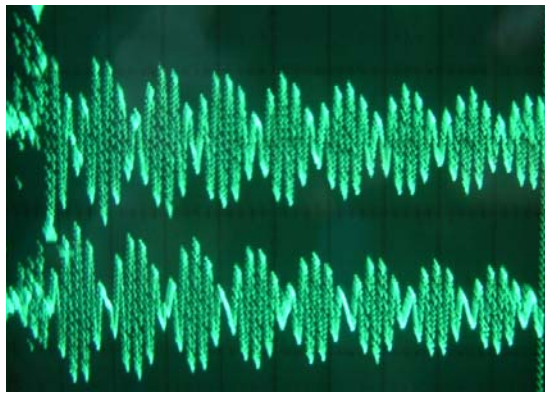


Fig. 6. Two elements interaction dynamics without oscilloscopes  
Straight contacts.

For more elements we have many interacting oscillators problem. As mention in [4] the situation is the same like in periodic crystals. In metamaterials cases instead of atoms the crystal structure elements are man-made. In solid state physics dispersion relations are characterized by energy-impulse dependence, in metamaterials it frequency-wave length one.

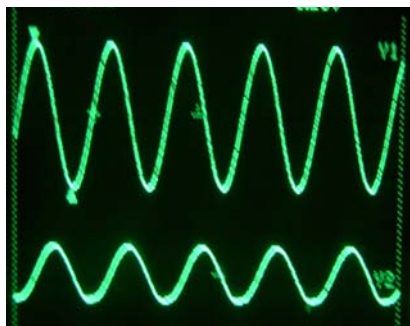


Fig. 7. Passive element excitation. Frequency 512 kHz,  
generators voltage 2V, passive element – 14 V.



Fig. 8. Model , that resonate at 50 Hz.

On fig. 8. as example is given element for 50 Hz region . It looks like element that have optimal parameters for 50 Hz need to be very large. It is shown experimentally that the characteristic dimension could be approximately 20-30 cm. It really resonates at magnetic and electrical components. If necessary dimension could be decreased.

### III THEORETICAL ASPECTS

First question is why the simple coil element have resonant active response on E and B field ? Really it is collective electrons oscillations that at definite frequency resonate. One way is imagine oscillators as one dimensional Lengmuir type electron oscillation along the coil wire that at the same time generate electrical current. Because it is coil system current generate magnetic field. When at one end electric charge increase and generate opposite electrical field, magnetic induction stimulate electrical charge increases. Than process due to electrical fields force start in opposite direction. At some frequency intensification process take place. It is like L-C resonance but in those cases some effective L and C are distributed along the coil. Another possibility is EM wave dispersion going from one coil end to another. Because between separate winding is C that are charged. EM field velocity decreases. It is like tsunami in shallow water. But in our cases due to vector character of field process stopped and starts in opposite direction. Then at next end the same increasing process are realized. One can use also interpretation using dynamic negative  $\epsilon$  and  $\mu$ . In fig.3 case we have two interacting oscillators [5]. Using L, C or E, B bound it is possible to detect resonant frequencies and dynamics of impulse excitations results fig. 4, 5. Situation is like two pendulum that are bounded by spring oscillations. Symmetrical case is when both pendulum move in the same directions. Asymmetrical when moving direction is opposite.

If both oscillators fig. 3 have the same resonant frequency  $w_0$  and interact with effective  $L_i$  and  $C_i$  then solution of interacting oscillator equations gives for potential at the elements end  $u_1$  and  $u_2$

$$\varphi = \varphi_0 e^{-i\omega_0 t} (u_1 \cos \omega_i t - i u_2 \sin \omega_i t), \quad (2) \text{ where } \omega_i = \frac{1}{\sqrt{L_i C_i}}, \quad L_i, C_i$$

effective interacting impedance and inductance. At times  $\omega_i t = (2n+1)\frac{\pi}{2}$  maximal amplitude have second element, at times  $\omega_i t = (2n+1)\pi$  first one. That is the

situation on fig. 4, 5. At  $t=0$   $u_1$  oscillator is excited by impulse force. Due to dissipation process oscillation amplitude decrease.

Experimentally results shown that  $w_i$  increases when the distance between elements decrease. Because effective  $C$  increase it means that there are essential decreases of effective  $L$ . Using the interpretation about wave velocity decreases interaction parameter  $w_i$  can be taken as  $v_{ef}/l$ , where  $v_{ef}$  – mean velocity and  $l$  – distance between elements. When there are sin type excitation the symmetric and asymmetric state are observed. Asymmetric state frequency is lower because in that cases elements is charged opposite and  $C$  between elements is larger ( $f_{re} \approx \frac{1}{\sqrt{C}}$ ).

On fig. 9 we have situation when there are two sin-type external sources. One source has frequency  $f_s$  and another  $f_{as}$ . The physics in this cases is little different but visually the interaction process is the same. Compare with impulse excitation process are without amplitude decreasing.

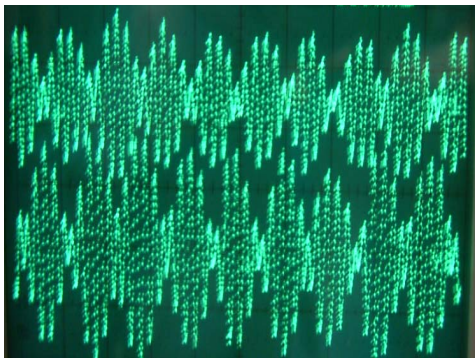


Fig. 9. Two elements excitation dynamics when there are two external sources.

For more elements, we need to solve many oscillatory interactive problem. Of course, we can use all the solid state physics ideas and results because in the plane or volume cases it is crystal type structure with man-mode elements instead of atoms. In atomic physics, every atom has many discrete energy levels for electrons. Due to interaction process, separate levels made energy band. There are closed bands as well as open one. It is known as conductive band. In our cases, we considered only the main resonant frequency level.

Returning to the situation fig. 3 where we have two resonant states, symmetric and asymmetric. Results of resonance frequency splitting by interaction are 472 an 510 kHz. It is small compare with next mode 2.38 MHz. Specific case is 50 Hz range. To have active element in 50 Hz range we need maximally increase interaction between element, it is increase  $C$  or  $L$  (or both) and as a result decrease resonance frequency. That is realized in model fig. 8. In that cases difference between asymmetric (50 Hz) and symmetric ( $\sim 2$  kHz) is essential.

If there are more elements the interacting process that is not very strong made some resonant frequency band. Results of fig. 4, 5 shows that interaction process depends of characteristic distance between elements. There exist optimal distance.

Really there are two resonant coil system investigated by Tesla [6]. When systems are close one to other resonant frequency splitting is maximal. If distance increase the resonant frequency for symmetrical and asymmetrical case is the same. It is analogy of degeneration levels in atomic physics. If the system's far away the question is about interaction mechanism. In [3] it is claimed that there are longitudinal EM wave's interaction. When distance between element in small there are 3-dimensional

EM field where both E and H have all three components. When distance is large it is something like entangled state in quantum field theory. Nobody exactly knows what do's it means entangled state.

Can we transfer energy using such entangled state? Results of Tesla investigations show that it is possible. But in that case we need two strictly identical elements. As we see fig. 4, 5 the energy transfers many time from one element to other when distances between elements are small. The transfers frequencies decrease if distance increase. Large distances need special investigations.

In the plane or volume cases, phases' transition could be possible. In symmetrical case, all oscillators give the same magnetic induction. It is not energy optimal case. When the neighbouring elements are opposite, the magnetic energy is decreased. It is analogy with phase transition in ferromagnetic where the domain structure appears. This and many another questions is for future investigation .

## CONCLUSIONS

There are no principal problems to realize metamaterials ideas in low frequencies range.

Metamaterials element can be made in a way to have resonant response to E and H field.

The important question is interaction effects between metamaterials elements.

At small distances between interacting elements pulse excitation of one element transfers to other and vice versa.

For resonant interacting elements need to be strictly identical.

Energy exchanges processes depend on distance between elements.

In resonance, interacting investigations there are necessary to take into account influence of measuring procedure.

Resonant interacting elements made collective system that is like entangled state in quantum field theory.

Active metamaterials element can be used as sensor in 50 – 60 Hz measuring techniques.

## REFERENCES

- [1] Веселаго Б. Г.: Электродинамика веществ с одновременно отрицательными значениями  $\epsilon$  и  $\mu$ . УФН, 92, 1967, стр. 515-526.
- [2] Веселаго Б.Г.: Электродинамика материалов с отрицательным коэффициентом преломления. УФН, 173, 2003, стр. 790-794.
- [3] Meyl K: Skalarwellentechnik. INDEL GmbH, Verlagsabteilung, Villingen-Schwenningen 2000, 1.Auflage, ISBN 3-9802 542-6-7.
- [4] Силян П. А.: Электромагнитные волны в искусственных периодических структурах. УФН 176, 2006, стр. 562-565.
- [5] Pierce J.: Almost all about waves. The MIT Press Cambridge, Massachusetts and London, England 1974, pp. 176.
- [6] Tesla N. & Childress D. H. The fantastic inventions of Nikola Tesla . Adventures Unlimited stelle, Illinois, USA, 1993, pp. 349.

**II apakšvirziens**  
**Magnētisko nanokoloīdu fizika**

**LU Fizikas institūta magnētisko šķidrumu pētījumu grupas rezultāti  
2008. gadā Vadītājs E. Blūms**

**LZP Sadarbības projekts 05. 0026-14 "Difuzīvā un konvektīvā nanodaļiņu pārnese neizotermiskos ferrokoloīdos un kapilāri-porainās vidēs"**

1. Veikti eksperimentāli pētījumi par magnētisko koloīdu pārneses parādībām kapilāri-porainā vidē. Novērotas būtiskas osmotiskā spiediena izmaiņas stēriski stabilizētos organosolos. Izdarīti analītiski pētījumi par termoosmotisko procesu relaksāciju plānā filtrējošā slānītī. Atrastas likumsakarības, kas apraksta osmotiskā spiediena līkņu dinamiku. Salīdzinot šīs likumsakarības ar eksperimentu rezultātiem, noskaidrots, ka dominējošās pārneses parādības slānītī ir filtrācija, termoosmoze un daļēji reversā osmoze. Prognozēta magnētiskā lauka ietekmes anizotropija uz osmotiskām parādībām atkarībā no lauka orientācijas pret temperatūras gradientu.
2. Veikti magnetizācijas un magnetizējošā lauka energijas termiskās disipācijas pētījumi nestacionārā magnētiskā laukā dažādu kompleksa ferītu nanodaļiņas saturošos koloīdos. Noskaidrots, ka kilohercu frekvenču diapazonā novērotais termiskais efekts atkarīgs no nanodaļiņu magnētiskās anizotropijas īpašībām, no ārējā lauka frekvences un intensitātes, kā arī no nanodaļiņu izmēriem un koncentrācijas, kā arī no koloīda viskozitātes.

**Valsts programma Nr. 3 "Modernu funkcionālu materiālu mikroelektronikai, nanoelektronikai, fotonikai, biomedicīnai un konstruktīvo kompozītu, kā arī atbilstošo tehnoloģiju izstrāde", Projekts Nr.3. 5. "Nanodaļiņu, nanostrukturālu materiālu un plāno kārtīju tehnoloģiju izstrāde funkcionālo materiālu un kompozītu izveidei".**

1. Veikti pētījumi par siltuma pārnesi termomagnētiskās konvekcijas plūsmās. Noskaidrota magnētiskā lauka perturbāciju ietekme uz brīvās konvekcijas siltumapmaiņu starp cilindrisku sildošo elementu un magnētisko šķidrumu. Izdarīti skaitliski pētījumi par termomagnētisko konvekciju divdimensionālā kanālā ar reversu šķidruma plūsmu zonā bez magnētiskā lauka. Noskaidrots, ka transversālas siltuma pārneses intensitāte būtiski pieaug, ja siltuma avots tuvināts konvekciju ierosinošā magneta poliem.
2. Veikti pētījumi par salikto ferītu nanodaļiņu saturošu koloīdu magnetizāciju un tās atkarību no temperatūras rajonā līdz 120 C. Formulētas rekomendācijas, lai radītu jaunus ferrokoloīdus ar īpašībām, kas nepieciešamas turpmākiem specifiskiem fizikāliem un lietišķiem pētījumiem, tai skaitā medicīniskās hipertermijas tematikā.
3. Izstrādāta hologrāfiska metode optiski ierosinātu nanodaļiņu struktūru vizualizācijai un magnētiskās mikrokonvekcijas pētījumiem. Izveidota „Forced Rayleigh Scattering” mēriekārtā, izmantojot kā termisko un termodifuzīvo struktūru ierosinātāju nepārtrauktas darbības lāzeri.

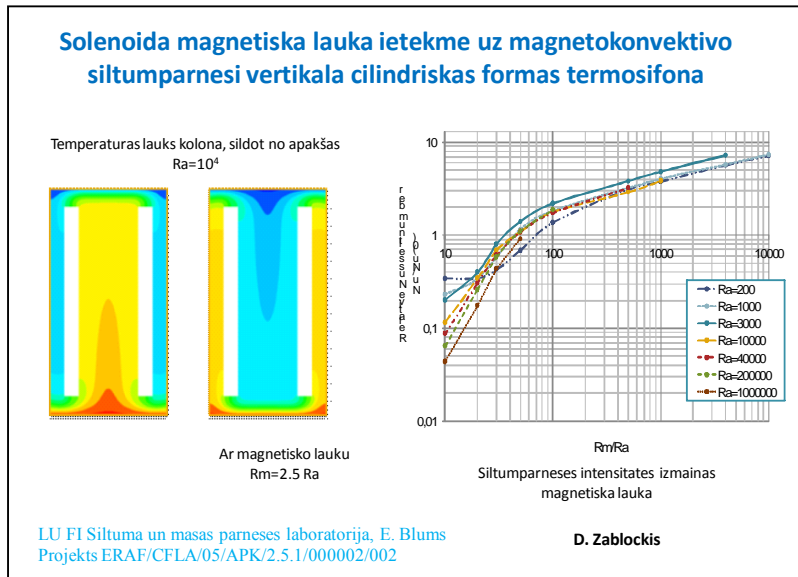
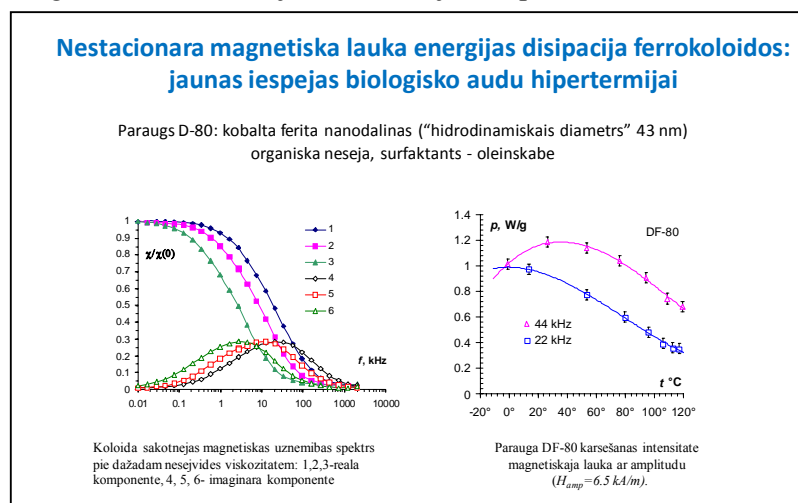
**ERAF līdzfinansētais projekts "Ferītu nanodaļiņas un koloīdi termomagnētiskās dzesēšanas sistēmām un audu hipertermijai", līguma Nr.  
VPD/ERAF/CFLA/05/APK/2.5.1./000002/002**

Nobeigti divu gadu pētījumi un apkopoti to rezultāti sekojošos jautājumos:

1. Izmantojot fundamentālo pētījumu rezultātus, uz salikto ferītu bāzes radīta virkne jaunu ferrošķidumu ar piesātinājuma magnetizāciju līdz 16 kA/m un

piromagnētisko koeficientu līdz  $0.0025 \text{ K}^{-1}$ , kā arī ar dažādām nanodalīju magnētiskās anizotropijas īpašībām, lai nodrošinātu paaugstinātu augstfrekvences lauka energijas disipāciju koloīdā.

2. Izveidots termomagnētiskā sifona eksperimentāls modelis. Izmantojot spēcīgus pastāvīgus magnētus un izveidojot konvekcijas kanālu ar magnētiskā šķidruma reversas plūsmas zonām ar nulles magnētisko lauku, panākta jūtama translācijas siltumplūsmas intensifikācija mangāna ferīta bāzes koloīdā.
3. Balstoties uz fundamentālo pētījumu rezultātiem, noskaidrotas iespējas izmantot magnētiskās nanodalīnas magnētiskās hipertermijas vajadzībām. Ferītu nanodalīnās ar paaugstinātām magnētiskās anizotropijas īpašībām (kobalta ferīti) pie relatīvi zemām nestacionārā magnētiskā lauka frekvencēm (22- 44 kHz) panākta energijas disipācija virs  $1 \text{ W/g}$ , kas pietiekama, lai realizētu magnētisko hipertermiju bioloģiskos audos.
4. Būtiski atjaunota laboratorijas telpu infrastruktūra (ERAF infrastruktūras projekts) un modernizēta eksperimentālās bāze. Aprīkota speciāla telpa optiskiem un hologrāfiskiem pētījumiem, papildināts aprīkojums termomagnētiskās konvekcijas un filtrācijas eksperimentiem.



**Dalība 2 starptautisku zinātnisko konferenču organizācijas komitejās:**

1. 7<sup>th</sup> th PAMIR International Conference on Fundamental and Applied MHD, September 2008,Grenoble-Presquile de Giens, Francija (E. Blums),
2. 12th International Magnetic Fluid Conference, Sendai, Japan, 2010 (E. Blums).

**12 referāti starptautiskās zinātniskās konferencēs:**

1. 7th International PAMIR Conference on Fundamental and Applied MHD, France, (E. Blums, G. Kroņkalns, A. Mežulis, D. Zablockis),
2. 8th International Meeting on Thermodiffusion, Bonn, Germany (E. Blums),
3. International Baltic Sea Region conference “Functional materials and nanotechnologies”, Riga (A. Mežulis, M. Majorovs, G. Kroņkalns, L. Tiļuga).

**Pakalpījumi ASV firmai “Ferotec-USA” uz LZA un Ferofluidics sadarbības līguma pamata: veikti aptuveni 40 firmas ferokoloīdu magnetizācijas mērījumi un izdarīta to magnetogranulometriskā analīze (M. Majorovs)**

**Publikācijas**

1. Vilnis Frishfelds, Elmars Blums, Drift of nonuniform ferocolloid through cylindrical grid by magnetic force, Journal of Physics: Condensed Mater, 20 (2008) 204130 (5pp)
2. D.Zablotsky, V. Frishfelds, E. Blums. Numerical investigation of thermomagnetic convection in heated cylinder under the magnetic field of a solenoid. Journal of Physics: Condensed Mater, 20 (2008) 204134 (5pp).
3. E. Blums, A. Mezulis, G. Kronkalns. Magnetoconvective heat transfer from a cylinder under the effect of a non-uniform magnetic field. Journal of Physics: Condensed Mater 20 (2008) 204128 (5pp)
4. G. Kroņkalns, A. Dreimane, M.M. Maiorov. The effect of thermal treatment on the magnetic properties of spinel ferrite nanoparticles in magnetic fluids, Magnetohydrodynamics, 44 (2008), No. 1, pp. 3–10
5. Segal I., Zablotskaya A., Lukevics E., Maiorov M., Zablotsky D., Blums E., Shestakova, I. Domracheva I. Synthesis, physico-chemical and biological study of trialkylsiloxyalkyl amine coated iron oxide/oleic acid magnetic nanoparticles for treatment of cancer. Appl. Organomet. Chem., 2008, 22, 82-88.
6. Segal I., Zablotskaya A., Lukevics E., Maiorov M., Zablotsky D., Blums E., Mishnev A., Shestakova I., Gulbe A. Iron oxide based magnetic nanoparticles bearing cytotoxic silylated alkanolamines. Proceedings of the 7th PAMIR Int. Conference on Fundamental and Applied MHD, Giens - France, September 8-12, 2008, p.697-701.
7. E. Blums, G. Kronkalns, M. Maiorov. Thermoosmosis in Magnetic Fluids in the Presence of a Magnetic Field, In: Proceedings of the 7th PAMIR Int. Conference on Fundamental and Applied MHD, Giens - France, September 8-12, 2008, p. 667 -671.
8. M. M. Maiorov, G. Kronkalns, E. Blums. Complex Magnetic Susceptibility of Cobalt Ferrite Ferrofluid: Influence of Carrier Viscosity and Particle Concentration, In: Proceedings of the 7th International PAMIR Conference on Fundamental and Applied MHD, September 8-12, 2008, Giens, France, pp.725-729 , p. 725-729

9. E. Blums, A. Mežulis, G. Kronkalns. Magnetoconvective Intensification of Heat Transfer Based on Permanent Magnets, In: Proceedings of the 7th International PAMIR Conference on Fundamental and Applied MHD, September 8-12, 2008, Giens, France, 803-807.
10. D. Zablockis, V. Frishfelds, E. Blums. Investigation of Heat Transfer Efficiency of Thermomagnetic Convection in Ferrofluids, In: Proceedings of the 7th International PAMIR Conference on Fundamental and Applied MHD, September 8-12, 2008, Giens, France, p. 715-720.
11. E. Blums, G. Kronkalns, M. Maiorov. Thermoosmotic Transfer of Ferrocolloids through a Capillary Porous Layer in the Presence of Transversal Magnetic Field, In: Thermal Nonequilibrium, 8th International Meeting on Thermodiffusion, Lecture notes, Eds. S. Wiegand, W. Kohler, J.K.G. Dhont, Forschungzentrum Julich GmbH, 2008, p. 169 - 174.
12. E. Blums, G. Kronkalns, M. Maiorov. Thermoosmotic transfer of ferrocolloids through a capillary porous layer in the presence of transversal magnetic field. Abstracts, 8th International Meeting on Thermodiffusion, Bonn, June 2008, p. 56 – 57.
13. Mezulis, A., L. Tiluga. Visualization of Optically Induced Gratings of Magnetic Nanoparticles, Abstracts, International Baltic Sea Region conference “Functional materials and nanotechnologies”, Institute of Solid State Physics, April 1 – 3, 2008, Riga.
14. D. Zablockis, V. Frishfelds, E. Blums. Numerical Investigation of Heat Transfer in Magnetic Nanocolloids under Inhomogeneous Magnetic Field, Abstracts, International Baltic Sea Region conference “Functional materials and nanotechnologies”, Institute of Solid State Physics, April 1 – 3, 2008, Riga.
15. M. Maiorov, G. Kronkalns, E. Blums. The Magnetic Susceptibility Spectrum of Cobalt Ferrite Ferrofluid, Abstracts, International Baltic Sea Region conference “Functional materials and nanotechnologies”, Institute of Solid State Physics, April 1 – 3, 2008, Riga.
16. Zablotskaya A., Segal I., Lukevics E., Zablotsky D., Maiorov M., Shestakova I. Mixed coated iron oxide magnetic nanoparticles containing organosilicon alkanolamine cover. The 15th International Symposium on Organosilicon Chemistry, June 1-6, 2008, Jeju, Korea, 2008, p.133.
17. Segal I., Zablotskaya A., Lukevics E., Maiorov M., Mishnev A., Shestakova I., Domracheva I. Sterically stabilized colloidal systems of magnetic nanoparticles for biomedical application. The International Baltic Sea Region conference ‘Functional materials and nanotechnologies 2008’, April 1-4, 2008, Institute of Solid State Physics University of Latvia, Riga, Latvia, 2008, p.115.

### **Studentu diplomdarbi:**

1. Dmitrijs Zablockis. Termomagnētiskās konvekcijas siltumpārneses efektivitātes pētījums magnētiskajā šķidrumā, Maģistra darbs, LU Fizikas un matemātikas fakultāte, Fizikas nodaļa, Rīga, 2008.
2. Līga Tiļuga, Termālā un koncentrācijas mikrorežģa inducēšana magnētiskajā koloīdā, un tā optiskā pētīšana, Bakalaura darbs, LU, 2008.g. jūnijs.

3. Aija Dreimane, Dažādas raudzes sudraba virsmas inhibēšana, Bakalaura darbs, RTU, 2008. g . jūnijs, 63 lpp.

**III apakšvirziens**  
**Degšanas procesu dinamikas izpēte.**

Dr.Phys. Maija Zaķes grupas darbs:

Laika posmā no 01.08 līdz 12.08. ir pabeigti eksperimentālie pētījumi un sagatavotas atskaites diviem projektiem, kuru vadītājs ir LU Fizikas institūta vad. pētn. Maija Zaķe. Pirmais projekts „VPD1/ERAF/CFLA/05/APK/2.5.1./000001/001” „Koksnes biomasa vietējo resursu racionāla izmantošana siltuma ražošanai kombinētā koksnes un gāzveida kurināmā degšanas procesā”, ir lietišķo pētījumu projekts, kura mērķis bija veikt kombinētā degšanas procesa eksperimentālos pētījumus, vienlaicīgi sadedzinot atjaunojamo kurināmo un gāzveida fosilo kurināmo, lai nodrošinātu stabili un ekoloģiski tīru degšanas procesu, sadedzinot dažāda mitruma un struktūras koksni (šķeldas, malku, granulas). Izmantojot eksperimentālo pētījumu rezultātus ir izveidots un aprobēts mazas jaudas (līdz 50 kW) vietējās apkures katls, siltuma ražošanai izmantojot kombinēto fosilā gāzveida kurināmā (propāns, dabas gāze) un atjaunojamā kurināmā (dažādu struktūru koksnes biomasa) degšanas procesu. Ir sagatavots un iesniegts patenta pieteikums katla konstrukcijai, kā arī ir saņemts paziņojums par pieteikuma atbilstību Patentu likuma 34.panta 1.daļai. Pieteikuma publicēšana notiks 20.08.2009. Pētījumu rezultāti ir aprobēti vairākās starptautiskās konferencēs, kā arī publicēti dažādos zinātniskos izdevumos (sk. lit. sarakstu). Darbs pie projekta tika pabeigts 07.08., sagatavojojot tehnisko un finansiālo atskaiti par projekta izpildi.

Vienlaikus ar pētījumiem, kas ir saistīti ar ERAF projekta izpildi, pārskata periodā tika veikti arī pētījumi saistībā ar ZP projekta Nr.05.1384 „Siltuma un masas pārneses pētījumi kombinētā gāzveida un cietā kurināmā degšanas procesā ārējo spēku laukā” (vispārējais projekts ar jauno zinātnieku un doktorantu piedalīšanos) izpildi. Dotais projekts apvieno fundamentālos degšanas procesa dinamikas pētījumus dažāda tipa liesmu virpuļplūsmās, izmantojot šo plūsmu kontrolei ārējo lauku (elektriskā, magnētiskā) un liesmas mijiedarbības efektus, kā arī lietišķos pētījumus, kas saistīti ar nepieciešamību ierobežot siltumnīcas efektu un skābo lietu izraisošo degšanas produktu ( $\text{CO}_2$ ,  $\text{NO}_x$ ) veidošanos degšanas procesā, izmantojot šim nolūkam gāzveida fosilā un cietā atjaunojamā kurināmā kombinēto degšanas procesu. Pārskata periodā pamatā tika veikti pētījumi, kas ir saistīti ar ārējo lauku (elektriskā, magnētiskā) un liesmas mijiedarbību, veicot detalizētus degšanas procesa dinamikas, kā arī ar dinamikas izmaiņām saistītos siltuma un masas pārneses procesu pētījumus un to izmaiņas ārējo spēku laukā. Pētījumu rezultāti ir aprobēti vairākās starptautiskās konferencēs (sk. Lit. pielikumu). Darbs pie dotā projekta ir pabeigts 12.08., sagatavojojot atskaiti par darba izpildi.

1. **zīm.** Vietējās apkures katls siltuma ražošanai kombinētā degšanas procesā.



## WOOD BIOMASS CO-FIRING FOR THE CLEAN HEAT ENERGY PRODUCTION

I. Barmina, M. Zake

Institute of Physics, University of Latvia

Miera Street 32, Salaspils-1, LV-2169, Phone: +371 7945838, Fax. +371 7901214, e-mail: [mzfi@sal.lv](mailto:mzfi@sal.lv)

**ABSTRACT:** The main objective of recent study is to provide a clean and effective burnout of a renewable fuel (wood pellets) by co-firing the wood fuel with a fossil fuel-propane. The effect of propane co-fire on the wet wood fuel burnout and composition of pollutant emissions is studied and analyzed at the different rates of propane co-fire and different duration time of additional heat input from propane flame flow. The results of experimental investigations have shown that co-firing of the wood biomass with propane flame flow results in a more effective and cleaner burnout of the wood fuel with reduced mass fraction of polluting (CO, NO) emissions in the products and dominant release of carbon –neutral CO<sub>2</sub> emissions.

**Keywords:** co-combustion, greenhouse gases, CO<sub>2</sub> emission reduction, emissions reduction

### 1 INTRODUCTION

By utilizing modern and efficient technologies of the heat energy production, biomass offers a source of sustainable energy that can gradually replace coal or other fossil fuels (natural gas, fuel oil, etc.). Biomass is considered as the renewable energy source with the highest potential to contribute to the energy needs of modern society world-wide [1, 2]. The biomass residues from agricultural or forestry-based activities are abundant and are possible supply up to three quarters of world energy demand. Globally, about 50% of the potentially available residues for the heat energy production are associated with forestry and wood-processing industries, about 40% are agricultural residues (mainly straw, rice husks, and sugarcane and cotton residues), while 10% are associated with animal manure [1]. The wood biomass as a fuel for heat production is a promising heat energy source for the private country houses, replacing fossil fuel use and mitigating global warming, because wood-fuel heating systems can achieve significant reductions in total emissions of greenhouse gases. Compared to the coal, biomass reduces SO<sub>2</sub>, NO<sub>x</sub>, CO<sub>2</sub>, and other air emissions. In the same time, the renewable wood fuels indicate a wide variation in their heat energy content, combustion and emission characteristics because of the differences in their structure, moisture content and bulk density, causing necessity for stabilization of the heat energy production during the burnout of the wood fuel. Traditionally co-firing is used at power plants where some biomass may be mixed with coal. It is estimated that typical coal-fired power plants can co-fire in excess of 10% biomass by weight, reducing SO<sub>2</sub>, NO<sub>x</sub>, CO<sub>2</sub> emissions during the heat energy production. In other words, if biomass fuel provides 10% of the heat input to a boiler, then 10% of the total heat energy produced can be designated as renewable or green. Co-firing greater proportions between the wood biomass and coal would require greater capital investment for modification and, therefore, is not preferable. The promising technique for stabilization of the heat energy production and improving combustion characteristics during the burnout of wood fuels is co-firing of the renewable wood fuel with a small amount of fossil gaseous fuel (natural gas, propane) [3-5]. There is experience for natural gas to be fired with a small amount (10%) of biomass, when practically applicable is separate wet biomass gasification and co-firing of the gas-phase products [3]. When used as a reburn fuel in power plants, firing coal or biomass with 5% - 25% of natural gas can be used to reduce NO<sub>x</sub> emissions up to 50-70% [6]. Similar proportions between

the wood biomass and fossil fuel by weight and total amount of heat release during the burnout of these fuels can be used, when the additional heat input by fossil fuel is used as a heat energy source for the wet wood fuel gasification and stabilization of the rate of heat energy production. Practically, for such conditions of wood biomass co-fire, when the heat input by fossil fuel into the wood biomass is limited to 20-30%, produced flow of CO<sub>2</sub> emissions mostly (up to 80%) refers to carbon-neutral emissions that are released during the burnout of the wood fuel. It should be noticed that the resulting effect of fossil fuel co-fire on the combustion and emission characteristics is influenced by altogether factors, such as structure and heating value of wet wood fuel, as well the rate, mode and duration of fossil fuel co-fire. To optimize the process of propane co-fire with application to the small-scale domestic boiler systems, the presented study was aimed to appreciate the main factors, affecting the resulting effect of fossil fuel co-fire on combustion and emission characteristics to provide the cleaner and more effective heat production.

### 2 EXPERIMENTAL

The experimental investigations of co-firing the renewable with fossil fuel were managed using a small-scale pilot device (6), designed for co-firing discrete portions of different types of the wet wood biomass pellets (Fig. 1) with propane flame flow. The pilot device is composed of such main components: (1)- the wood biomass gasifier (2)- swirling propane/air burner, (3), (4)- inlet ports of the primary and secondary swirling air supply, (5) -water cooled sections of the combustor, (6)- diagnostic sections with peepholes for the local injection of the diagnostic tools (thermocouples and gas sampling probes) into the flame reaction zone. (7, 8)- inlet and outlet ports of the cooling water flow. The total volume of the gasifier can be varied by varying number of the sections and, hence, can be charged by different total mass of the wet wood pellets (180g or 500g), providing the variation of the moisture content in the pellets from 7% up to 30%. The primary and secondary swirling airflows were used to initiate the process of wood biomass gasification and provide complete burnout of the volatiles. The total rate of the air supply into the combustor could be varied in a range from 80 up to 160 l/min. The tangential air nozzle provides the strongly swirled secondary airflow formation above the layer of the wood biomass ( $S \approx 0.6-3.5$ ), providing the formation of the inner and outer recirculation zones with an intensive

mixing of the flame compounds above the wood layer. The rate of propane supply into the swirl burner can be varied in a range from 0,5 l/min to 0,8 l/min, determining the variation of additional heat supply rate into the system from 770 J/s up to 1100 J/s. For such conditions the total additional heat supply that is released during the propane combustion in these experiments is limited by 25-30% of the total heat value produced by co-firing the wood pellets with propane flame flow.

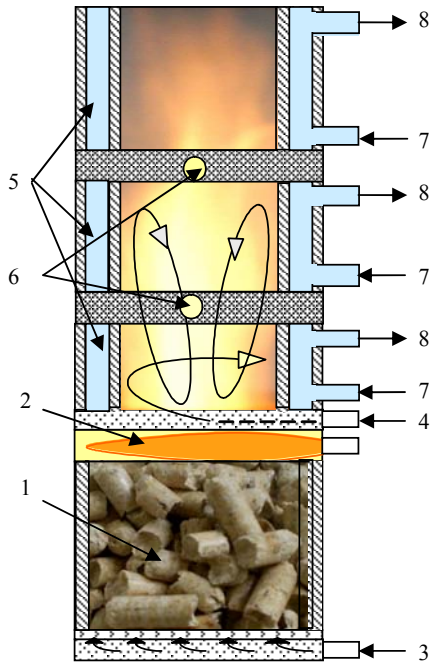


**Figure 1:** The pilot device for the experimental study of co-firing the wood biomass with propane flame flow.

The experimental investigations of co-firing the wood co-fire with propane flame flow involve a test and optimization of combustion characteristics and composition of polluting emissions with respect of a rate, mode and duration of propane co-fire for the clean heat energy production. The investigations of combustion and emission characteristics were conducted providing simultaneous on-line measurements of the flame characteristics with data registration using a plate PC-20 and software. The data registration was carried out with time interval of 1sec. The time-dependent measurements of the flame characteristics were carried out at different stages of the wet wood fuel gasification, ignition and burnout of the volatiles and different rates of propane co-fire, providing statistical analysis of repeated experimental measurements. The average values of the flame temperature, heat production rate and emission characteristics at different stages of the wood fuel burnout and different rates of propane co-fire were estimated from the 500 up 800 measurements, displaying on a chart a mathematical approximation of the relation between the average values of the flame characteristics and the rate of propane co-fire. The flame temperature was measured using the Pt/Pt-Rh thermocouples and providing the local injection of the thermocouples in the different parts of the flame reaction zone, while the heat

production rate was estimated from the calorimetric measurements of the cooling water flow for all sections of combustor. The measurements of the time-dependent variations of emission characteristics at different stages of wood fuel burnout were carried out providing continuous on-line monitoring of the products composition ( $O_2$ ,  $CO$ ,  $CO_2$ ,  $NO$ ,  $NO_x$  and  $NO_2$ ) using the gas analyzer Testo 350XL.

### 3 THE EXPERIMENTAL RESULTS AND DISCUSSION

The modeling parametric study of the wet wood biomass (at moisture content up to 30%) co-firing with the propane flame flow for the given system configuration (Fig. 1) is carried out with the aim to estimate the main factors, determining efficiency of the wet wood fuel burnout. Among them, the experimental research estimates the effects of the heat input rate during the propane co-fire ( $\dot{Q}_{co\text{-fire}}$ ) and duration time of additional heat input ( $t_{co\text{-fire}}$ ), as well equivalence ratio the propane flame flow ( $a_{prop}$ ) on the combustion and emission characteristics and the rate of heat production during the burnout of the wet wood fuel.

#### 3.1 The effect of propane co-fire on combustion characteristics of the wet wood fuel

By co-firing the wet wood pellets with propane flame flow the wood biomass undergo fast thermal decomposition with an intensive release of the volatiles –  $CO$ ,  $H_2O$ ,  $CO_2$ ,  $N_2$  and hydrocarbon fragments ( $C_xH_y$ ). For the wet wood fuel moisture content ( $MC_w$ ) is the most critical factor determining the total amount of heat value that can be produced during the burnout of the wet wood fuel. For completely dry and ash free wood biomass, the higher heating value (HHV) is in the order of 20 MJ/kg ( $\pm 15\%$ ). The higher the moisture content, the lower the energy content of the wet wood fuel and less amount of the heat can be produced during the burnout of the wood fuel. The relation between the heating value of the wet wood fuel and the moisture content and can be expressed as follows [7, 8]:

$$GHV = HHV (1 - MC_w/100). \quad (1)$$

Thus GHV represents the available potential heat at given moisture content and is equal to HHV only if the wood is dry. Generally, wood and bark fuels can contain considerable moisture content with direct influence on the rate of heat release, ignition time of the volatiles and total amount of heat produced during the wet wood fuel burnout. The time-dependent measurements of the rate of heat production ( $\dot{Q}_{wood,sum}$ ) during the stages of thermal decomposition of the wet wood pellets and burnout of the volatiles confirm that increasing of moisture content in the wet wood fuel results in a decrease of the rate of heat production with pronounced ignition delay (Fig. 2). The measurements of the average rate of heat production during the burnout of the wet wood pellets ( $\dot{Q}_{wood,av}$ ) by varying the moisture content in the wood pellets (Fig. 3) and approximate estimation of the effect of moisture content on the average rate of heat production confirm that the average rate of heat production decreases by

increasing the moisture content in the wet wood fuel and can be expressed as a power function of the moisture content in the wet wood fuel:

$$\dot{Q}_{\text{wood,av.}} = 350(MC_w / 100)^{-0.8} \quad (2)$$

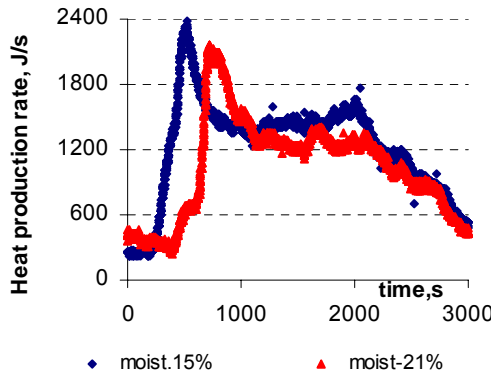


**Figure 2:** The effect of moisture content in the wet wood fuel on the time-dependent variations of the heat production rate.

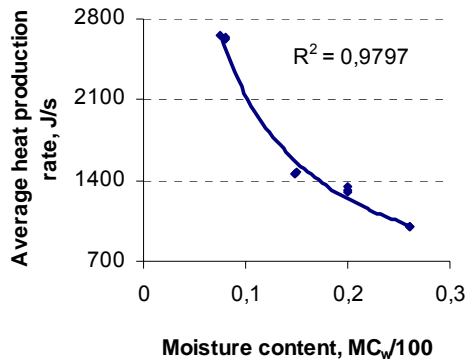


**Figure 3:** The effect of moisture content in the wet wood fuel on the average rate of heat production during the burnout of the wet wood fuel.

With the aim to obtain an increased rate of the heat production during the burnout of the wet wood fuel, the effect of propane co-fire on combustion and emission characteristics of the wet wood fuel was studied and analyzed. To appreciate the effect of propane co-fire on the rate of heat release during the wet wood fuel burnout, the time-dependent measurements of the flame temperature and heat production rates were carried out at different rates of the stoichiometric propane/air ( $\alpha_{\text{prop}}=1$ ) supply, different moisture contents in the wet wood pellets and lasting propane co-fire up to the complete burnout of the wet wood fuel ( $t_{\text{co-fire}}=3000$ s). The results show that the effect of a rate of propane co-fire on combustion characteristics of the wet wood fuel is quite different at different stages of propane co-fire. The local measurements of the time-dependent variations of the flame temperature and heat production rate at different

stages of propane co-fire indicate that the most pronounced effect of propane co-fire is detected during the primary stage of the thermal decomposition of the wet wood pellets ( $t < 1000$ s), when increasing of the rate of propane co-fire initiates faster and more intensive wood fuel drying, gasification and ignition of the volatiles with rapid increase of the flame temperature and heat production rate up to the peak values (Fig. 4-a,b).

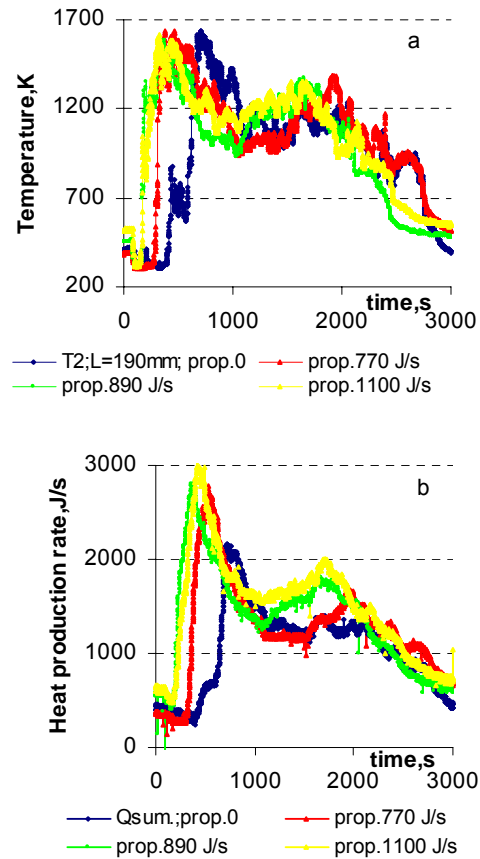


**Figure 4:** The effect of propane co-fire on the time-dependent variations of the flame temperature (a) and heat production rates (b) during the burnout of the wet wood fuel (moisture 21%).

The measurements of peak rate of heat production at different rates of propane co-fire have shown that the mathematical approximation of the relation between the peak heat production rate during the propane co-fire ( $\dot{Q}_{\text{sum,max}}$ ) of the wet wood pellets, rate of propane co-fire ( $\dot{Q}_{\text{co-fire}}$ ) and peak rate of heat production during the burnout of the wet wood fuel pellets ( $\dot{Q}_{\text{wood,max}}$ ) can be expressed as:

$$\dot{Q}_{\text{sum,max}} = (1 - MC_w / 100) \dot{Q}_{\text{co-fire}} + \dot{Q}_{\text{wood,max}}. \quad (3)$$

Moreover, the local measurements of the flame characteristics confirm that increasing the rate of propane

co-fire promotes a faster transition to the stage of self-sustaining wood biomass burnout. During this stage of propane co-fire the wood layer gradually slows down below the inlet port of propane flame flow and propane co-fire mostly is used to complete the burnout of the volatiles. At this stage of the wood fuel burnout the effect of propane co-fire on the rate of heat production is less pronounced (Fig. 5) and can be estimated using the mathematical approximation of the relation between the average rate of heat production during the propane co-fire ( $\dot{Q}_{sum.av.}$ ), rate of propane co-fire ( $\dot{Q}_{co-fire}$ ) and the average rate of heat production during the burnout of wet wood pellets ( $\dot{Q}_{wood.av.}$ ) that can be expressed as:

$$\dot{Q}_{sum.av.} = 0,7(1-MC_w/100)\dot{Q}_{co-fire} + \dot{Q}_{wood.av.} \quad (4)$$

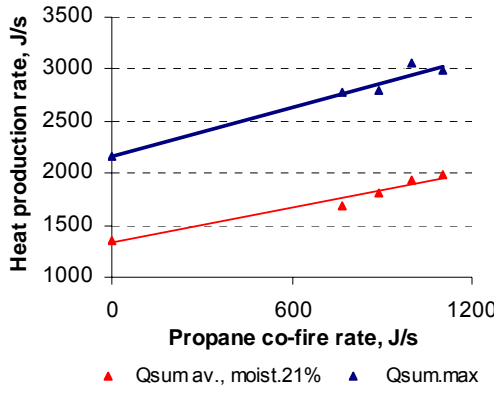


**Figure 5:** The effect of propane co-fire on the peak and average rates of heat production by co-firing the wet wood pellets.

### 3.2 The effect of duration time of additional heat input on combustion characteristics

As shown above, the dominant and more pronounced effect of propane co-fire is observed at the initial stage of the wood fuel gasification and ignition of the volatiles, when the propane flame flow helps as ignition source by enhancing the wood fuel gasification and ignition of the volatiles. In accordance with (3) and (4) the effect of propane co-fire on the rate of heat production significantly reduces during the next stage of the self-sustaining wood fuel burnout, when the propane co-fire is used to complete the burnout of the volatiles. Therefore, with the aim to improve combustion and emission characteristics of the wet wood fuel, there is essential so to consider usefulness of lasting propane co-fire over the all stages of the wood fuel burnout ( $t_{co-fire}$ ) up to complete burnout of the wet wood fuel. The effect of duration of propane co-fire on the time-dependent variations of the flame temperature and heat production rate at different stages of the wood fuel co-fire is illustrated in Figure 6-a,b.

Figure 6 shows the variations of an ignition time of volatiles at constant rate of propane co-fire, resulting in a rapid increase of the flame temperature and heat production rate. As one can see, decreasing duration of

propane co-fire at constant rate of co-fire results in pronounced ignition delay with an intensive heat consumption from the propane flame flow and correlating decrease of the flame temperature during the primary stage of the thermal decomposition of the wet wood fuel. Hence, the time-dependent variations of the flame temperature and rate of the heat production have shown that, not only enough heat production rate during the propane co-fire, but also enough duration of propane co-fire must be provided to prevent an ignition delay. As a consequence of resulting effect of these two main factors on the rate of wood fuel gasification and ignition of the volatiles, an ignition time of the volatiles can be decreased by increasing duration of propane co-fire, as well increasing the rate of propane co-fire and can be approximately expressed as a power function of the total additional heat input produced during the time of propane co-fire ( $\dot{Q}_{sum.prop.} = \dot{Q}_{co-fire} t_{co-fire}$ ) (Fig. 7):

$$t_{ign} = 63,5 \dot{Q}_{sum.prop.}^{-0,5} \quad (5)$$

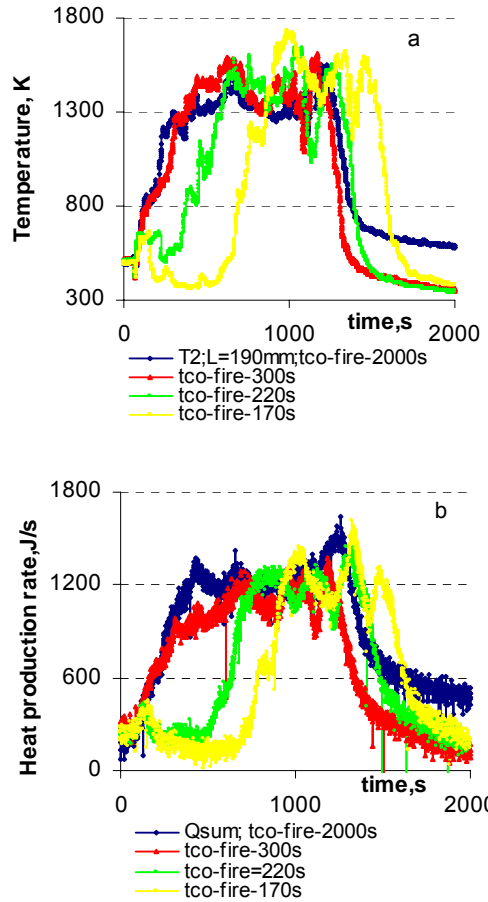


**Figure 6:** The effect of duration of propane co-fire on the time-dependent variations of the flame temperature (a) and the heat production rate (b) at constant rate of propane co-fire ( $\dot{Q}_{co-fire} = 1,1 \text{ kJ/s}$ ).

Moreover, it should be noticed that by limiting duration of propane co-fire and switching out the propane co-fire during the stage of the self-sustaining wet wood fuel burnout promotes the formation of combustion instability, resulting in the formation of the intensive pulsations of the flame temperature, rate of the heat production and rate of the formation of main product -  $\text{CO}_2$  (Fig. 8). The amplitude of temperature pulsations with no propane co-fire increases up to  $\pm 300\text{K}$ , the amplitude of heat production rate increases up to  $\pm 300\text{J/s}$ , while pulsations of the volume fraction of  $\text{CO}_2$  in the products increases up to  $\pm 3,5\%$  (Fig. 6-a,b and Fig. 8).

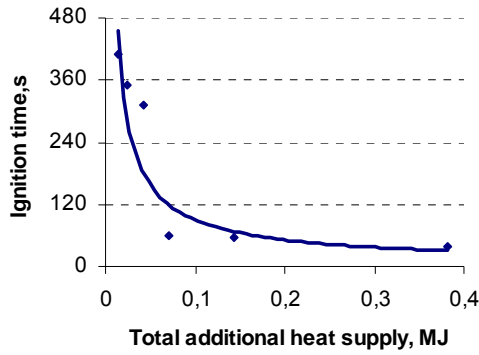


**Figure 7:** The effect of additional heat input by the propane flame flow into the wood biomass on the ignition time of the volatiles.

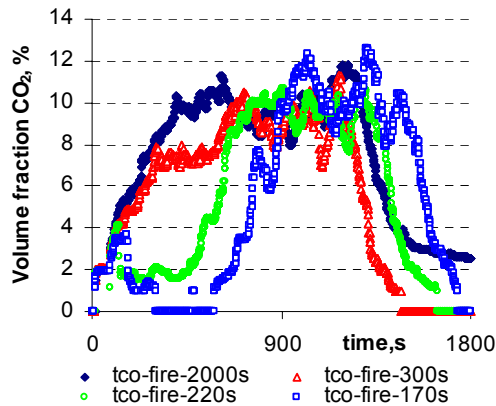


**Figure 8:** The effect of duration of propane co-fire at constant rate of propane co-fire ( $1,1\text{ kJ/s}$ ) on the time-dependent variations of the formation of the main product -  $\text{CO}_2$ .

Substantial stabilization of combustion and emission characteristics can be achieved for the conditions, if the propane co-fire is lasting yet over the stage of the self-sustaining burnout up to complete burnout of wood fuel, resulting in correlating increase of the total amount of produced heat during the wood fuel burnout (Fig. 9). Consequently, the propane co-fire of the wet wood fuel is quite desirable not only as a tool to provide the enhanced wood fuel gasification and faster ignition of the volatiles at the initial stage of the wood fuel co-fire, but so as a tool to provide stabilization of combustion characteristics

and to complete burnout of the volatiles during the stage of the self-sustaining wood fuel burnout. In general, increasing duration of propane co-fire and the total heat amount ( $Q_{sum.prop}$ ) injected into the system during the propane co-fire promotes an increase of the average volume fraction of carbon neutral  $\text{CO}_2$  in the products from 5-6% with no propane co-fire up to 9-10% that is fixed at the rate of propane co-fire  $1-1,2\text{ kJ/s}$  (Fig. 10).

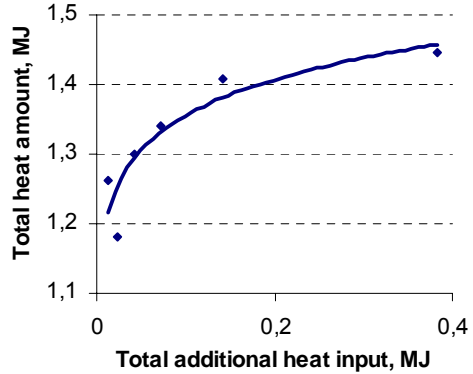


**Figure 9:** The effect of additional heat input by the propane flame on the total amount of produced heat during the stage self-sustaining burnout of the wood fuel

As follows from Figure 10, increasing duration of propane co-fire and the total additional heat input during the stage of the self-sustaining wood fuel burnout results in an increase of the average  $\text{CO}_2$  volume fraction in the products with correlating decrease of the average mass fraction of the flammable volatiles ( $\text{CO}$ ,  $\text{H}_2$ ) below  $100\text{ppm}$  (Fig. 11-a), so decreasing the volume fraction of free oxygen and air excess in the products (Fig. 11-b). Hence, the results of experimental study confirm that the additional lasting heat input during the propane co-fire improves combustion characteristics of the wet wood fuel and composition of polluting emissions.

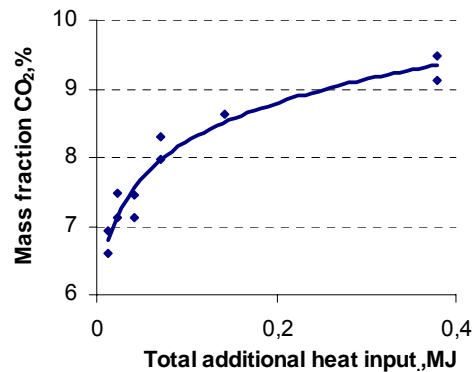


**Figure 10:** The effect of propane co-fire of the wood fuel on the average volume fraction of  $\text{CO}_2$  in the products

Finally, it should be noticed that the very important problem of wood biomass co-firing for the stoichiometric combustion conditions of the propane flame flow ( $\alpha=1$ ) is an increased rate of thermal NO production with relative

high mass fraction of  $\text{NO}_x$  emissions in the products— by increasing the total heat input into by the propane flame into the system, the average mass fraction of  $\text{NO}_x$  emissions in the products increases from 60–70 ppm with no propane co-fire up to 90–100 ppm at 30% of propane co-fire (Fig. 12).

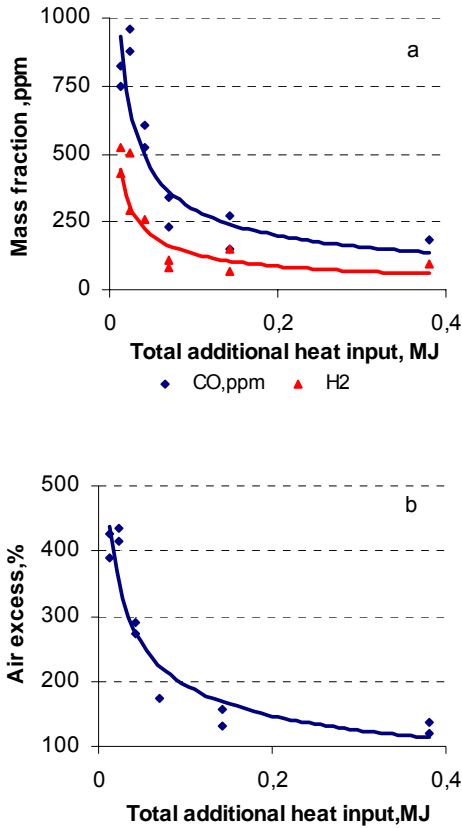


**Figure 11:** The effect of propane co-fire of the wood biomass on the average volume fraction of CO, H<sub>2</sub> and the air excess in the products

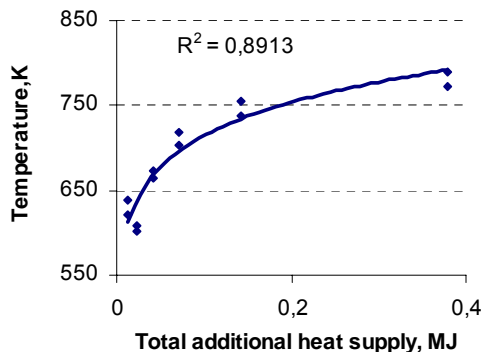


**Figure 12:** The effect of fuel-rich ( $\alpha < 1$ ) propane co-fire on the average temperature of emissions.

Hence, as a consequence of the effect of propane co-fire on the enhanced formation of  $\text{NO}_x$ , the additional measures must be used to restrict the thermal  $\text{NO}_x$  formation and reduce the levels of  $\text{NO}_x$  in the products. In this account the investigations of  $\text{NO}_x$  formation are carried out by varying the equivalence ratio of propane/air supply ( $\alpha_{\text{prop}}$ ) and providing the propane co-fire at the fuel-rich conditions of the propane flame flow. In accordance with [6] propane supply into the flame reaction zone can be used as reburn fuel to reduce  $\text{NO}_x$  emissions. The measurements of the composition of products confirm that a slight increase of propane excess ( $\alpha_{\text{prop}}=0,8$ ) during the propane co-fire allows provide the enhanced wood fuel gasification and burnout of the volatiles with an increased rate of heat release, the rate of CO<sub>2</sub> formation and the average temperature of the products (Fig. 12), while rapidly decreases the air excess and the average mass fraction of  $\text{NO}_x$  (Fig. 13) in the products.

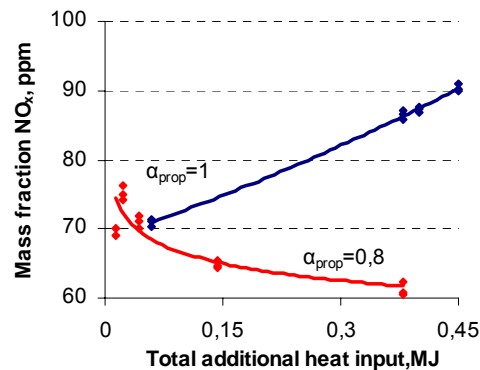


**Figure 13:** The effect of total additional heat supply and equivalence ratio of propane/air supply on the variations of NO<sub>x</sub> mass fraction in the products

The observed variations of the products composition and temperature allows suggest that co-firing of the wood pellets with propane flame flow at the fuel rich conditions ( $\alpha < 1$ ) can promote destruction of NO by enhancing the reburn reactions between unburned hydrocarbons (C<sub>x</sub>H<sub>y</sub>) and NO. The detailed experimental study of NO destruction in slightly rich premixed methane/air flame have shown [9] that the more significant changes of NO concentration occur in the flame front due to the reburning phenomenon with the rapid reaction between CH and NO:



The intensive CH band radiation of premixed propane flame flow at 431.25 nm close to the swirl burner outlet confirms [10] that the propane flame contains the free CH radicals that can promote the reburn reactions between CH and NO with resulting reburn of NO, so decreasing the mass fraction of NO<sub>x</sub> in the products (Fig. 13) and providing cleaner and more effective wood fuel burnout with reduced levels of NO<sub>x</sub> in the products.

#### 4 SUMMARY

In summary, the results of experimental study of the effect of propane co-fire on combustion and emission characteristics clearly show that:

- Co-firing of renewable with fossil fuel improves the wood fuel drying, gasification and ignition of the volatiles at the initial stage of the additional heat input into the wood biomass, so improving the combustion and emission characteristics during the stage of the self-sustaining wood fuel burnout.
- Moreover, the propane co-fire of the wet wood fuel provides stabilization of combustion characteristics, completing the burnout of volatiles during the stage of the self-sustaining wood fuel burnout.
- Therefore, the results of experimental study confirm that co-firing of wood biomass with propane is both feasible and practical for cleaner, more stable and effective heat energy production with reduced mass fraction of polluting (CO, NO) emissions in the products with dominant release (up to 80%) of carbon –neutral CO<sub>2</sub> emissions.

#### REFERENCES

1. Ausilio Bauen, Jeremy Woods and Rebecca Hailes, BIOPOWERSWITCH! A Biomass blueprint to Meet 15 % of OECD Electricity Demand by 2020, WWF Climate Change Programme, 2004, pp.74: <http://assets.panda.org/downloads/biomassreportfinal.pdf>
2. K. Maniatis, Progress in Biomass gasification: An Overview, Belgium, 2001, pp. 31: [http://www.intrinergy.com/pdf/Biomass\\_Gasification\\_Overview.pdf](http://www.intrinergy.com/pdf/Biomass_Gasification_Overview.pdf)
3. Gray Davis, Biomass Co- firing with Natural Gas in California, report P500-02-050F, 2002, pp.36: [http://www.energy.ca.gov/reports/2002-11-12\\_500-02-050F.PDF](http://www.energy.ca.gov/reports/2002-11-12_500-02-050F.PDF).
4. Miles Perry and Frank Rosillo-Calle, Sustainable International BioEnergy Trade: Securing supply and demand, Co-firing Report T40UK02R, United Kingdom, 2006, pp. 75 : <http://www.bioenergytrade.org/downloads/ukcofiringfinal.pdf>.
5. Barmina, A. Desnickis, A. Meijere, M. Zake, Development of Biomass and Gas Co-firing Technology to Reduce Greenhouse Gaseous Emissions, Advanced combustion and Aerothermal Technologies, 2007 Springer, pp 221-230.
6. Rajesh Kapoor and George Rizeq, Utilization of Waste Renewable Fuels in Boilers with Minimization of Pollutant Emissions, Project Fact Sheet, 2002, pp.2: [http://www.energy.ca.gov/pier/renewable/documents/GE\\_EERC.pdf](http://www.energy.ca.gov/pier/renewable/documents/GE_EERC.pdf)
7. P. J. Ince, How to estimate Recoverable Heat Energy in Wood or Bark Fuels, U.S. Department of Agriculture, Forest Service, 1979, pp.7. <http://www.fpl.fs.fed.us/documents/fplgr29.pdf>
8. The Engineering ToolBox, 2005, [http://www.engineeringtoolbox.com/wood-combustion-heat-d\\_372.html](http://www.engineeringtoolbox.com/wood-combustion-heat-d_372.html)
9. M. Tamura, J. Luque, J.E. Harrington, P.A. Berg, G.P. Smith, J.B. Jeffries, D.R. Crosley, Laser-induced fluorescence of seeded nitric oxide as a flame thermometer, Appl. Phys. 1998, B 66, pp. 503–510.
10. M. Zake, I. Barmina, M. Lubāne Swirling Flame. Part1. Experimental Study of the Effect of Stage Combustion on Soot Formation and Carbon Sequestration from the Non-Premixed Swirling Flame // Magnetohydrodynamics, Vol.40 (2004), N2, pp.161-181.

#### ACKNOWLEDGMENT

The financial support by the European Regional Development Funding (ERDF): 2.5.1. Financial Support of Applied Research in the State Research Institutions is gratefully acknowledged.

## COMBUSTION AND EMISSION CHARACTERISTICS OF GRANULATED NON-HYDROLYZED RESIDUES FROM LIGNOCELLULOSICS ETHANOL PRODUCTION.

A. Arshanitsa\*, I Barmina\*\*, T Dizhbite\*, G Telysheva\*, M. Zake\*\*

\*Latvian State Institute of Wood Chemistry

Dzerbenes Street 27, Riga, LV-1006; fax. +371 7550635, e-mail:ligno@edi.lv

\*\* Institute Of Physics, University of Latvia

Miera Street 32, Salaspils-1, LV-2169, fax. +371 7901214, e-mail: [mzfi@sal.lv](mailto:mzfi@sal.lv)

**ABSTRACT:** The paper presents results of the experimental study of composition, heating values and combustion characteristics of rich in lignin-hydrolyzed residues (LHRs) of different configuration of spruce wood bioethanol processing. Combustion and emission characteristic of LHRs granules were tested using small pilot-scale combustion system, composed of the plant biofuel gasifier and water-cooled combustor and results compared with those parameters for commercial softwood granules. In comparison with softwood granules LHRs granules differ by higher heating value, faster gasification and faster burning out, determining an increase of heat production rate at 23-75% with higher rate of CO<sub>2</sub> production and higher average volume fraction of CO<sub>2</sub> in the combustion products. It was established that LHRs produced by enzymatic hydrolysis of different configurations contain more sulphur and nitrogen than LHR produced by acid hydrolysis although the emission of SO<sub>2</sub> does not exceed the domestic requirements. At the same time NO<sub>x</sub> emission exceeded the same requirements negligibly.

Keywords: bio-ethanol, biomass characteristic, CO<sub>2</sub> balance

### 1 INTRODUCTION

The still increased exhaustion of fossil fuels reserves and environmental considerations have led to an intensive research and development of alternative energy sources [1, 2]. An important study in this raw is the lignocellulosic biomass ethanol production, which is considered as real alternative of gasoline for transport needs today. In fact, the biomass hydrolysis during biomass ethanol production cannot be processed completely and about 40-50% of raw materials remain as non-hydrolyzed residues, containing lignin and non-hydrolyzed carbohydrates. LHRs (in fine dispersed form or granulated) can combusted to provide heat energy so increasing the value of this residue and significantly enhancing the competitiveness of bioethanol production technology. Significant differences in plants structure and its chemical composition produce the wide variations of combustion and emission characteristics of the plant biofuel. Significant impact in variation of above mentioned LHRs can be connected with conditions of biomass processing during which LHRs were obtained. The aim of the present study was estimation of combustion and emission characteristics of fuel granules on LHRs basis obtained from spruce wood by dilute acid hydrolysis (LHR AH), enzymatic (Enz.) hydrolysis with separate hydrolysis and fermentation (LHR SHF), as well enzymatic hydrolysis with simultaneous hydrolysis and fermentation (LHR SSF).

### 2 EXPERIMENTAL

#### 2.1. Materials and method of it investigation

LHRs samples were prepared by pilot plant in Ornskoldsvik (Sweden). Due to the conditions of both types of enzymatic hydrolysis were varied all corresponding LHRs were investigated separately (Tab.I). Lignin content determination was accomplished in accordance with Klason procedure [3]. C, H N and S total (S<sub>tot</sub>) determination was accomplished using Elemental Analysis System Vario Macro CHNS. Water content and ash content was determined according CEN /TS 14774-1 and CEN /TS 14775 correspondingly.

Higher heating value (HHV) of LHRs samples and softwood samples was founded by burning sample in the calorimetric bomb according ISO1928. Combustion sulphur content (S<sub>comb</sub>) was measured spectrophotometrically, after burning samples in calorific bomb [4].

Table I: Composition of different types of dry plant biofuel

Biofuel and hydrolysis type.	Element content, %				
	C	H	N	S <sub>tot</sub>	S <sub>comb</sub>
Softwood (sw)	50.2	6.2	0.33	0.14	0.02
LHR AH	59.4	6.0	0.19	0.21	0.04
Dilute acid					
LHR SHF-1 Enz.	55.0	6.2	0.42	0.22	0.03
LHR SHF-2 Enz.	57.7	6.0	0.40	0.21	0.05
LHR SSF-1 Enz.	58.0	5.9	0.56	0.23	0.13
LHR SSF-2 Enz.	59.7	5.9	0.80	0.20	0.13
LHR SSF-3 Enz.	60.9	5.9	1.13	0.34	0.21

Pilot extruder with capacity up 20 kg of material per hour, equipped with six-channel die of channel diameter 7 mm has been used in experiment for manufacturing of LHRs pellets. Water contents in LHRs before granulation were in the range 47-62%. After air-drying LHRs pellets with water content 6-7% and diameter 5.5-5.6 mm were obtained. Commercial softwood granules (6.2 mm in diameter) with water content 7.2% were used as reference material.

Particles density, bulk density of granules were determined according CEN /TS 15150:2005, CEN /TS 151030:2005 correspondingly.

## 2.2. Pilot-scale combustion system

The testing of combustion and emission characteristics for different types of plant biofuel granules was conducted using a small pilot-scale combustion system, composed of biofuel gasifier with discrete mass load (180g) of the biofuel granules and water-cooled combustor [5]. The primary and secondary swirling airflows are used to promote the biofuel gasification and to provide complete burnout of the volatiles downstream of the water-cooled channel. The gasification of the wood fuel and ignition of volatiles were initiated using the propane flame flow as a heat source. Between the sections of the water-cooled channel access ports for the kinetic measurements of the flame temperature at the different stages of thermal decomposition of plant biofuel were installed. The diagnostic tools for the complex experimental study of combustion and emission characteristics included: Pt/Pt-Rh thermocouples for the local time-dependent measurements of the flame temperature; a portable gas-analyzer Testo 350XL that is used for investigation of emissions composition ( $\text{CO}$ ,  $\text{CO}_2$ ,  $\text{NO}_x$ ,  $\text{SO}_2$ ). The calorimetric measurements of the cooling water flow are used to estimate the rate of the heat energy production at different stages of the biofuel burnout. The all time-dependent variations of combustion and emission characteristics during the burnout of different biofuels were recorded on-line by using the data recording plate PC-20.

## 3 RESULTS AND DISCUSSION.

### 3.1 Fuel characteristic of LHRs

In general lignocellulosic materials are composed of three natural components; cellulose, hemicellulose and lignin. Each of these natural components exhibit very different characteristics of heat energy release when combusted. It was reported [6] that cellulose and hemicelluloses have a HHV of 18,6 MJ/kg, whereas lignin has a HHV of 23,3 to 26,6 MJ/kg. Actually, the HHV of lignocellulosic fuel increase with increase of their lignin content (LC) that was reflected by the regression equation proposed recently [6]:

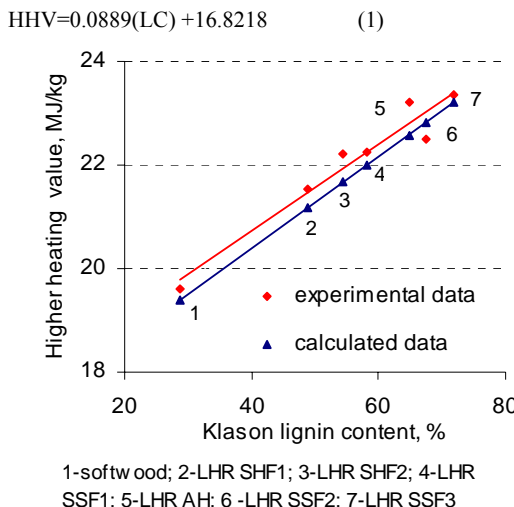


**Figure 1:** The effect of Klason lignin content on HHV of dry biofuel

The experimental measurements of HHV for softwood and LHRs samples confirm that heating value of biofuel samples correlates with Klason lignin content in these samples. Only a small deviation from calculated data was observed (Fig.1), indicating usefulness of equation proposed.

Results presented above show that HHV of investigated LHRs up 10-18% exceed the value of softwood. Moreover, when additional hydrolysis of LHR SHF-2 sample has been performed in laboratory conditions to remove the main part of non-hydrolyzed carbohydrates, the carbon content and HHV increases up to 69.2% and 27.3 MJ/kg correspondingly, that is near to the same characteristic of fossil coal (carbon content 65-85%, HHV-23-28 MJ/kg) [7].

Another important characteristic of plant biofuel is amount of ash in material. It was established that ash content in LHR AH (0.6%), LHR SHF (0.4-0.6%) and softwood (0.5%) differs insignificantly. At that time LHR SSF have lower ash content 0.1-0.3%. According to this results no fouling and slagging problems can be prognosed during combustion of fuels on LHRs basis.

The usage of  $\text{SO}_2$  or sulphuric acid in the pretreatment step of hydrolytic treatments and enzymes at SHF and SSF hydrolysis results in an increase of total nitrogen (for enzymatic products), total and combustion sulphur content in LHRs in comparison with softwood (Tabl. I). However, the combustion sulphur and total nitrogen content correspond to demand of CEN /TC 335 standard for chemically treated biomass.

Since the difference granulating technologies (pellet mills for softwood and screw extruder for LHRs) have been used, particle density of softwood granules (1150 kg/m<sup>3</sup>) is higher than the density of LHRs granules (1030-730 kg/m<sup>3</sup>). In fact, the granules density is one of the factors that can affect the heat transfer rate into the biomass and the process of biofuel volatilisation. This factor have no been investigated in this paper and will be investigated in further.

### 3.2 COMBUSTION AND EMISSION CHARACTERISTICS OF DIFFERENT TYPES OF PLANT BIOFUEL GRANULES

#### 3.2.1 The effect of propane co-firing on the thermal degradation and ignition of the different types of plant biofuel granules.

In order to initiate the primary endothermic process of thermal degradation of softwood and LHRs (in this case LHR SHF-2) granules, resulting in the formation of the mixture of combustible volatiles ( $\text{CO}$ ,  $\text{H}_2$ ,  $\text{C}_x\text{H}_y$ ) and carbonaceous char, the additional heat energy (propane flame flow in this case) must be injected into the layer of the plant biofuel. The primary endothermic reactions of biofuel degradation promote intensive heat absorption from the system before an ignition and exothermic combustion occurs. To provide ignition of the volatiles with transition to the stage of self-sustaining exothermic combustion, the mix of volatiles with swirling airflow must be heated by the external heat source up to the 900-1000K. It was established that at constant heat supply rate of propane-air mixture (1.2 kJ/s) and constant biofuel mass the ignition time is highly sensitive to the type of biofuel and depends on the amount of heat introduced into the system by the propane flame. The very important factor, determining the rate of the thermal degradation of biofuel and ignition of the volatiles, is duration of co-firing the biofuel with propane. Actually, the time-

dependent variations of the flame temperature, heat production rates and composition of the products have shown that decreasing duration of co-firing biofuel with propane can result in an ignition delay (Fig 2, a-d).

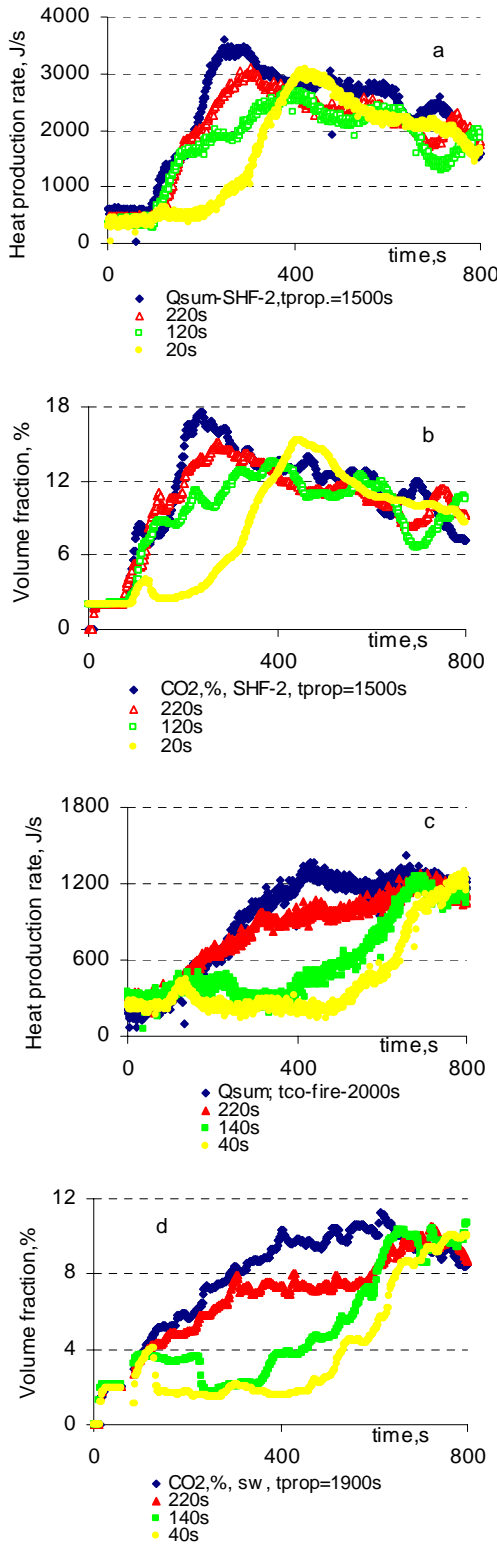


**Figure 2:** The effect of duration of propane co-firing on the rate of the heat production (a, c) and  $\text{CO}_2$  formation (b, d) for: (a, b) - LHR SHF-2, (c, d) – softwood granules.

As follows from Figure 2, the more pronounced ignition delay is observed for the softwood granules, because the thermal decomposition of main softwood compounds (cellulose and hemicelluloses) results in an intensive heat consumption during the endothermic degradation of cellulose, promoting decrease of the flame temperature with pronounced decrease of the heat production rate and rate of  $\text{CO}_2$  formation during the primary stage of the thermal degradation (Fig.2-c, d). In contrary, the reduced content of volatile matter with higher heating value of LHRs samples allows decreasing duration of propane co-firing with higher rate of the heat production and faster  $\text{CO}_2$  formation (Fig.2-a, b). Hence, the time-dependent variations of combustion and emission characteristics have shown that ignition of the volatiles and transition from the primary stage of endothermic reactions to the next stage of exothermic reactions is mostly affected by the structural and elemental composition of the plant biofuel. In fact, proportion between the level of the volatiles and char is quite different for the different types of the plant biofuels [7,8]. It was established by the thermogravimetry analysis that char residue at 1000 °C for softwood is 12.9% and 27.6 % for LHR SHF-2. As a result, the higher level of volatiles with lower heat of combustion for softwood granules results in an ignition delay, while higher char yield and lower percent of volatiles with higher combustion heat for LHR-SSF-2 granules promotes the faster ignition of the volatiles. Therefore, lower duration of propane co-firing is needed to provide transition to the self-sustaining LHRs granules burnout in comparison with softwood granules.

### 3.2.2 The effect of the plant biofuel composition on the combustion and emission characteristics

The time-dependent measurements of the combustion process have shown that at the equal rates of the primary (55 l/min) and secondary (85 l/min) air supply in a system, equal rates of the additional heat supply during the primary stage of the biofuel gasification and equal moisture content in the granules (6-8%), the granules of LHRs in comparison with softwood granules are subjected to faster gasification during the primary stage of the thermal degradation (Fig.2, 5), resulting in a faster ignition and faster transition to the next stage of self-sustaining biofuel burnout.

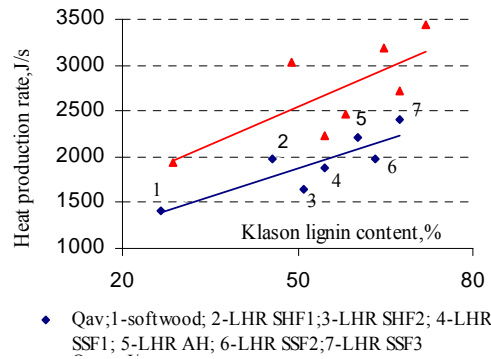


**Figure 3:** The dependence of average and peak heat production rates on the Klason lignin content during the stage of self-sustaining wood fuel burnout.

The measurements of the heat production rates for the softwood and different types of LHRs granules during the stage of self-sustaining biofuel burnout have shown that the average ( $Q_{av}$ ) and peak rate ( $Q_{max}$ ) of heat production can be approximately expressed with linear dependence on the lignin content in the biofuel (Fig. 3)

The measurements of the average volume fraction of  $\text{CO}_2$  in the combustion products have shown that for different types of the plant biofuel under investigation these parameters can be approximately expressed with linear dependence on the carbon content (Fig. 4)

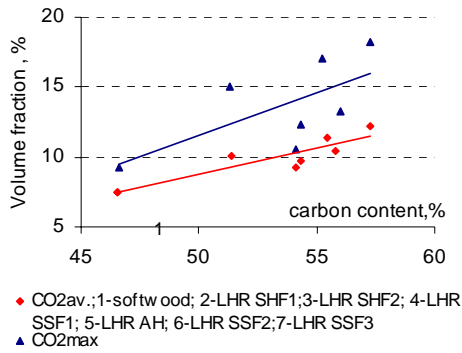


**Figure 4:** The correlation between the volume fraction of  $\text{CO}_2$  in the combustion products and carbon content in different types of biofuel granules.

As one can see from Fig.7, the average volume fraction of  $\text{CO}_2$  in the products during the active burning stage (air excess  $\leq 200\%$ ) of different types of biofuels can be increased from 7% for the softwood granules up to 10-12.5% for LHRs granules. Hence, the results of experimental study indicate that the LHRs are applicable for the clean and effective heat energy production with reduced impact on the global warming.

The local measurements of the flame temperature at the distance  $L=25\text{mm}$  above the inlet port of propane flame have shown that the average flame temperature during the active burning stage of LHRs granules exceeds that observed for softwood (sw) granules by 250 K (Fig.5).

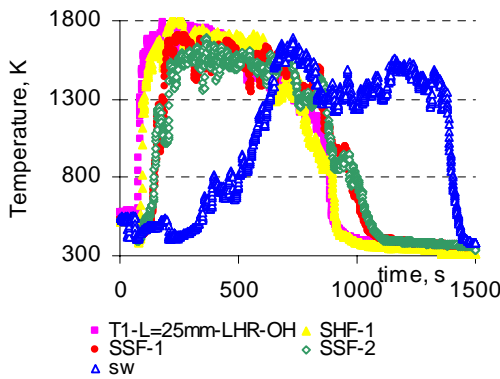


**Figure 5:** The variations of flame temperature during the burnout stage for different types of biofuel granules.

The higher rate of heat release together with higher temperature of the flame reaction zone during the burnout of LHR granules allows suggest the faster formation of temperature-sensitive  $\text{NO}_x$  in the products. The average concentration of  $\text{NO}_x$  in the products during the active burning stage increases from 48 ppm for softwood granules up 68-380 ppm for LHRs granules (Fig.6).

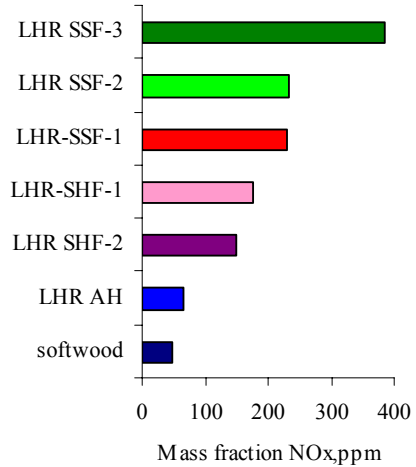


**Figure 6:** The variation of  $\text{NO}_x$  content in combustion products of different types of biofuel granules.

In fact, the analysis of correlation between the variations of the mass fraction of  $\text{NO}_x$  in the products and the average flame temperature for different types of wood fuels have shown that for given combustion conditions  $\text{NO}_x$  formation can not be expressed with exponential dependence on the flame temperature, as it follows from Zeldovich mechanism [9]. The better correlation is observed between the average mass fraction of  $\text{NO}_x$  in the products and nitrogen content in the biofuel. (Fig.7).

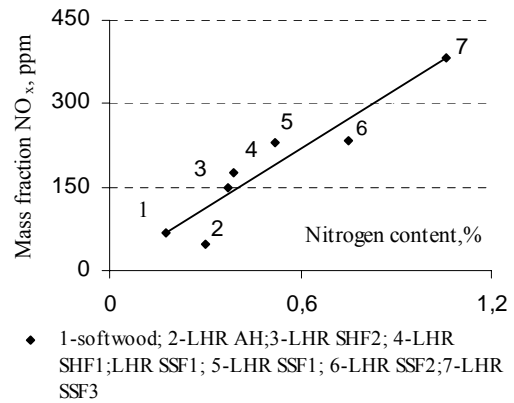


**Figure 7:** The correlation between mass fraction of  $\text{NO}_x$  in combustion products and nitrogen content in different types of biofuel granules.

The investigation of  $\text{SO}_2$  content in the burning products of biofuel granules show that the burnout of

LHR granules produces the relatively high levels of sulphur dioxide. The highest sulphur dioxide content (up 80ppm in the products) is fixed for LHR-SSF-3 pellets that actually refers to the highest elemental content of S<sub>comb</sub> (0,20%) in this type of the pellets. The minimum value of SO<sub>2</sub> (2-3%) in the products was established for the softwood granules with minimum value of elemental S<sub>comb</sub> content (0,02%) in the wood (Figure 8).

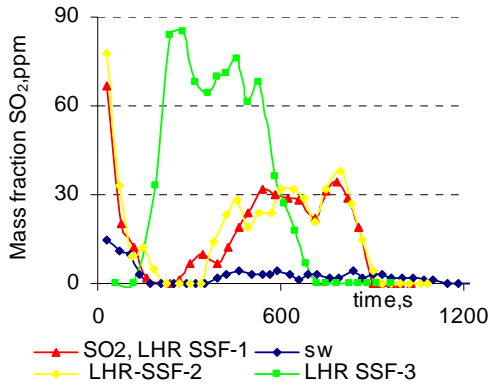


**Figure 8:** The variations of SO<sub>2</sub> content in the products during the burnout of the different types of biofuels granules.

Finally it should be noticed that for the investigated conditions the average levels of SO<sub>2</sub> ( $\leq 175 \text{ mg/m}^3$ ) and CO ( $\leq 1700 \text{ mg/m}^3$ ) in the combustion products measured during the active burning stage of different LHRs granules do not exceed the Latvian standards, determining the maximal emission of harmful products at solid fuels combustion as follow: SO<sub>2</sub> -2500 mg/m<sup>3</sup>, NO<sub>x</sub>-600 mg/m<sup>3</sup>, CO-2000 mg/m<sup>3</sup>. Hence, the average levels of NO<sub>x</sub> (800 mg/m<sup>3</sup>), fixed during the burnout of LHR SSF-3, exceed the standard requirements and conventional methods for NO<sub>x</sub> emission decreasing could be used.

#### 4 SUMMARY

- Liner correlation between Klason lignin content and higher heating values of soft wood and LHRs was established.
- Because of higher carbon content and reduced content of volatile matter in LHRs in comparison with softwood, lower amount of heat is needed for the beginning of the thermal degradation of LHR granules in comparison with softwood pellets and faster ignition of the volatile is preceded.
- The higher heating value of LHR granules and higher carbon content in LHR pellets results in higher average value of the heat production rate and higher average value of CO<sub>2</sub> in the products during the active burning stage of self-sustaining burnout of LHR granules
- Because of higher nitrogen and combustion sulphur content in enzymatic LHRs in comparison with softwood, the burnout of LHRs granules produces the higher levels of NO<sub>x</sub> and SO<sub>2</sub> in the products. Additional measures should be undertaken to decrease NO<sub>x</sub> and SO<sub>2</sub> emission in LHRs products up to values obtained for softwood granules if it would be necessary.

#### REFERENCES

- [1] M. Asif, T. Muneer, Energy supply, its demand and security issues for developed and emerging economies. *Renewable and sustainable Energy Reviews*, Vol.. 11, (2006), pp. 1388-1413.
- [2] A.C Dimian, Renewables raw materials, chance and challenge for computer –aided Process engineering. *Computer Aided Chemical Engineering*, Vol.24, (2007), pp. 309-318.
- [3] S.Y Lin, C.W. Dence (Eds.). Methods in lignin chemistry. Springer-Verlag, Berlin-Heidelberg-New York (1992).
- [4] F. Egami, N. Takashi. Bull. Soc. Chem. Japan, Vol.30, 5, (1957), p.442.
- [5] I. Barmina, A. Desnickis, M. Gedrovics, M. Zaķe, Co-firing of Renewable with Fossil Fuel for the Cleaner Heat Energy Production, Proceedings of 10<sup>th</sup> Biennial Conference on Environmental Science and Technology, CEST-2007, Cos island Greece, 2007, pp. B44-B51.
- [6] A. Demirbas, Relationships between lignin contents and heating values of biomass, *Energy Convers. Manage*, 2001, 42:183-8.
- [7] A. Demirbas, Combustion characteristics of different biomass fuels, *Progress in Energy and Combustion Science* 30, 2004, pp. 219-230
- [8] R.M. Rowell, G. Ballard-Tremeer, Emissions of Rural Wood-Burning Cooking Devices, A thesis submitted to the Faculty of Engineering, University of the Witwatersrand, Johannesburg, for the degree of Doctor of Philosophy, Johannesburg, 1997: (<http://ecoharmony.com/thesis/PhDIntro.htm#Contents>)
- [9] F.Shafizadeh ,S.S. Sofer, O.R. Zaborsky, Basic Principles of Direct Combustion, in *Biomass Conversion Processes for Energy and Fuels*, Plenum Publishing Corporation, 1981, New York, pp. 103-124.

#### ACKNOWLEDGMENTS.

The financial support Project NILE (Contract N 019882) and the financial support by the European Regional Development Funding (ERDF): 2.5.1. Applied Research in the State Research Institutions are gratefully acknowledged.